Supporting Information for

One Stone Two Birds: β-Fluoropyrrolyl-Cysteine S_NAr Chemistry Enabling Functional Porphyrin Bioconjugation

Guo-Qing Jin[1], Jing-Xiang Wang[1], Jianhua Lu[1], Hang Zhang[1], Yuhang Yao[1], Yingying Ning[1], Hua Lu[1], Song Gao[1,2,3], and Jun-Long Zhang[1,2]*

[1]Beijing National Laboratory for Molecular Sciences, College of Chemistry and Molecular Engineering, Peking University, Beijing 100871, P. R. China

[2]Chemistry and Chemical Engineering Guangdong Laboratory, Shantou 515031, P. R. China

[3] Spin-X Institute, School of Chemistry and Chemical Engineering, State Key Laboratory of Luminescent Materials and Devices, Guangdong-Hong Kong-Macao Joint Laboratory of Optoelectronic and Magnetic Functional Materials, South China University of Technology, Guangzhou 510641, China

Contents

I. Materials and Methods 3
Materials. 3
Methods. 4
General procedures 4
Synthesis of substrates. 6
Reaction rate 17
P_{12} reacted with GSH 18
P_{13} reacted with GSH 18
Click chemistry 18
Protein bioconjugation 18
Synthesis of P_{13}-EGFP-PDS and IAA-EGFP-PDS 19
Metabolic labeling of Sialoglycoproteins 19
Measurement of $^1O_2$ generation efficiency 19
Cytotoxicity evaluation *in vitro* 20
Cellular internalization measured by confocal laser scanning microscopy (CLSM) 20
Enzymatic assay of caspase-3 in solutions. 20
Fluorescence imaging of caspase-3 in live HeLa cells 20
Fluorescence imaging of A549/MCF7 21
In vivo photodynamic therapy assay 21
Structures of β-peptidyl porphyrins 22
II. Supporting Tables and Figures 33
III. Reference 154

I. Materials and Methods

Materials.

All reagents were purchased from commercial suppliers and used as received unless otherwise indicated below. Chemical reagents used in this work are listed in the format of (trade name; agency, article number): 1-dimethylamino-2-propyne (HEOWNS, 7223-38-3), dibenzocyclooctyne-PEG_4-N-hydroxysuccinimidyl ester (DBCO-PEG_4-NHS; Sigma-Aldrich, 764019), disulfo-Cy5-DBCO (Confluore, BCD-34), sulfo-DBCO-amine (Click Chemistry Tools, 1227), tris[(1-hydroxypropyl-1H-1,2,3-triazol-4-yl)methyl]amine (THPTA; Sigma-Aldrich, 762342), 2-iminothiolane (J & K Scientific, 455901), Biotin-PEG4-alkyne (Confluore, BCP-14), Ac_4ManNAz (Confluore, BSMB-3), lipoic acid (LA; Macklin, A835604), Staurosporine (STS, Amethyst, 970545), 5-[(S)-(+)-2-(methoxymethyl)pyrrolidino]sulfonylisatin (MPS, EFEBIO, E005702). H_2O was obtained from Milli-Q integral, HPLC grade methanol was purchased from Fisher. All mobile phase were filtered with 0.22 μm filter membrane in advance.

3,4-Difluoropyrrole was synthesized according to literature methods. [1]

Peptides were purchased from ChinaPeptides. Streptavidin (Sav) was purchased from Thermo Fisher Scientific. Bovine serum albumin (BSA) was purchased from Sigma-Aldrich. Recombinant human Caspase-3 and recombinant human Caspase-7 were both purchased from Sino Biological Inc. (Beijing, China). The EGFP was expressed according to literature method.[2,3] The sequence is shown as following:

MENLYFQCGKGEELFTGVVPILVELDGDVNGHKFSVSGEGEGDATYGKLTLKFICTTGKLPVPWPTLVTTL
TYGVQCFSRYPDHMKQHDFFKSAMPEGYVQERTIFFKDDGNYKTRAEVKFEGDTLVNRIELKGIDFKEDG
NILGHKLEYNYNSHNVYIMADKQKNGIKVNFKIRHNIEDGSVQLADHYQQNTPIGDGPVLLPDNHYLSTQ
SALSKDPNEKRDHMVLLEFVTAAGITLGMDELYKLPETGGLEHHHHHH

HPLC procedures were performed on an Auno High-Performance Liquid Chromatography System (P2010 high pressure infusion pump; UV (190-400 nm) detector; 7725i manual injection valve; *Easychrom* chromatography workstation) using the Dr. Maisch GmbH packed reversed-phase column (ReproSil-Pur Basic-C18, 5 μm, 250×4.6 mm for analysis; ReproSil-Pur Basic-C18, 5 μm, 250×10 mm for purification, respectively).

NMR (^{1}H NMR/^{13}C NMR/^{19}F NMR) spectrum were recorded on Bruker 400MHz or Brucker 500MHz NMR or Brucker 600MHz NMR spectrophotometer. High resolution mass spectroscopy was recorded on Bruker Solarix XR

mass spectrometer or AB Sciex 5800 MALDI-TOF mass spectrometer. IR spectra were recorded on a Bruker Tensor 27 FTIR Spectrometer.

UV-vis spectra were conducted on an Agilent Cary 8454 UV-vis spectrometer equipped with an Agilent 89090A thermostat (±0.1 °C) at 25 °C. The emission spectra were obtained on an Edinburgh Analytical Instruments FLS980 lifetime and steady state spectrometer (450 W Xe lamp/60 W microsecond flash lamp, PMT R928 for visible emission spectrum, HAMAMATSU R5509-73 PMT with C9940-02 cooler for NIR emission spectrum and luminescence lifetime). The excited state lifetime decay curves were obatained on an Edinburgh LifeSpec II picosecond time-resolved fluorescence spectrometer (260-1100 nm laser, 77-500K variable temperature, and MCP detector). All animal procedures were approved by the Institutional Animal Care and Use Committee of Sinoresearch (Beijing) Biotechnology Co., Ltd. (protocol number: 20211205)

Methods.

General procedures

General procedure 1 for *β*-fluoropyrrolyl-cysteine S_NAr chemistry between P_4 and peptides. **P_4** was dissolved in water to prepare a stock solution (100 mM). 500 μL Tris buffer (pH 8.0), **P_4** (5 μL, 100 mM), and corresponding peptide in H_2O or DMSO (2.5 μL, 50 mM) was successively added to a 1 mL centrifuge tube, and stirred for 15 min in dark. The reaction mixture was quenched by 5 μL trifluoroacetic acid (TFA). The crude mixture was analysed on analytical HPLC with **Method B** (ReproSil-Pur Basic-C18, 5 μm, 250 × 4.6 mm) and major peaks were identified by high resolution mass spectroscopy (HRMS). The yield of **P_4-a** was determined according to calibrated HPLC integral area using the formula:

$$\text{Yield } (\mathbf{P_4\text{-}a}) = \frac{4N(\mathbf{P_4\text{-}a})}{N(\mathbf{P_4\text{-}a})+N(\mathbf{P_4\text{-}2a})+N(\mathbf{P_4})}$$

N(**P_4**): final content of **P_4** (nM); N(**P_4-a**): final content of **P_4-a** (nM); N(**P_4-2a**): final content of **P_4-2a** (nM).

The product was isolated by reverse phase RP–HPLC system with **Method C** (ReproSil-Pur Basic-C18, 5 μm, 250 × 10 mm).

General procedure 2 for *β*-fluoropyrrolyl-cysteine S_NAr chemistry between *β*-octafluoroporphyrins ($P_{4\text{-}11}$) and glutathione (GSH). *β*-octafluoroporphyrin was dissolved in water to prepare a stock solution (100 mM). 500

μL Tris buffer (pH 8.0), *β*-octafluoroporphyrin (5 μL, 100 mM), and GSH in H_2O (2.5 μL, 50 mM) was successively added to a 1 mL centrifuge tube, and stirred for 15 min in dark. The reaction mixture was quenched by 5 μL TFA. The crude mixture was analysed on analytical HPLC with **Method B** (ReproSil-Pur Basic-C18, 5 μm, 250×4.6 mm) and major peaks were identified by HRMS. The yield was determined as described above.

The product was isolated by reverse phase RP–HPLC system with **Method C** (ReproSil-Pur Basic-C18, 5 μm, 250 ×10 mm).

Synthesis of substrates.

2,3,7,8,12,13,17,18-octafluoro-5,10,15,20-tetrakis[4-bromomethylphenyl]porphyrin

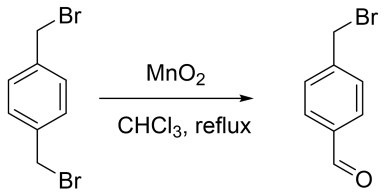

A solution of *p*-xylene dibromide (8 g, 30 mmol) and activated manganese dioxide (12 g, 140 mmol) in chloroform (300 mL) was refluxed for 3 days. The reaction mixture was filtered and washed with chloroform. The combined filtrates were evaporated and separated on silica gel using petroleum ether-dichloromethane (3:1) as eluent. The product (1.2 g, 20%) was obtained as a white solid.

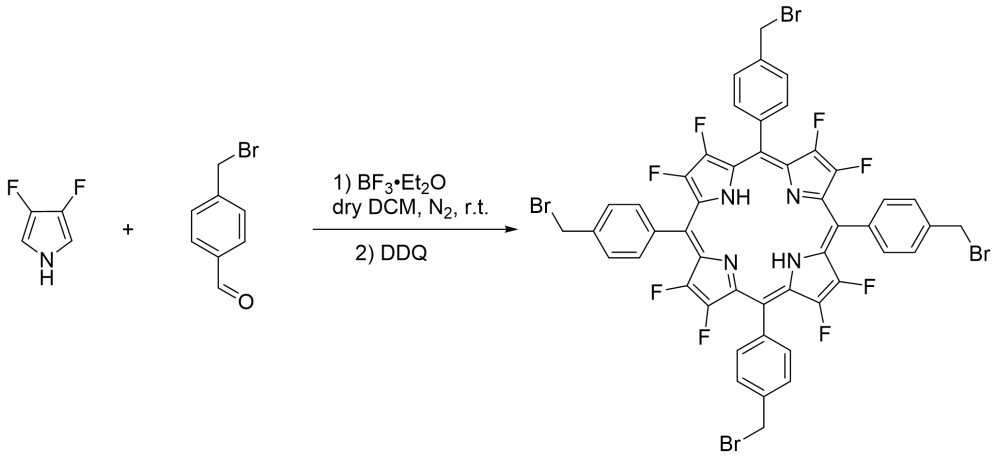

3,4-Difluoropyrrole (206 mg, 2.0 mmol) and 4-bromomethylbenzaldehyde (400 mg, 2.0 mmol) were dissolved in 400 mL anhydrous dichloromethane (DCM). The mixture was stirred for 5 min, then boron trifluoride etherate ($BF_3 \cdot Et_2O$) (100 μL) was added. The mixture was then stirred for 2 h at room temperature. 2,3-Dichloro-5,6-dicyano-1,4-benzoquinone (DDQ) (476 mg, 2.1 mmol) was added. After stirring for 2 h, the reaction mixture was transferred to a silica flash column and eluted by DCM. The obtained solution was evaporated *in vacuo* and isolated on silica gel column with petroleum ether/dichloromethane (v/v = 3:1) as eluent to give dark brown 2,3,7,8,12,13,17,18-octafluoro-5,10,15,20-tetrakis[4-bromomethylphenyl]porphyrin (150 mg, 66%). ^{1}H NMR (400 MHz, Chloroform-*d*) δ 8.01 (d, *J* = 8.0 Hz, 8H), 7.75 (d, *J* = 8.0 Hz, 8H), 4.80 (s, 8H), -4.18 (s, 2H). ^{19}F NMR (471 MHz, Chloroform-*d*) δ -140.03 (s, 4F), -145.14 (s, 4F). HRMS (MALDI-FTICR), $[M+H]^+$ calcd. For $[C_{48}H_{27}Br_4F_8N_4]^+$ 1126.8836; Found: 1126.8805.

2,3,7,8,12,13,17,18-Octafluoro-5,10,15,20-tetrakis(*α*-pyridinio-*p*-tolyl)porphyrin (P$_4$)

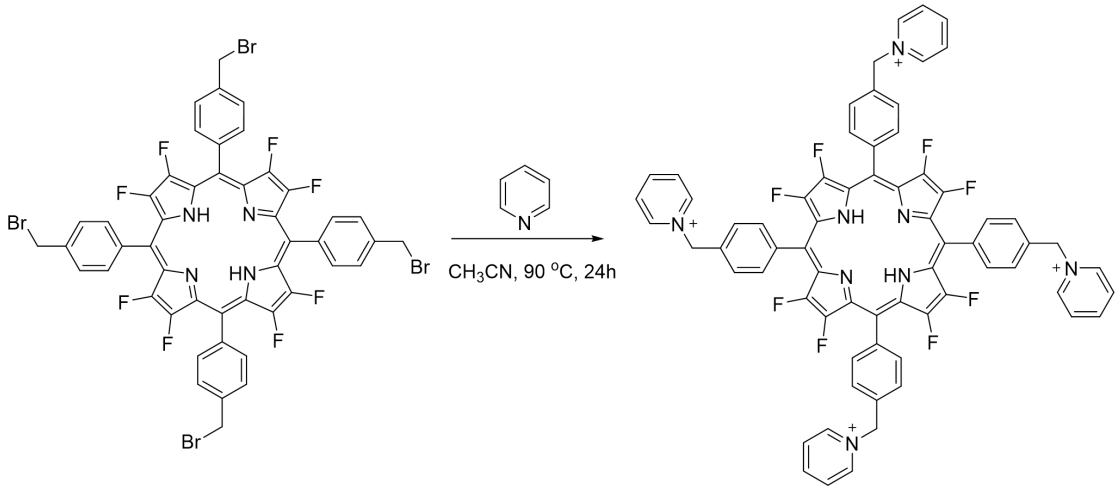

2,3,7,8,12,13,17,18-octafluoro-5,10,15,20-tetrakis[4-bromomethylphenyl]porphyrin (115 mg, 0.1 mmol), pyridine (79 mg, 1 mmol) was dissolved in 5 mL CH_3CN in a Schlenk tube and refluxed at 90 °C for 24 h. After cooling to room temperature, the reaction mixture was filtered and the solid residue was washed with DCM (5 mL × 3), acetone (5 mL × 3), hexane (5 mL × 3) to give crude product as dark solid. Furthermore, the crude compound was purified by RP-HPLC using **Method C** to give the desired compound **P$_4$** as a dark brown solid (82 mg, 73%). ^{1}H NMR (500 MHz, Methanol-d_4) δ 9.40 (d, J = 5.5 Hz, 4H), 8.81 (t, J = 7.9 Hz, 2H), 8.40 – 8.33 (m, 3H), 8.27 (d, J = 8.1 Hz, 3H), 7.96 (d, J = 8.1 Hz, 3H), 6.28 (s, 3H). ^{13}C NMR (126 MHz, Methanol-d_4) δ 146.32, 144.94, 138.60, 133.21, 128.66, 127.79, 64.33. ^{19}F NMR (471 MHz, Methanol-d_4) δ -142.89 (s, 4F), -148.50 (s, 4F). HRMS (ESI$^+$-FTICR) m/z [M^{4+}-H^+] calcd. for C68H45F8N8 375.1208 found: 375.1206; [M^{4+}] calcd. for C68H46F8N8 281.5924 found: 281.5922

2,3,7,8,12,13,17,18-Octafluoro-5,10,15,20-tetrakis(N, N', N''-trimethylamonium-*p*-tolyl)porphyrin (P$_5$)

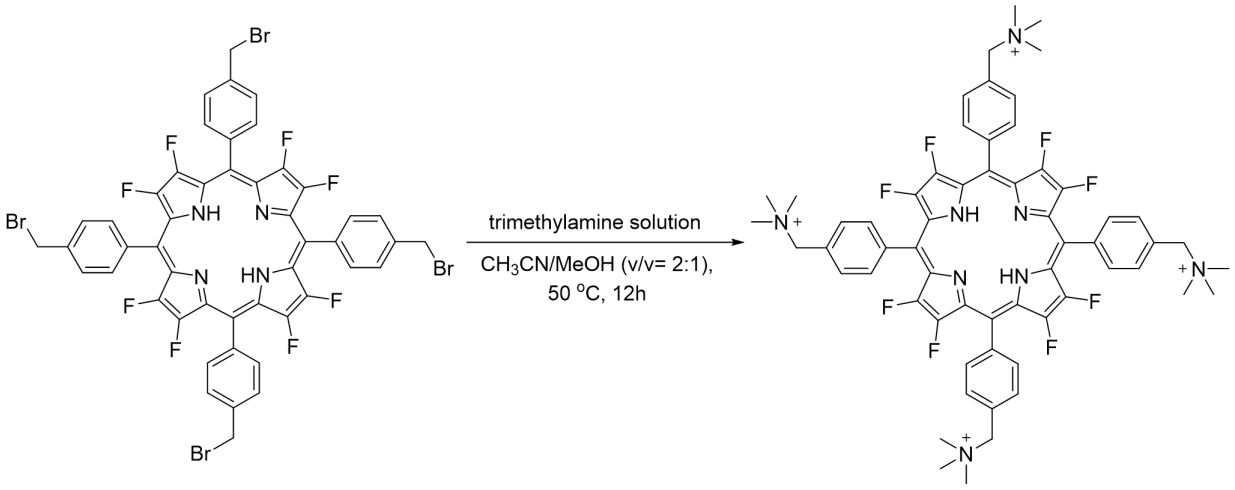

2,3,7,8,12,13,17,18-octafluoro-5,10,15,20-tetrakis[4-bromomethylphenyl]porphyrin (38 mg, 0.033 mmol), 33% trimethylamine ethanol solution (0.5 mL) was dissolved in CH_3CN/MeOH (3 mL, v/v = 2:1) in a Schlenk tube and

stirred at 50 °C for 12 h. After cooling to room temperature, the reaction mixture was evaporated *in vacuo* to give crude product as dark solid. Furthermore, the crude compound was purified by RP-HPLC using **Method C** to give the desired product **P_5** as dark brown solid (29 mg, 85%). ^{1}H NMR (400 MHz, Methanol-d_4) δ 8.37 (s, 8H), 8.05 (s, 8H), 4.94 (s, 8H), 3.37 (d, J = 5.8 Hz, 36H). ^{19}F NMR (471 MHz, Methanol-d_4) δ -142.81 (s, 4F), -148.37 (s, 4F). HRMS (ESI$^+$-FTICR) m/z [M^{4+}] calcd. for $C_{60}H_{62}F_8N_8^{4+}$ 261.6228 found: 261.6234.

2,3,7,8,12,13,17,18-Octafluoro-5,10,15,20-tetrakis(N-benzyl-2-hydroxy-N,N-dimethylethanammonium) porphyrin (P$_6$)

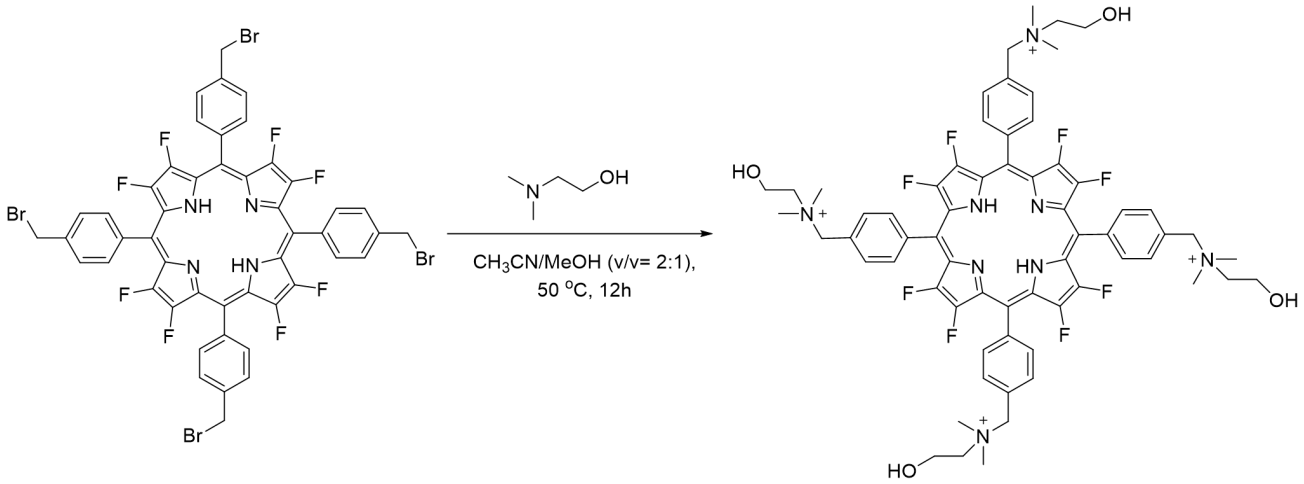

2,3,7,8,12,13,17,18-octafluoro-5,10,15,20-tetrakis[4-bromomethylphenyl]porphyrin (38 mg, 0.033 mmol), newly distilled 2-(N, N-dimethylamino)ethanol (1 mL) was dissolved in CH_3CN/MeOH (3 mL, v/v = 2:1) in a Schlenk tube and stirred at 50 °C for 12 h. After cooling to room temperature, the reaction mixture was evaporated *in vacuo* and the oily solid residue was purified by RP-HPLC using **Method C** to give the desired product compound **P_6** as a dark brown solid (25 mg, 65%). ^{1}H NMR (400 MHz, Methanol-d_4) δ 8.34 (d, J = 7.3 Hz, 8H), 8.06 (d, J = 7.4 Hz, 8H), 5.03 (s, 9H), 4.27 (s, 8H), 3.75 (s, 8H), 3.38 (s, 23H). ^{19}F NMR (471 MHz, Methanol-d_4) δ -142.77 (s, 4F), -148.33 (s, 4F). HRMS (ESI$^+$-FTICR) m/z [M^{4+}-H^+] calcd. for $C_{64}H_{69}F_8N_8O_4^{3+}$ 388.5099 found: 388.5103; [M^{4+}] calcd. for $C_{64}H_{70}F_8N_8O_4^{4+}$ 291.6343 found: 291.6338.

2,3,7,8,12,13,17,18-Octafluoro-5,10,15,20-tetrakis(benzyl-[2-(2-hydroxyethoxy)ethyl]-dimethylazanium) porphyrin (P$_7$)

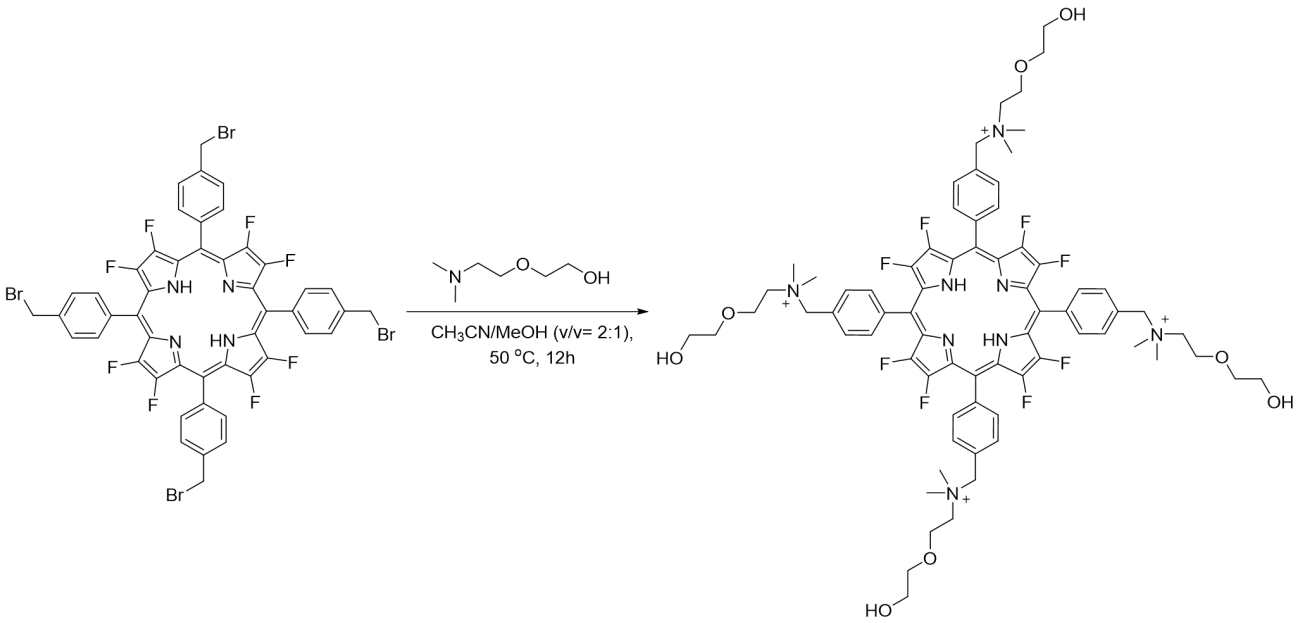

The synthetic procedure of **P$_7$** is similar to that of **P$_6$** by using corresponding newly distilled 1-O-dimethylaminoethyl-ethylenglykol.

2,3,7,8,12,13,17,18-octafluoro-5,10,15,20-tetrakis[4-bromomethylphenyl]porphyrin (38 mg, 0.033 mmol), newly distilled 1-O-dimethylaminoethyl-ethylenglykol (1 mL) was dissolved in CH_3CN/MeOH (3 mL, v/v = 2:1) in a Schlenk tube and stirred at 50 °C for 12 h. After cooling to room temperature, the reaction mixture was evaporated *in vacuo* and the oily solid residue was purified by RP-HPLC using **Method C** to give the desired product compound **P$_7$** as a dark brown solid (32 mg, 71%). ^{1}H NMR (400 MHz, Methanol-d_4) δ 8.31 (d, J = 8.2 Hz, 8H), 8.04 (d, J = 8.2 Hz, 8H), 5.00 (s, 8H), 4.17 (s, 8H), 3.86 – 3.79 (m, 16H), 3.76 – 3.71 (m, 8H), 3.35 (s, 24H). ^{19}F NMR (471 MHz, Methanol-d_4) δ -142.78 (s, 4F), -148.37 (s, 4F). HRMS (ESI$^+$-FTICR) m/z [M^{4+}] calcd. for $C_{72}H_{86}F_8N_8O_8^{4+}$ 335.6605 found: 335.6604; [M^{4+}-H^+] calcd. for $C_{72}H_{85}F_8N_8O_8^{3+}$ 447.2115 found: 447.2115; [M^{4+}-H^++CF_3COOH] calcd. for $C_{74}H_{86}F_{11}N_8O_{10}^{3+}$ 485.2092 found: 485.2093.

2,3,7,8,12,13,17,18-Octafluoro-5,10,15,20-tetrakis(benzyldimethyl(2-propynyl)ammonium)porphyrin (P$_8$)

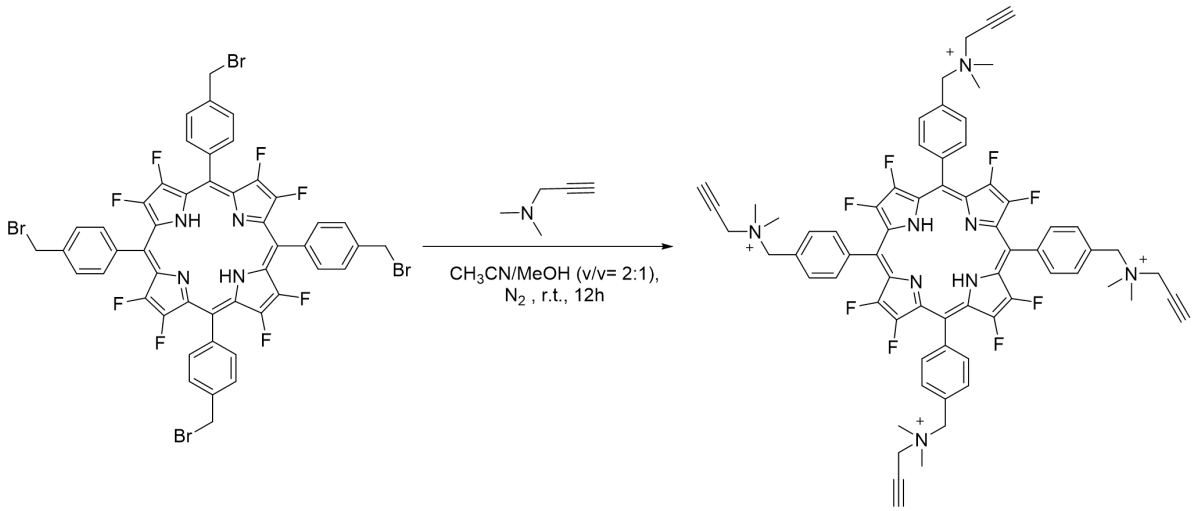

2,3,7,8,12,13,17,18-octafluoro-5,10,15,20-tetrakis[4-bromomethylphenyl]porphyrin (38 mg, 0.033 mmol), newly distilled N,N-Dimethylpropargylamine (1 mL) was dissolved in CH_3CN/MeOH (3 mL, v/v = 2:1) in a Schlenk tube. The reaction mixture was degassed at -78 ^oC and flushed with nitrogen for three times. After stirring at room temperature for 12 h, the reaction mixture was evaporated *in vacuo* and the dark brown solid residue was purified by RP-HPLC using **Method C** to give the desired product compound **P$_8$** as a dark brown solid (18 mg, 47%). **P$_8$** was stored in -20 ^oC refrigerator for following experiments. ^{1}H NMR (400 MHz, Methanol-*d*$_4$) δ 8.40 (d, *J* = 7.9 Hz, 8H), 8.11 (d, *J* = 8.0 Hz, 8H), 5.06 (s, 8H), 4.54 (s, 8H), 3.84 (s, 4H), 3.45 (s, 24H). ^{19}F NMR (471 MHz, Methanol-*d*$_4$) δ -142.80 (s, 4F), -148.36(s, 4F). HRMS (ESI$^+$-FTICR) m/z [M^{4+}] calcd. for $C_{66}H_{62}F_8N_8^{4+}$ 285.6237 found: 285.6233; [M^{4+}-H^+] calcd. for $C_{66}H_{61}F_8N_8^{3+}$ 380.4958 found: 380.4959.

2,3,7,8,12,13,17,18-Octafluoro-5,10,15,20-tetrakis(benzyldimethyl(2-azido)ammonium)porphyrin (P$_9$)

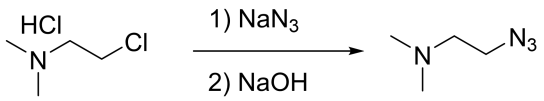

2-chloro-N,N-dimethylethylamine hydrochloride (1.4 g, 10.0 mmol) was dissolved in deionized water (40 mL), and then add sodium azide (1.9 g, 30.0 mmol). The mixture was stirred at 80 °C for 24 h. The reaction mixture was cooled to room temperature, the pH of the solution was adjusted to 10 using 1M NaOH solution, and extracted with dichloromethane for three times. Organic layer was collected and dried with anhydrous Na_2SO_4. Finally, extract was evaporated *in vacuo* to give 2-azido-N, N-dimethylethan-1-amine as a colorless oil (0.98 g, 85 %). ^{1}H NMR (400 MHz, Chloroform-*d*) δ 3.31 (t, *J* = 6.1 Hz, 1H), 2.46 (t, *J* = 7.0 Hz, 1H), 2.23 (s, 3H). HRMS (ESI$^+$-FTICR) m/z [M+H] $^+$ calcd. for $C_4H_{11}N_4^+$ 115.0978 found: 115.0978.

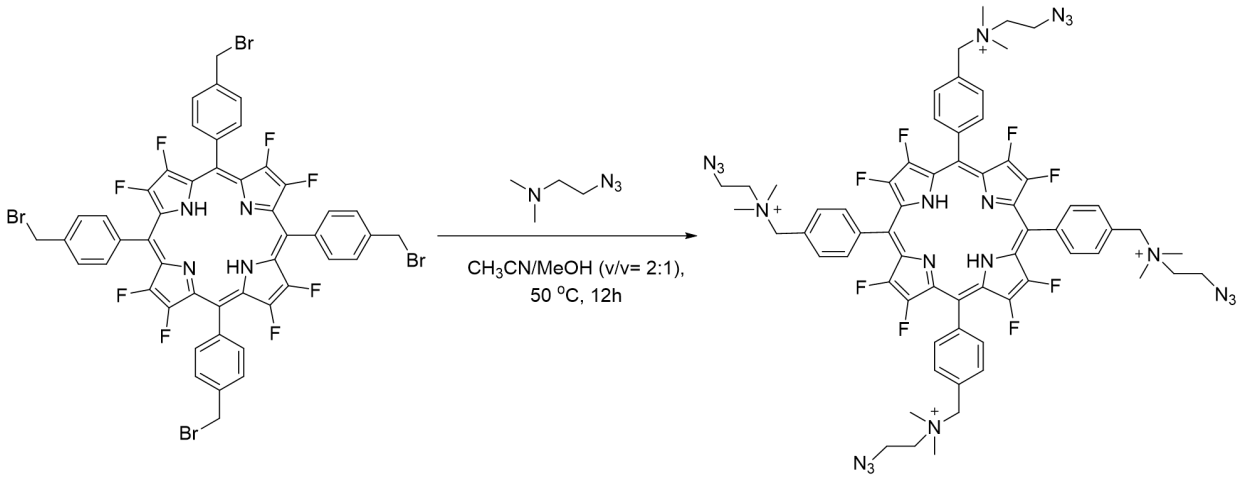

2,3,7,8,12,13,17,18-octafluoro-5,10,15,20-tetrakis[4-bromomethylphenyl]porphyrin (38 mg, 0.033 mmol), newly distilled 2-azido-N,N-dimethylethan-1-amine (0.2 mL) was dissolved in CH_3CN/MeOH (3 mL, v/v = 2:1) in a Schlenk tube. The reaction mixture was stirred at 50 °C for 6 h, then the solution was evaporated *in vacuo* and the dark brown solid residue was purified by RP-HPLC using **Method C** to give the desired product compound **P_9** as dark brown solid (21 mg, 51%). ^{1}H NMR (400 MHz, Methanol-d_4) δ 8.32 (d, J = 7.7 Hz, 8H), 8.01 (d, J = 7.8 Hz, 8H), 4.95 (s, 8H), 4.19 (t, J = 5.0 Hz, 8H), 3.86 – 3.73 (m, 8H), 3.32 (s, 24H). ^{19}F NMR (471 MHz, Methanol-d_4) δ -142.70 (s, 4F), -148.29 (s, 4F). HRMS (ESI$^+$-FTICR) m/z [M^{4+}] calcd. for $C_{64}H_{66}F_8N_{20}^{4+}$ 316.6407 found: 316.6405; [M^{4+}-H^+] calcd. for $C_{64}H_{65}F_8N_{20}^{3+}$ 421.8519 found: 421.8524.

2,3,7,8,12,13,17,18-Octafluoro-5,10,15,20-tetrakis(benzyltrimethyl phosphonium)porphyrin (P_{10})

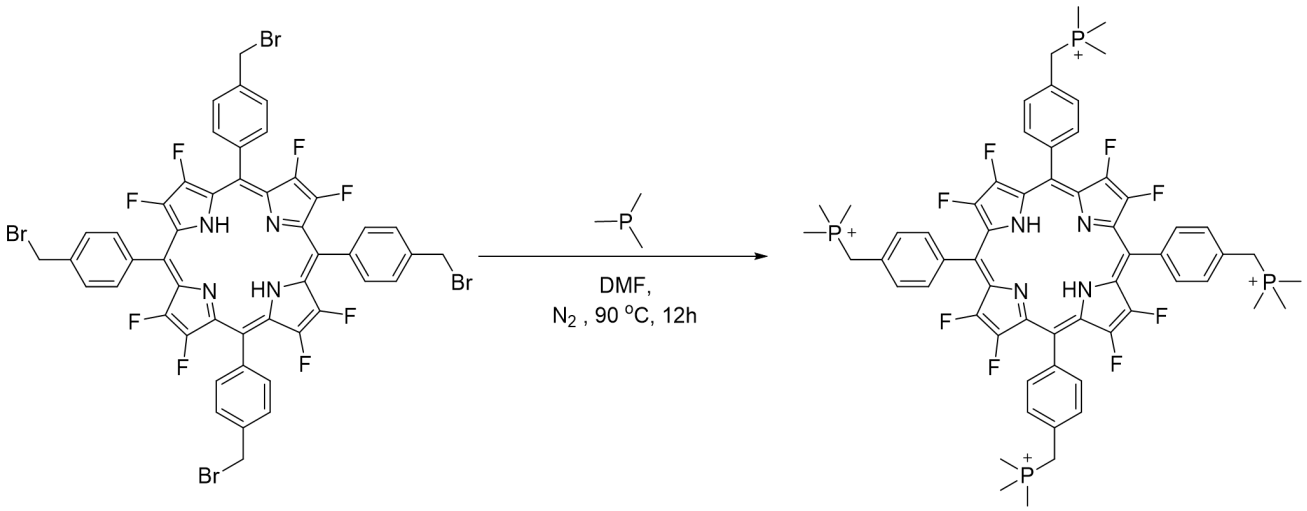

2,3,7,8,12,13,17,18-octafluoro-5,10,15,20-tetrakis[4-bromomethylphenyl]porphyrin (38 mg, 0.033 mmol), newly distilled trimethylphosphane (1 mL) was dissolved in N, N-dimethylformamide (DMF) in a Schlenk tube. The reaction mixture was degassed at -78 °C and flushed with nitrogen for three times. After stirring at 90 °C for 12 h, the solvent was distilled *in vacuo* and the dark brown solid residue was purified by RP-HPLC using **Method C** to

give the desired product compound **P_{10}** as dark brown solid (27 mg, 74%). ^{1}H NMR (400 MHz, Methanol-d_4) δ 8.24 (d, J = 7.7 Hz, 8H), 7.78 (d, J = 10.7 Hz, 8H), 4.11 (d, J = 16.2 Hz, 8H), 2.06 (d, J = 14.3 Hz, 36H). ^{19}F NMR (565 MHz, Methanol-d_4) δ -143.18 (s, 4F), -148.73 (s, 4F). HRMS (ESI$^+$-FTICR) m/z [M^{4+}] calcd. for $C_{60}H_{62}F_8N_4P_4^{4+}$ 278.5944 found: 278.5944; [M^{4+}-H^+] calcd. for $C_{60}H_{62}F_8N_4P_4^{3+}$ 371.1234 found: 371.1244.

2,3,7,8,12,13,17,18-2,3,7,8,12,13,17,18-Octafluoro-5,10,15,20-tetrakis(benzyldimethylsulfonium)porphyrin (P$_{11}$)

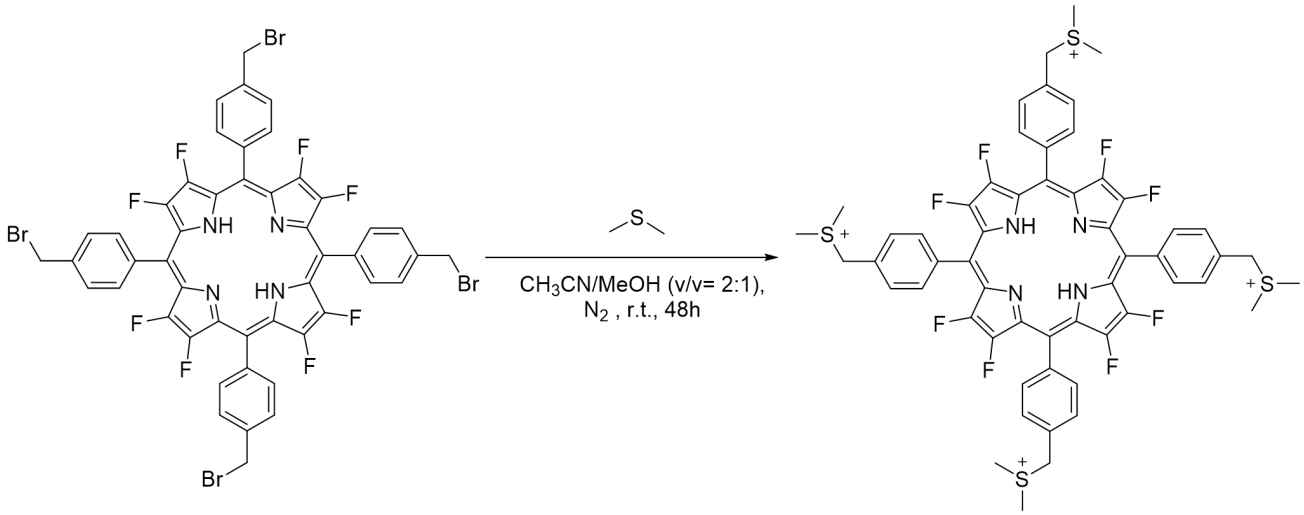

2,3,7,8,12,13,17,18-octafluoro-5,10,15,20-tetrakis[4-bromomethylphenyl]porphyrin (38 mg, 0.033 mmol), dimethylsulfane (1 mL) was dissolved in CH_3CN/MeOH (3 mL, v/v = 2:1) in a Schlenk tube. The reaction mixture was degassed at -78 ^{o}C and flushed with nitrogen for three times. After stirring at room temperature for 48 h, the solvent was distilled *in vacuo* and the dark brown solid residue was purified by RP-HPLC using **Method C** to give the desired product compound **P_{11}** as a dark brown solid (16 mg, 46%). ^{1}H NMR (400 MHz, Methanol-d_4) δ 8.28 (d, J = 8.1 Hz, 8H), 7.90 (d, J = 8.1 Hz, 8H), 4.97 (s, 8H), 3.03 (s, 24H). ^{19}F NMR (471 MHz, Methanol-d_4) δ -142.94 (s, 4F), -148.52 (s, 4F). HRMS (ESI$^+$-FTICR) m/z [M^{4+}] calcd. for $C_{56}H_{50}F_8N_4S_4^{4+}$ 264.5692 found: 264.5688.

2,3,7,8,12,13,17,18-Octafluoro-5,10,15,20-tetrakis(3-(2-[2-(2-methoxy-ethoxy)-ethoxy]-ethoxy)-phenyl) porphyrin (P$_{12}$)

3-(2-[2-(2-methoxy-ethoxy)-ethoxy]-ethoxy)-benzaldehyde

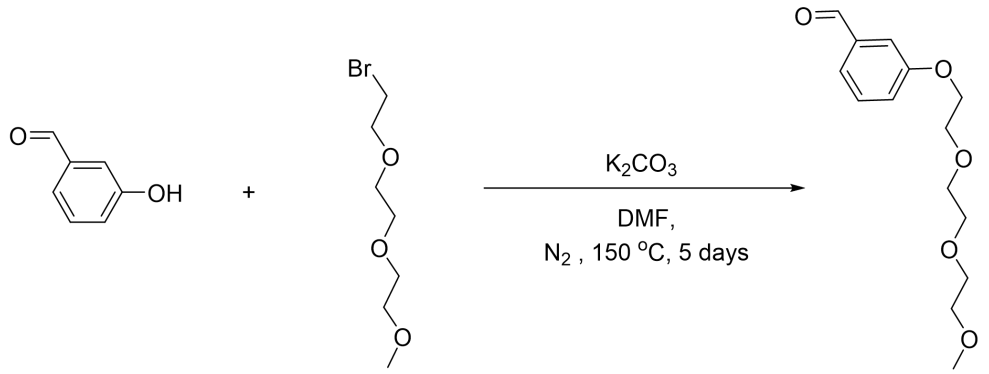

3-hydroxybenzaldehyde (1.22 g, 10 mmol), 1-bromo-2-(2-(2-methoxyethoxy)ethoxy)ethane (3.4 g, 15 mmol), and K_2CO_3 (4.14 g, 30 mmol) were mixed in DMF (20 mL). The reaction mixture was degassed at -78 °C and flushed with nitrogen for three times, then refluxing at 150 °C for 5 days. After cooling to room temperature, the solvent was distilled *in vacuo* to give crude product 3-(2-[2-(2-methoxy-ethoxy)-ethoxy]-ethoxy)-benzaldehyde as the faint yellow oil. Furthermore, it was purified using reversed phase column with MeOH/H_2O (v/v from 20%/80%-60%/40%) on Biotage Isolera Prime (1.9 g, 72%). ^{1}H NMR (400 MHz, Chloroform-*d*) δ 9.97 (s, 1H), 7.44 (s, 2H), 7.41 (s, 1H), 7.21 (d, J = 7.2 Hz, 1H), 4.20 (s, 2H), 3.89 (s, 2H), 3.75 (s, 2H), 3.68 (d, J = 16.9 Hz, 4H), 3.56 (s, 2H), 3.38 (s, 3H). HRMS (ESI$^+$-FTICR) m/z [M+Na$^+$] calcd. for C14H20NaO5$^+$ 291.1203 found: 291.1196.

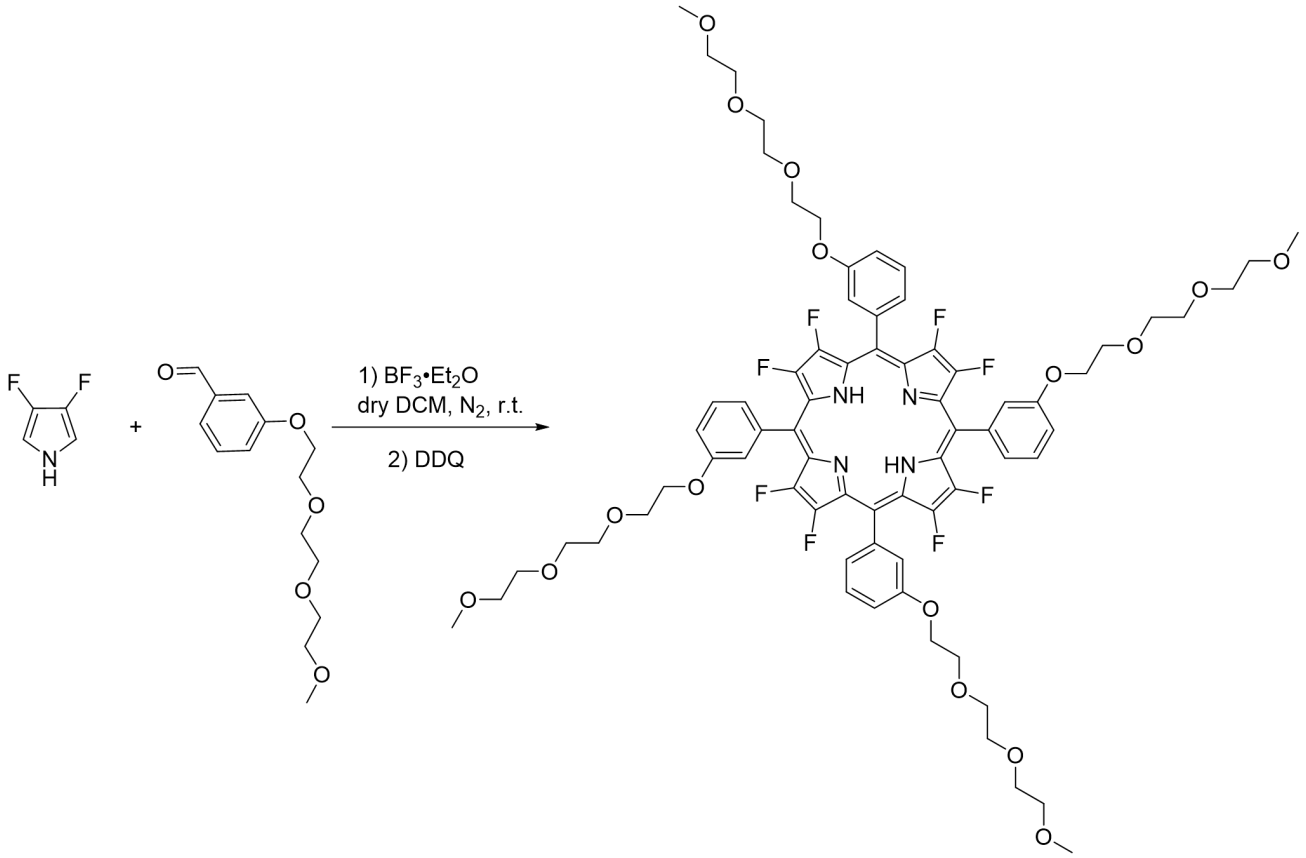

3,4-Difluoropyrrole (206 mg, 2.0 mmol) and 3-(2-[2-(2-methoxy-ethoxy)-ethoxy]-ethoxy)-benzaldehyde (540 mg,

2.0 mmol) were dissolved in 400 mL anhydrous dichloromethane (DCM). The mixture was stirred for 5 min after which, boron trifluoride etherate ($BF_3 \cdot Et_2O$) (100 μL) was added. The mixture was then stirred for 12 h at room temperature. 2,3-Dichloro-5,6-dicyano-1,4-benzoquinone (DDQ) (475 mg, 2.1 mmol) was added. After reacting for 2 h , the reaction mixture was transferred to a silica flash column and eluted by ethyl acetate. The obtained solution was evaporated *in vacuo* and isolated on silica gel column with petroleum ether/ethyl acetate (v/v, 90%/10%-1%/99%) as eluent on Biotage Isolera Prime to give dark brown **P_{12}** (81 mg, 29%). ^{1}H NMR (400 MHz, Chloroform-*d*) δ 7.63 (s, 12H), 7.35 (s, 4H), 4.32 (s, 8H), 3.94 (s, 8H), 3.78 (s, 8H), 3.69 (s, 8H), 3.64 (s, 8H), 3.51 (s, 8H), 3.33 (s, 12H), -4.23 (s, 2H). ^{19}F NMR (471 MHz, Chloroform-*d*) δ -140.26 (s, 4F), -145.29 (s, 4F). HRMS (ESI$^+$-FTICR) m/z [M+H$^+$] calcd. for $C_{72}H_{79}F_8N_4O_{16}^+$ 1407.5358 found: 1407.5340; [M+H$^+$+NH$_4^+$] calcd. for $C_{72}H_{83}F_8N_5O_{16}^{2+}$ 712.7848 found: 712.7851.

2,3,7,8,12,13,17,18-Octafluoro-5,10,15,20-tetrakis(2,6-difluorophenyl)porphyrin

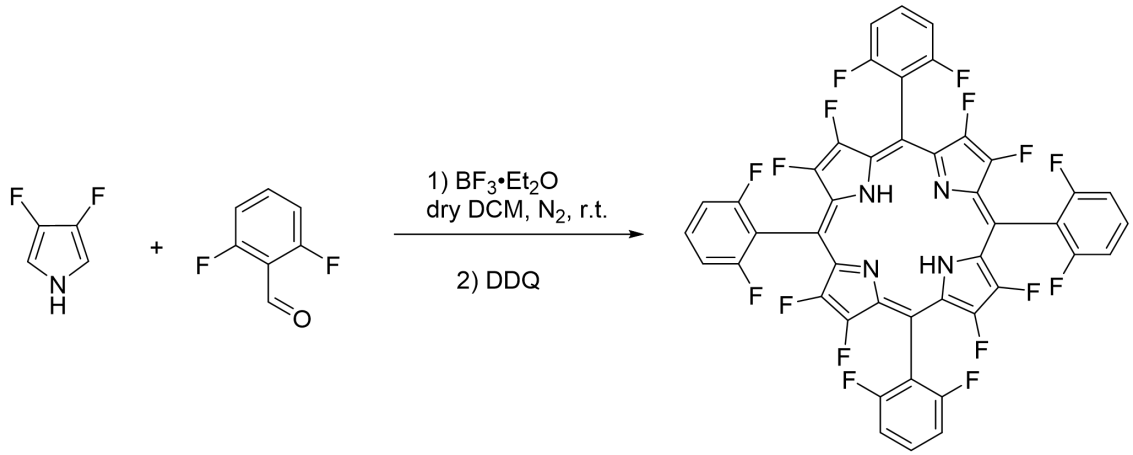

3,4-Difluoropyrrole (206 mg, 2 mmol), 2,6-difluorobenzaldehyde (285 mg, 2 mmol), and anhydrous DCM (300 mL) were mixed under N_2 in a 500 mL round-bottom flask. Boron trifluoride etherate ($BF_3 \cdot Et_2O$) (200 μL) was dropped slowly into the mixture and the resulting solution was stirred for 2 h. Then, DDQ (400 mg, 2 mmol) was added. The reaction mixture was stirred overnight and eluted through a flash silica gel column with DCM/petroleum ether (v/v = 1:5). The solvent was removed under reduced pressure, and the crude product was chromatographed through a silica gel column with DCM/petroleum ether (v/v, 1:50) to give desired product 2,3,7,8,12,13,17,18-octafluoro-5,10,15,20-tetrakis(2,6-difluorophenyl)porphyrin (80 mg, 44%) as dark brown solid. ^{1}H NMR (400 MHz, Chloroform-*d*) δ 7.78 (p, *J* = 7.4 Hz, 4H), 7.34 (t, *J* = 7.5 Hz, 8H), -4.13 (s, 2H). ^{19}F NMR (471 MHz, Chloroform-*d*) δ -110.62 (s, 8F), -144.31 (s, 4F), -149.60 (s, 4F). HRMS (ESI$^+$-FTICR) m/z [M+H$^+$] calcd. for $C_{44}H_{15}F_{16}N_4$, [M+H$^+$]: 903.1036; Found: 903.1036.

2,3,7,8,12,13,17,18-Octafluoro-5,10,15,20-tetrakis(3-sulfonato-2,6-difluorophenyl)porphyrin (P_{13})

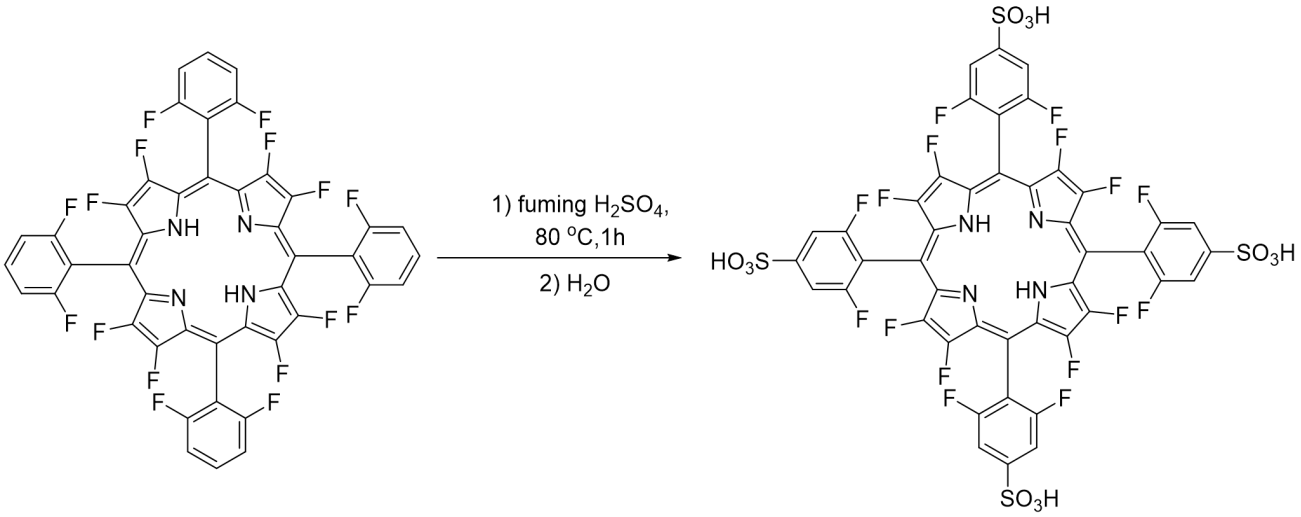

2,3,7,8,12,13,17,18-Octafluoro-5,10,15,20-tetrakis(2,6-difluorophenyl)porphyrin was dissolved (50 mg, 0.055 mmol) in fuming H_2SO_4 (18-20% free SO_3, 1 mL) and heated at 80 °C for 1 h. The mixture was cooled to room temperature before carefully adding H_2O (20 mL). After neutralization with 1 M NaOH aqueous solution, the solvent was removed *in vacuo*. Followingly, the remaining solid was dissolved in CH_3OH and filtered to remove excessive Na_2SO_4. The desired product **P_{13}** (54 mg, 80%) was precipitated from CH_3OH by adding anhydrous diethyl ether into the solution. ^{1}H NMR (400 MHz, Methanol-*d*$_4$) δ 8.40 (q, *J*=8.3, 4H), 7.54 (tt, *J*=8.1, 3.1, 4H). ^{19}F NMR (471 MHz, Methanol-*d*$_4$) δ -108.67 (br, 4F), -109.30 – -109.50 (m, 4F), -146.43 (s, 4F), -151.59 (s, 4F). HRMS (ESI-FTICR), [M-3H] $^{3-}$ calcd. For $[C_{44}H_{11}F_{16}N_4O_{12}S_4]^{3-}$ 406.4006; Found: 406.3007; [M-4H] $^{4-}$ calcd. for $[C_{44}H_{10}F_{16}N_4O_{12}S_4]^{4-}$ 304.4736; Found: 304.4739.

Computational details. In this work, we performed geometry optimizations for ground (S_0) and excited states (S_1, T_1-T_4) followed by harmonic vibrational frequencies calculation with hybrid density functional, B3LYP[4] with "D3BJ"[5] dispersion corrections, using the program package Gaussian 09 (Revision E.01). [4,5,6] The 6-311G(d) basis set[5,6] was used for all atoms. Solvent effects (including the geometry optimizations and frequencies) were considered by means of SMD[7,8,9] model for dichloromethane to match the experimental conditions. Frequency calculations were performed on the optimized structures to ensure that they were in minimum energy structures by the absence of imaginary frequency. Stability calculations were also performed for all the optimized structures to ensure that all the wavefunctions were stable.

The spin-orbit coupling (SOC) constants between the spin states of S_1 and T_n, $\langle T_n|\hat{H}|S_1\rangle$, were estimated using effective atomic charge (Zeff) method by PySOC[8,9] following the guidance in http://sobereva.com/411. The intersystem crossing rate constants (k_{ISC}s) were calculated by MOMAP program package[10-14] using a thermal vibration correlation function formalism for the transition between two adiabatic electronic states considering displacements, distortions, and Duschinsky rotations of potential energy surfaces within the framework of multidimensional harmonic oscillator model and Franck-Condon principle.

Reaction rate. For the kinetic study, compound **P4** (1 mM, 1.126 mg/mL in ultrapure water stock solution) and GSH (1 mM, 0.307 mg/mL in ultrapure water stock solution) were reacted in 1000 μL Tris buffer (pH 8.0) at room temperature. At certain time point (e. g. 1 min, 3 min, 5 min, 7 min, 9 min, 11 min, 13 min, 15 min, 20 min, 25 min, 30 min, 35 min, 40 min, 45 min, 50 min, 55 min, 60 min, 70 min, and 80 min), 20 μL of reaction mixture was withdrawn and immediately quenched by 1 μL trifluoroacetic acid. After that, the mixture was frozen before injecting to analytical HPLC. HPLC analysis clearly indicated that the peak for compound **P4** gradually decreased while the peak for conjugates increased. The quantification was obtained based on the calibrated integration of the absorbance peak of compound **P4** and conjugates at 395 nm, which correspond to the conversion during the reaction progress.

The rate constant *k* of the reaction between compound **P4** and GSH was obtained based on the second-order reaction kinetics. The rate constant *k* was determined by the following formula:

$$\frac{1}{[A]} = \frac{1}{[A_0]} + kt$$

[A]: real-time concentration of **P4**, [A_0]: initial concentration of compound **P4** (1 mM), *k*: rate constant

Based on the HPLC analysis, $\frac{1}{[A]}$ over time was linearly-plotted which is shown in **Figure S12** and the slope is the rate constant (1.44 $\mathbf{M^{-1} \cdot s^{-1}}$).

P_{12} reacted with GSH. **P_{12}** was dissolved in dimethylsulfoxide (DMSO) to prepare a stock solution (100 mM). 242.5 μL Tris buffer (pH 8.0), 250 μL DMSO, **P_{12}** (5 μL, 100 mM), and GSH in H_2O (2.5 μL, 50 mM) was successively added to a 1 mL centrifuge tube, and stirred for 15 min in dark. After that, the reaction mixture was quenched by 5 μL TFA. The crude mixture was analysed on analytical HPLC with **Method D** (ReproSil-Pur Basic-C18, 5 μm, 250×4.6 mm) and major peaks were identified by HRMS.

P_{13} reacted with GSH. **P_{13}** was dissolved in H_2O to prepare a stock solution (100 mM). 490 μL Tris buffer (pH 8.0), **P_{13}** (5 μL, 100 mM), and GSH in H_2O (5 μL, 200 mM) was successively added to a 1 mL centrifuge tube, and stirred for 15 min in dark. After that, the reaction mixture was quenched by 5 μL TFA. The crude mixture was analysed by UV-vis spectrometer and HRMS, respectively.

Click chemistry.

Strain-promoted azide-alkyne cycloaddition (SPAAC) between *β*-peptidyl azido-porphyrin (**P_9-a**) and dibenzocyclooctyne reagent (**h**/**i**/**j**).

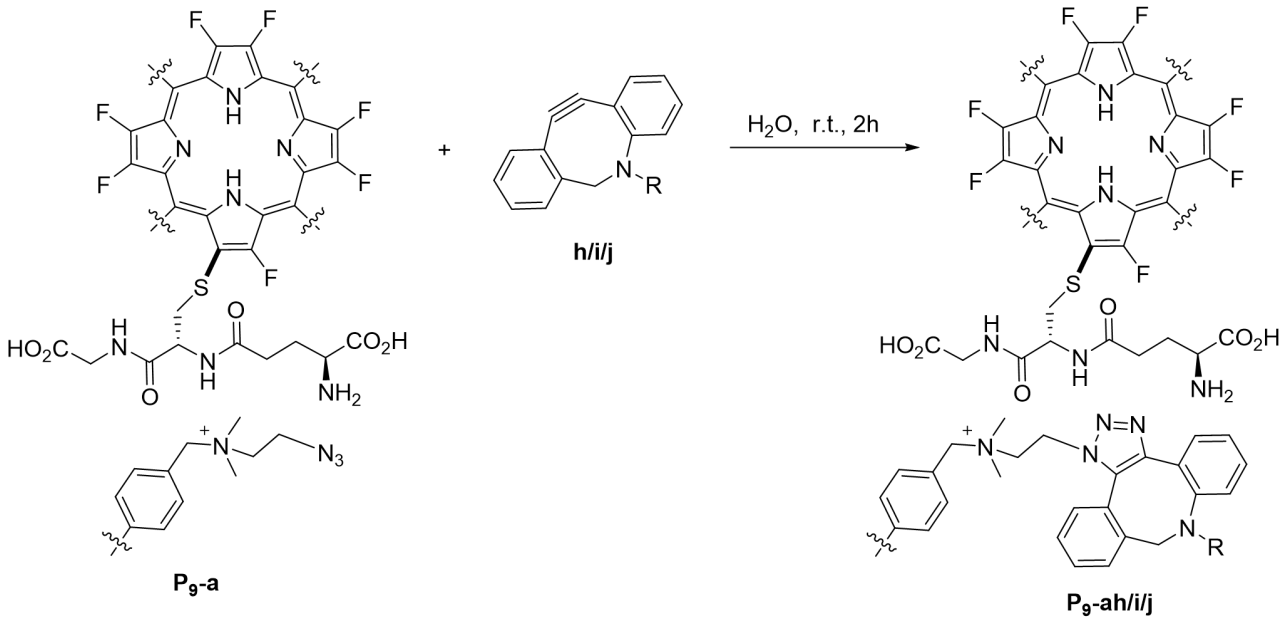

In a 0.2 mL centrifuge tube, *β*-peptidyl azido-porphyrin (**P_9-a**) in H_2O (1.00 μL, 20.0 mM) and dibenzocyclooctyne reagent (**h/i/j**) in DMSO (1.1 μL, 80 mM, 4.4 equiv.) were combined. The resulting mixture was stirring for 30 minutes at room temperature. After that, the reaction mixture was diluted with H_2O (17.9 μL) and analyzed by HPLC. The desired products **P_9-ah/i/j** were confirmed by HRMS (ESI^+-FTICR).

Protein bioconjugation.

P_4/**P_8**/**P_{13}** (0.5 μL, 100 mM), protein (5 μL, 0.5 mM in 1×PBS), and NaCl (10 μL, 5 M) were mixed in a Tris buffer (34.5 μL, pH 8.0) and reacted at room temperature for 8 h. After that, the solution was desalted by passing through

Bio-Rad desalting column (10 K) to give corresponding protein conjugate, respectively. The protein conjugate was analyzed by MALDI-TOF and SDS-PAGE gel (in gel fluorescence and coomassie brilliant blue staining).

Streptavidin (Sav, 5 μL, 10 mg/mL in 1×PBS), 2-iminothiolane hydrochloride (Traut's reagent, 0.42 μL, 20 mM in H_2O) were mixed in Tris buffer (44.6 μL, pH 8.0). The mixture was incubated at 25 °C for 60 min before removing all the unreacted Traut's reagent by passing through Bio-Rad desalting column (10 K). The obtained solution was mixed with **P_{13}** (0.42 μL, 20 mM in H_2O), incubated at 4 °C overnight, and then desalted. MALDI-TOF indicated a complete conversion of Sav into **P_{13}-Sav**.

EGFP (5 μL, 0.5 mM 1×PBS), and iodoacetamide (**IAA**, 0.63 μL, 20 mM in H_2O) were mixed in Tris buffer (44.4 μL, pH 8.0) and reacted at room temperature for 1 h. After that, the solution was desalted to give **IAA-EGFP**.

Synthesis of P_{13}-EGFP-PDS and IAA-EGFP-PDS. The neutralized stock lipoic acid (LA) solution with a final concentration of 100 mM was prepared by dissolving lipoic acid (206.33 mg, 1.0 mmol) with stoichiometric NaOH in an aqueous solution (0.1 M in 10 mL). The pH of the LA solution was then carefully adjusted to 7.0. Next, EGFP solution (2 μL, 25 mg/mL) was added to the freshly prepared LA solution (48 μL, 100 mM) and the mixture was incubated at -30 ℃ for 2 h. The reaction was quenched with **P_{13}** or **IAA** (10 μL, 100 mM in H_2O) at room temperature for 30 min. The result was evidenced by non-reducing (DTT free) SDS-PAGE gel analysis (Coomassie brilliant blue staining).

Metabolic labeling of Sialoglycoproteins. For O-GlcNAc labeling, HeLa cells were incubated with 50 μM Ac_4ManNAz for 48 h. The cells were fixed with 4% (w/v) formaldehyde in 1×PBS for 15 min, washed three times with 1 × PBS. After three washes with 1 × PBS, the cells were incubated with 50 μ M biotin-PEG4-alkynyl, THPTA-$CuSO_4$ complex (50 μM $CuSO_4$, THPTA/$CuSO_4$ 6:1, mol/mol) and 2.5 mM sodium ascorbate in PBS at room temperature for 30 min, followed by three washes with 0.1% (v/v) Tween 20 in 1×PBS. The cells were then incubated with 5 μg/ml **P_{13}-Sav** in 1×PBS containing 1% (w/v) BSA for 1 h and washed three times with PBS for confocal microscopy.

Measurement of $^1O_2$ generation efficiency. The singlet oxygen generated by compound **P_4**, **P_4-a**, and **P_4-2a** were measured using 1, 3-diphenylisobenzofuran (DPBF). The relative quantum yields were calculated with that of the standard reference (tetraphenylporphyrin, TPP) in toluene. Briefly, an oxygen-saturated solution of photosensitizer containing 4 μ M DPBF was prepared in the dark. Then, the cuvette was irradiated with a 405 nm laser at 5 mW/cm^2 for 60 s. Φ_Δ was calculated by the following equation:

$$\Phi_{\Delta sam} = \Phi_{\Delta std} \frac{k_{sam}}{k_{std}} \frac{F_{std}}{F_{sam}}$$

Where "*sam*" and "*std*" represent the "complex" and "TPP", respectively. "*k*" is the slope of absorbance change curve of DPBF at 415 nm, $F=1-10^{-OD}$ (OD is the absorbance of the solution at 405 nm).

Cytotoxicity evaluation *in vitro*. CCK-8 assay was carried out to evaluate the dark toxicity and phototoxicity of compound **P_4**, **P_4-a**, and **P_4-2a**. HeLa cells were seeded into 96-well plates at the density of 1×10^4 per well and incubated at 37 °C for 24 h. After removal of the medium and rinsing with PBS, HeLa cells were pretreated with compound **P_4**, **P_4-a**, and **P_4-2a** (final concentration contains 0, 0.25, 0.5, 1, 2 or 4 μM), respectively. One plate was kept in the dark for studying dark toxicity, and another plate was irradiated using the 400-700 nm laser at a power of 10 mW cm^{-2} for 10 min. All group cells were incubated for another 24 h, the cell viability was detected by added of Cell Counting Kit-8 (CCK-8, 10 μL), and the absorbance at a wavelength of 450 nm of each well was measured using a 96-well plate reader. The cell viability was then determined *via* the following equation: cell viability (%) = (mean of abs. value of treatment group/mean abs. value of control) × 100%.

Cellular internalization measured by confocal laser scanning microscopy (CLSM). HeLa cells were seeded in a cell culture chamber and incubated for 24 h at 37 °C in 5% CO_2 before the experiment. After medium aspiration, the cells were incubated with EGFP (250 nM × 200 μL) or **P_{13}-EGFP** (250 nM × 200 μL) or **P_{13}-EGFP-PDS** (250 nM × 200 μL) for 1 h at 37 °C before three 1×PBS washes. Next, HeLa cells were fixed with 4% PFA, then co-stained with Hoechst 33258 for 5 min, washed and reintroduced with PBS buffer (1×, pH = 7.4) and imaged with CLSM.

Enzymatic assay of caspase-3 in solutions. The enzymatic assays were first carried out with a recombinant caspase-3 solution. The mixtures of the probe (**P_4-k**, 10 μM) and caspase-3 (150 ng/mL) were incubated in PBS buffer (1×, pH = 7.4) at 37 °C in a centrifuge tube for 1 h. Then, the reaction solution was transferred to a cuvette with 1 cm optical length for fluorescence measurements excited by 470 nm. In the meantime, the blank solution without caspase-3 and the inhibition solution with caspase-3 inhibitor (5-[(S)-(+)-2-(methoxymethyl)pyrrolidino] sulfonylisatin, 5 μM) was also measured under the same condition for comparison.

Fluorescence imaging of caspase-3 in live HeLa cells. **P_4-k** was diluted with DMEM to work concentration (10 μM). For untreated HeLa cells, probe solution (**P_4-k**) was added to the chamber and incubating at 37 °C for 1 h, then washed twice with PBS buffer (1×, pH = 7.4), and kept in fresh FBS-free DMEM for observation under a microscope. For apoptotic cells, the cells were first treated with 3 μM apoptosis inducer STS for 1 h. After washing twice with PBS buffer (1×, pH = 7.4), probe solution (**P_4-k**) was added and incubated at 37 °C for 1 h. After washing twice with PBS buffer (1×, pH = 7.4), the STS-treated cells were kept in fresh FBS-free DMEM for

observation under a microscope. For apoptotic inhibited cells, the cells were first incubated with 3 μM apoptosis inducer STS and 5 μM apoptosis inhibitor (5-[(S)-(+)-2-(methoxymethyl)pyrrolidino] sulfonylisatin) for 2 h. After washing twice with PBS buffer (1×, pH = 7.4), probe solution (**P_4-k**) was added and incubated at 37 °C for 1 h. After washing twice with PBS buffer (1×, pH = 7.4), the STS-treated cells were kept in fresh FBS-free DMEM for observation under a microscope. Confocal fluorescence microscopy of live cells was performed using an ISS Alba5 FLIM/FFS confocal system equipped with a Nikon TE2000 inverted microscope, and a 488 nm laser using the Semrock 525/50 nm band pass filters.

Fluorescence imaging of A549/MCF7. For A549, **P_4** or **P_4-a** or **P_4-f** was diluted with DMEM to work concentration (8 μM). For untreated A549 cells, probe solution (**P_4** or **P_4-a** or **P_4-f**) was added to the chamber and incubating at 37 °C for 30 min, the cells were washed twice with PBS buffer (1×, pH = 7.4) and kept in fresh FBS-free DMEM for observation under a microscope. For iRGD inhibited group, cells were incubated with iRGD (20 μM) for 1 h, then incubated with **P_4-f** (8 μM) at 37 °C for 30 min, washed twice with PBS buffer (1×, pH = 7.4), and kept in fresh FBS-free DMEM for observation under a microscope. Quantitative relative fluorescence intensity of A549 and MCF7 was analysed via ImageJ software.

For MCF7, fluorescence imaging of MCF7 cells was performed in the same experimental protocol as A549.

In vivo **photodynamic therapy assay**. The dosage of 2 mg/kg body weight for A549 tumor mice model was selected. A549 cells at 1×106 in 100 μL of serum-free medium was injected into the right back of SCID female mice. When the average tumor volume reached about 20 mm^3 after 15 days, mice were randomly divided into four groups (3 mice/group) for the control group (PBS+light (white light, 100 $mW \cdot cm^{-2}$, 10 min)), **P_4** treatment group, **P_4**+light (white light, $mW \cdot cm^{-2}$, 10 min) group, **P_4-f**+light (white light, 100 $mW \cdot cm^{-2}$, 10 min), and **P_4-a**+light (white light, 100 $mW \cdot cm^{-2}$, 10 min) group. Mice were treated with 100 μL PBS or 2 mg/kg body weight of corresponding compounds by i.v. injection at the first day. After the 2 h post-injection, mice were exposed to white light at a density of 100 $mW \cdot cm^{-2}$ for 10 min. Tumor volume was calculated using the formula: volume = $(L \times W \times W)/2$, with "L" refers to the maximal length of tumors and "W" being the width. At the end of the experiments, the tumor tissues and major organs of each group were harvested. The tumor and organ sections were subjected to Hematoxylin and eosin (H&E) staining.

Structures of *β*-peptidyl porphyrins.

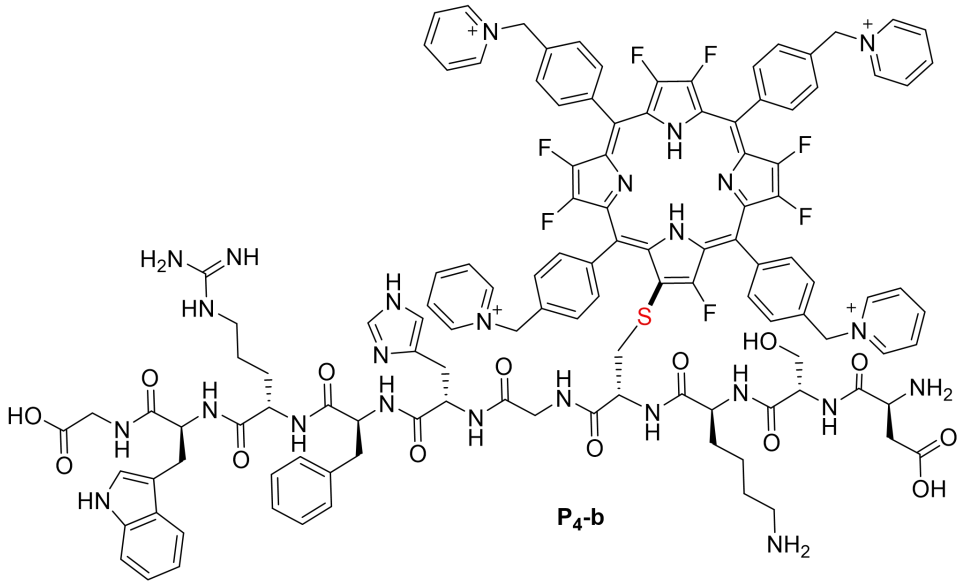

P_4-b: HRMS (ESI$^+$-FTICR) m/z [M^{4+}+H^+] calcd. for $C_{120}H_{119}F_7N_{25}O_{14}S^{5+}$ 459.7790 found: 459.7794; [M^{4+}] calcd. for $C_{120}H_{118}F_7N_{25}O_{14}S^{4+}$ 574.4719 found: 574.4727; [M^{4+}-H^+] calcd. for $C_{120}H_{117}F_7N_{25}O_{14}S^{3+}$ 765.6272 found: 765.6262; [M^{4+}-H^++TFA] calcd. for $C_{122}H_{118}F_{10}N_{25}O_{16}S^{3+}$ 803.6244 found: 803.6257.

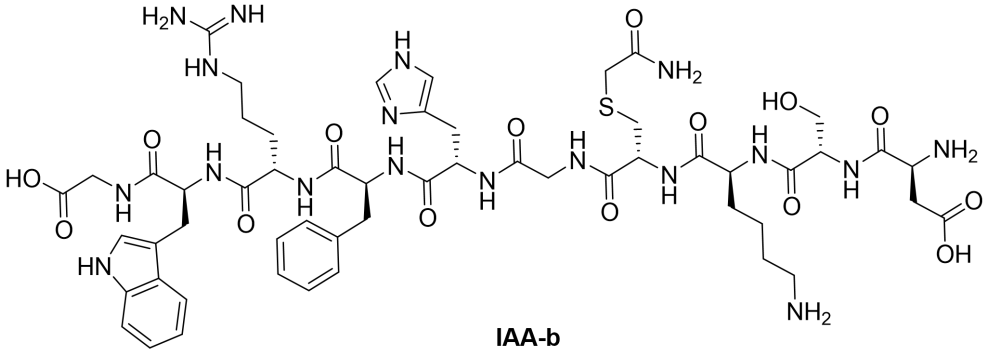

IAA-b: HRMS (ESI$^+$-FTICR) m/z [M+2H^+] calcd. for $C_{54}H_{78}N_{18}O_{15}S$ 625.2802 found: 625.2803.

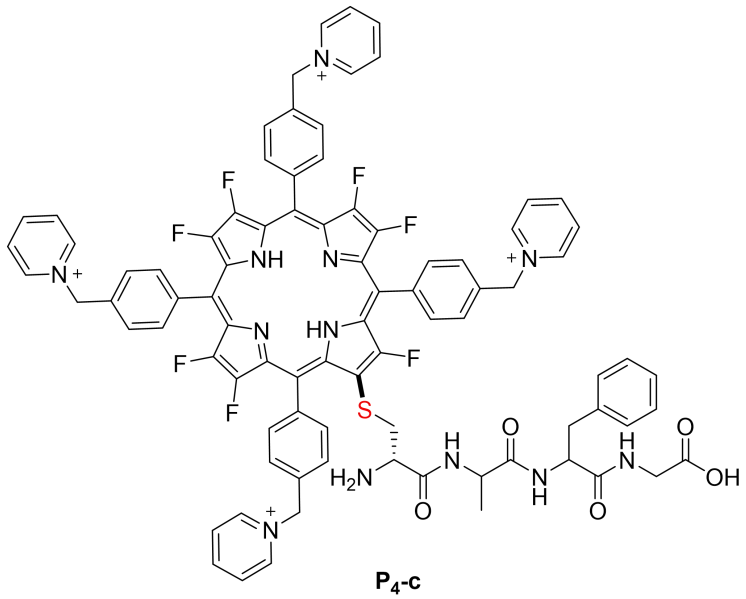

P_4-c

P_4-c: ^{1}H NMR (600 MHz, Deuterium Oxide, 1%MeOH) δ 9.11 – 9.05 (m, 6H), 9.00 (d, *J* = 5.7 Hz, 2H), 8.63 – 8.42 (m, 11H), 8.33 (s, 1H), 8.14 (t, *J* = 7.2 Hz, 6H), 8.10 – 8.05 (m, 2H), 7.90 (d, *J* = 8.0 Hz, 7H), 7.80 (d, *J* = 7.8 Hz, 1H), 6.99 (s, 3H), 6.78 (s, 2H), 6.11 (s, 6H), 6.01 (s, 2H), 4.17 (s, 1H), 3.77 (q, *J* = 7.1 Hz, 1H), 3.58 (d, *J* = 3.3 Hz, 2H), 3.16 – 3.13 (m, 1H), 2.84 – 2.68 (m, 3H), 2.49 (s, 1H), 0.69 (d, *J* = 7.1 Hz, 3H). ^{13}C NMR (151 MHz, Deuterium Oxide, 1%MeOH) δ 173.17, 163.30, 147.06, 145.32, 143.62, 138.20, 136.57, 135.75, 132.36, 129.35, 127.66, 121.43, 120.55, 120.15, 119.77, 119.24, 117.84, 115.90, 113.97, 64.92, 52.16, 49.50, 35.44, 16.96. ^{19}F NMR (565 MHz, Deuterium Oxide, 1%MeOH) δ -124.74, -145.05 – -147.83 (m). HRMS (ESI^{+}-FTICR) m/z [M^{4+}] calcd. for $C_{85}H_{69}F_7N_{12}O_5S^{4+}$ 375.6275 found: 375.6270; [M^{4+}-H^{+}] calcd. for $C_{85}H_{68}F_7N_{12}O_5S^{3+}$ 500.5009 found: 500.5012; [M^{4+}-H^{+}+TFA] calcd. for $C_{87}H_{69}F_{10}N_{12}O_7S^{3+}$ 538.4986 found: 538.4997.

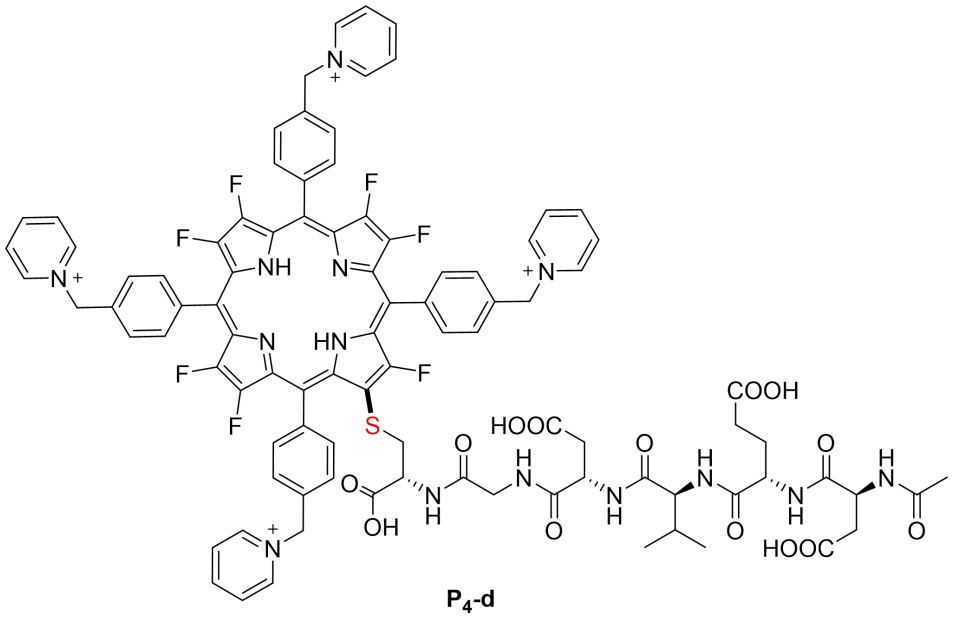

P_4-d

P_4-d: HRMS (ESI^{+}-FTICR) m/z [M^{4+}] calcd. for $C_{93}H_{83}F_7N_{14}O_{14}S^{4+}$ 446.1450 found: 446.1452; [M^{4+}-H^{+}] calcd.

for $C_{93}H_{83}F_7N_{14}O_{14}S^{3+}$ 594.8602 found: 594.8590.

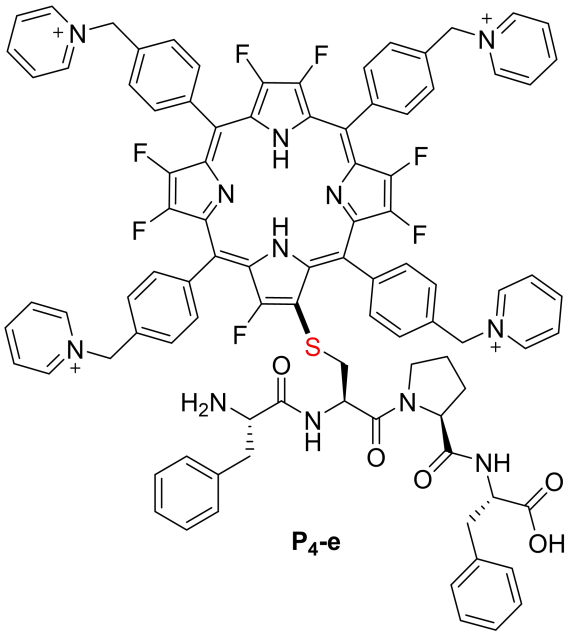

P$_4$-e

P$_4$-e: ^{1}H NMR (600 MHz, Deuterium Oxide, 1%MeOH) δ 9.13 – 9.02 (m, 8H), 8.58 (dd, *J* = 25.6, 8.6 Hz, 7H), 8.40 (d, *J* = 43.6 Hz, 5H), 8.17 – 8.10 (m, 7H), 8.08 (d, *J* = 6.9 Hz, 1H), 7.97 – 7.83 (m, 8H), 7.11 – 6.67 (m, 9H), 6.16 – 6.08 (m, 6H), 6.05 (d, *J* = 16.0 Hz, 3H), 3.92 – 3.46 (m, 3H), 3.01 – 2.84 (m, 1H), 2.81 (dd, *J* = 13.8, 6.5 Hz, 1H), 2.75 – 2.65 (m, 1H), 2.65 – 2.59 (m, 1H), 2.54 – 2.43 (m, 2H), 2.35 – 1.45 (m, 4H), 1.38 – 1.13 (m, 2H), 1.12 – 0.77 (m, 1H). ^{13}C NMR (151 MHz, Deuterium Oxide, 1%MeOH) δ 172.62, 168.41, 163.34, 147.06, 145.39, 137.21, 136.02, 133.88, 130.12, 129.61, 129.35, 128.32, 119.83, 117.89, 115.96, 114.03, 64.92, 60.39, 54.34, 53.77, 51.26, 47.77, 47.32, 37.02, 36.88, 30.42, 29.08, 24.28. ^{19}F NMR (565 MHz, Deuterium Oxide, 1%MeOH) δ -124.65, -146.63 (dd, *J* = 174.6, 90.0 Hz). HRMS (ESI$^+$-FTICR) m/z [M^{4+}] calcd. for $C_{94}H_{77}F_7N_{12}O_5S^{4+}$ 404.6432 found: 404.6435; [M^{4+}-H^+] calcd. for $C_{94}H_{76}F_7N_{12}O_5S^{3+}$ 539.1885 found: 539.1891; [M^{4+}-H^++TFA] calcd. for $C_{96}H_{77}F_{10}N_{12}O_7S^{3+}$ 577.1861 found: 577.1876.

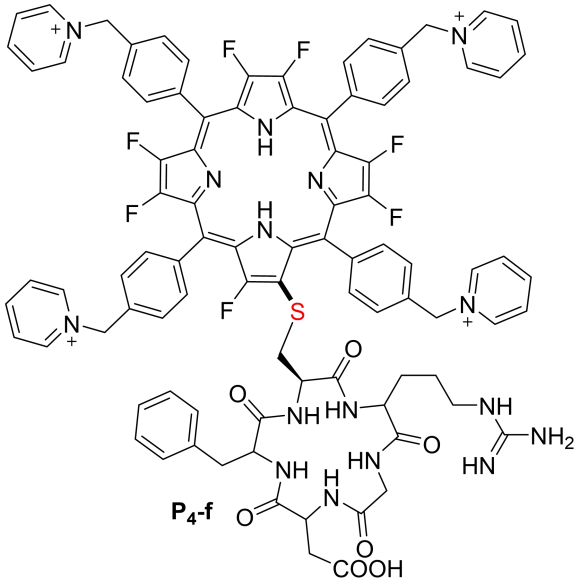

P₄-f: HRMS (ESI⁺-FTICR) m/z [M^{4+}+H^+] calcd. for $C_{92}H_{80}F_7N_{16}O_7S^{5+}$ 337.1195 found: 337.1196; [M^{4+}] calcd. for $C_{92}H_{79}F_7N_{16}O_7S^{4+}$ 421.1476 found: 421.1476; [M^{4+}-H^+] calcd. for $C_{92}H_{79}F_7N_{16}O_7S^{3+}$ 561.5303 found: 561.5302.

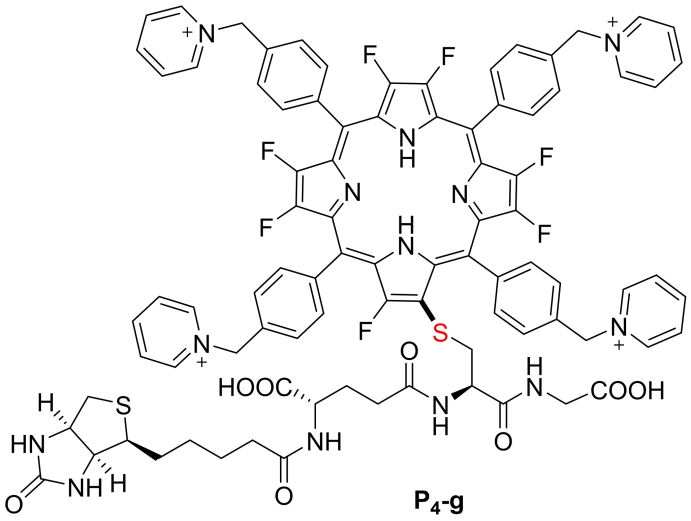

P₄-g: HRMS (ESI⁺-FTICR) m/z [M^{4+}] calcd. for $C_{88}H_{76}F_7N_{13}O_8S_2^{4+}$ 409.8812 found: 409.8809; [M^{4+}-H^+] calcd. for $C_{88}H_{75}F_7N_{13}O_8S_2^{3+}$ 546.1725 found: 546.1724.

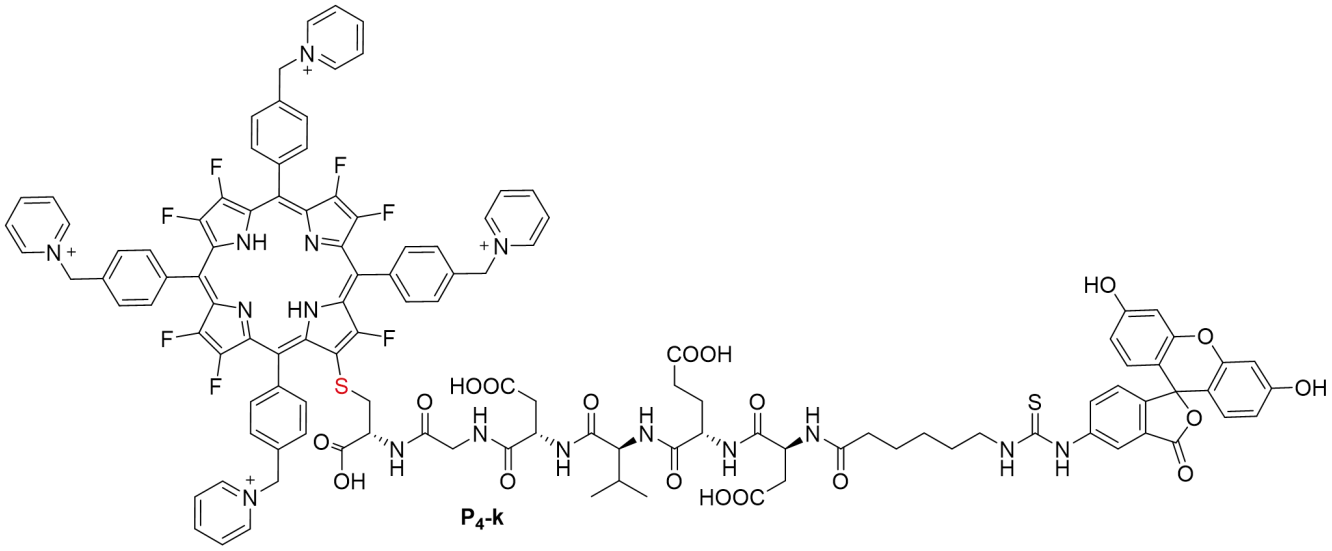

P_4-k

P_4-k: HRMS (ESI$^+$-FTICR) m/z [M^{4+}+H^+] calcd. for $C_{118}H_{105}F_7N_{16}O_{19}S_2^{5+}$ 449.3409 found: 449.3400; [M^{4+}] calcd. for $C_{118}H_{104}F_7N_{16}O_{19}S_2^{4+}$ 561.4243 found: 561.4232; [M^{4+}-H^+] calcd. for $C_{92}H_{79}F_7N_{16}O_7S^{3+}$ 747.8940 found: 747.8937.

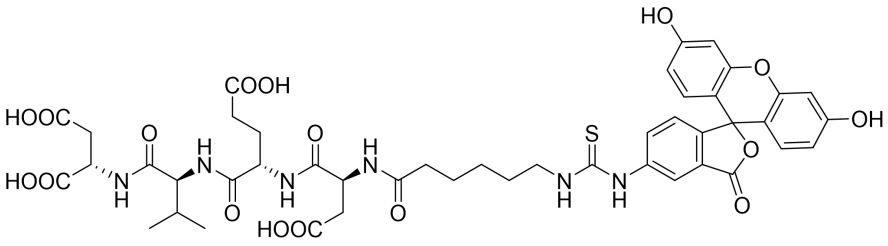

FITC-DEVD

FITC-DEVD: HRMS (ESI$^+$-FTICR) m/z [M+H]$^+$ calcd. for $C_{45}H_{51}N_6O_{17}S^+$ 979.3026 found: 979.3045.

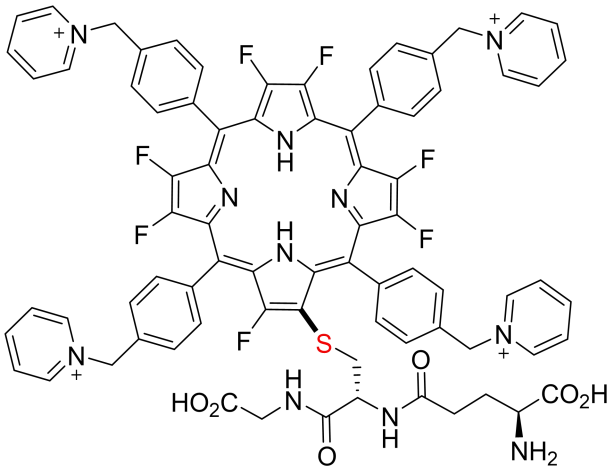

P_4-a

P_4-a: ^{1}H NMR (600 MHz, Deuterium Oxide) δ 9.16 – 9.05 (m, 8H), 8.67 – 8.33 (m, 12H), 8.15 (q, *J* = 6.4, 5.5 Hz, 8H), 7.92 (d, *J* = 4.2 Hz, 8H), 6.19 – 6.07 (m, 8H), 3.46 (dd, *J* = 11.7, 6.5 Hz, 1H), 3.38 (q, *J* = 6.0 Hz, 1H), 3.06 – 2.91 (m, 3H), 2.60 (dd, *J* = 14.6, 7.9 Hz, 1H), 1.87 (d, *J* = 5.8 Hz, 2H), 1.61 – 1.41 (m, 2H). ^{13}C NMR (151 MHz, Deuterium Oxide) δ 170.75, 146.46, 146.37, 144.72, 144.69, 136.02, 135.87, 129.05, 128.73, 128.67, 119.15, 115.29, 64.26, 52.01, 34.64, 30.61, 25.40. ^{19}F NMR (565 MHz, Deuterium Oxide) δ -124.83 (d, *J* = 81.0 Hz, 1F), -146.00 – -147.60 (m, 6F). HRMS (ESI$^+$-FTICR) m/z [M^{4+}-H^+] calcd. for $C_{78}H_{61}F_7N_{11}O_6S^{3+}$ 470.8133 found: 470.8143.

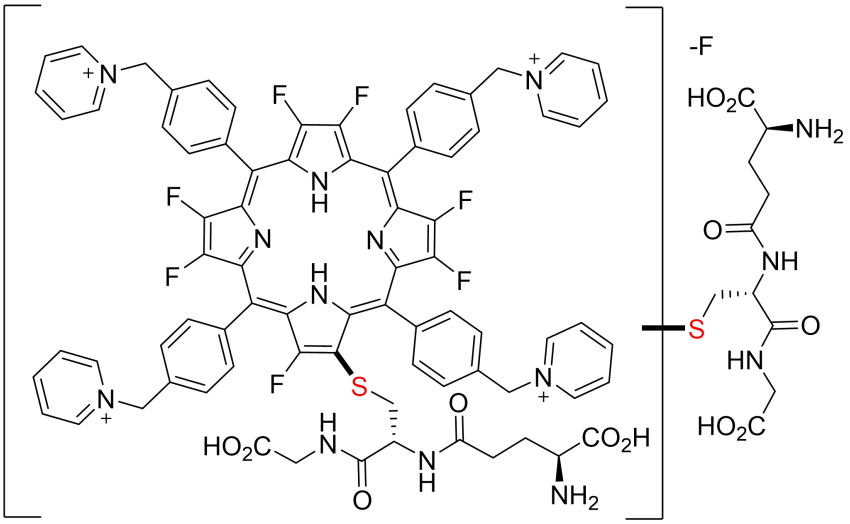

P_4-2a

P_4-2a: ^{1}H NMR (400 MHz, Deuterium Oxide) δ 9.07 (d, *J* = 6.0 Hz, 8H), 8.69 – 8.31 (m, 12H), 8.12 (t, *J* = 6.8 Hz, 8H), 7.91 (d, *J* = 6.0 Hz, 8H), 6.10 (d, *J* = 3.4 Hz, 8H), 3.46 – 3.26 (m, 4H), 3.06 – 2.81 (m, 6H), 2.72 – 2.44 (m, 2H), 1.89 (q, *J* = 7.7 Hz, 4H), 1.67 – 1.39 (m, 4H). ^{13}C NMR (151 MHz, Deuterium Oxide) δ 173.46, 172.20, 170.80, 146.46, 146.38, 144.73, 144.69, 142.48, 138.03, 136.58, 136.18, 136.05, 135.73, 135.17, 129.45, 129.33, 129.12, 128.73, 128.69, 120.55, 118.64, 117.22, 115.28, 64.26, 52.88, 52.20, 52.06, 40.64, 34.73, 30.79, 25.46. ^{19}F

NMR (565 MHz, Deuterium Oxide) δ -124.27(1F), -124.83 (1F), -146.66 (d, J = 69.5 Hz, 2F), -147.28 (2F). HRMS (ESI$^+$-FTICR) m/z [M^{4+}] calcd. for $C_{88}H_{78}F_6N_{14}O_{12}S_2^{4+}$ 425.1312 found: 425.1315; [M^{4+}-H^+] calcd. for $C_{88}H_{77}F_6N_{14}O_{12}S_2^{3+}$ 566.5058 found: 566.5063; [M^{4+}-2H^++Na^+] calcd. for $C_{88}H_{76}F_6N_{14}NaO_{12}S_2^{3+}$ 573.8331 found: 573.8337; [M^{4+}-2H^++K^+] calcd. for $C_{88}H_{76}F_6KN_{14}O_{12}S_2^{3+}$ 579.1578 found: 579.1567.

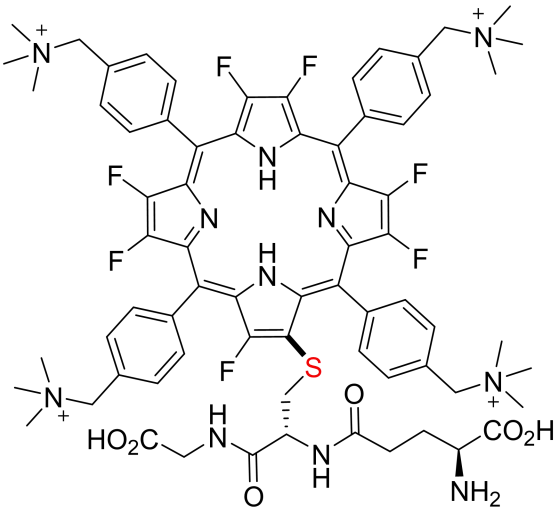

P_5-a

P_5-a: HRMS (ESI$^+$-FTICR) m/z [M^{4+}] calcd. for $C_{70}H_{78}F_7N_{11}O_6S^{4+}$ 333.3931 found: 333.3928; [M^{4+}-H^+] calcd. for $C_{70}H_{77}F_7N_{11}O_6S^{3+}$ 444.1884 found: 444.1886.

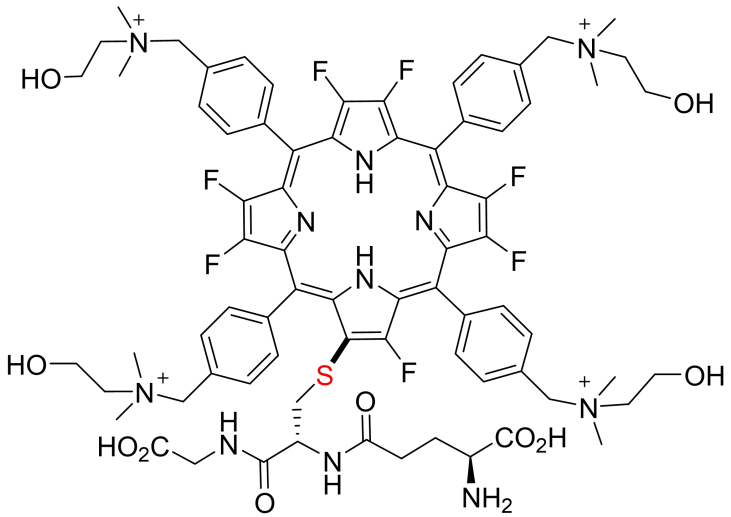

P_6-a

P_6-a: HRMS (ESI$^+$-FTICR) m/z [M^{4+}] calcd. for $C_{74}H_{86}F_7N_{11}O_{10}S^{4+}$ 363.4037 found: 363.4034; [M^{4+}-H^+] calcd. for $C_{74}H_{85}F_7N_{11}O_{10}S^{3+}$ 444.1884 found: 444.1886.

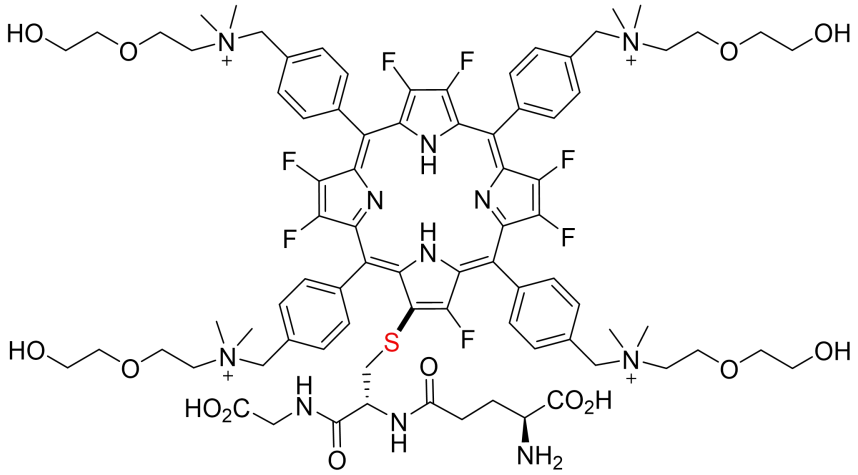

P_7-a

P_7-a: HRMS (ESI$^+$-FTICR) m/z [M^{4+}] calcd. for $C_{82}H_{102}F_7N_{11}O_{14}S^{4+}$ 407.4299 found: 407.4298; [M^{4+}-H^+] calcd. for $C_{82}H_{101}F_7N_{11}O_{14}S^{3+}$ 542.9041 found: 542.9049.

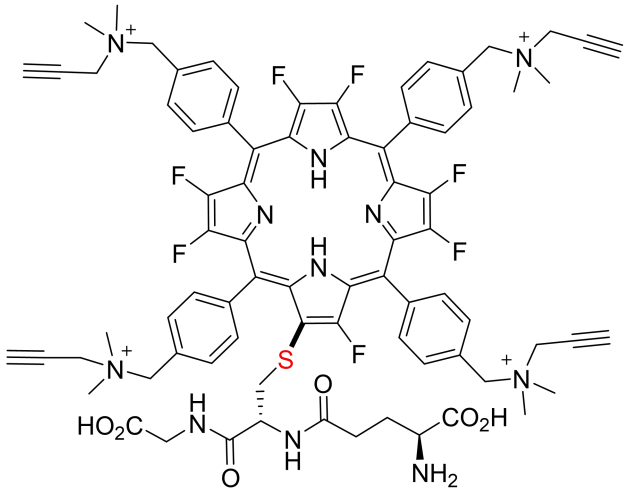

P_8-a

P_8-a: HRMS (ESI$^+$-FTICR) m/z [M^{4+}] calcd. for $C_{78}H_{78}F_7N_{11}O_6S^{4+}$ 357.3931 found: 357.3924; [M^{4+}-H^+] calcd. for $C_{78}H_{77}F_7N_{11}O_6S^{3+}$ 476.1884 found: 476.1892.

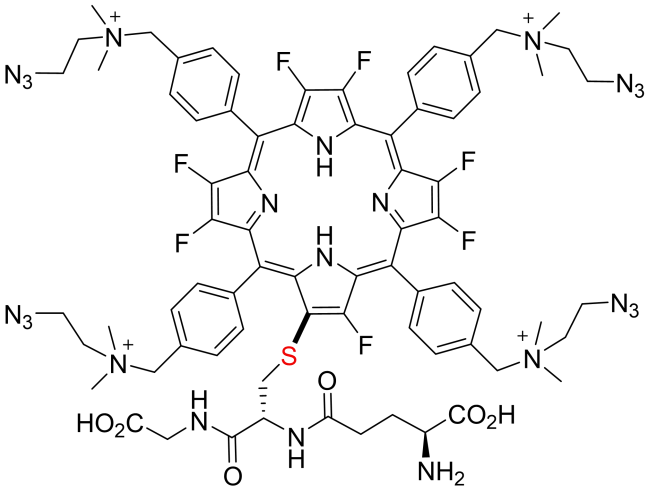

P_9-a

P_9-a: HRMS (ESI$^+$-FTICR) m/z [M^{4+}] calcd. for $C_{74}H_{82}F_7N_{23}O_6S^{4+}$ 388.4101 found: 388.4103; [M^{4+}-H^+] calcd. for $C_{74}H_{81}F_7N_{23}O_6S^{3+}$ 517.5444 found: 517.5447.

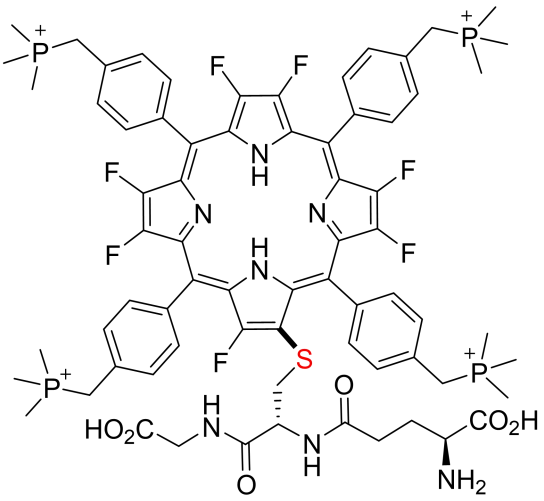

P_{10}-a

P_{10}-a: HRMS (ESI$^+$-FTICR) m/z [M^{4+}] calcd. for $C_{70}H_{78}F_7N_7O_6P_4S^{4+}$ 350.3638 found: 350.3628; [M^{4+}-H^+] calcd. for $C_{70}H_{77}F_7N_7O_6P_4S^{3+}$ 466.8160 found: 466.8161.

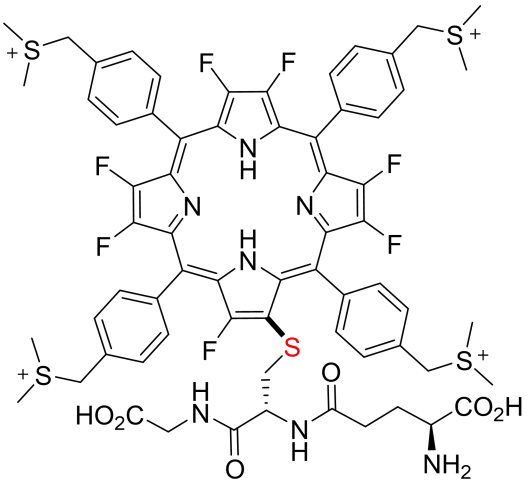

P_{11}-a

P_{11}-a: HRMS (ESI$^+$-FTICR) m/z [M^{4+}] calcd. for $C_{66}H_{66}F_7N_7O_6S_5^{4+}$ 336.3386 found: 336.3384; [M^{4+}-H^+] calcd. for $C_{66}H_{65}F_7N_7O_6S_5^{3+}$ 427.4427 found: 427.4432.

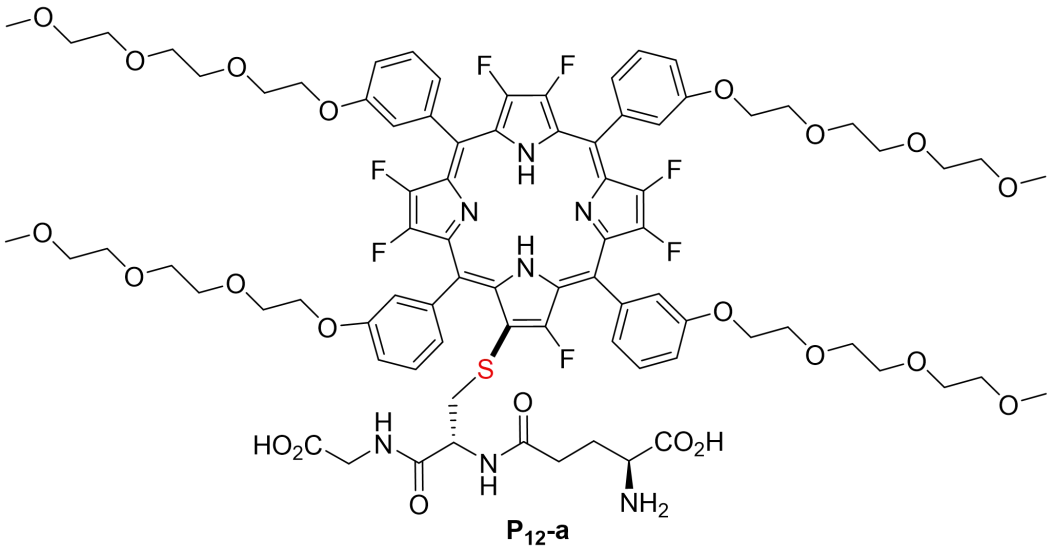

P_{12}-a

P_{12}-a: HRMS (ESI$^+$-FTICR) m/z [$M+H^{2+}$] calcd. for $C_{82}H_{96}F_7N_7O_{22}S^{4+}$ 847.8103 found: 847.8080.

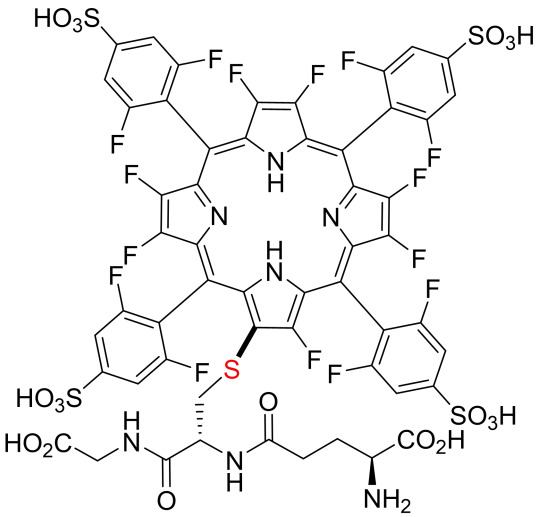

P_{13}-a

P_{13}-a: HRMS (ESI$^-$-FTICR) m/z [M^{4-}] calcd. for $C_{54}H_{26}F_{15}N_7O_{18}S_5^{4-}$ 376.32430 found: 376.3384; [M^{4-}+H^+] calcd. for $C_{54}H_{26}F_{15}N_7O_{18}S_5^{3-}$ 501.9931 found: 501.9928; [M^{4-}+Na^+] calcd. for $C_{54}H_{26}F_{15}N_7NaO_{18}S_5^{3-}$ 509.3204 found: 509.3202.

II. Supporting Tables and Figures

Solvent A – water (0.05% v/v TFA), Solvent B – MeOH. Detection wavelength – 395 nm.

Time/min	Rate of flow mL/min	A%	B%
0	1	80	20
2	1	48	52
17	1	30	70
17.1	1	5	95
18.9	1	5	95
19	1	80	20
20	1	80	20

Table S1. **Method A** was adopted during optimizing reaction conditions.

Solvent A – water (0.05% v/v TFA), Solvent B – MeOH. Detection wavelength – 395 nm.

Time/min	Rate of flow mL/min	A%	B%
0	1	80	20
5	1	55	45
22	1	25	75
22.1	1	5	95
23.9	1	5	95
24	1	80	20
25	1	80	20

Table S2. **Method B**.

Solvent A – water (0.05% v/v TFA), Solvent B – MeOH. Detection wavelength – 395 nm.

Time/min	Rate of flow mL/min	A%	B%
0	5	80	20
5	5	55	45
22	5	25	75
22.1	5	5	95
23.9	5	5	95
24	5	80	20
25	5	80	20

Table S3. **Method C**.

Solvent A – water (0.05% v/v TFA), Solvent B – acetonitrile. Detection wavelength – 395 nm.

Time/min	Rate of flow mL/min	A%	B%
0	1	90	10
40	1	40	60
41	1	0	100
55	1	0	100

Table S4. **Method D**.

		$\mathbf{P_1}$	$\mathbf{P_2}$	$\mathbf{P_3}$
ΔE_{ST} /eV	S_1-T_1, S_1-T_2	1.24	0.658	0.714
	S_1-T_3	-0.0197	0.0432	0.0405
SOC constants /cm^{-1}	S_1-T_1, S_1-T_2	0.0418	0.604	1.26
	S_1-T_3	--	1.70	1.85
k_{ISC} /s^{-1}	S_1-T_1, S_1-T_2	2.48×10^5	2.63×10^7	6.35×10^7
	S_1-T_3	--	6.98×10^5	5.58×10^5

Table S5. Computational calculation data of $\mathbf{P_{1\text{-}3}}$.

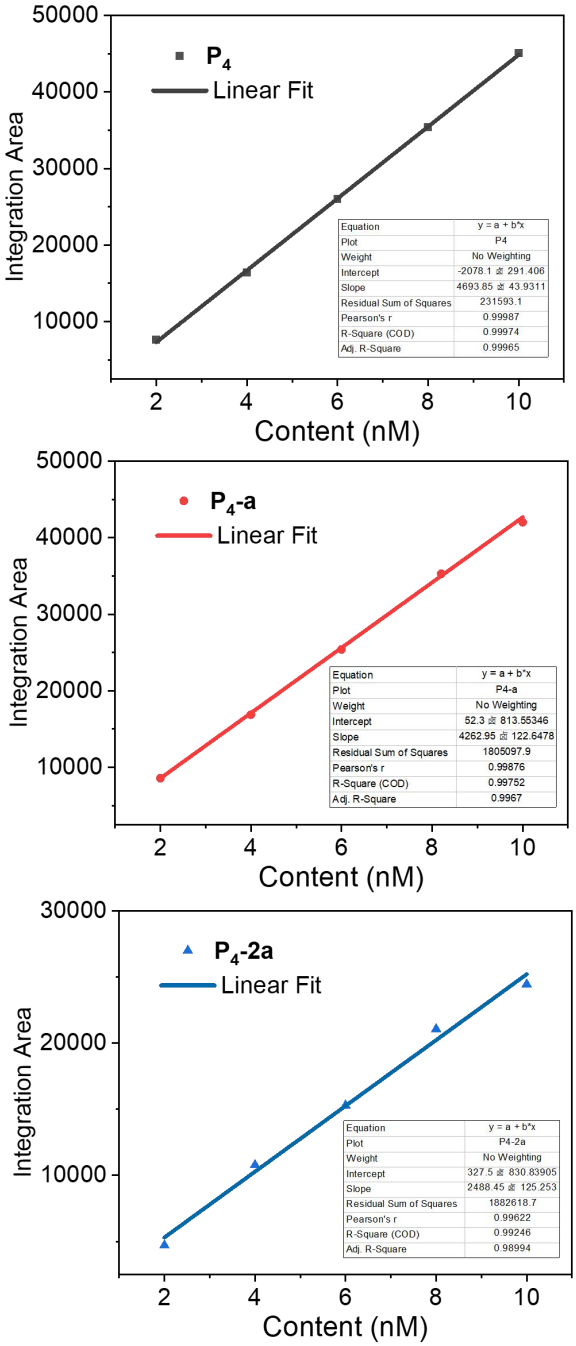

Figure S1. Correlations between integration area and content of **P**$_4$, **P**$_4$**-a**, and **P**$_4$**-2a** at 395 nm.

HPLC spectra of reaction optimization between P_4 and a.

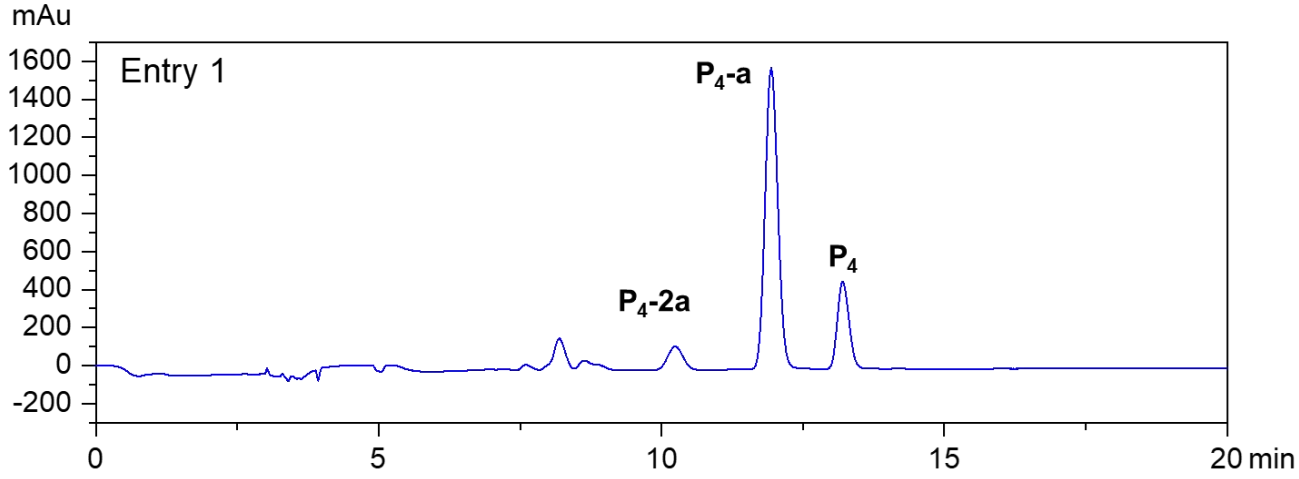

Figure S2. HPLC analysis of reaction mixture in Entry 1.

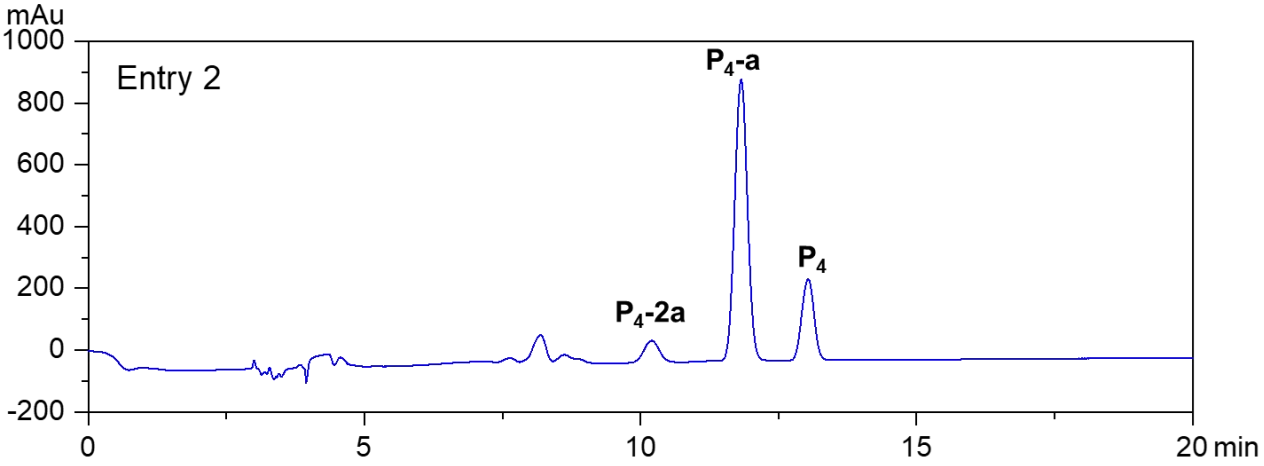

Figure S3. HPLC analysis of reaction mixture in Entry 2.

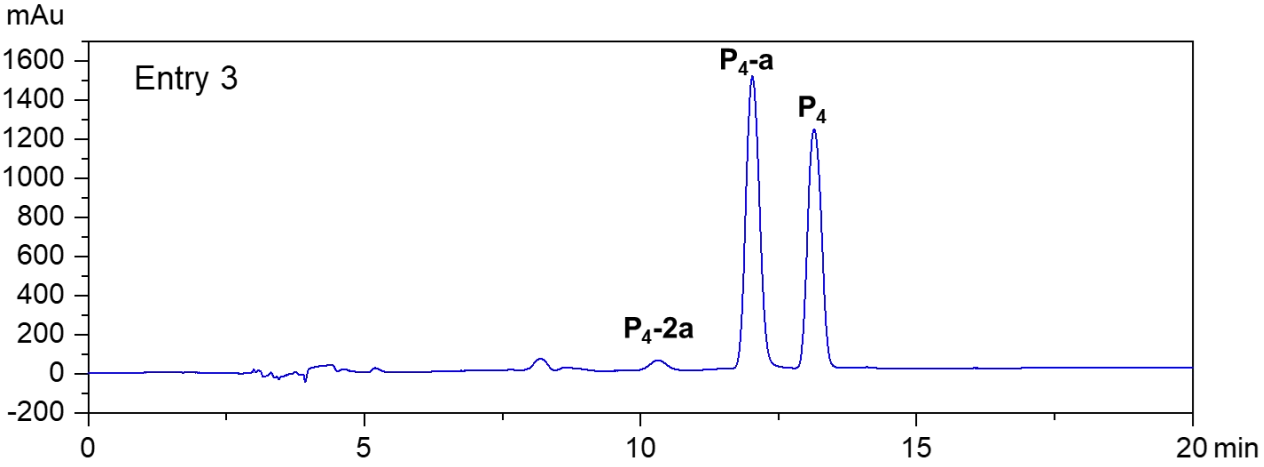

Figure S4. HPLC analysis of reaction mixture in Entry 3.

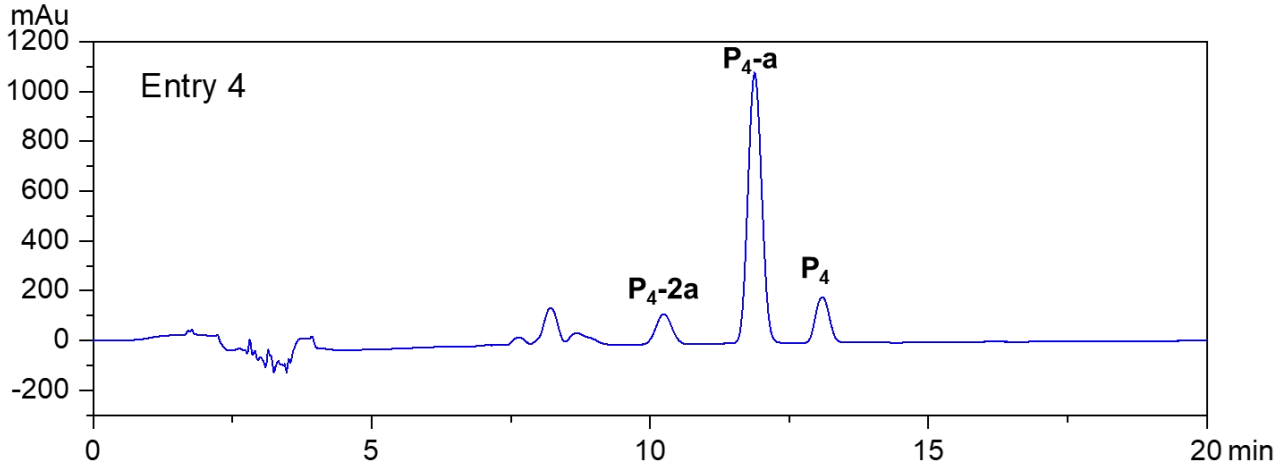

Figure S5. HPLC analysis of reaction mixture in Entry 4.

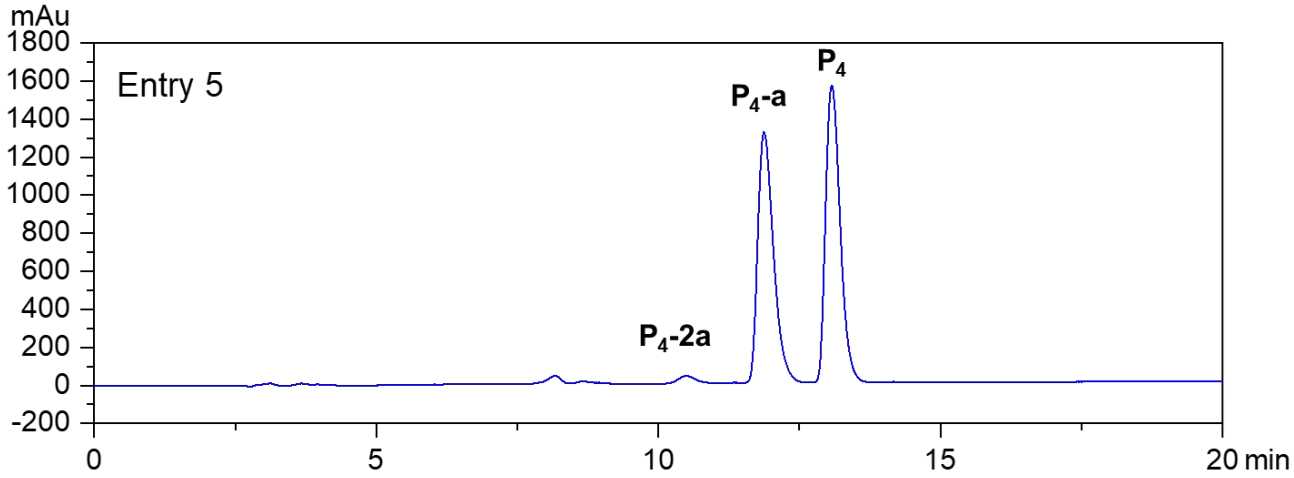

Figure S6. HPLC analysis of reaction mixture in Entry 5.

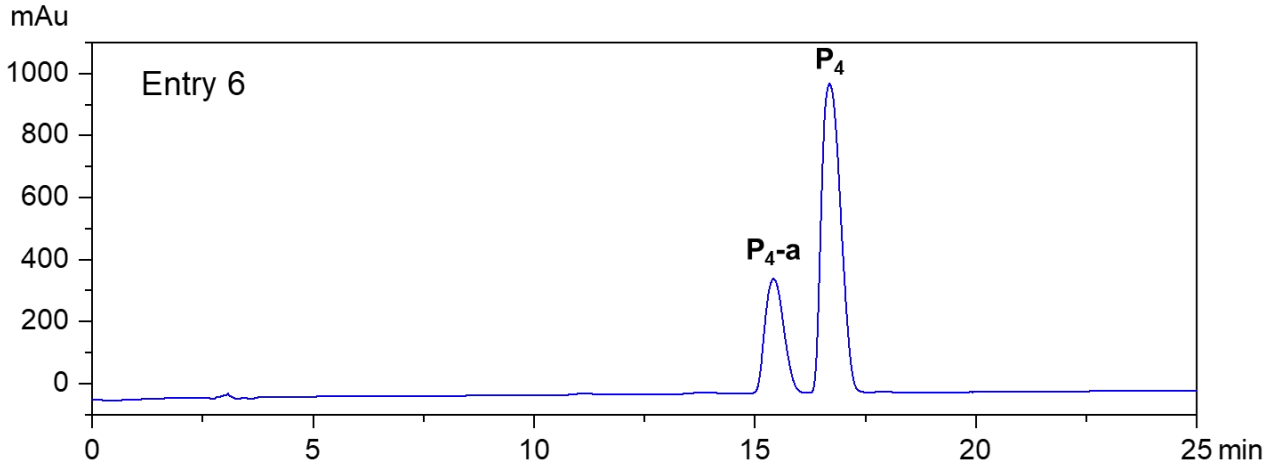

Figure S7. HPLC analysis of reaction mixture in Entry 6.

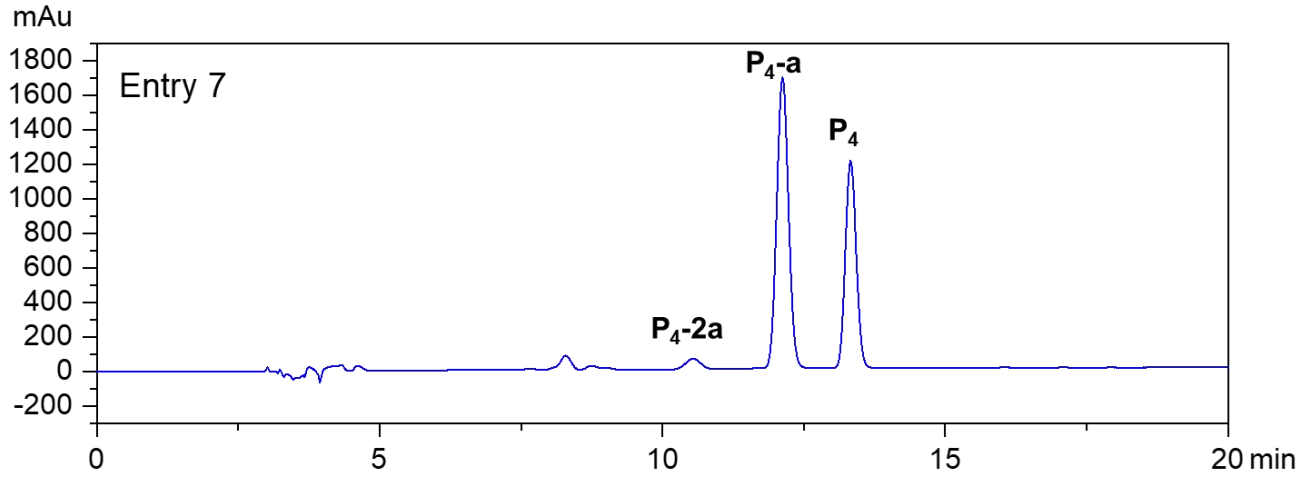

Figure S8. HPLC analysis of reaction mixture in Entry 7.

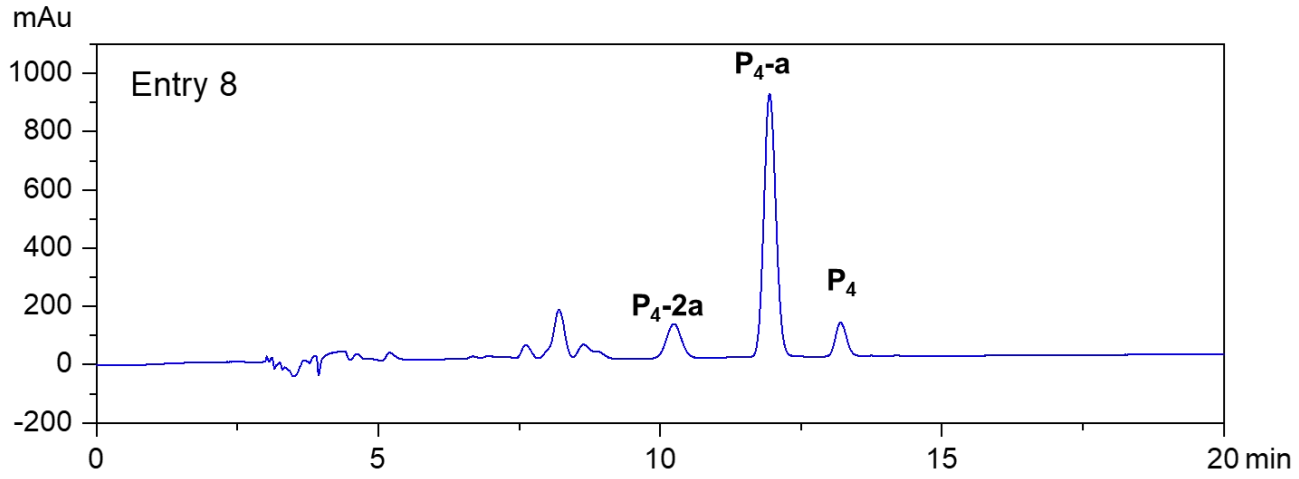

Figure S9. HPLC analysis of reaction mixture in Entry 8.

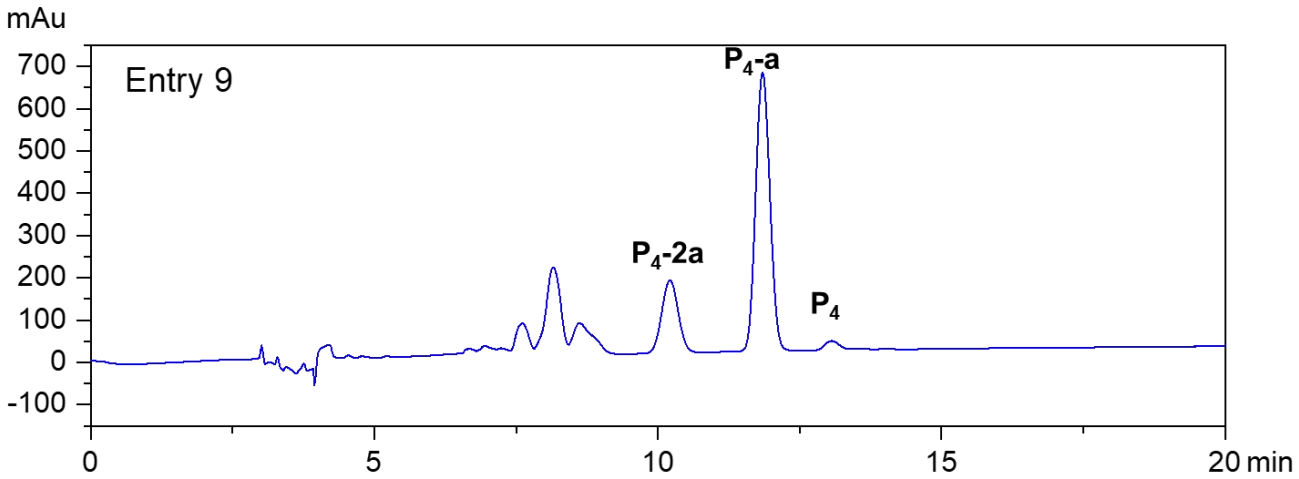

Figure S10. HPLC analysis of reaction mixture in Entry 9.

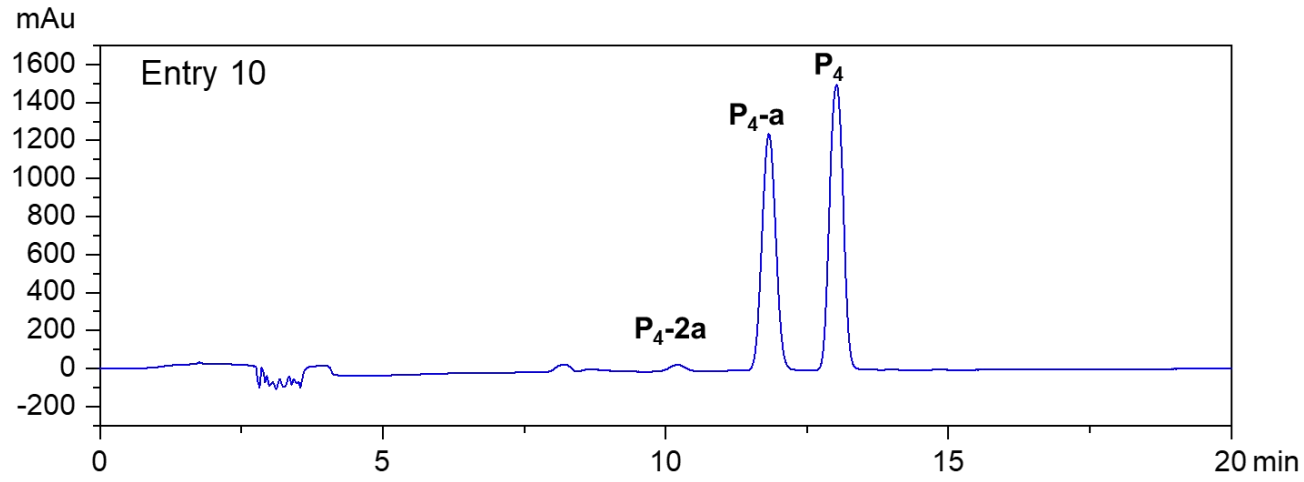

Figure S11. HPLC analysis of reaction mixture in Entry 10.

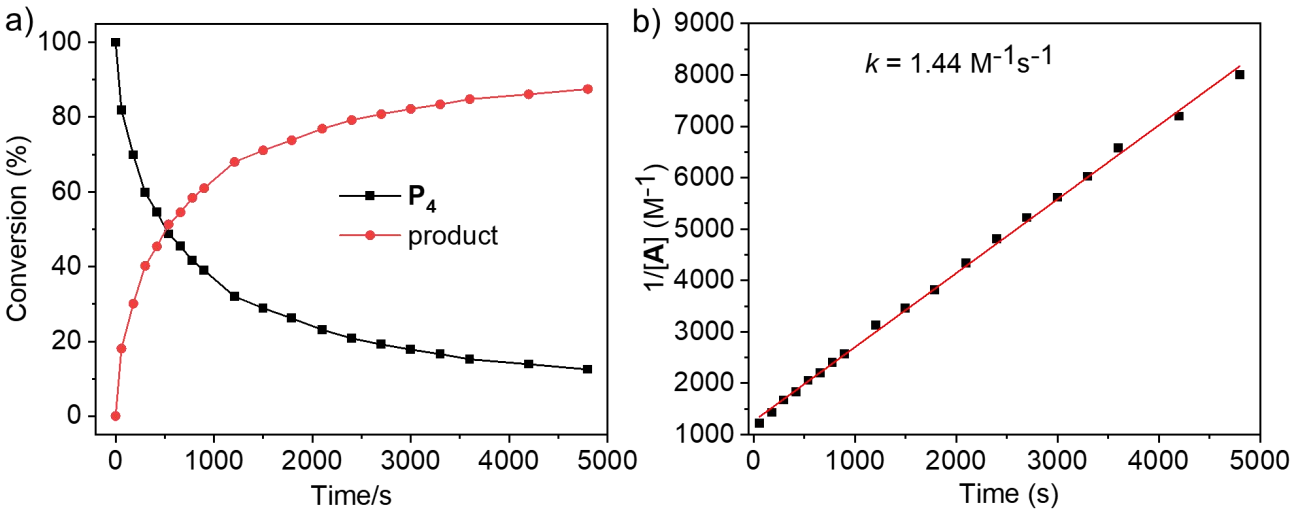

Figure S12. a) Percentage of $\mathbf{P_4}$ (1 mM) and its bioconjugate when reacting with GSH (**a**, 1 mM) at different time points. b) Experimental determination of the reaction rate constant.

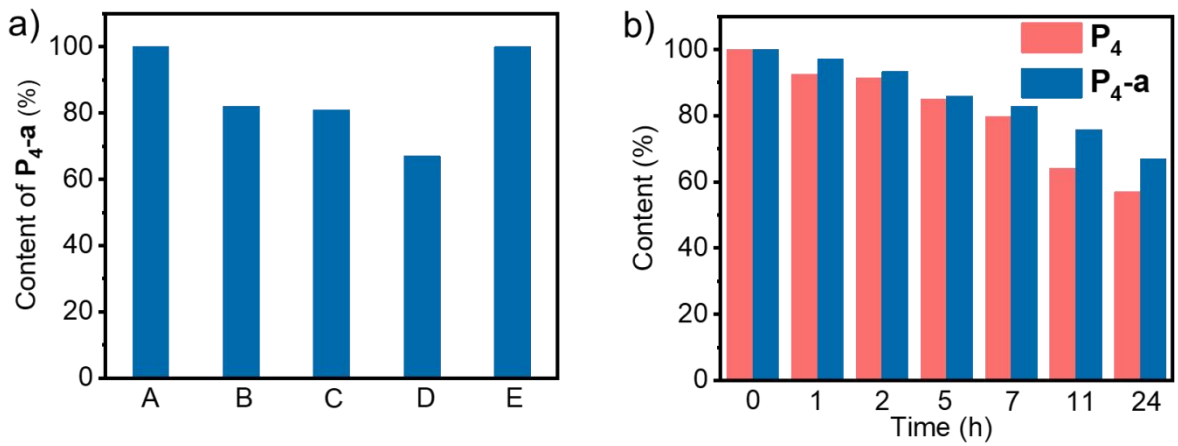

Figure S13. a) Stability of **P₄-a** at GSH abundant conditions determined by HPLC analysis. A: PBS (pH 7.4), 37 °C, 24 h. B: GSH (2 mM), PBS (pH 7.4), 37 °C, 24 h. C: GSH (5 mM), PBS (pH 7.4), 37 °C, 24 h. D: GSH (10 mM), PBS (pH 7.4), 37 °C, 24 h. E: GSH (10 mM), PBS (pH 6.8), 37 °C, 24 h. b) Content of **P₄** (red) and **P₄-a** (blue) in GSH (10 mM), PBS (pH 7.4) at 37 °C at different time points determined by HPLC analysis.

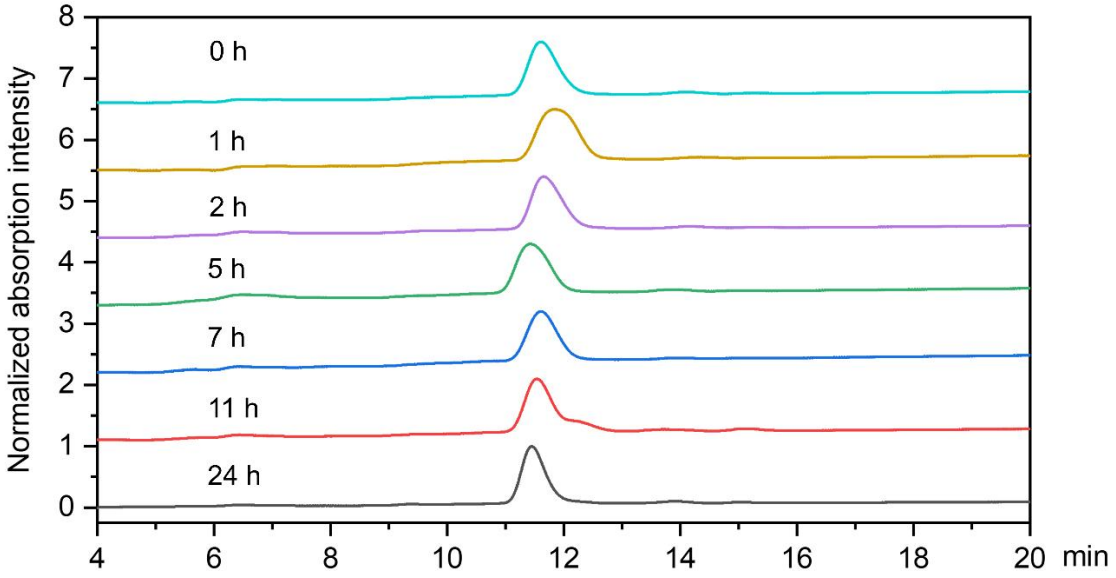

Figure S14. HPLC analysis of cell lysates of HeLa cells treated with **P_4-a** (10 μM) for different time period (0, 1, 2, 5, 7, 11, 24 h).

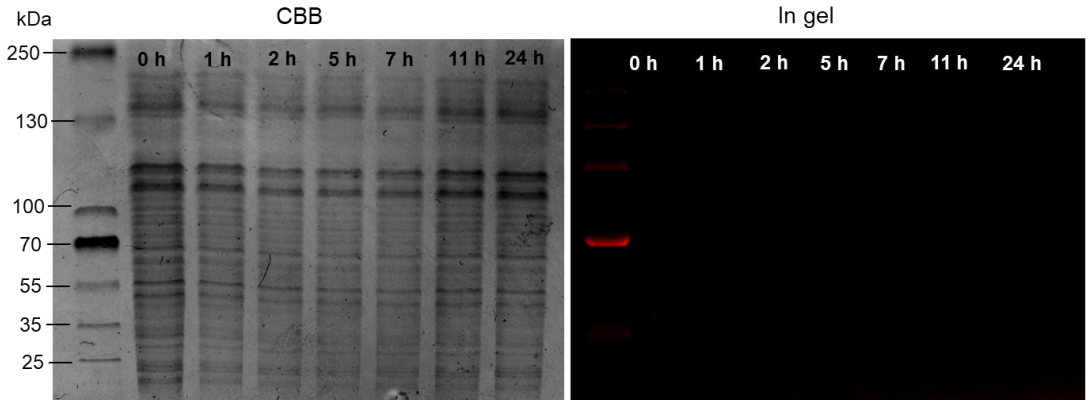

Figure S15. Determination of cell stability of **P_4-a** by SDS-PAGE. Coomassie brilliant blue (CBB)-stained gel showed protein weights of cell lysates in which HeLa cells were incubated with **P_4-a** for different time period (0, 1, 2, 5, 7, 11, 24 h). In gel fluorescence scanning showed no porphyrinic emission (red).

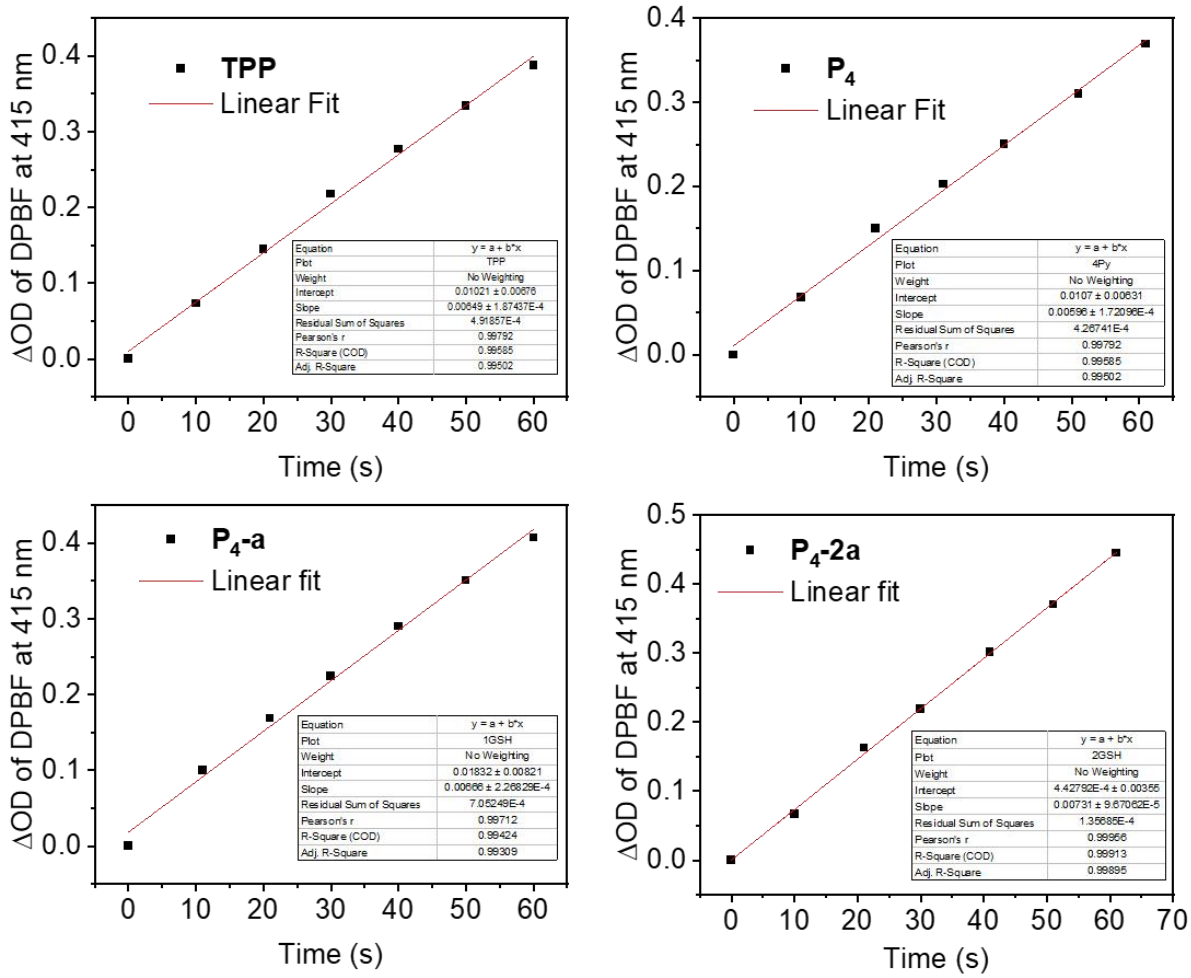

Figure S16. ΔOD of DPBF absorbance change at 415 nm for **P$_4$**, **P$_4$-a**, and **P$_4$-2a** in toluene (0.1% v/v DMSO) at room temperature.

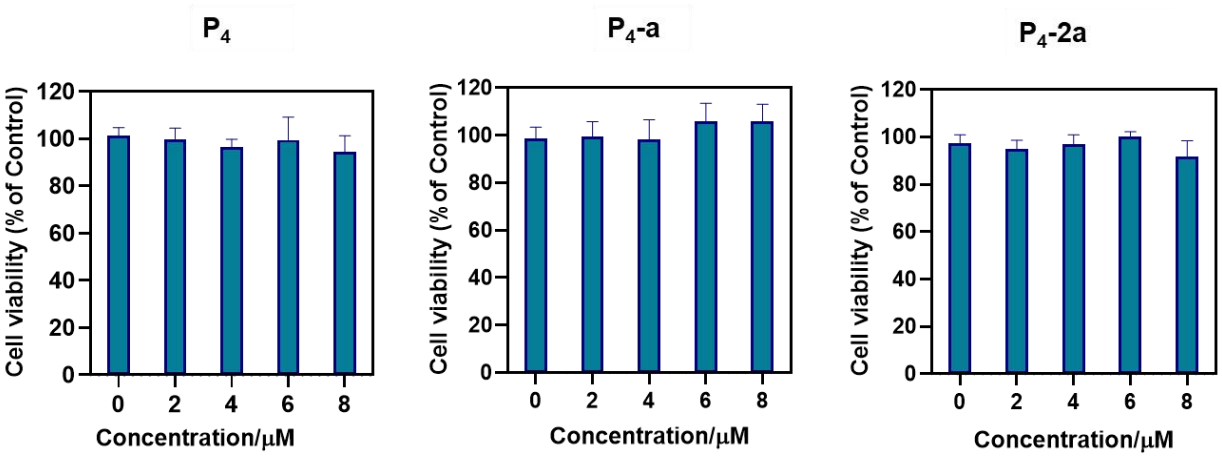

Figure S17. Dark cytotoxicity evaluation (mean ± SD, three biological repeats) of **P**$_4$, **P**$_4$**-a**, and **P**$_4$**-2a** in HeLa cells.

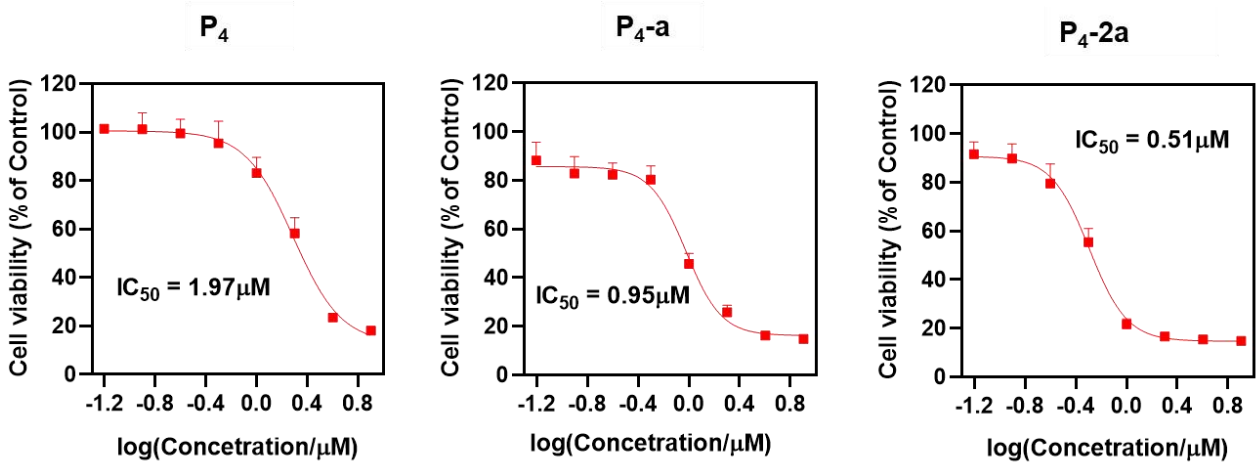

Figure S18. Photocytotoxicity evaluation (mean ± SD, three biological repeats) of **P**$_4$, **P**$_4$**-a**, and **P**$_4$**-2a** in Hela cells.

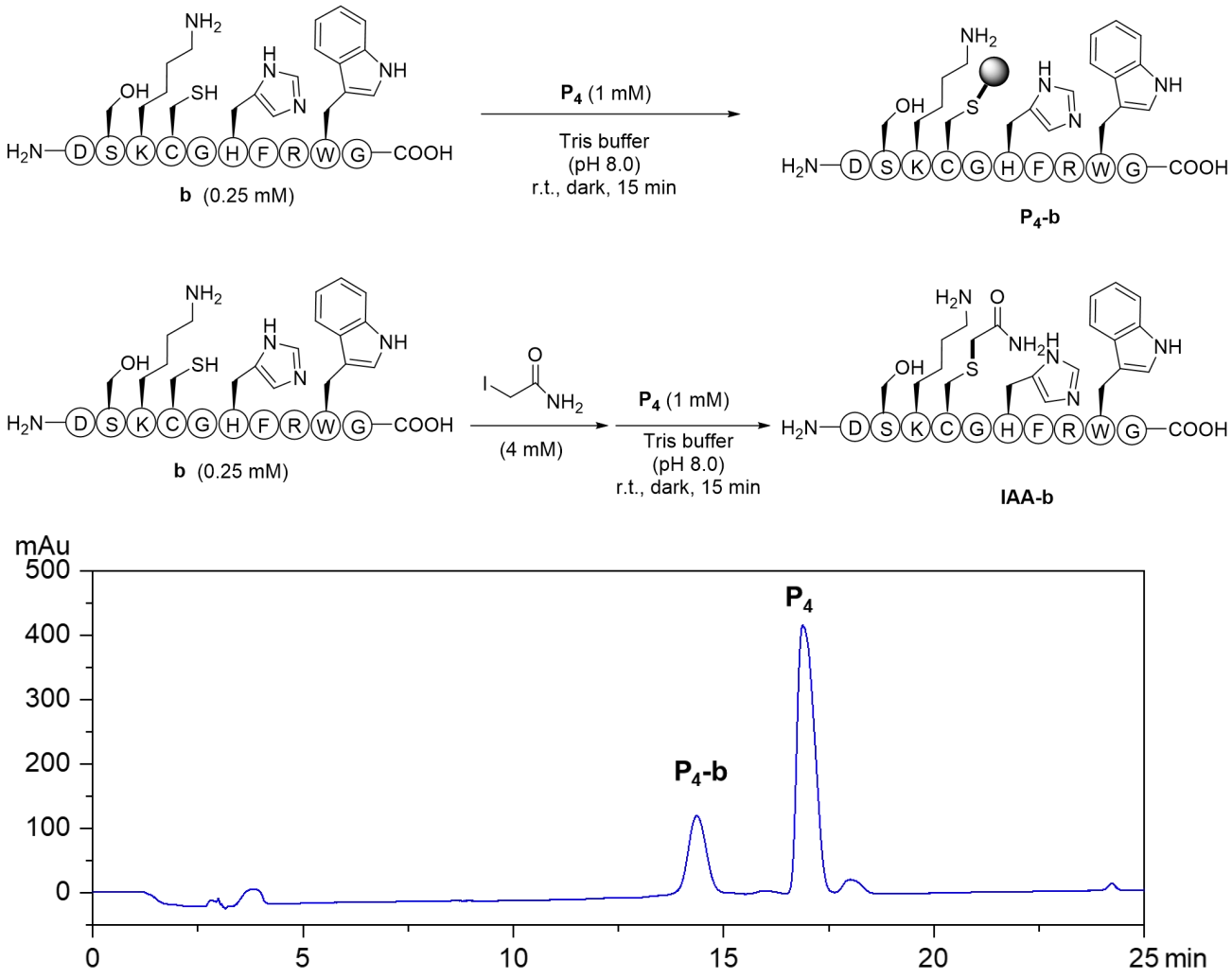

Figure S19. HPLC-UV chromatogram at 395 nm of reaction mixture between **P4** and **b**.

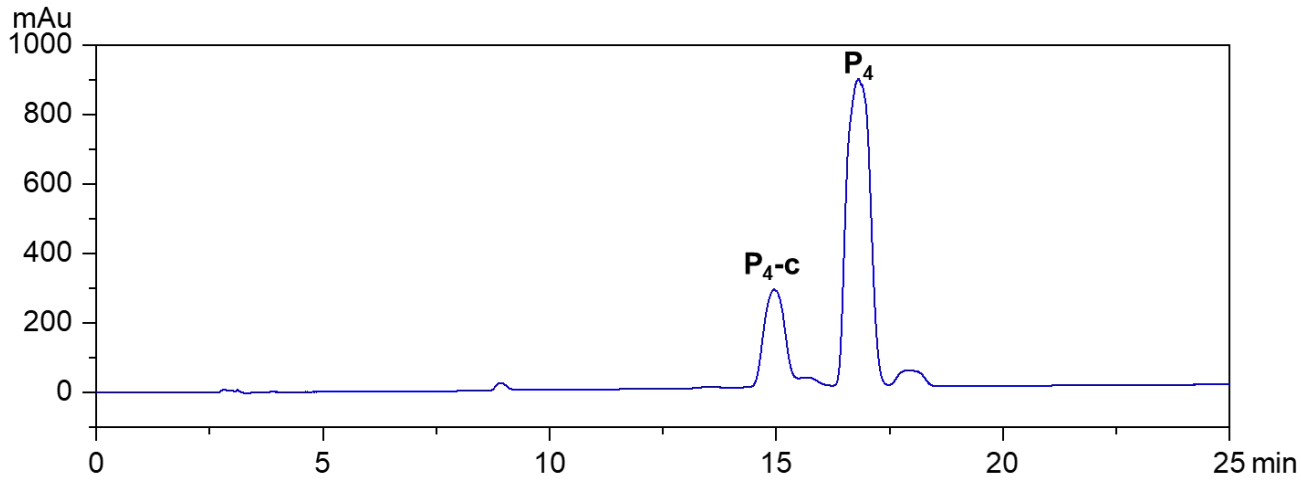

Figure S20. HPLC-UV chromatogram at 395 nm of reaction mixture between **P4** and **c**.

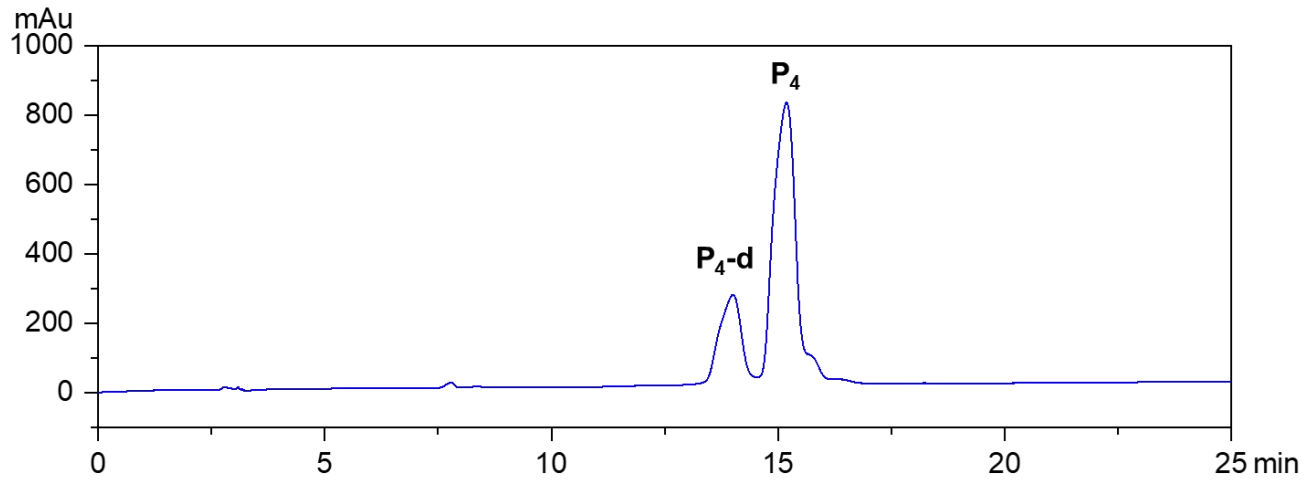

Figure S21. HPLC-UV chromatogram at 395 nm of reaction mixture between **P4** and **d**.

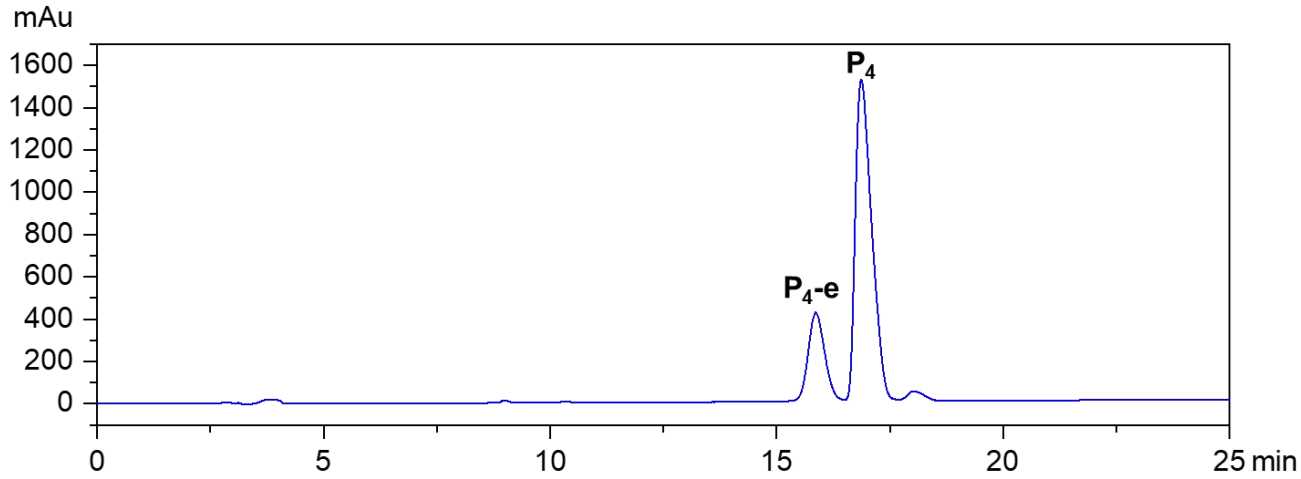

Figure S22. HPLC-UV chromatogram at 395 nm of reaction mixture between $\mathbf{P_4}$ and **e**.

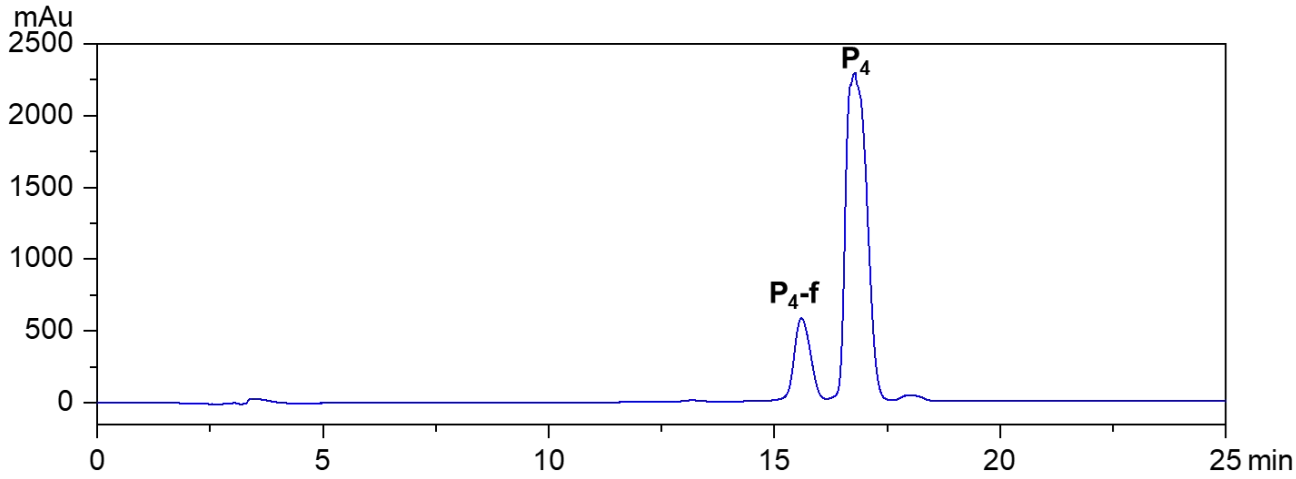

Figure S23. HPLC-UV chromatogram at 395 nm of reaction mixture between **P4** and **f**.

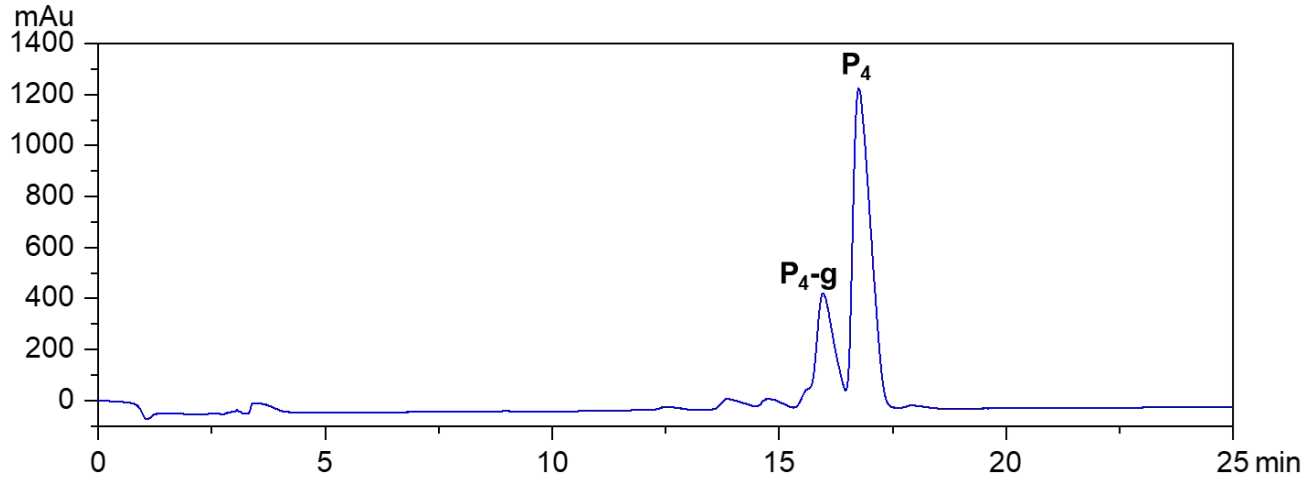

Figure S24. HPLC-UV chromatogram at 395 nm of reaction mixture between **P4** and **g**.

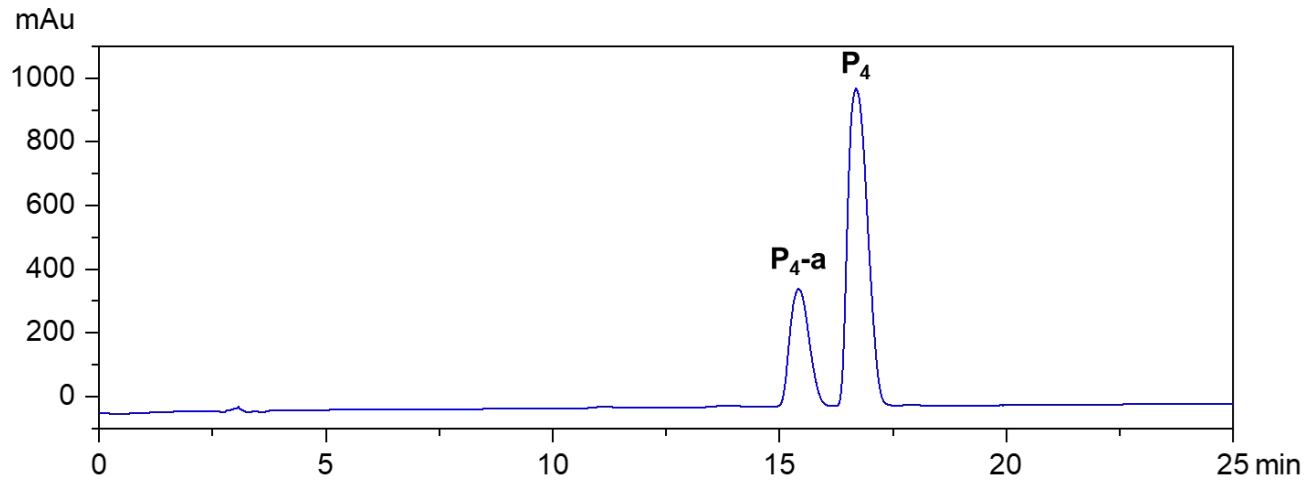

Figure S25. HPLC-UV chromatogram at 395 nm of reaction mixture between $\mathbf{P_4}$ and **a**.

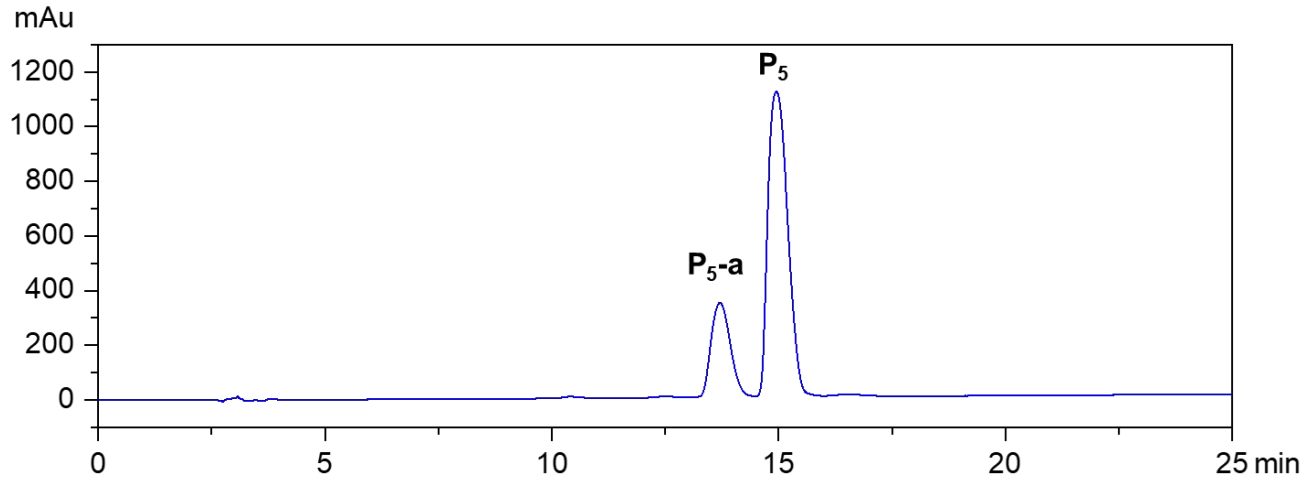

Figure S26. HPLC-UV chromatogram at 395 nm of reaction mixture between $\mathbf{P_5}$ and **a**.

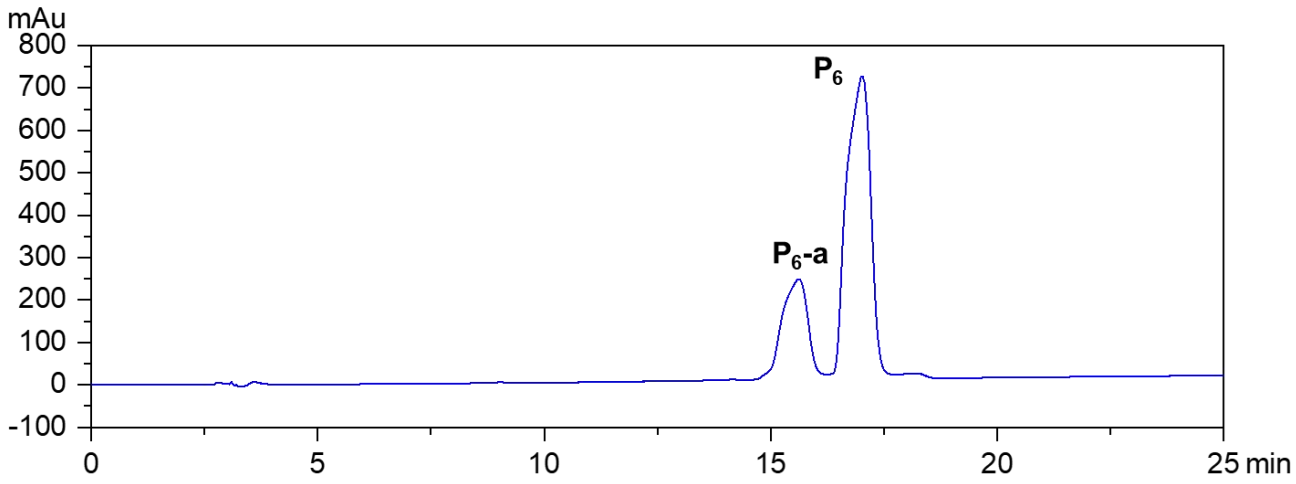

Figure S27. HPLC-UV chromatogram at 395 nm of reaction mixture between $\mathbf{P_6}$ and **a**.

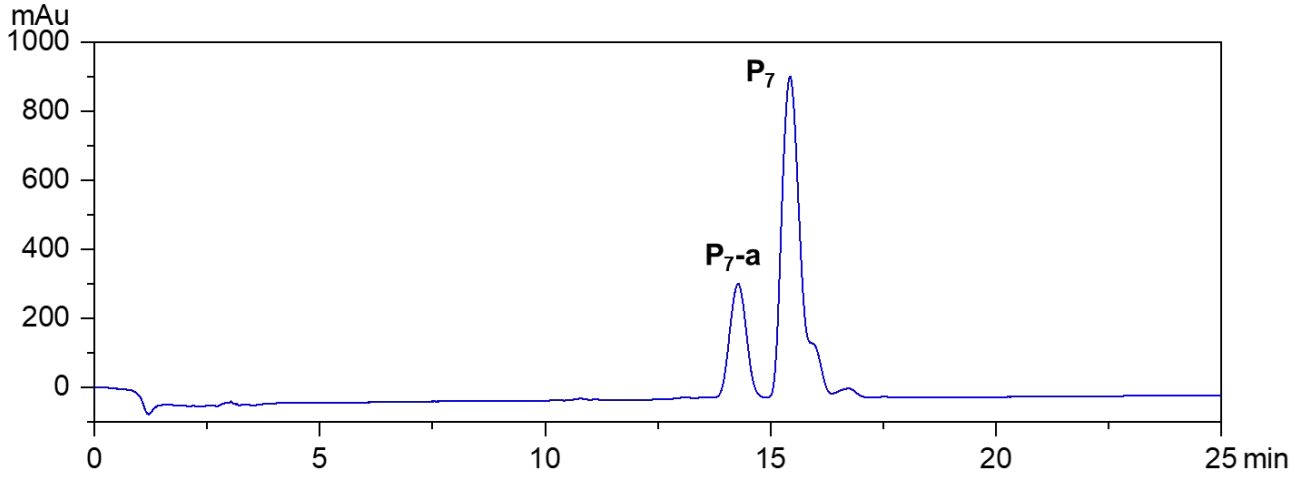

Figure S28. HPLC-UV chromatogram at 395 nm of reaction mixture between $\mathbf{P_7}$ and **a**.

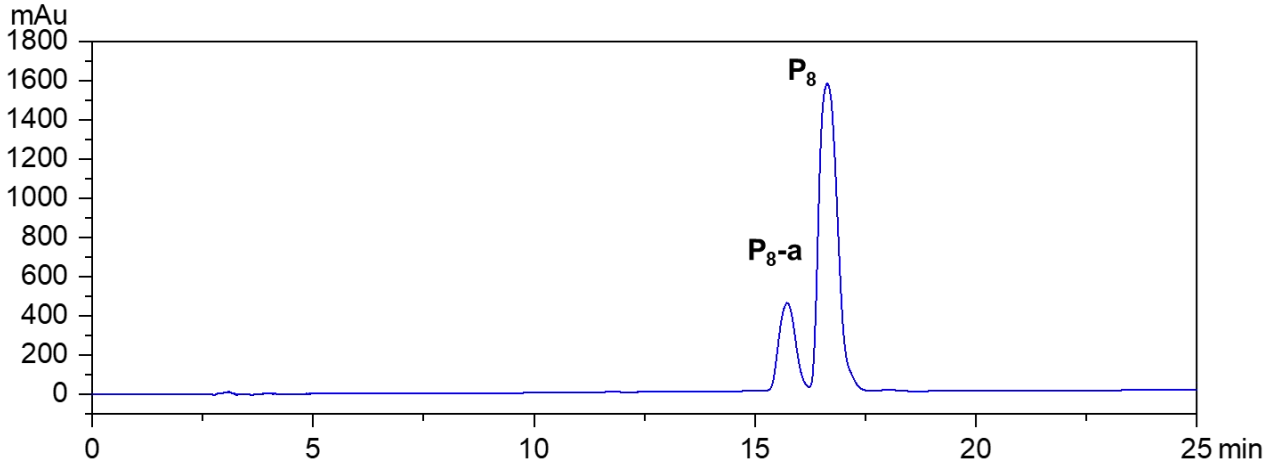

Figure S29. HPLC-UV chromatogram at 395 nm of reaction mixture between $\mathbf{P_8}$ and **a**.

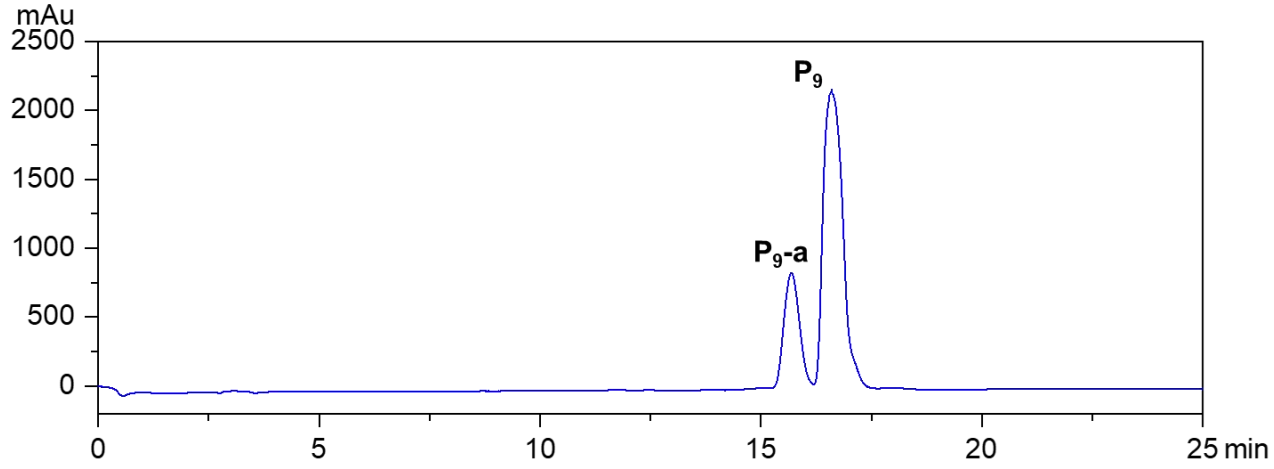

Figure S30. HPLC-UV chromatogram at 395 nm of reaction mixture between **P9** and **a**.

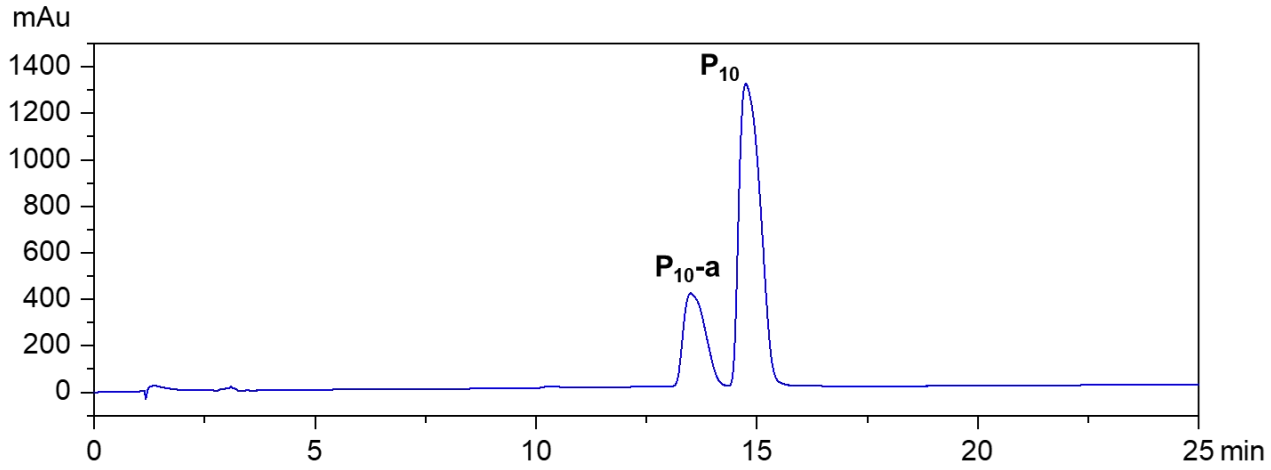

Figure S31. HPLC-UV chromatogram at 395 nm of reaction mixture between $\mathbf{P_{10}}$ and **a**.

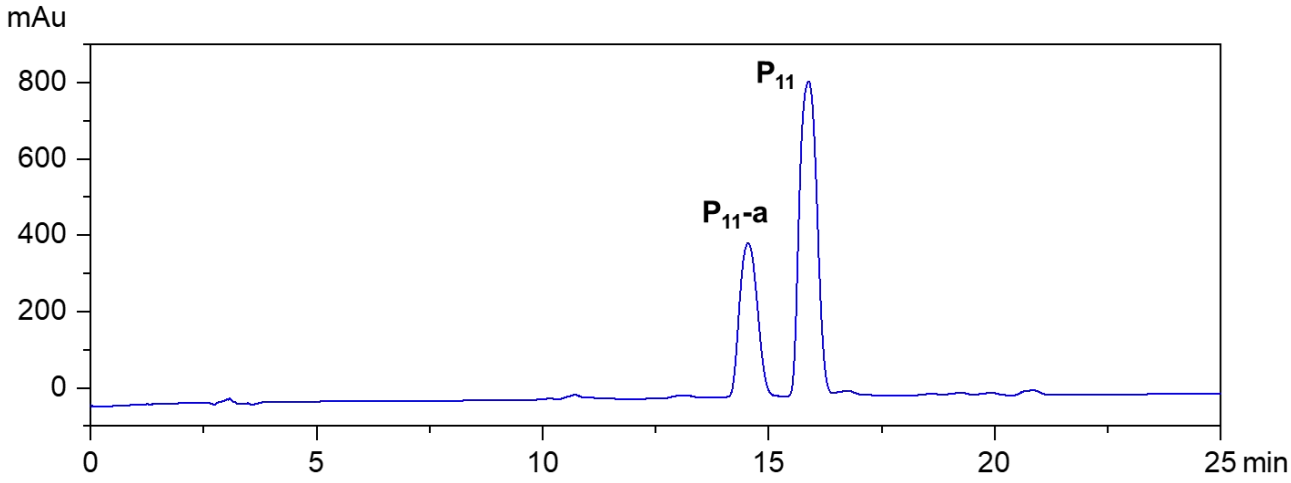

Figur S32. HPLC-UV chromatogram at 395 nm of reaction mixture between $\mathbf{P_{11}}$ and **a**.

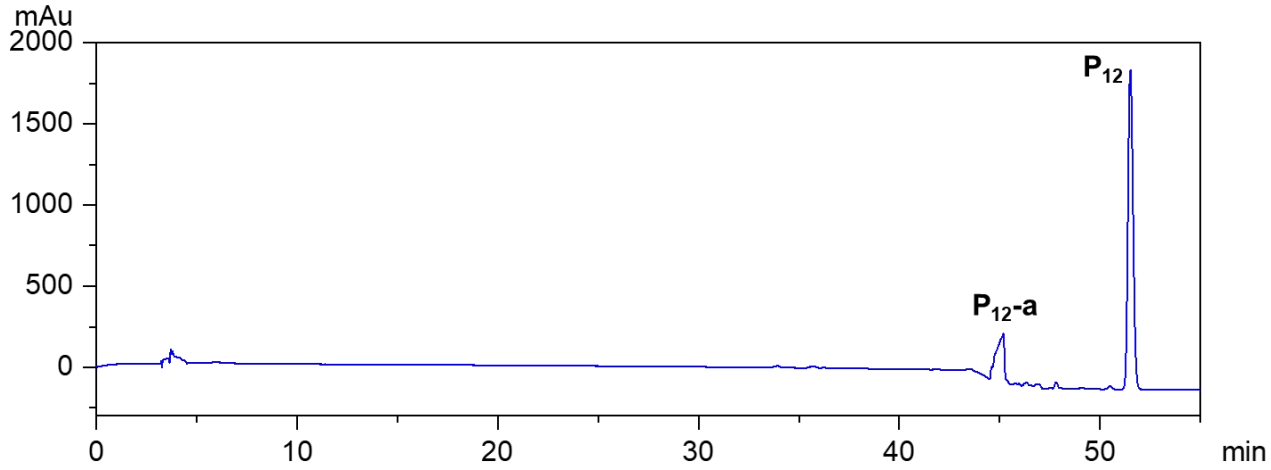

Figure S33. HPLC-UV chromatogram at 395 nm of reaction mixture between $\mathbf{P_{12}}$ and **a**.

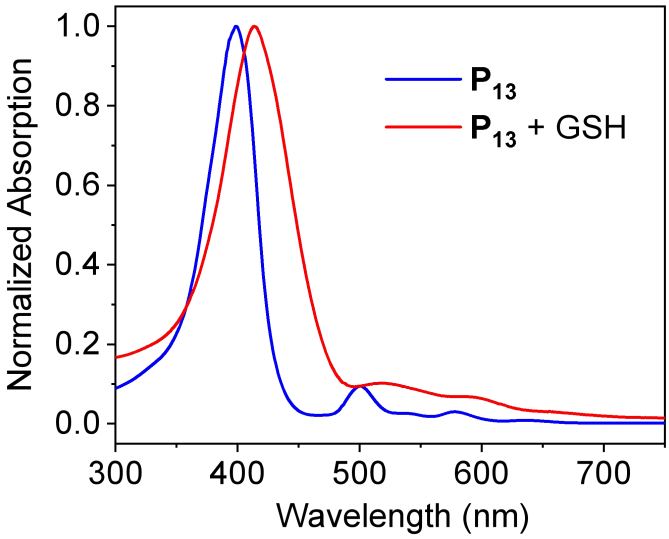

Figure S34. UV-Vis spectrum of of reaction mixture between $\mathbf{P_{13}}$ and **a**.

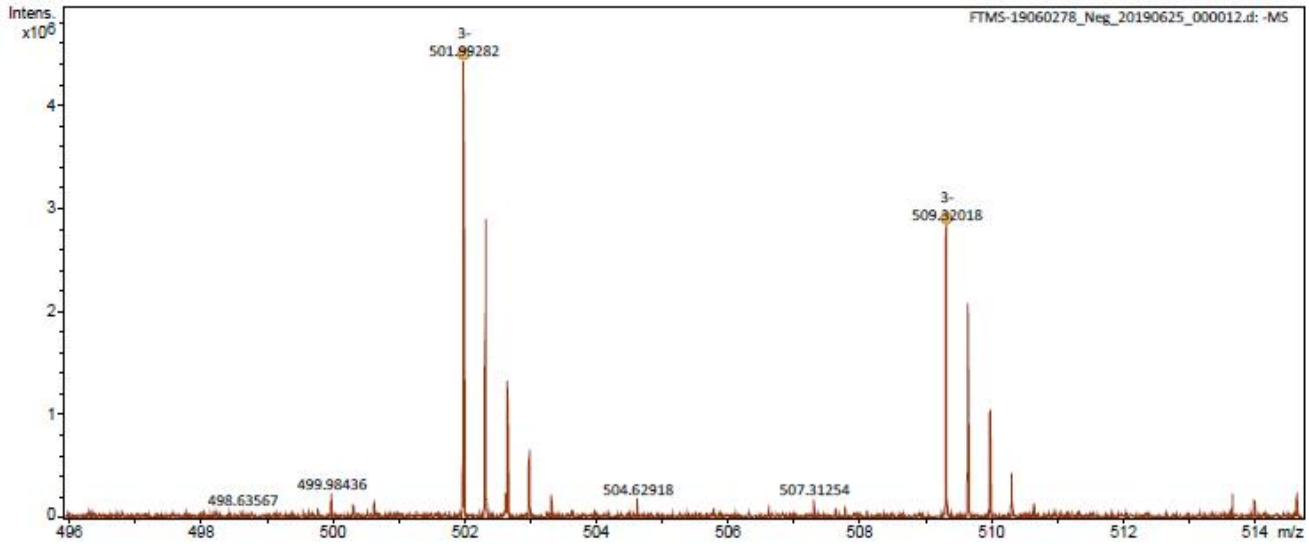

Figure S35. HRMS (ESI$^-$-FTICR) spectrum of **P_{13}-a**.

Using sulfo-DBCO- NH_2 (**h**):

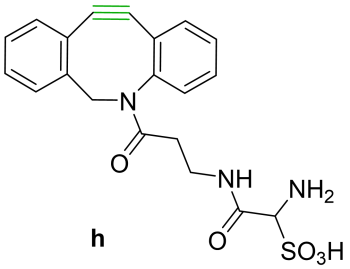

h

P$_9$-ah: HRMS (ESI$^+$-FTICR) m/z [M^{4+}] calcd. for $C_{158}H_{167}F_7N_{35}O_{26}S_5^{4+}$ 815.7823 found: 815.7809.

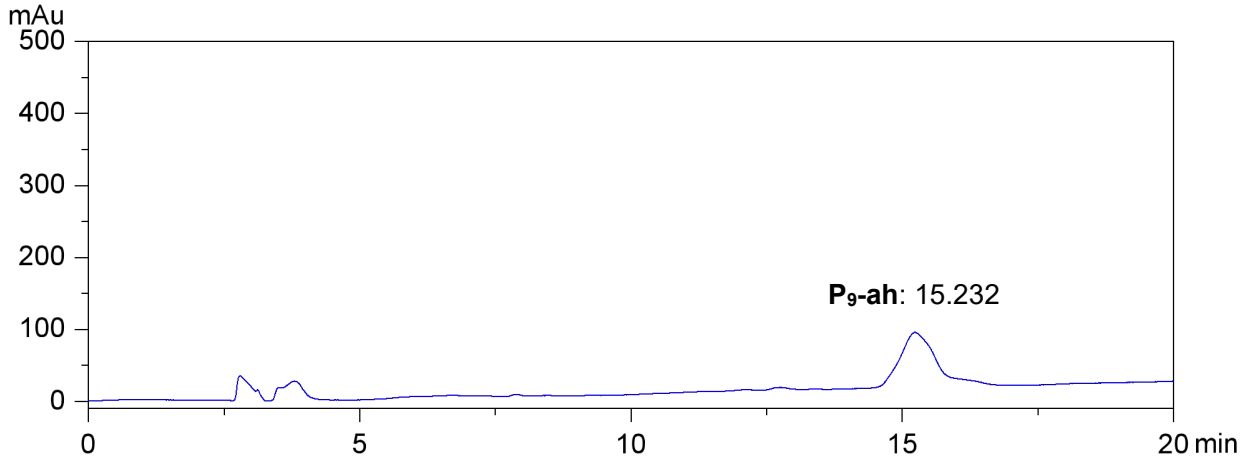

Figure S36. HPLC-UV chromatogram at 395 nm of reaction mixture between **P$_9$-a** and **h**.

Using DBCO-PEG4-NHS (**i**):

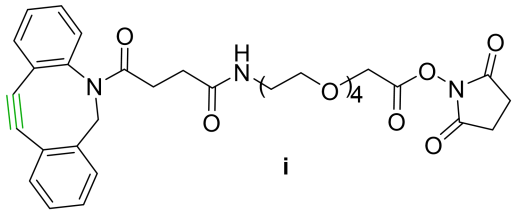

i

P$_9$-ai: HRMS (ESI$^+$-FTICR) m/z [M^{4+}] calcd. for C210H240F7N35O46S^{4+} 1038.1776 found: 1038.1747.

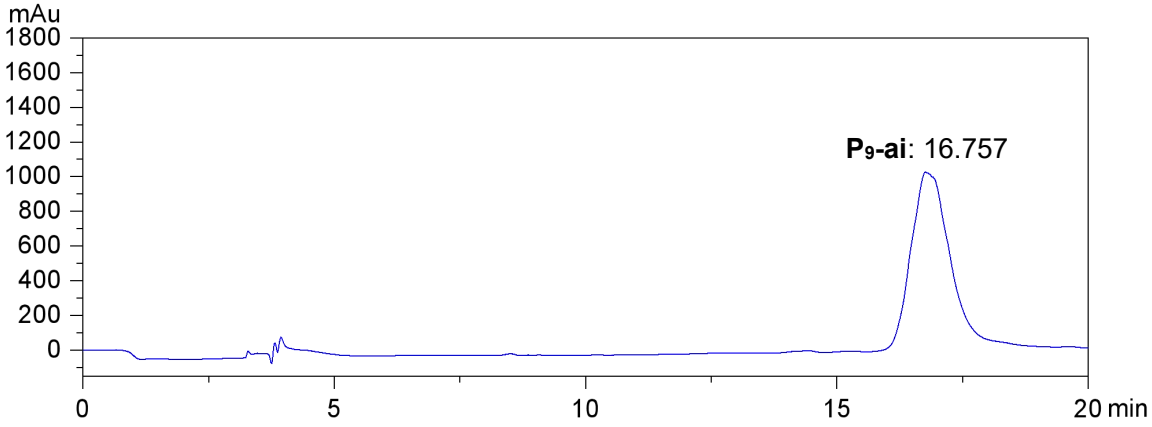

Figure S37. HPLC-UV chromatogram at 395 nm of reaction mixture between **P$_9$-a** and **i**.

Using Disulfo-Cy5-DBCO (**j**):

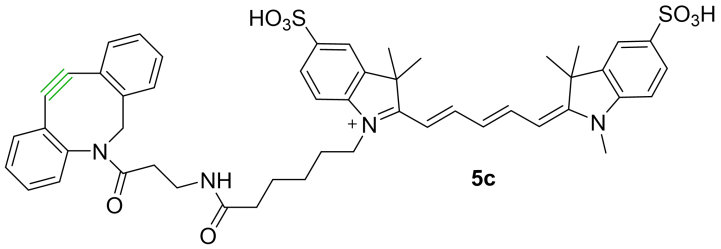

5c

P$_9$-aj: HRMS (ESI$^+$-FTICR) m/z [M-H]$^{3+}$ calcd. for C274H292F7N39O38S9^{3+} 1718.9825 found: 1718.9794.

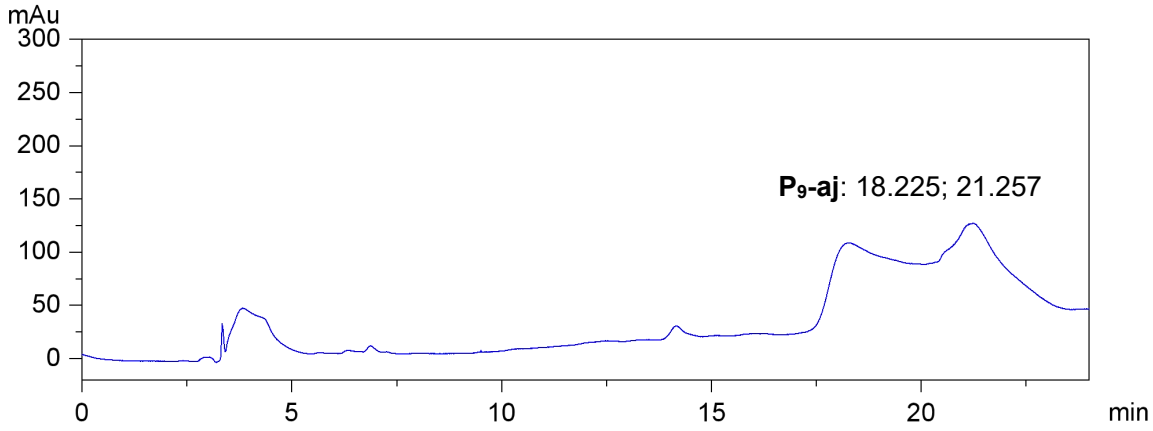

Figure S38. HPLC-UV chromatogram at 395 nm of reaction mixture between **P$_9$-a** and **j**.

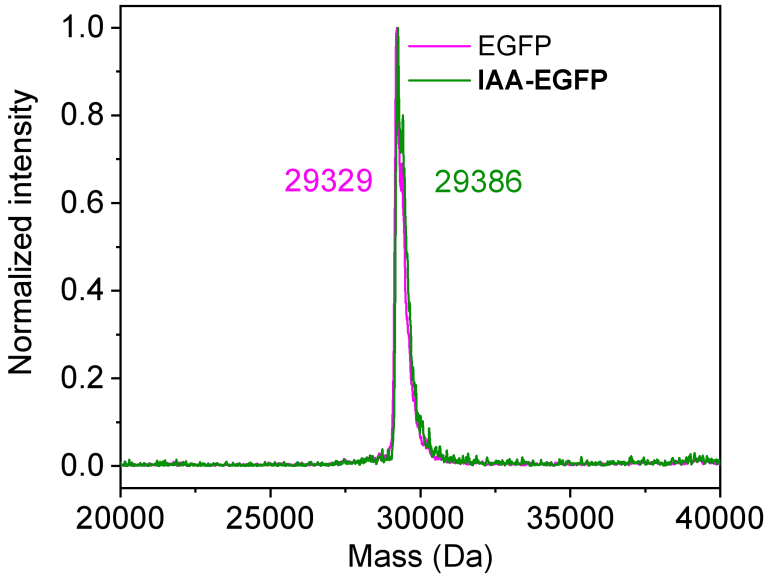

Figure S39. MALDI-TOF spectra of EGFP (magenta) and **IAA-EGFP** (green).

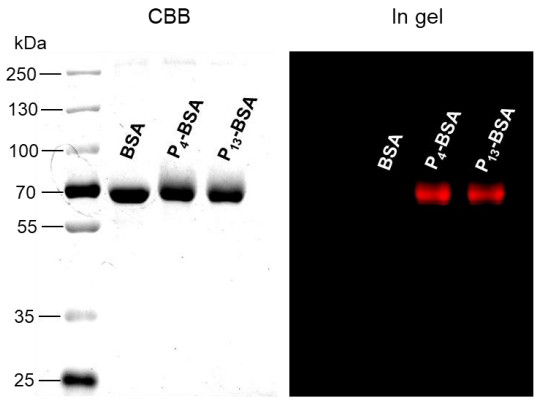

Figure S40. SDS-PAGE gel of *β*-fluorine-cysteine S_NAr reaction mixtures between BSA and **P4**/**P13**. Coomassie brilliant blue (CBB)-stained gel showed increased protein weights after *β*-fluorine-cysteine S_NAr reaction. In gel fluorescence scanning showed porphyrinic emission (red).

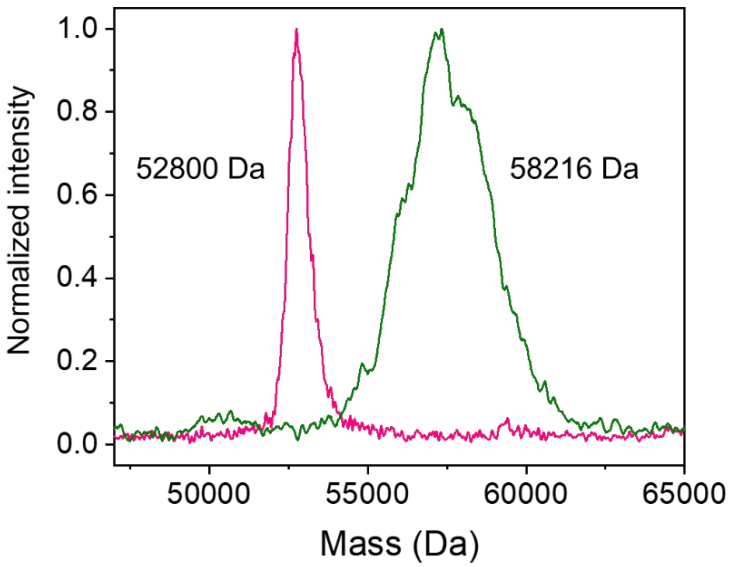

Figure S41. MALDI-TOF spectrum of free Sav (magenta) and **P_{13}-Sav** (green).

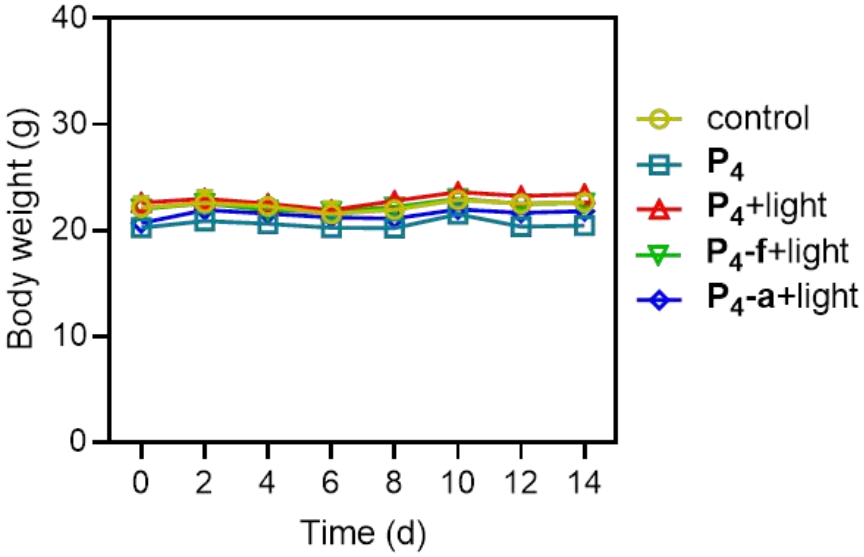

Figure S42. Body weight curves of tumor mice in each treatment group (n = 3, mean ± SD).

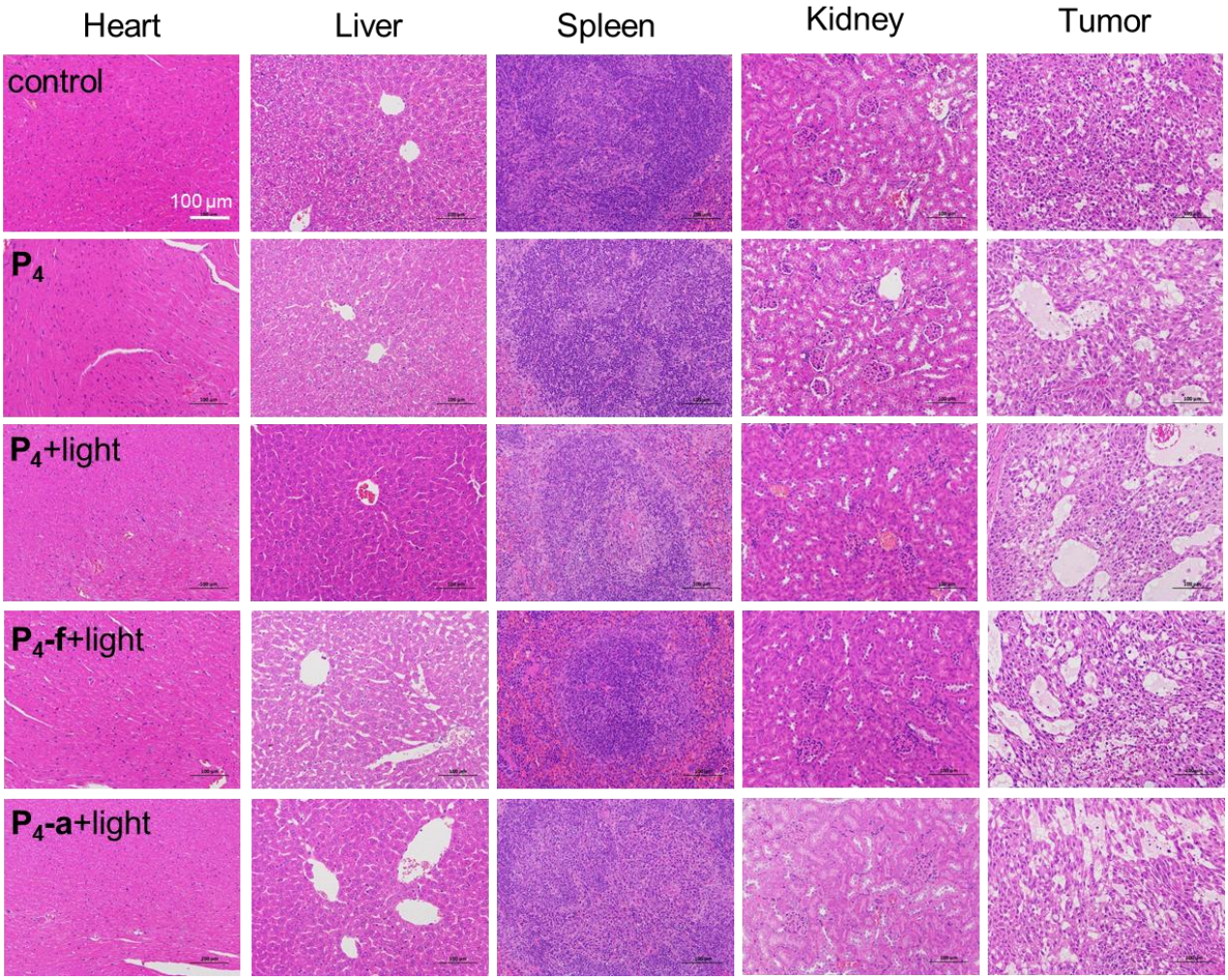

Figure S43. Hematoxylin and eosin (H&E)-stained slice images of major organs from different groups. All images share the same scale bar: 100 μm.

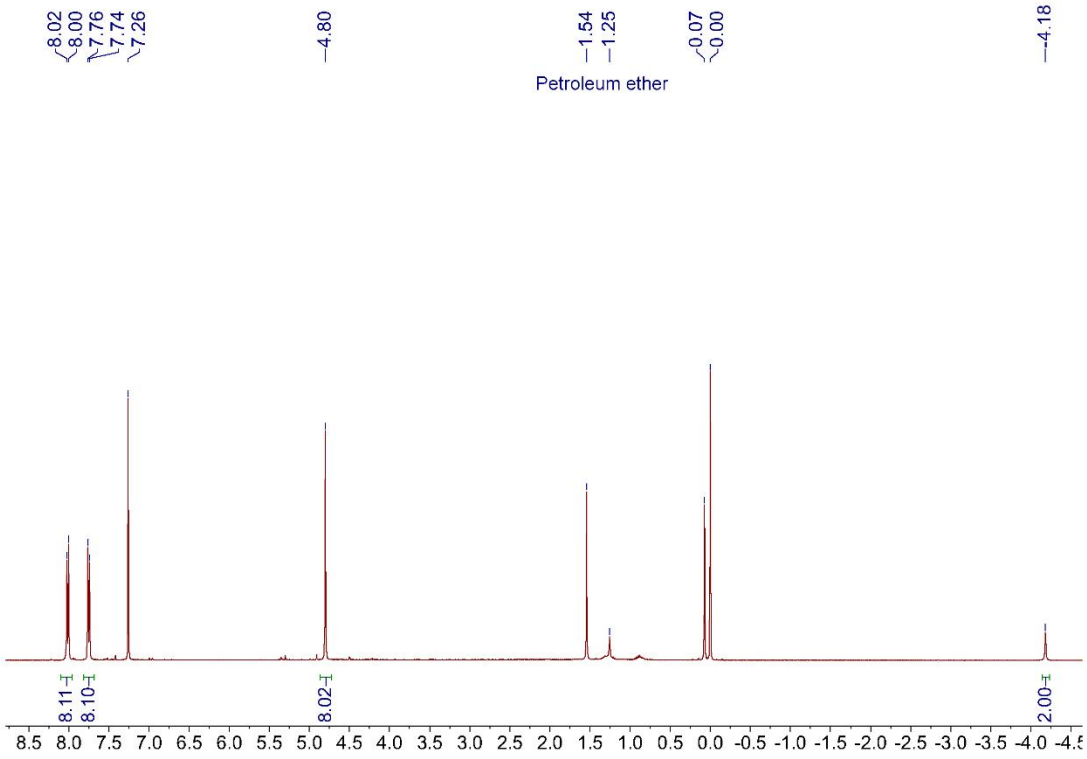

Figure S44. ^{1}H NMR spectrum (400 MHz, Chloroform-*d*) of 2,3,7,8,12,13,17,18-octafluoro-5,10,15,20-tetrakis[4-bromomethylphenyl]porphyrin.

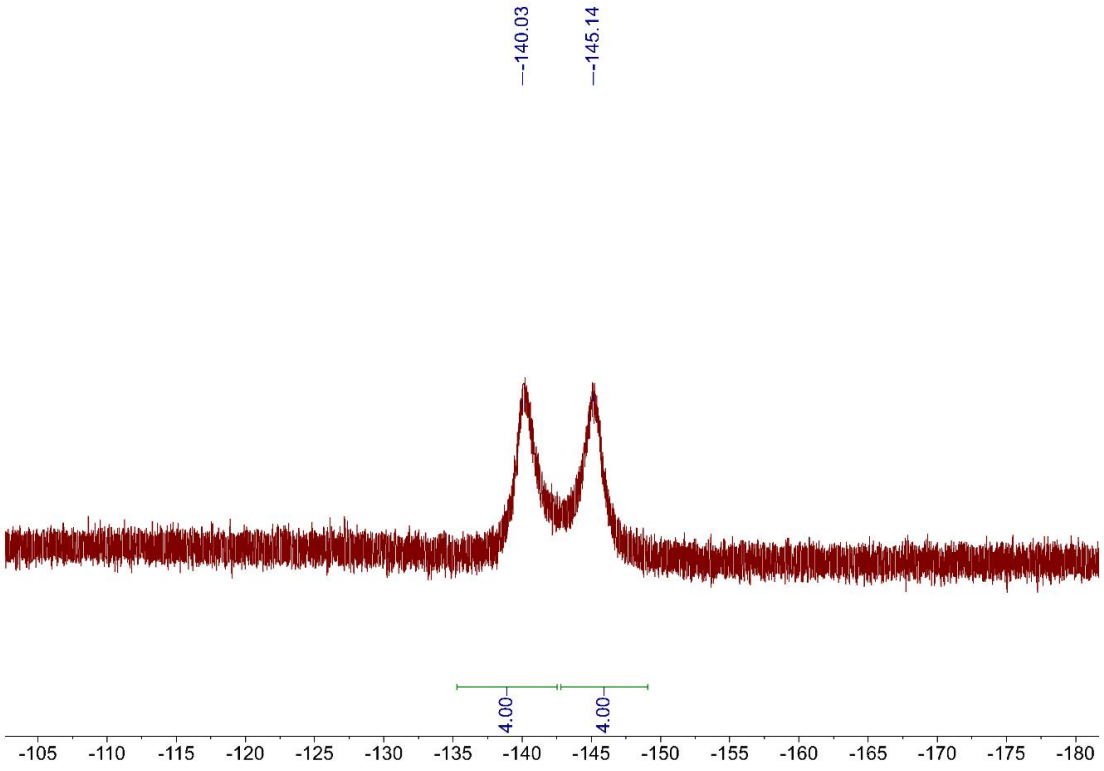

Figure S45. ^{1}H NMR spectrum (400 MHz, Chloroform-*d*) of 2,3,7,8,12,13,17,18-octafluoro-5,10,15,20-tetrakis[4-bromomethylphenyl]porphyrin.

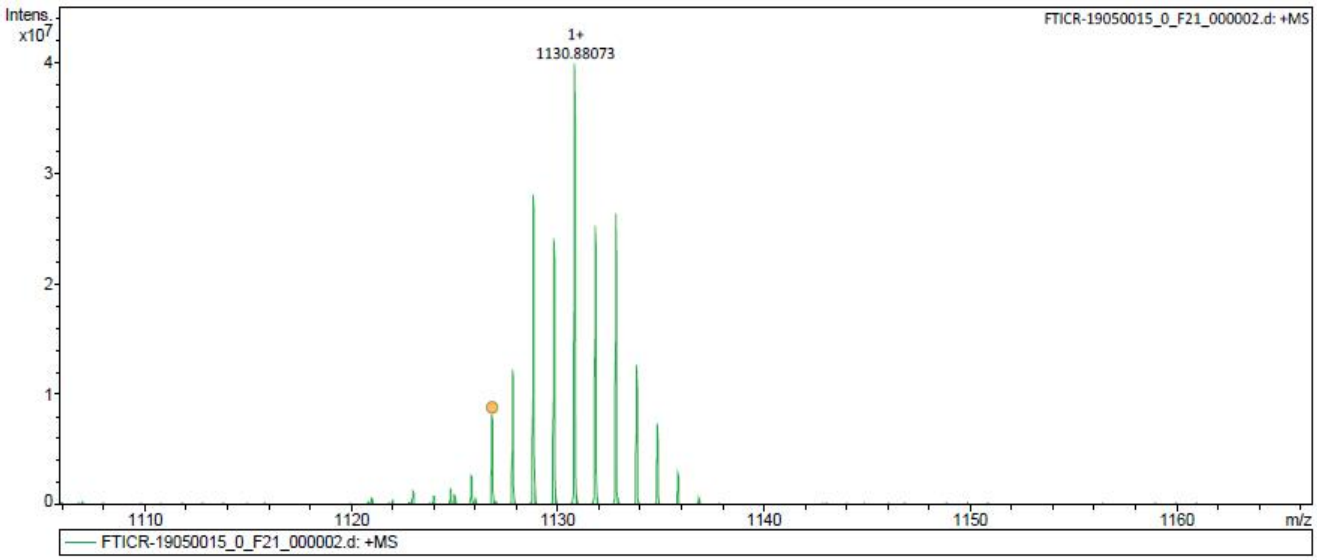

Meas. m/z	#	Ion Formula	Score	m/z	err [ppm]	Mean err [ppm]	mSigma	rdb	e¯ Conf	N-Rule
1126.880516	1	C48H27Br4F8N4	100.00	1126.883599	2.7	-0.5	118.0	40.0	even	ok

Figure S46. HRMS (MALDI-FTICR) spectrum of 2,3,7,8,12,13,17,18-octafluoro-5,10,15,20-tetrakis[4-bromomethylphenyl]porphyrin.

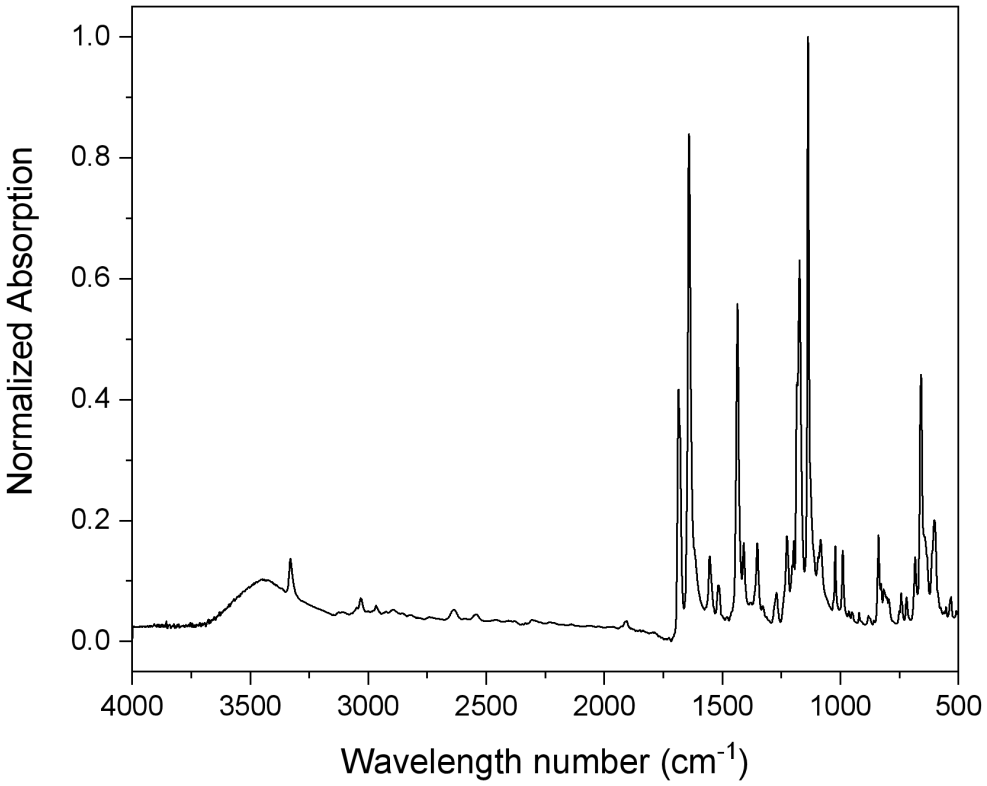

Figure S47. Normalized FT-IR spectrum of 2,3,7,8,12,13,17,18-octafluoro-5,10,15,20-tetrakis[4-bromomethylphenyl]porphyrin.

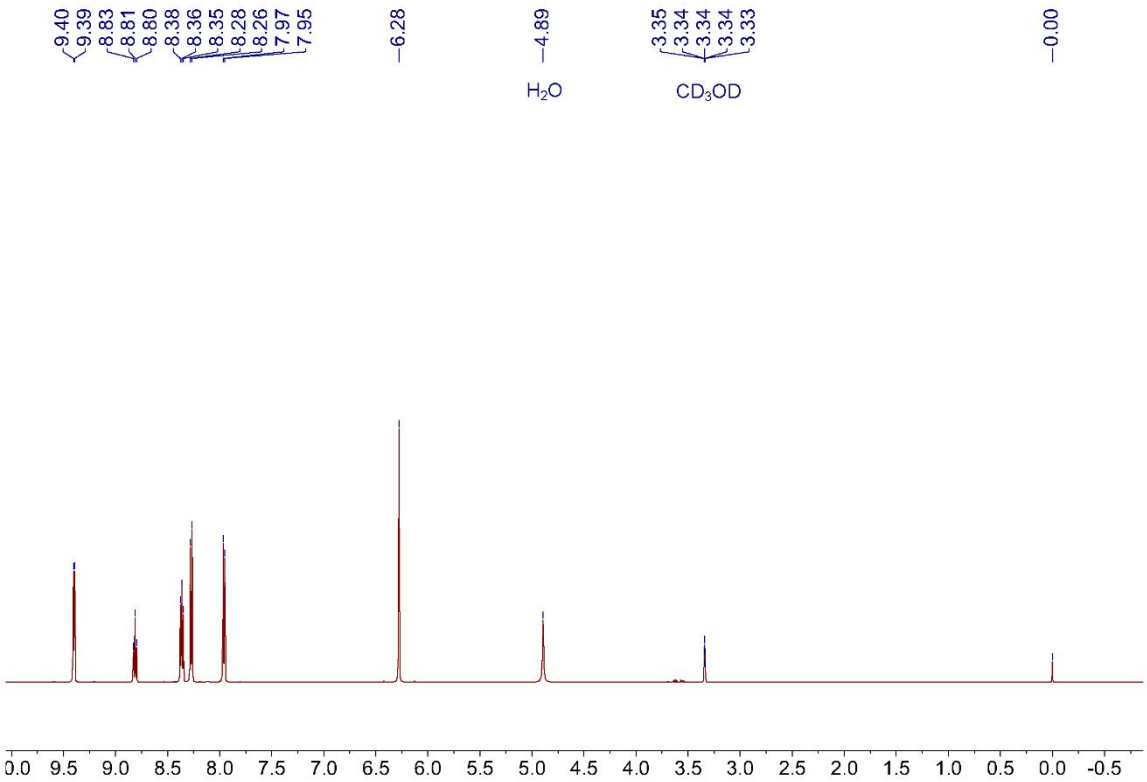

Figure S48. ^{1}H NMR spectrum (500 MHz, Methanol-d_4) of **P$_4$**.

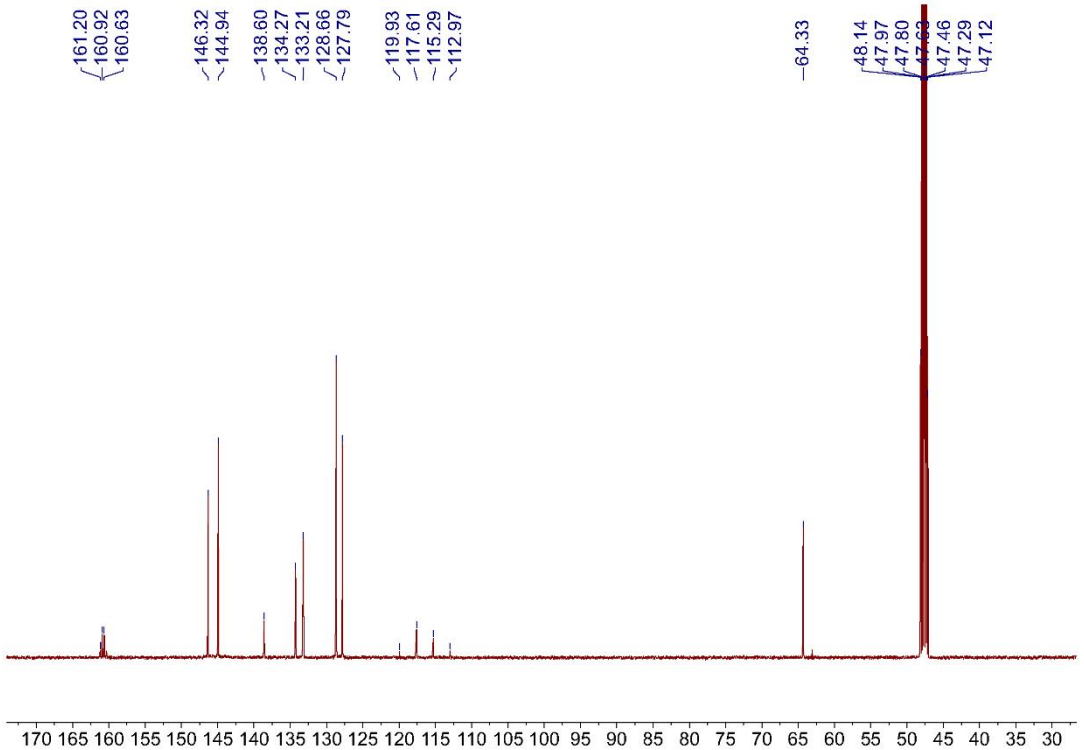

Figure S49. ^{13}C NMR spectrum (126 MHz, Methanol-d_4) of **P$_4$**.

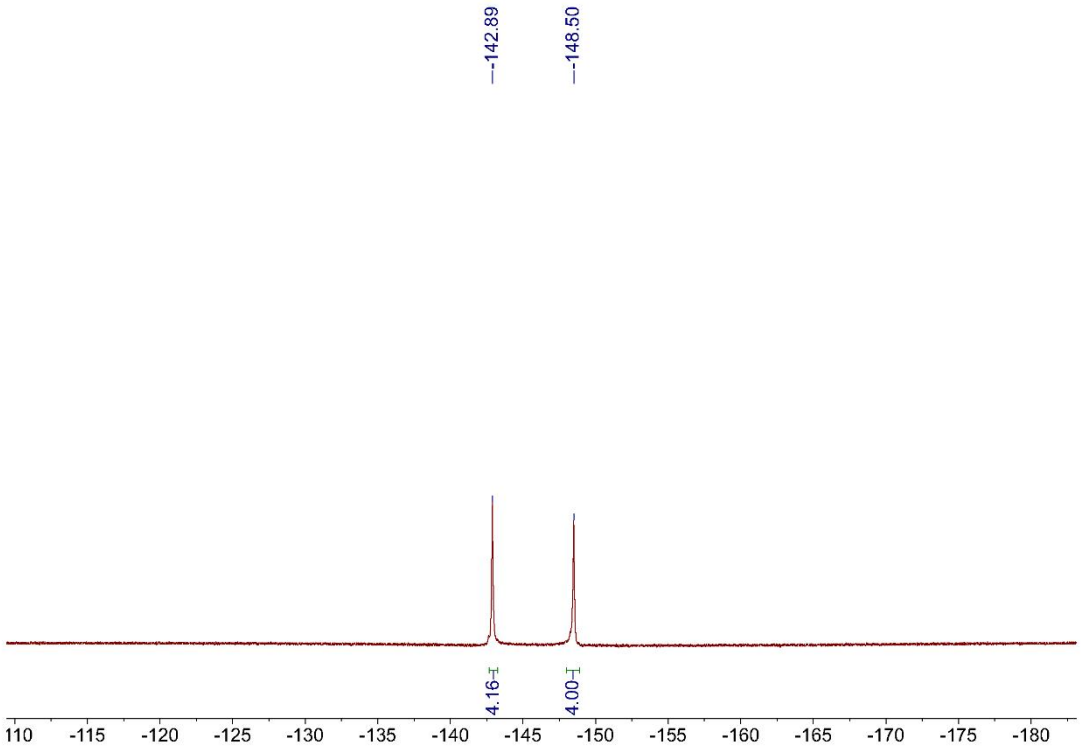

Figure S50. ^{19}F NMR spectrum (471 MHz, Methanol-d_4) of **P$_4$**.

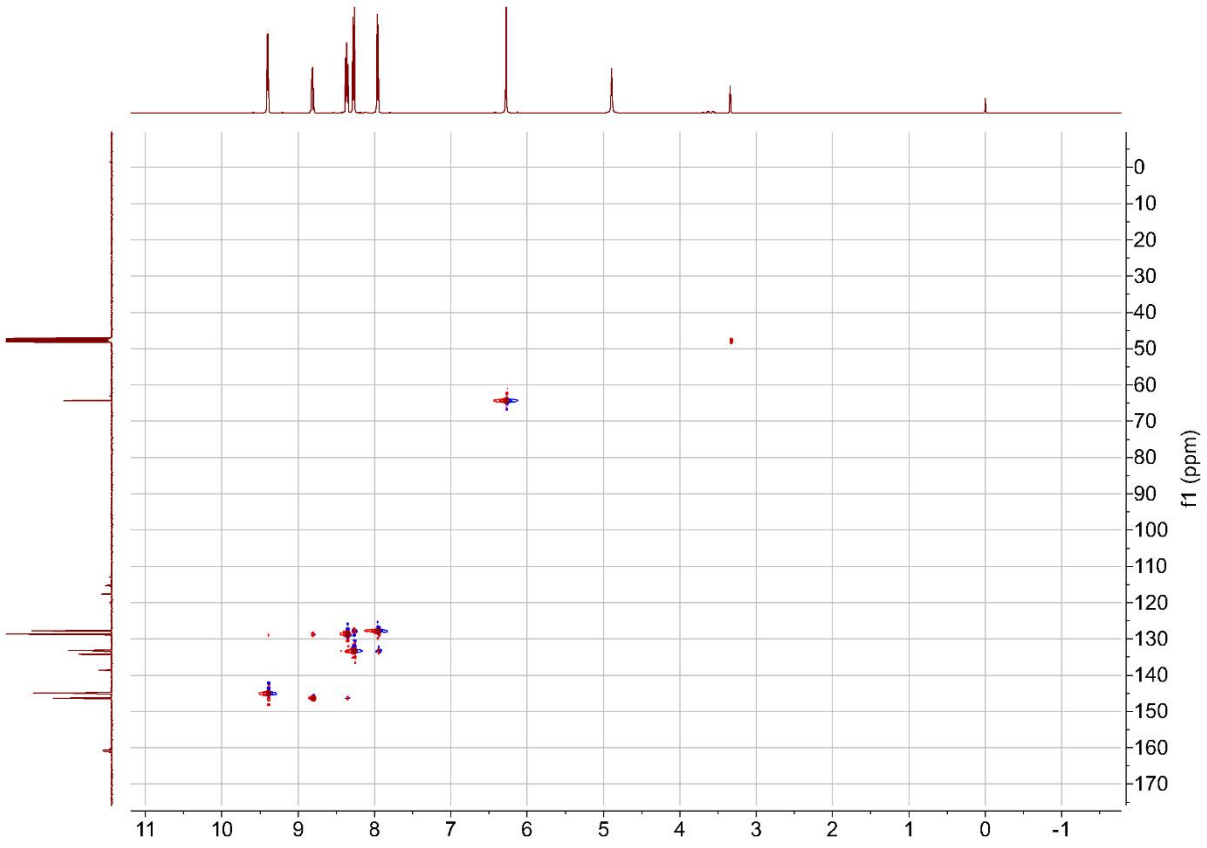

Figure S51. HSQC NMR spectrum (500 MHz) of **P$_4$**.

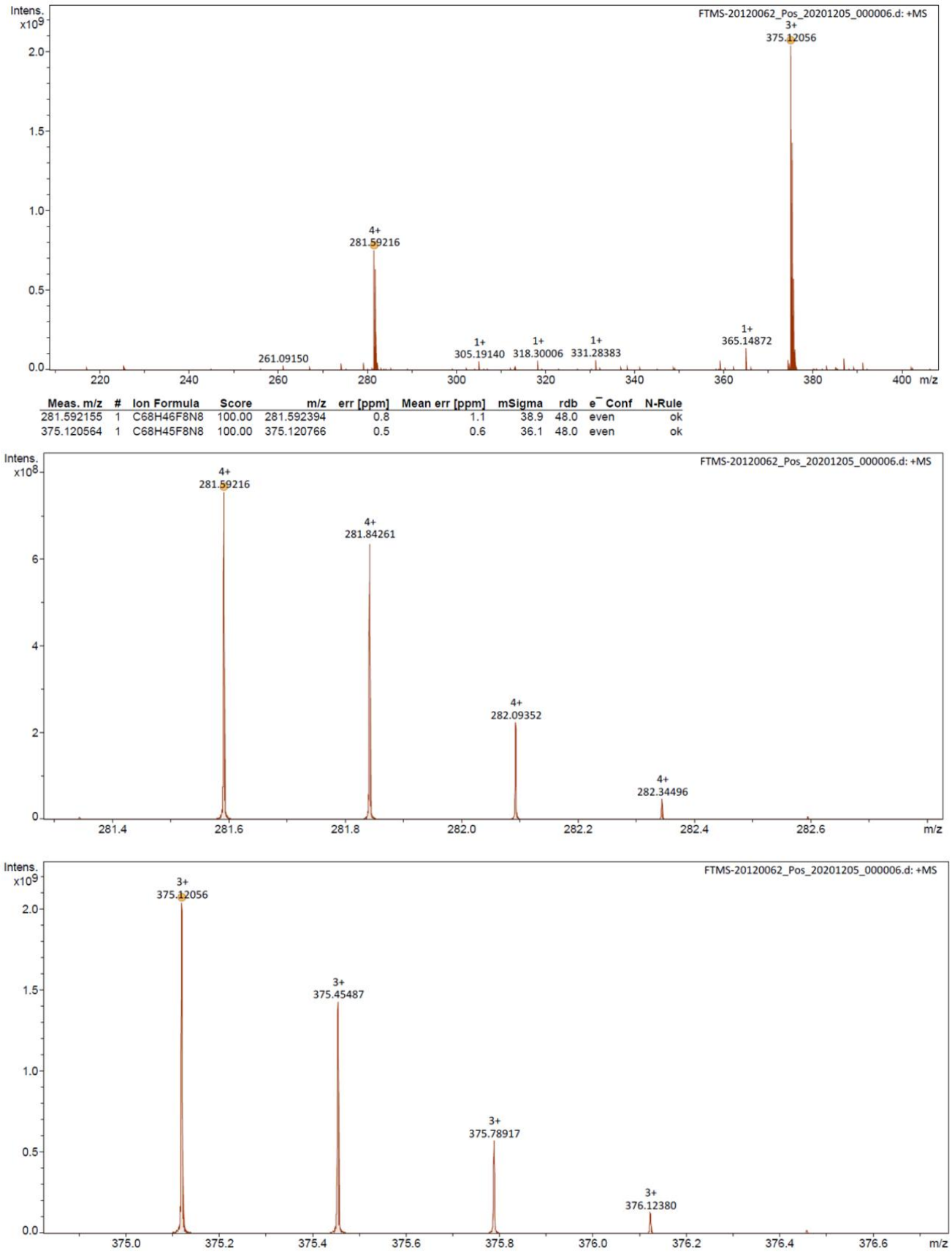

Meas. m/z	#	Ion Formula	Score	m/z	err [ppm]	Mean err [ppm]	mSigma	rdb	e⁻ Conf	N-Rule
281.592155	1	C68H46F8N8	100.00	281.592394	0.8	1.1	38.9	48.0	even	ok
375.120564	1	C68H45F8N8	100.00	375.120766	0.5	0.6	36.1	48.0	even	ok

Figure S52. HRMS (ESI$^+$-FTICR) spectrum of **P$_4$**.

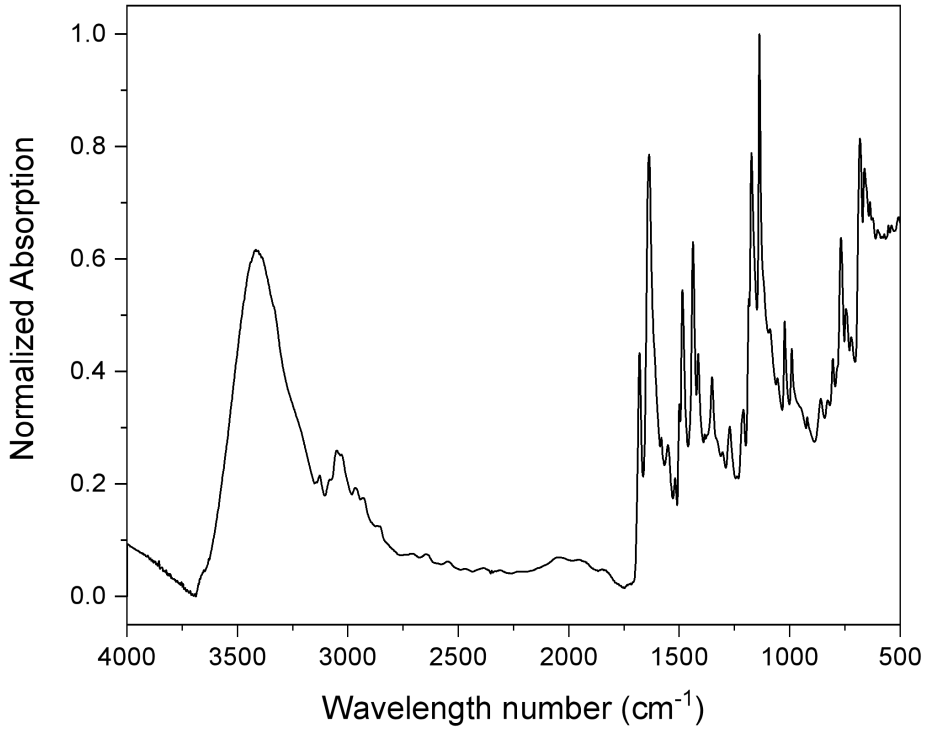

Figure S53. Normalized FT-IR spectrum of $\mathbf{P_4}$.

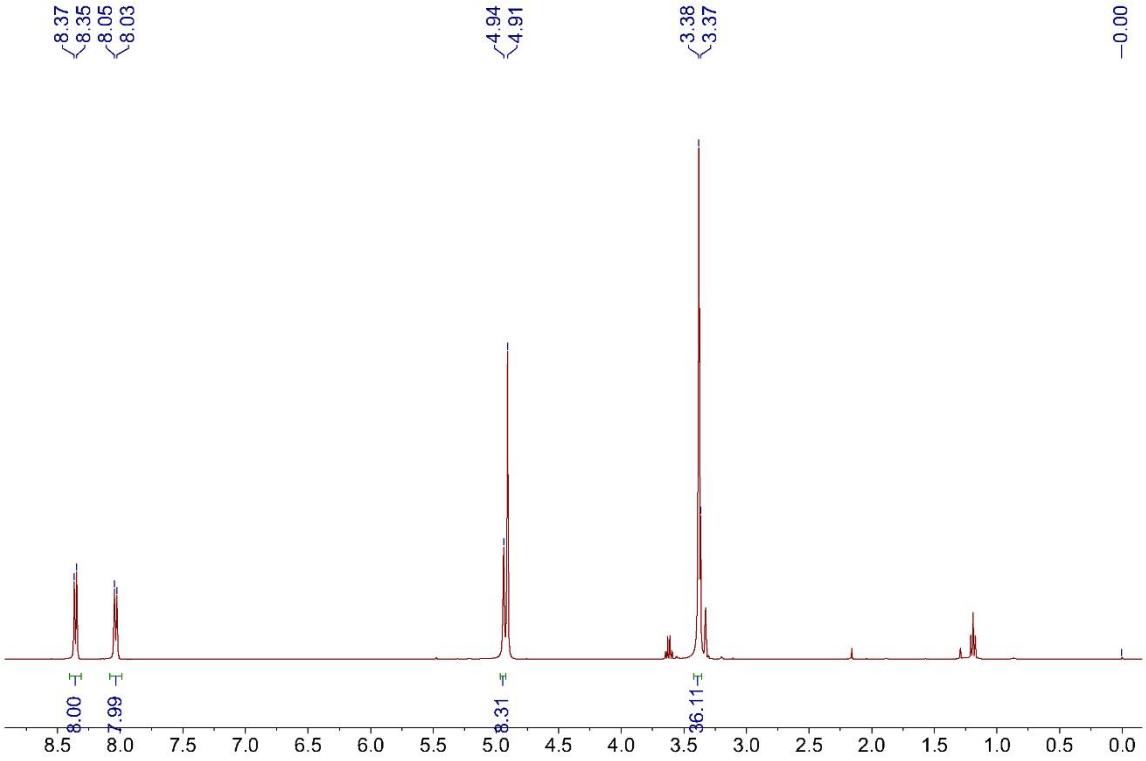

Figure S54. ^{1}H NMR spectrum (400 MHz, Methanol-d_4) of $\mathbf{P_5}$.

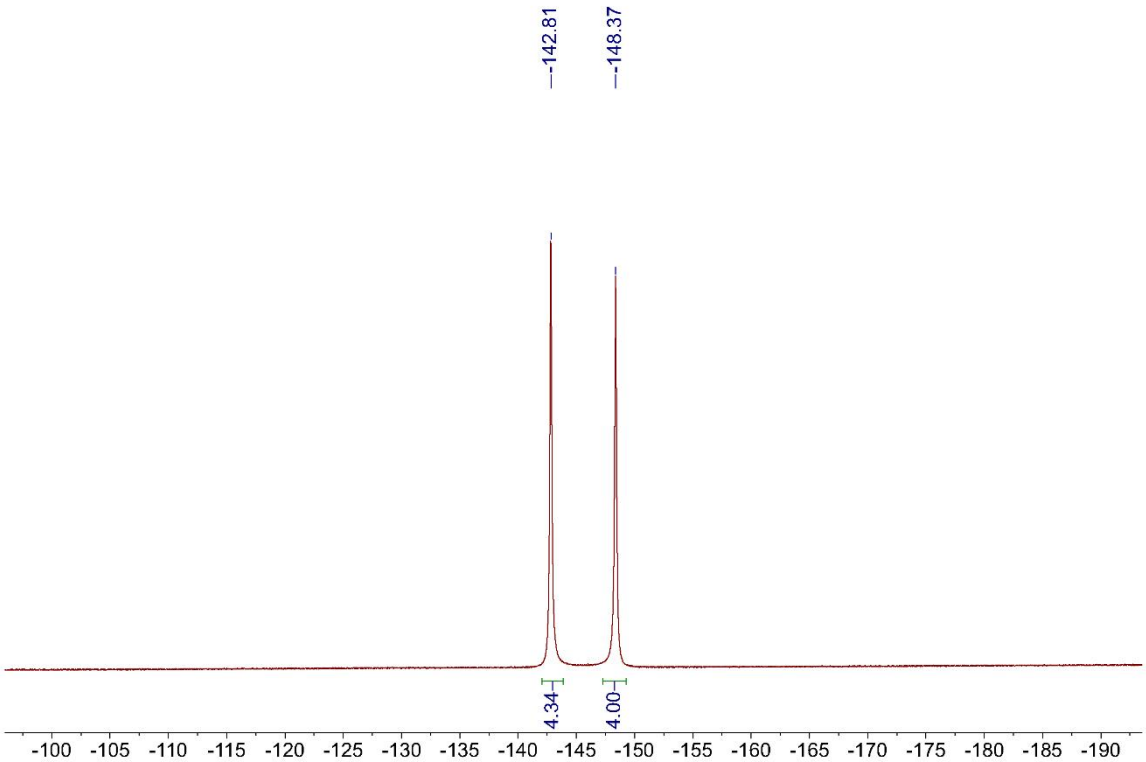

Figure S55. ^{19}F NMR spectrum (471 MHz, Methanol-d_4) of $\mathbf{P_5}$.

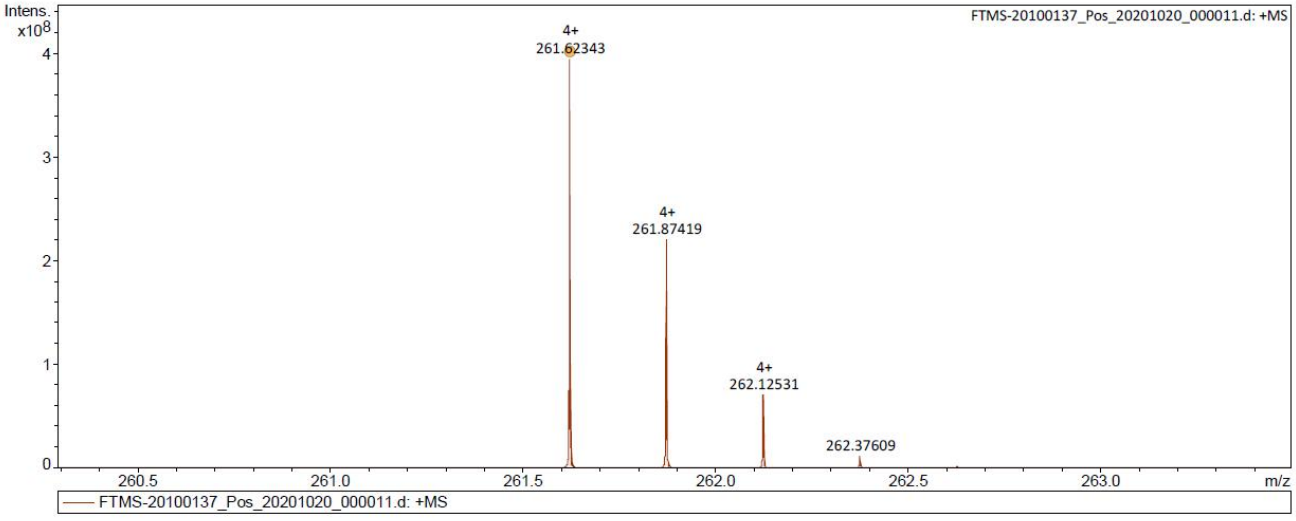

Meas. m/z	#	Ion Formula	Score	m/z	err [ppm]	Mean err [ppm]	mSigma	rdb	e⁻ Conf	N-Rule
261.623432	1	C60H62F8N8	100.00	261.622816	-2.4	-2.9	34.6	10.0	even	ok

Figure S56. HRMS spectrum (ESI$^+$-FTICR) spectrum of **P_5**.

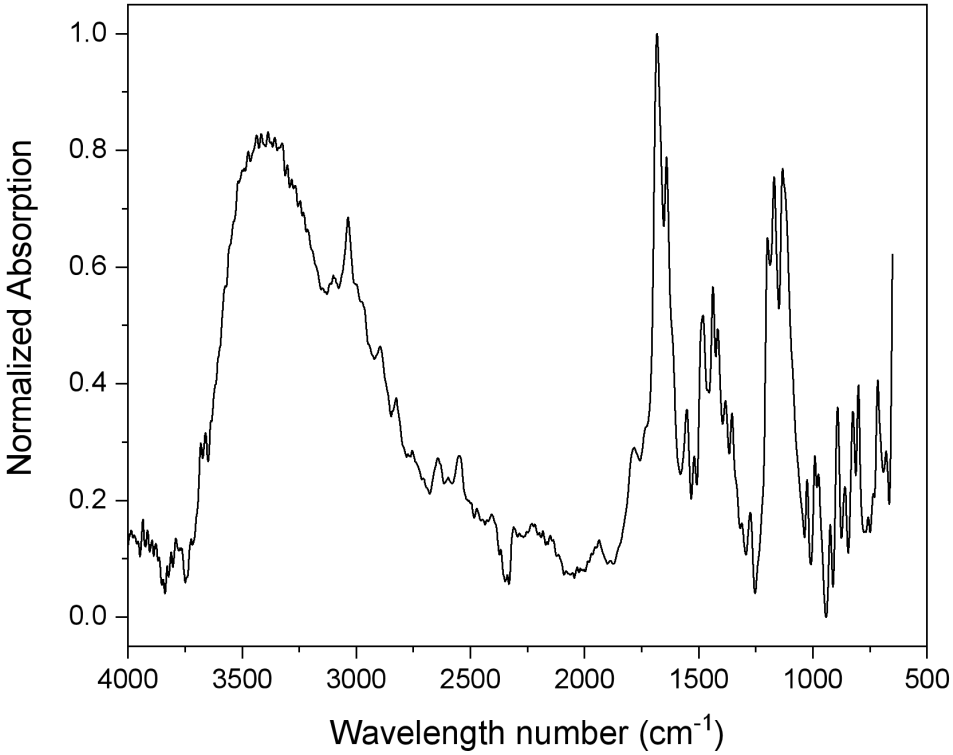

Figure S57. Normalized FT-IR spectrum of $\mathbf{P_5}$.

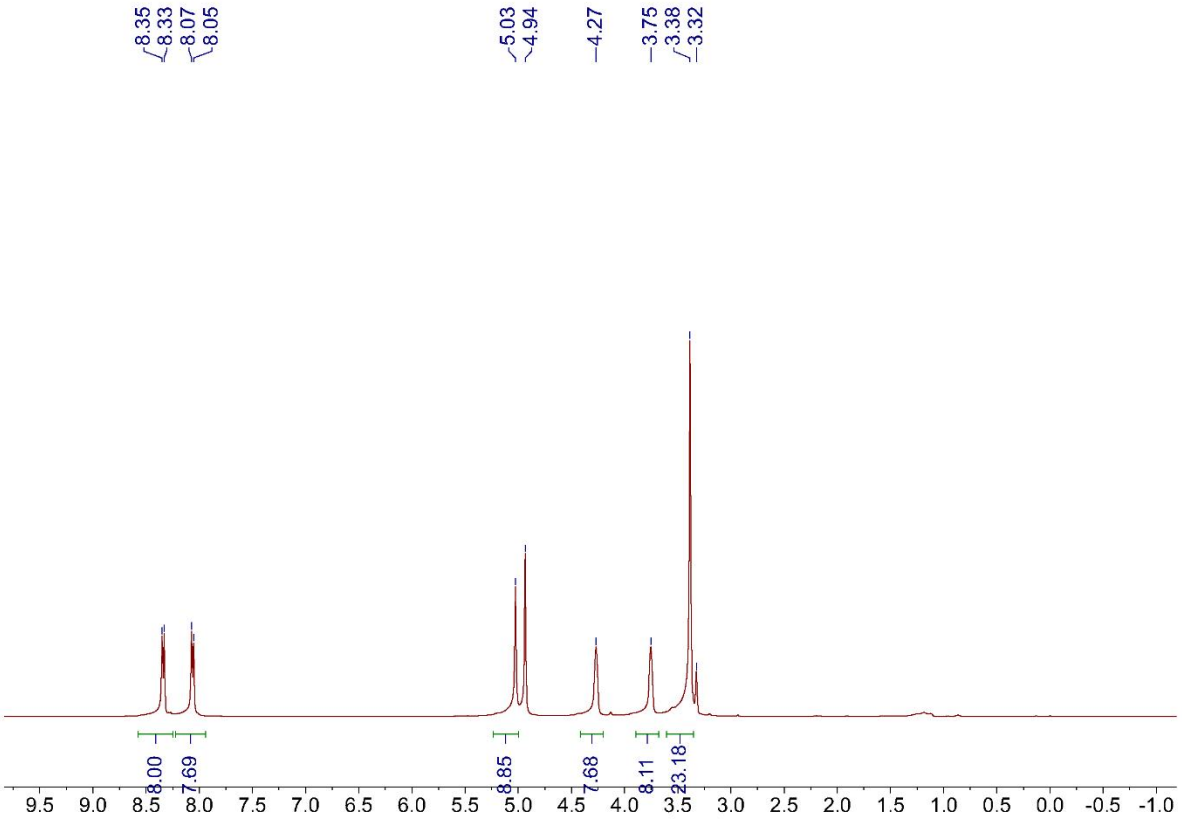

Figure S58. ^{1}H NMR spectrum (400 MHz, Methanol-d_4) of $\mathbf{P_6}$.

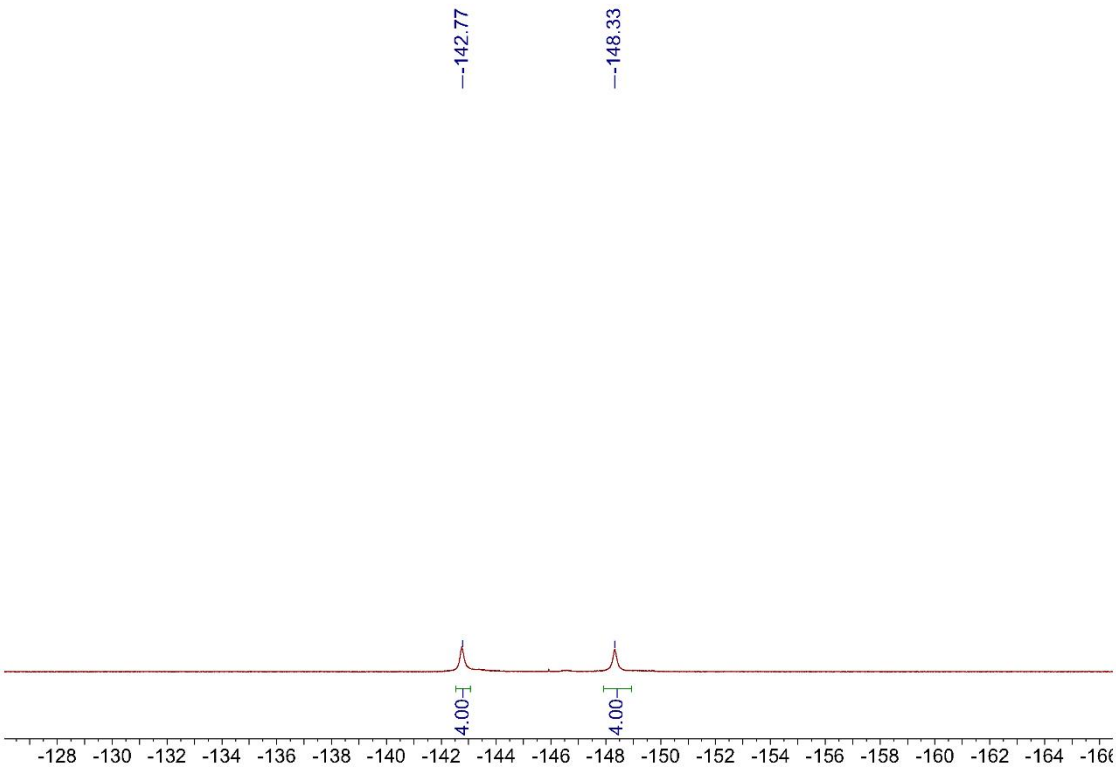

Figure S59. ^{19}F NMR spectrum (471 MHz, Methanol-d_4) of $\mathbf{P_6}$.

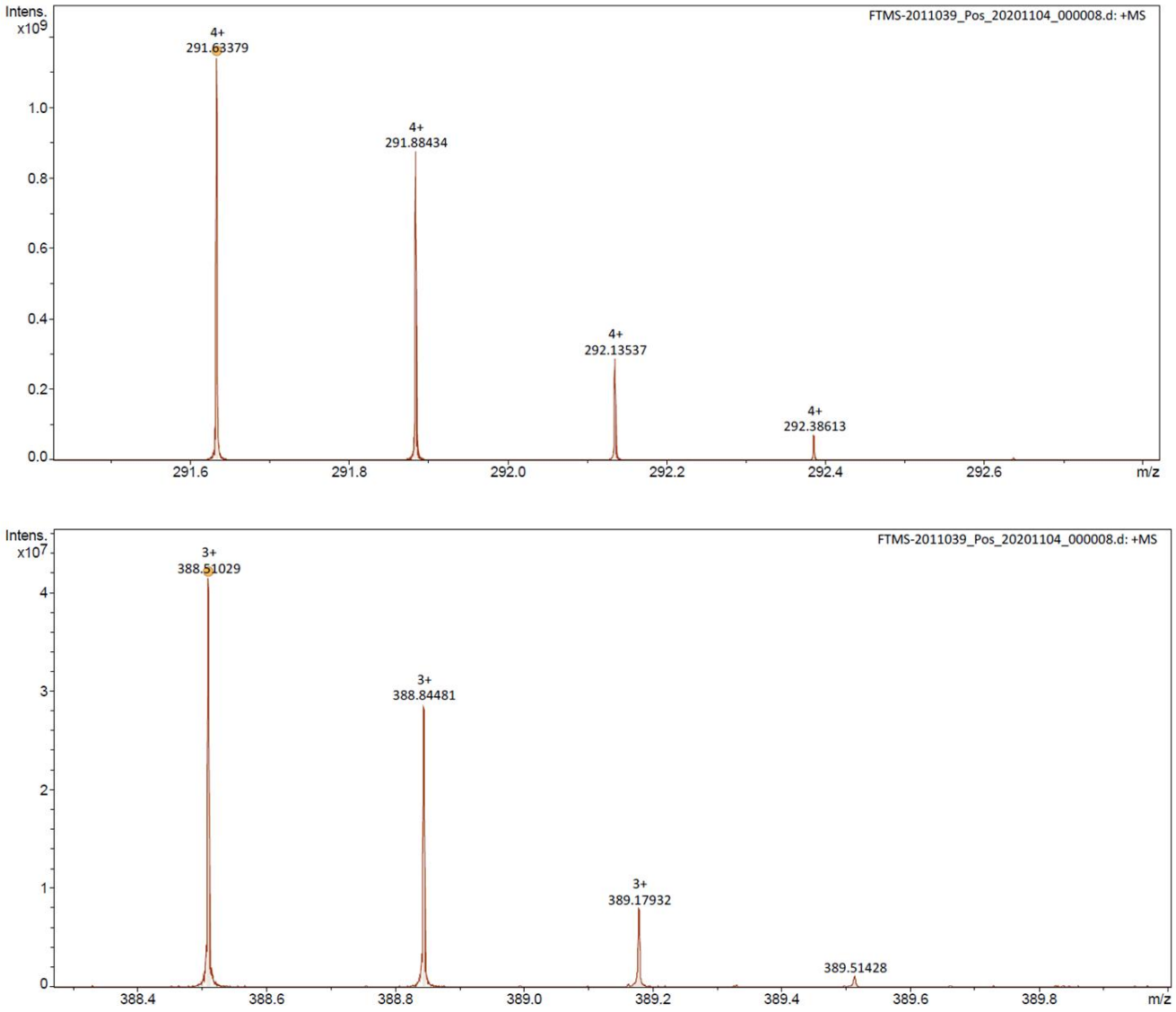

Figure S60. HRMS (ESI$^+$-FTICR) spectrum of $\mathbf{P_6}$.

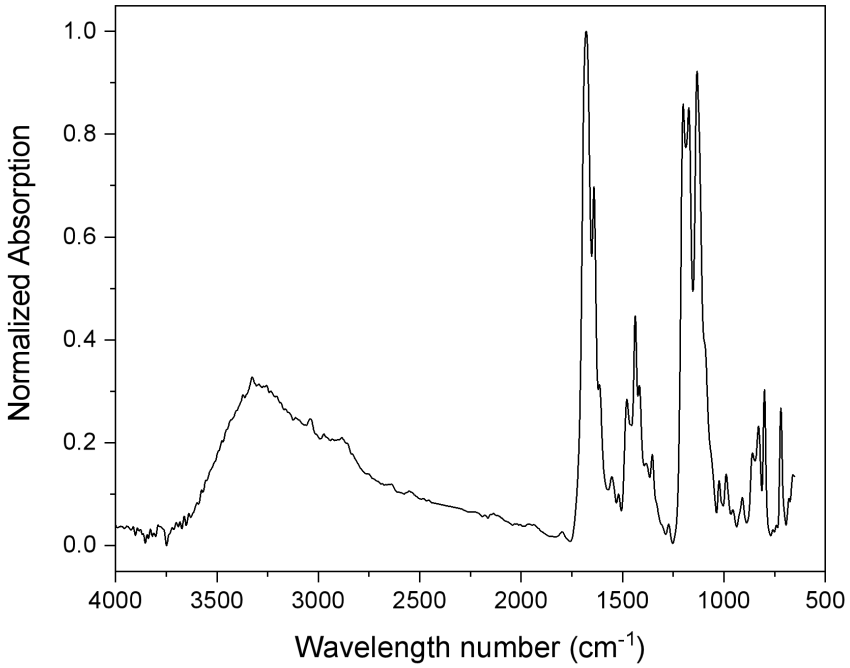

Figure S61. Normalized FT-IR spectrum of $\mathbf{P_6}$.

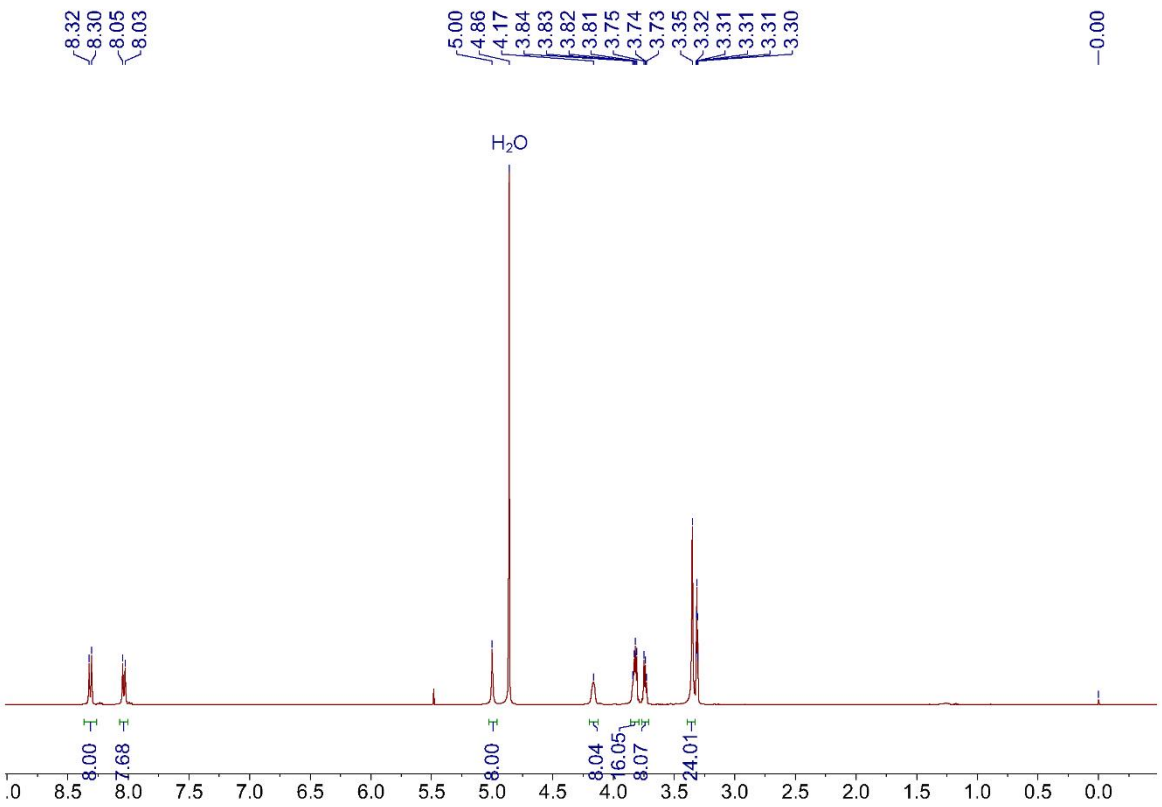

Figure S62. ^{1}H NMR spectrum (400 MHz, Methanol-d_4) of $\mathbf{P_7}$.

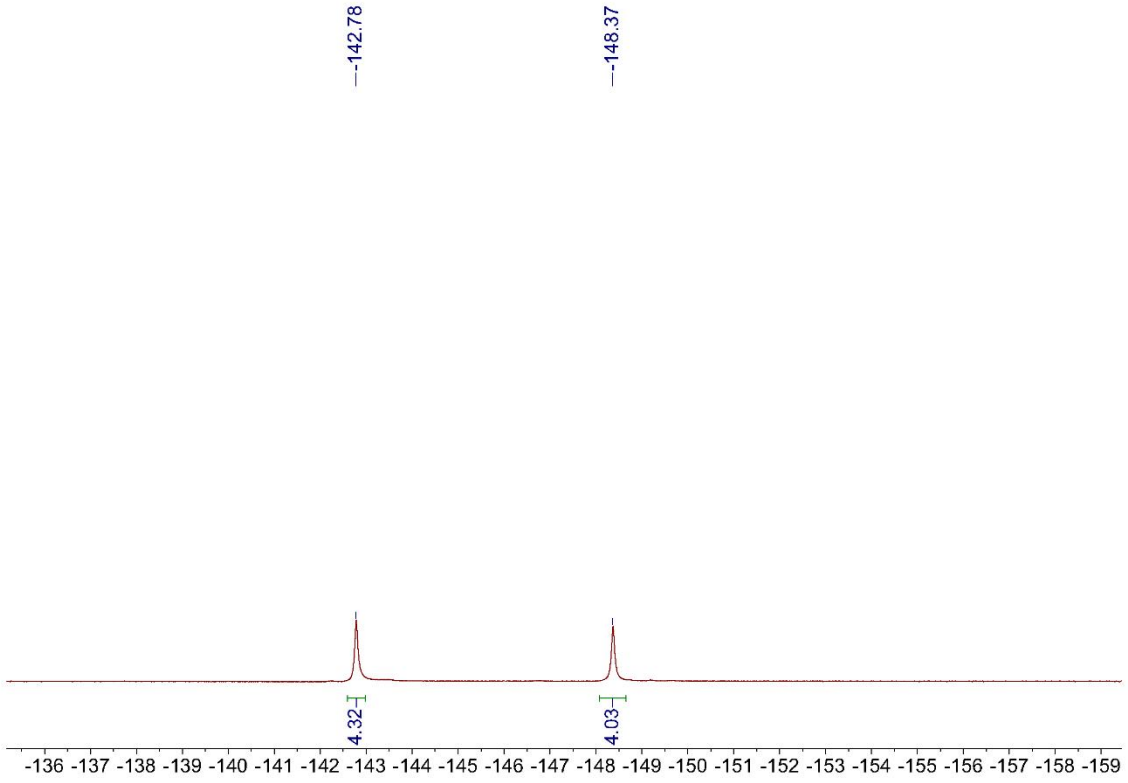

Figure S63. ^{19}F NMR spectrum (471 MHz, Methanol-d_4) of $\mathbf{P_7}$.

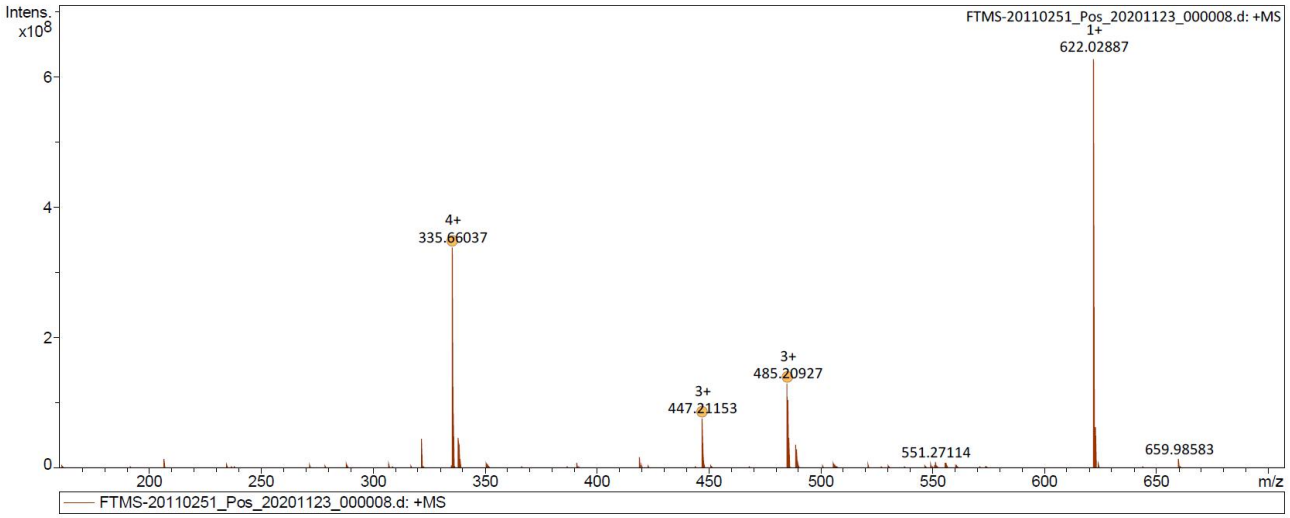

Meas. m/z	#	Ion Formula	Score	m/z	err [ppm]	Mean err [ppm]	mSigma	rdb	e⁻ Conf	N-Rule
335.660366	1	C72H86F8N8O8	100.00	335.660473	0.3	0.0	52.5	32.0	even	ok
447.211531	1	C72H85F8N8O8	100.00	447.211539	0.0	-0.8	16.8	32.0	even	ok
485.209271	1	C74H86F11N8O10	100.00	485.209160	-0.2	-0.7	23.5	32.0	even	ok

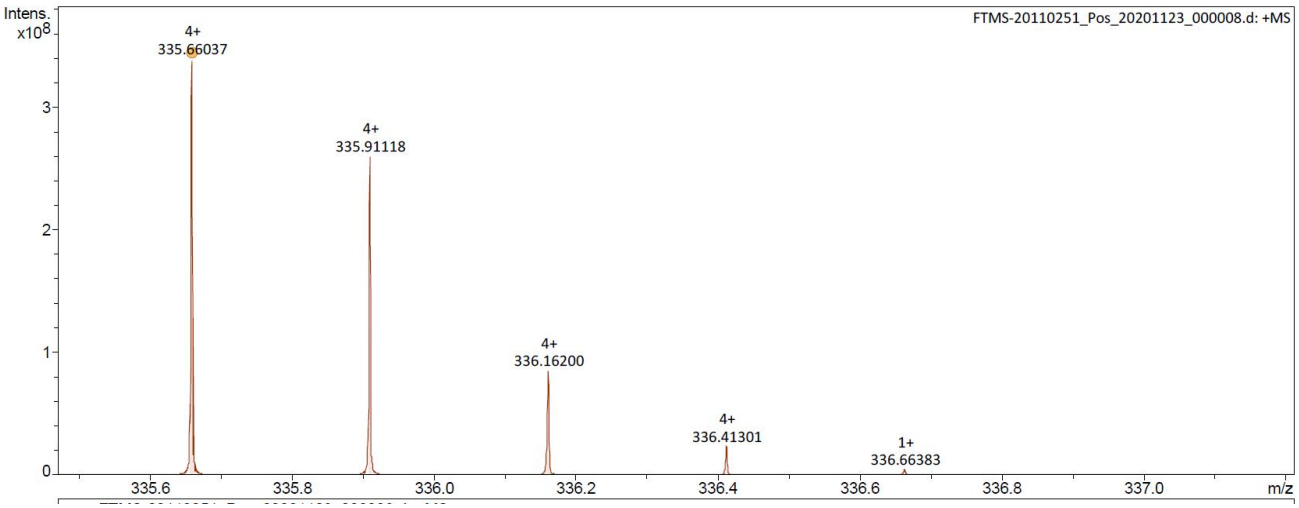

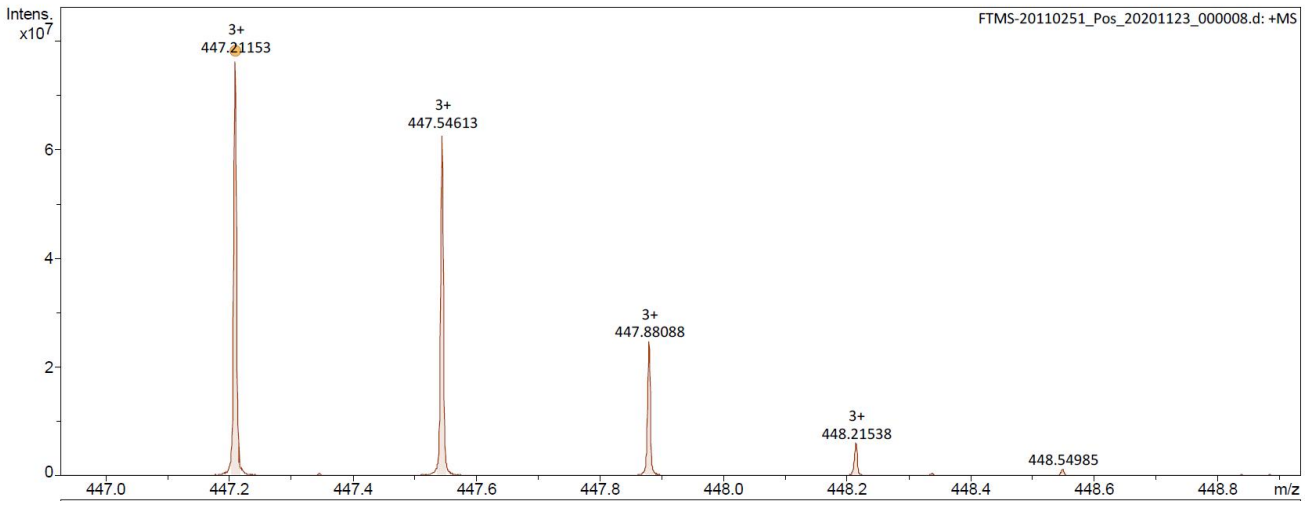

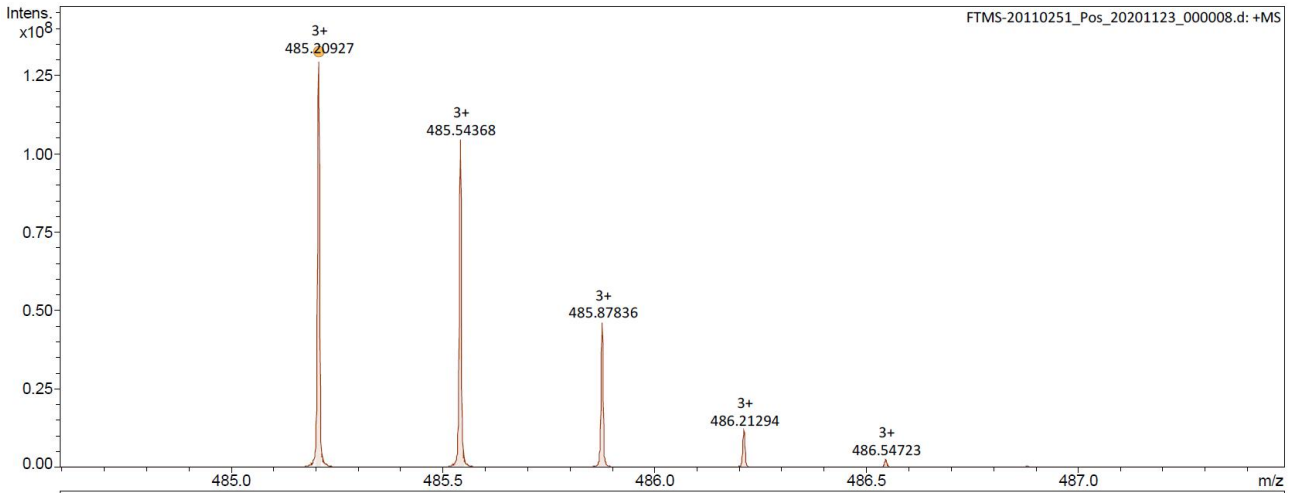

Figure S64. HRMS (ESI+-FTICR) spectrum of $\mathbf{P_7}$.

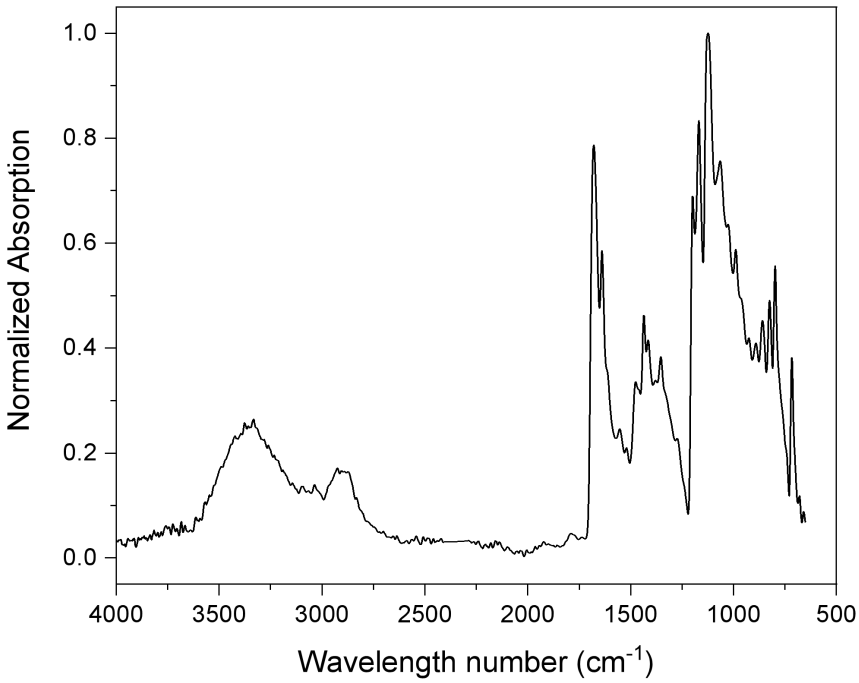

Figure S65. Normalized FT-IR spectrum of $\mathbf{P_7}$.

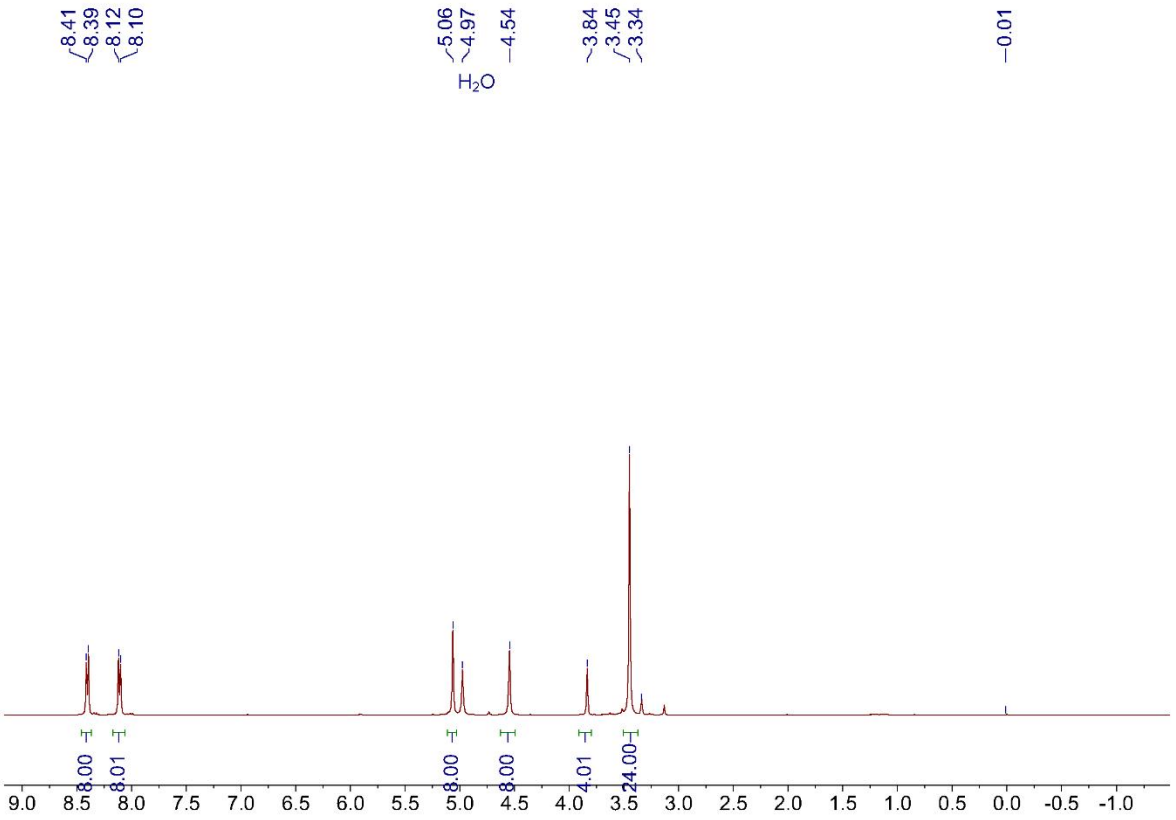

Figure S66. ^{1}H NMR spectrum (400 MHz, Methanol-d_4) of **P$_8$**.

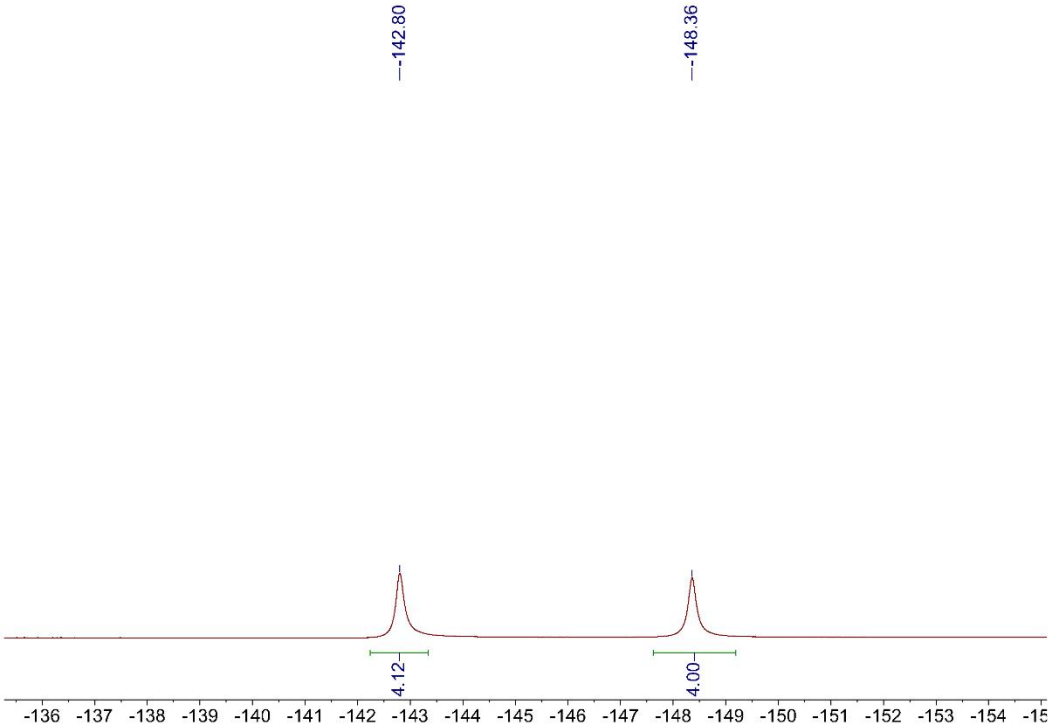

Figure S67. ^{19}F NMR spectrum (471 MHz, Methanol-d_4) of **P$_8$**.

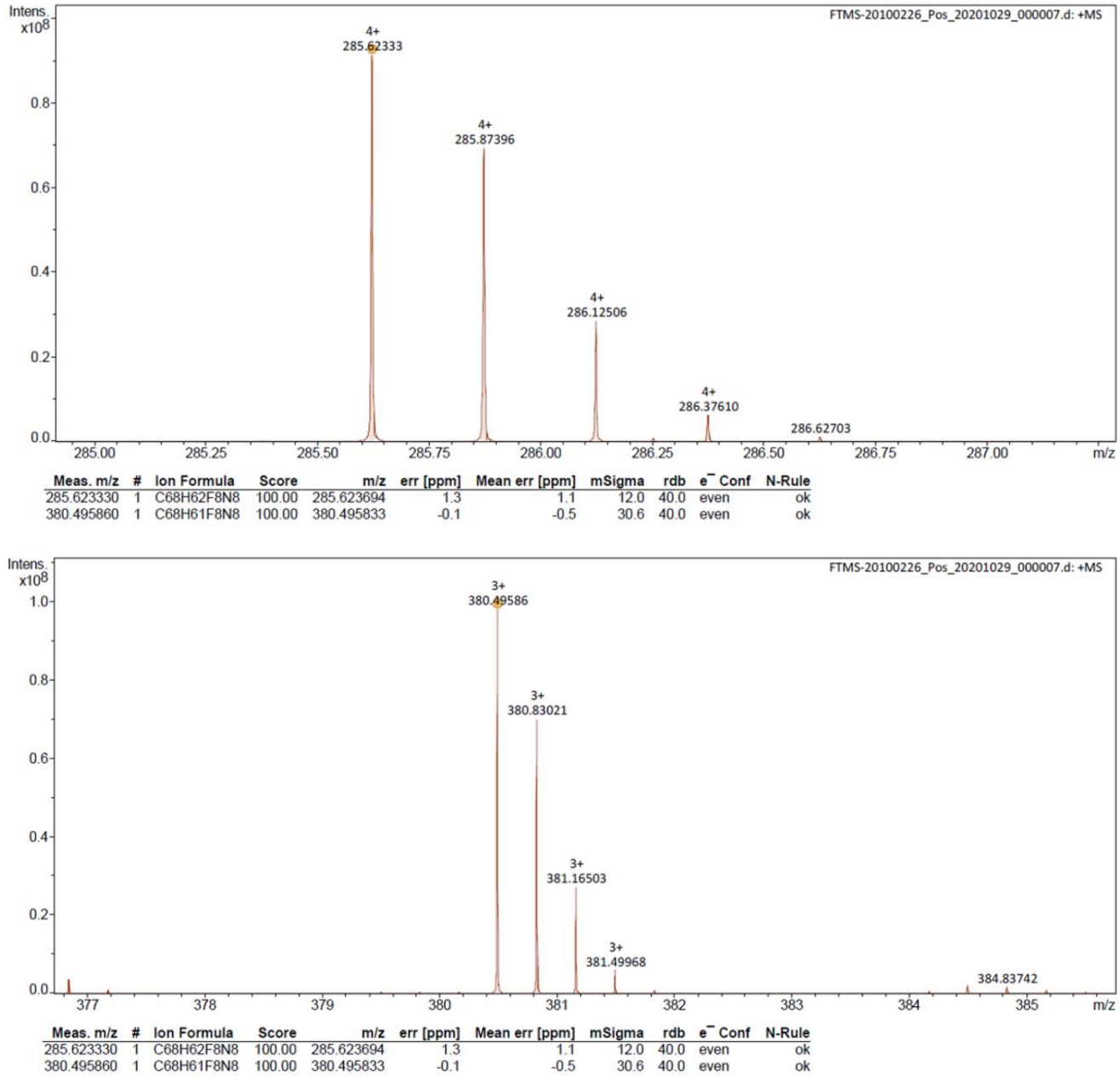

Meas. m/z	#	Ion Formula	Score	m/z	err [ppm]	Mean err [ppm]	mSigma	rdb	e⁻ Conf	N-Rule
285.623330	1	C68H62F8N8	100.00	285.623694	1.3	1.1	12.0	40.0	even	ok
380.495860	1	C68H61F8N8	100.00	380.495833	-0.1	-0.5	30.6	40.0	even	ok

Meas. m/z	#	Ion Formula	Score	m/z	err [ppm]	Mean err [ppm]	mSigma	rdb	e⁻ Conf	N-Rule
285.623330	1	C68H62F8N8	100.00	285.623694	1.3	1.1	12.0	40.0	even	ok
380.495860	1	C68H61F8N8	100.00	380.495833	-0.1	-0.5	30.6	40.0	even	ok

Figure S68. HRMS (ESI$^+$-FTICR) spectrum of **P$_8$**.

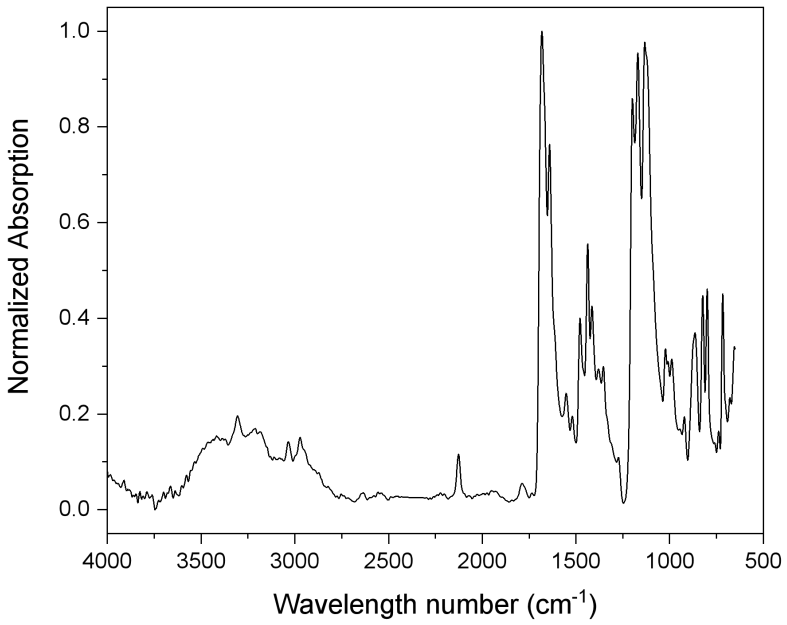

Figure S69. Normalized FT-IR spectrum of $\mathbf{P_8}$.

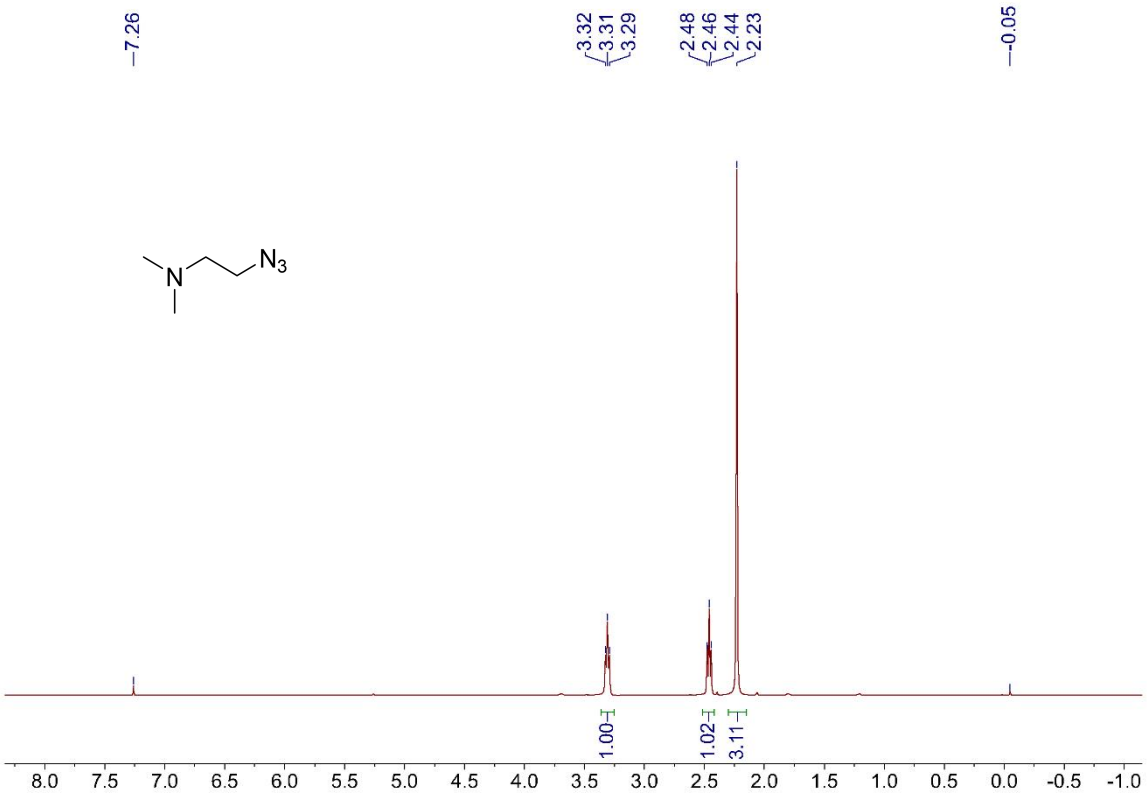

Figure S70. ^{1}H NMR spectrum (400 MHz, Chloroform-*d*) of 2-azido-N,N-dimethylethan-1-amine.

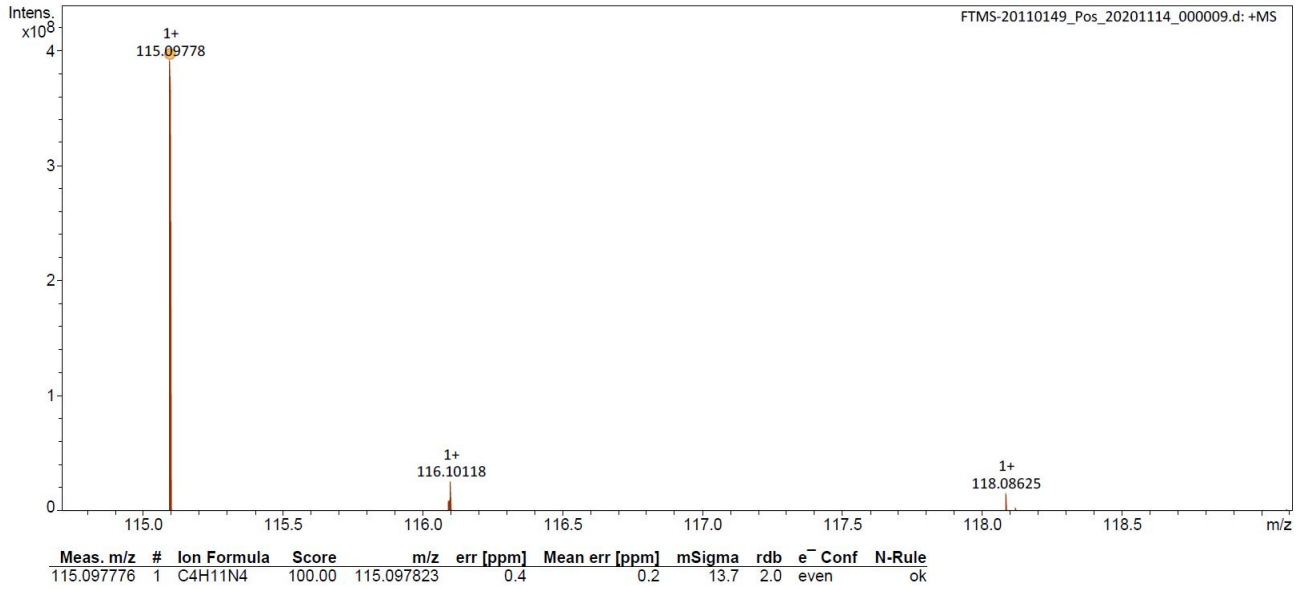

Meas. m/z	#	Ion Formula	Score	m/z	err [ppm]	Mean err [ppm]	mSigma	rdb	e⁻ Conf	N-Rule
115.097776	1	C4H11N4	100.00	115.097823	0.4	0.2	13.7	2.0	even	ok

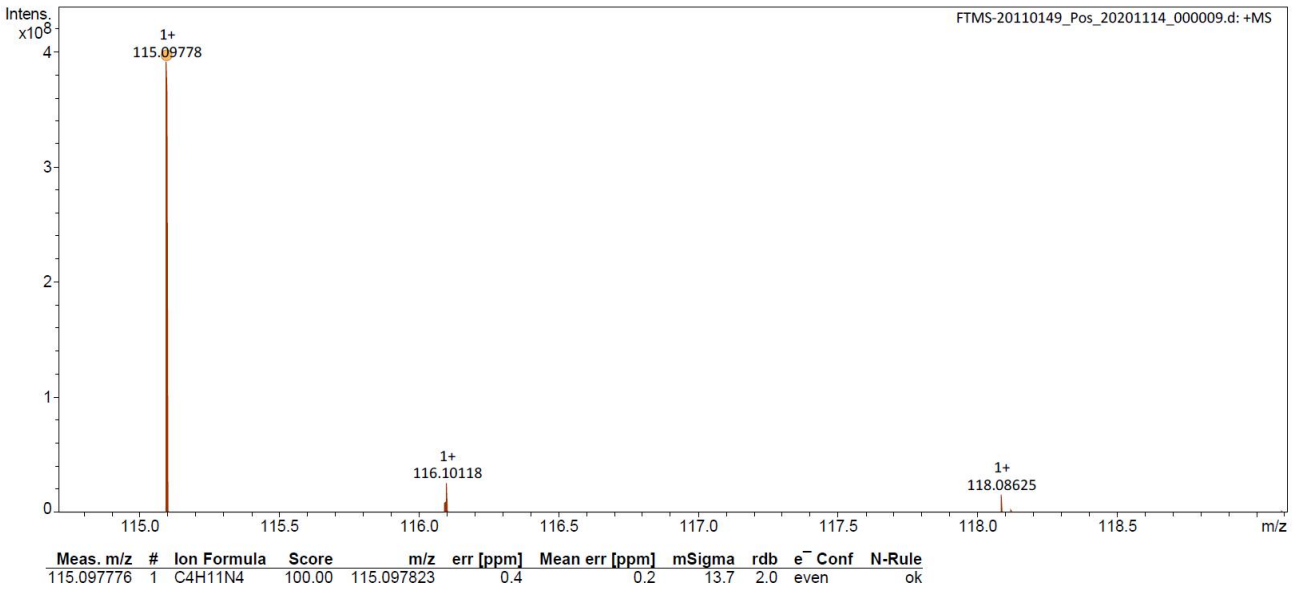

Meas. m/z	#	Ion Formula	Score	m/z	err [ppm]	Mean err [ppm]	mSigma	rdb	e⁻ Conf	N-Rule
115.097776	1	C4H11N4	100.00	115.097823	0.4	0.2	13.7	2.0	even	ok

Figure S71. HRMS (ESI$^+$-FTICR) spectrum of 2-azido-N,N-dimethylethan-1-amine.

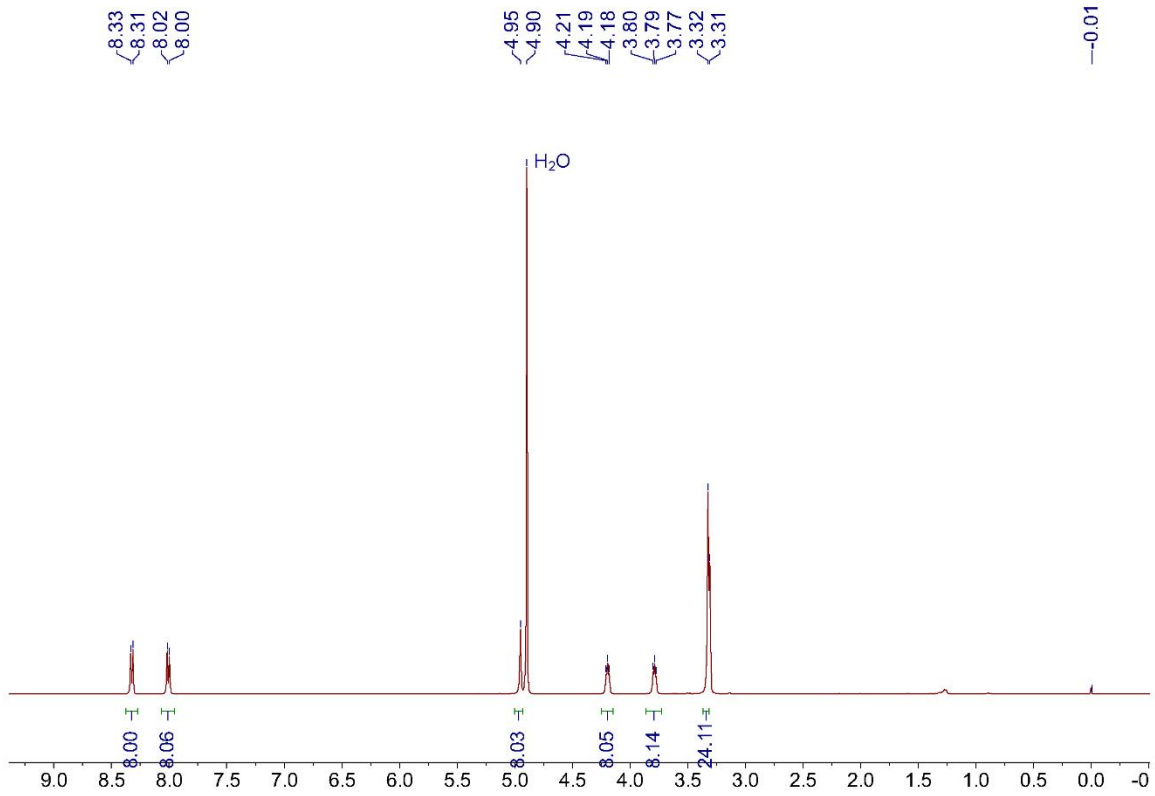

Figure S72.[1]H NMR spectrum (400 MHz, Methanol-d_4) of **P9**.

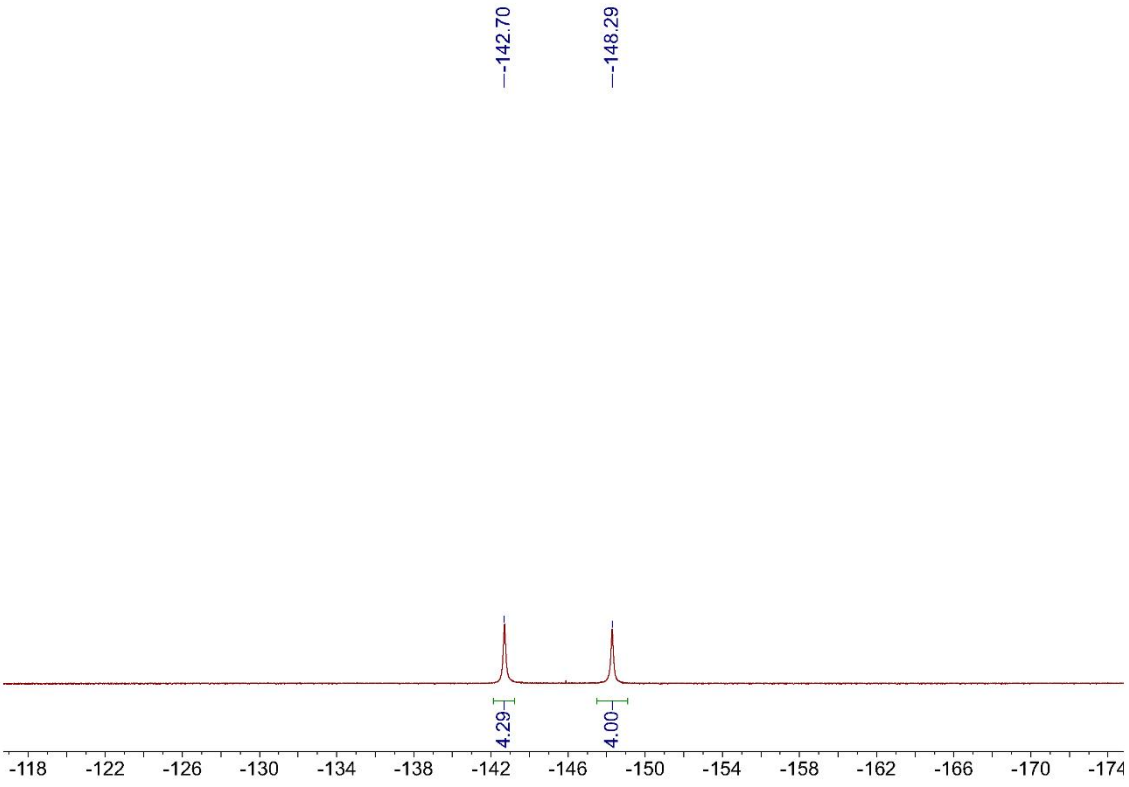

Figure S73. [19]F NMR spectrum (471 MHz, Methanol-d_4) of **P9**.

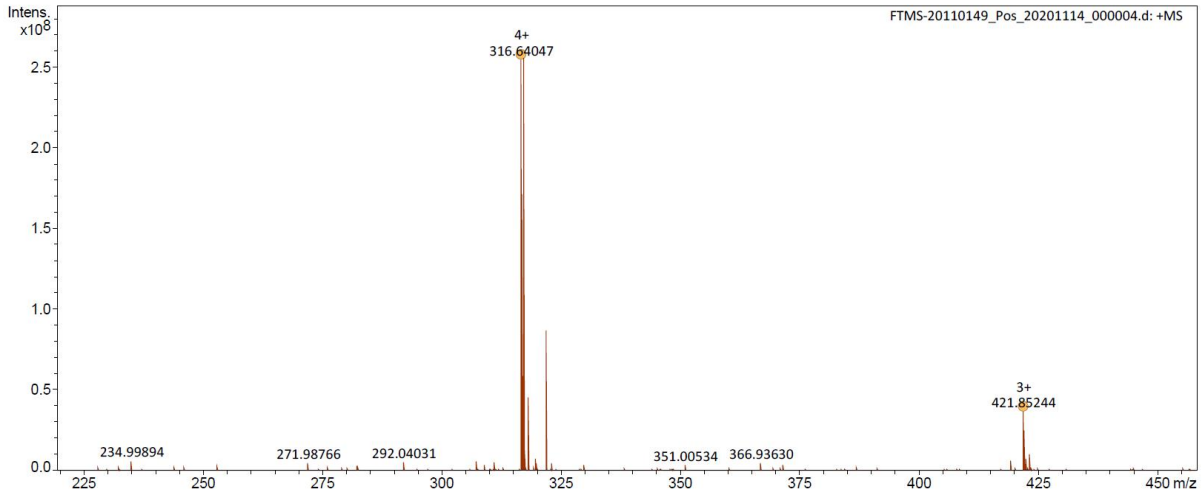

Meas. m/z	#	Ion Formula	Score	m/z	err [ppm]	Mean err [ppm]	mSigma	rdb	e⁻ Conf	N-Rule
316.640472	1	C64H66F8N20	100.00	316.640741	0.8	0.2	57.7	40.0	even	ok
421.852442	1	C64H65F8N20	100.00	421.851896	-1.3	-2.1	73.7	40.0	even	ok

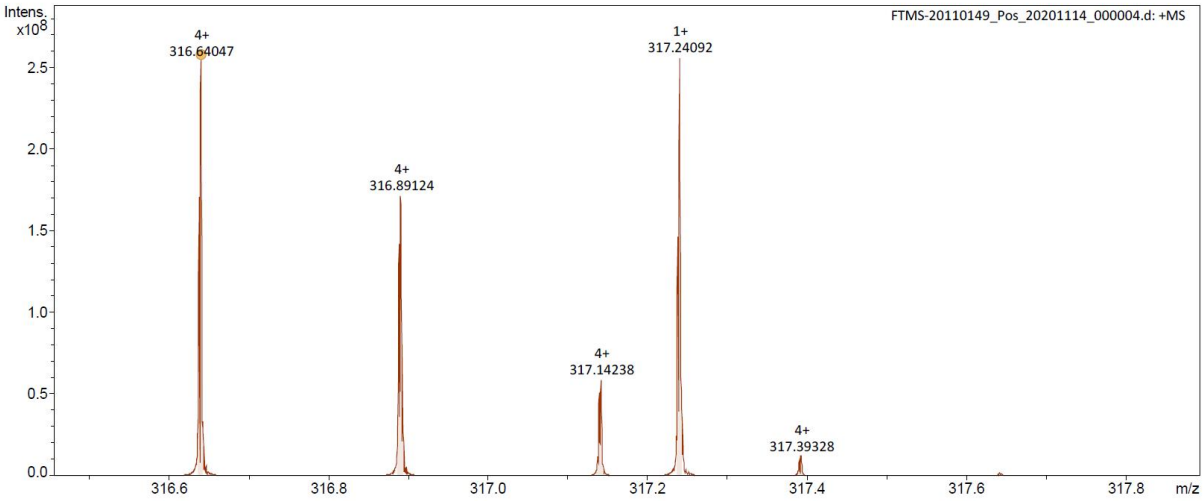

Meas. m/z	#	Ion Formula	Score	m/z	err [ppm]	Mean err [ppm]	mSigma	rdb	e⁻ Conf	N-Rule
316.640472	1	C64H66F8N20	100.00	316.640741	0.8	0.2	57.7	40.0	even	ok
421.852442	1	C64H65F8N20	100.00	421.851896	-1.3	-2.1	73.7	40.0	even	ok

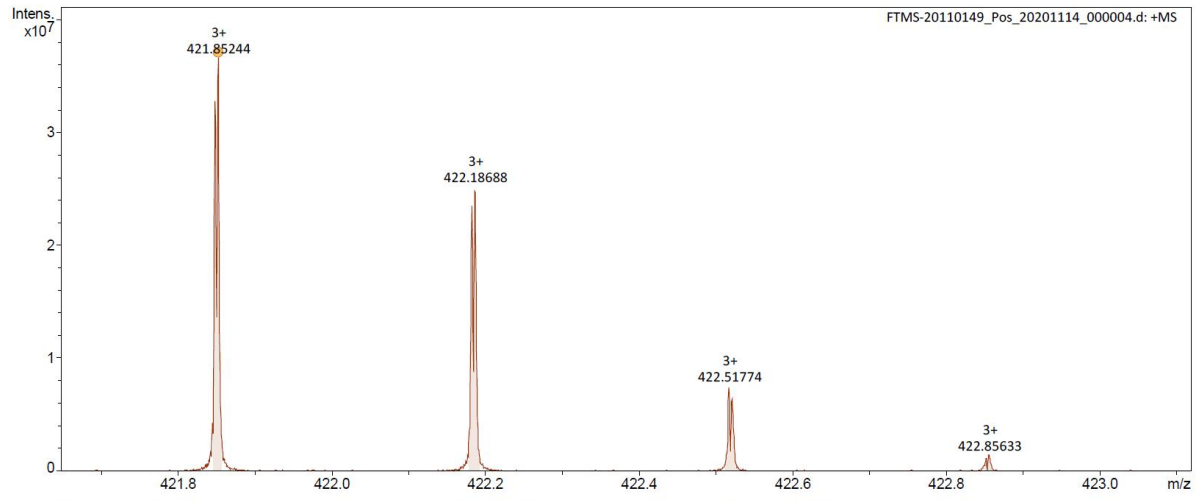

Meas. m/z	#	Ion Formula	Score	m/z	err [ppm]	Mean err [ppm]	mSigma	rdb	e⁻ Conf	N-Rule
316.640472	1	C64H66F8N20	100.00	316.640741	0.8	0.2	57.7	40.0	even	ok
421.852442	1	C64H65F8N20	100.00	421.851896	-1.3	-2.1	73.7	40.0	even	ok

Figure S74. HRMS spectrum (ESI$^+$-FTICR) of **P$_9$**.

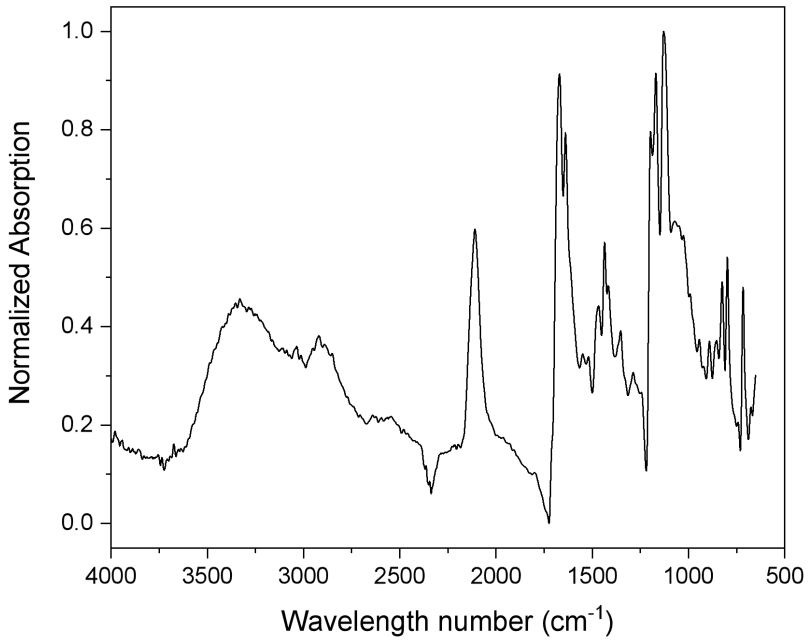

Figure S75. Normalized FT-IR spectrum of $\mathbf{P_9}$.

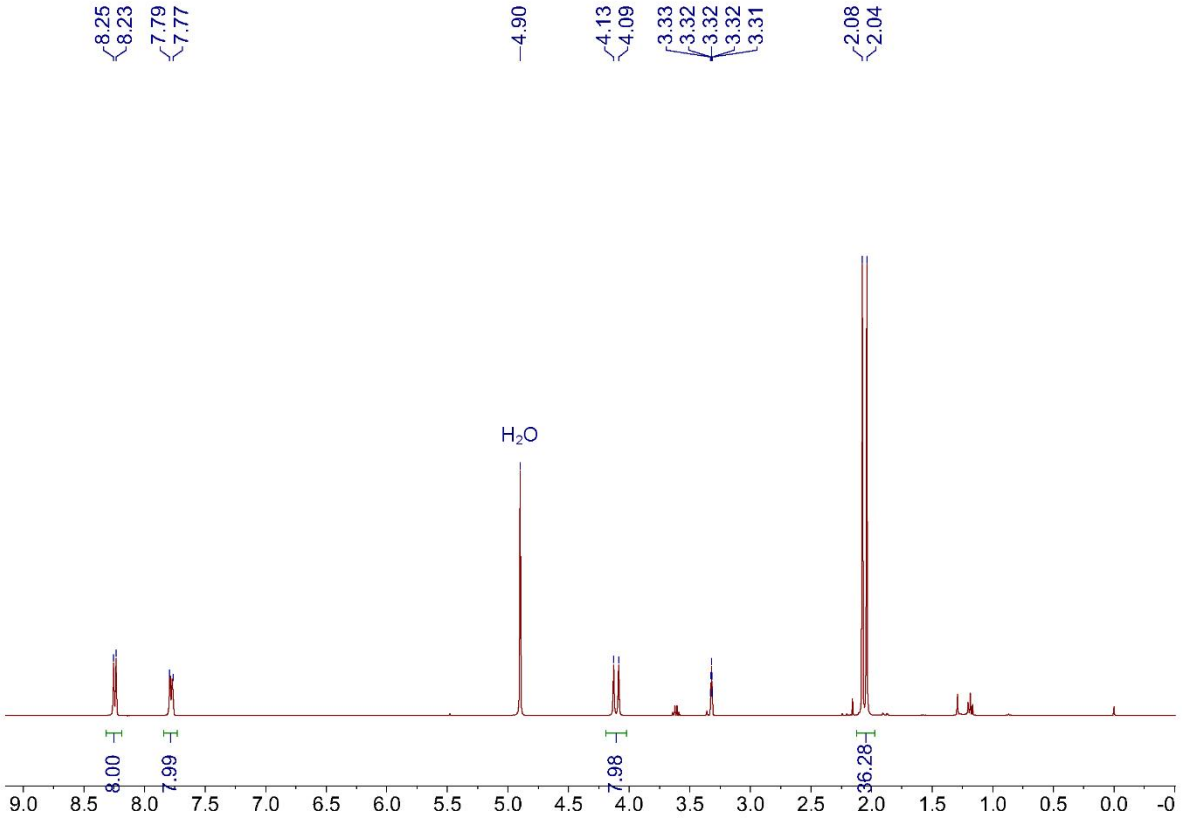

Figure S76. ^{1}H NMR spectrum (400 MHz, Methanol-d_4) of $\mathbf{P_{10}}$.

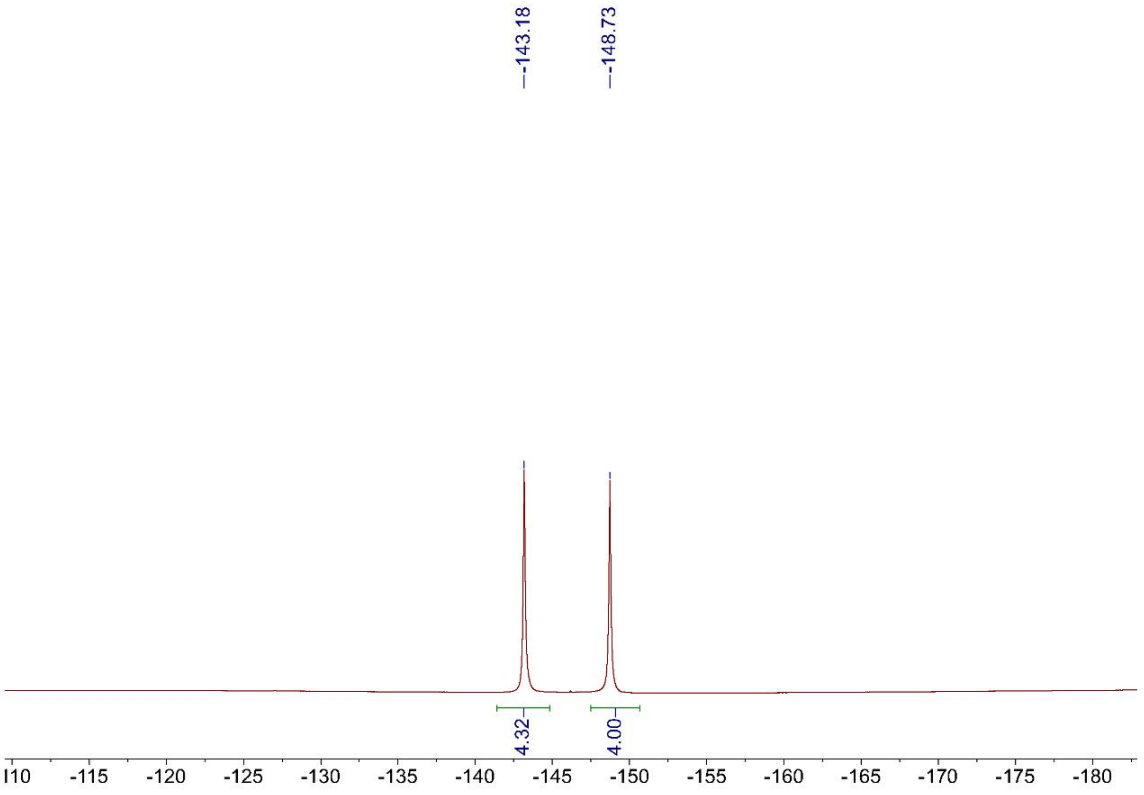

Figure S77. ^{19}F NMR spectrum (565 MHz, Methanol-d_4) of $\mathbf{P_{10}}$.

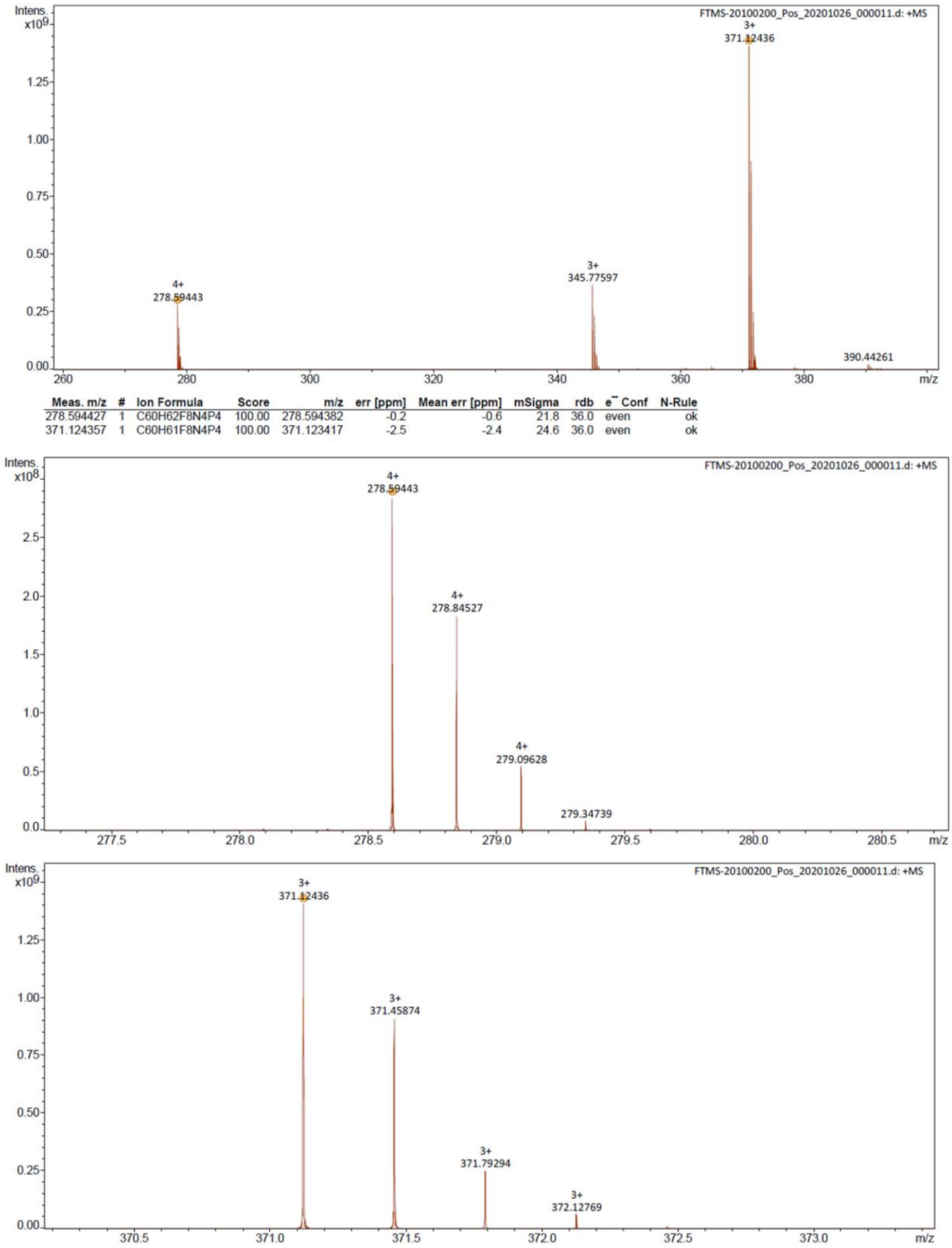

Meas. m/z	#	Ion Formula	Score	m/z	err [ppm]	Mean err [ppm]	mSigma	rdb	e⁻ Conf	N-Rule
278.594427	1	C60H62F8N4P4	100.00	278.594382	-0.2	-0.6	21.8	36.0	even	ok
371.124357	1	C60H61F8N4P4	100.00	371.123417	-2.5	-2.4	24.6	36.0	even	ok

Figure S78. HRMS spectrum (ESI$^+$-FTICR) of **P_{10}**.

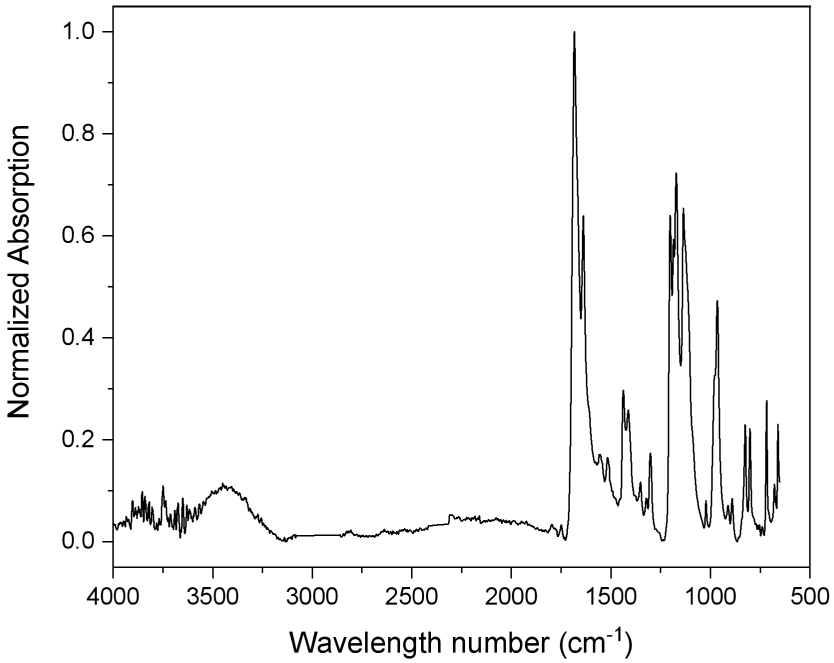

Figure S79. Normalized FT-IR spectrum of $\mathbf{P_{10}}$.

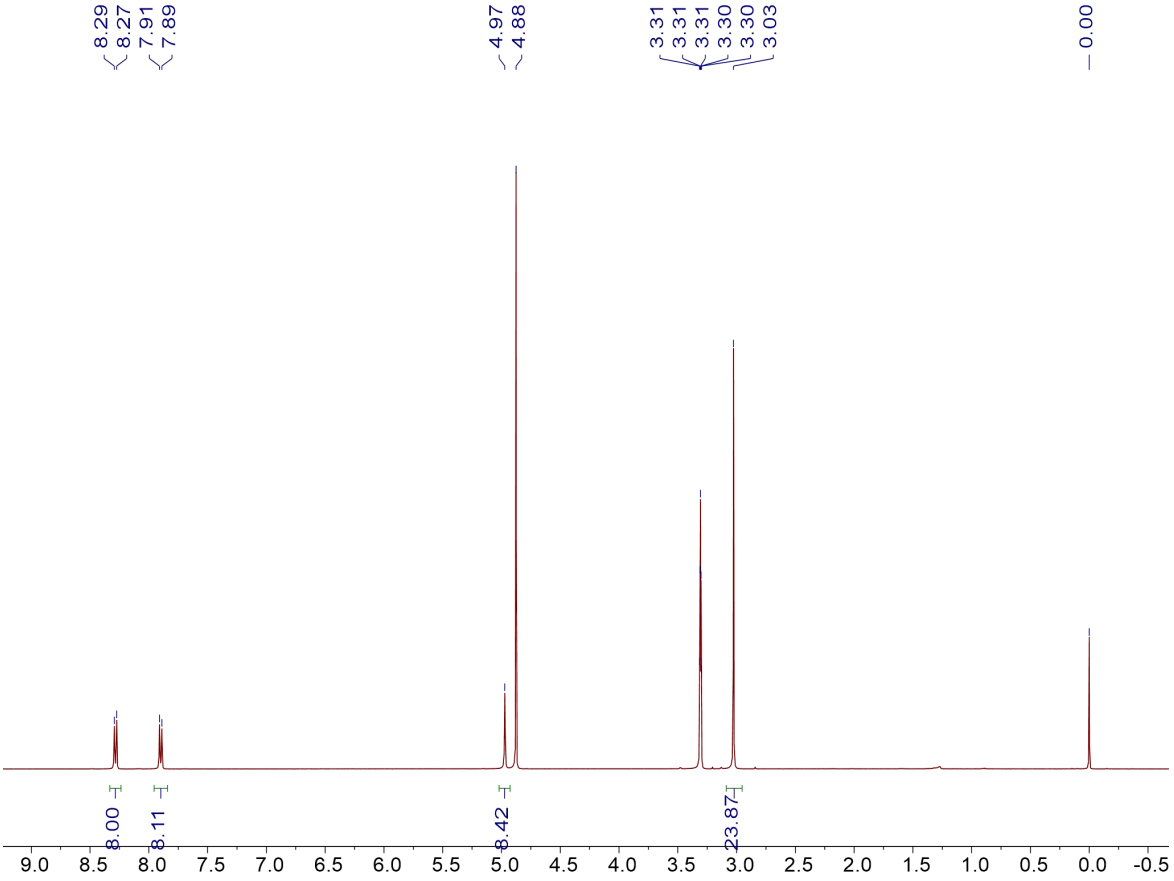

Figure S80. [1]H NMR spectrum (400 MHz, Methanol-d_4) of $\mathbf{P_{11}}$.

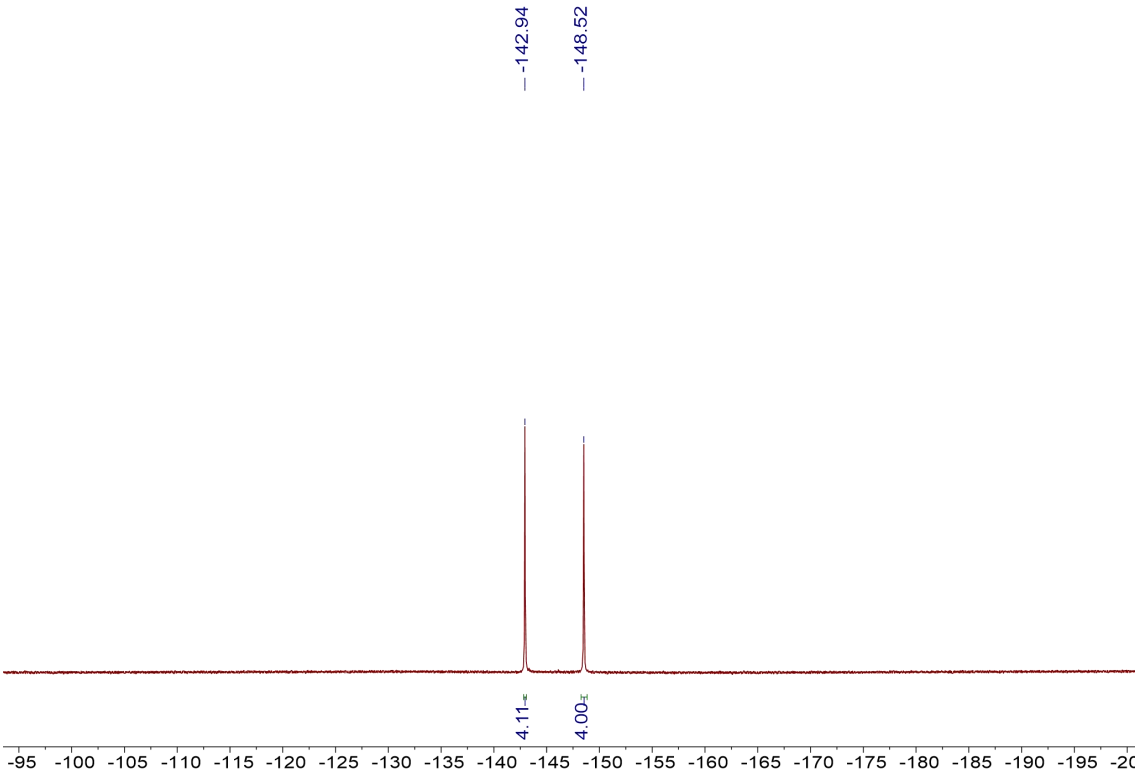

Figure S81. [19]F NMR spectrum (471 MHz, Methanol-d_4) of $\mathbf{P_{11}}$.

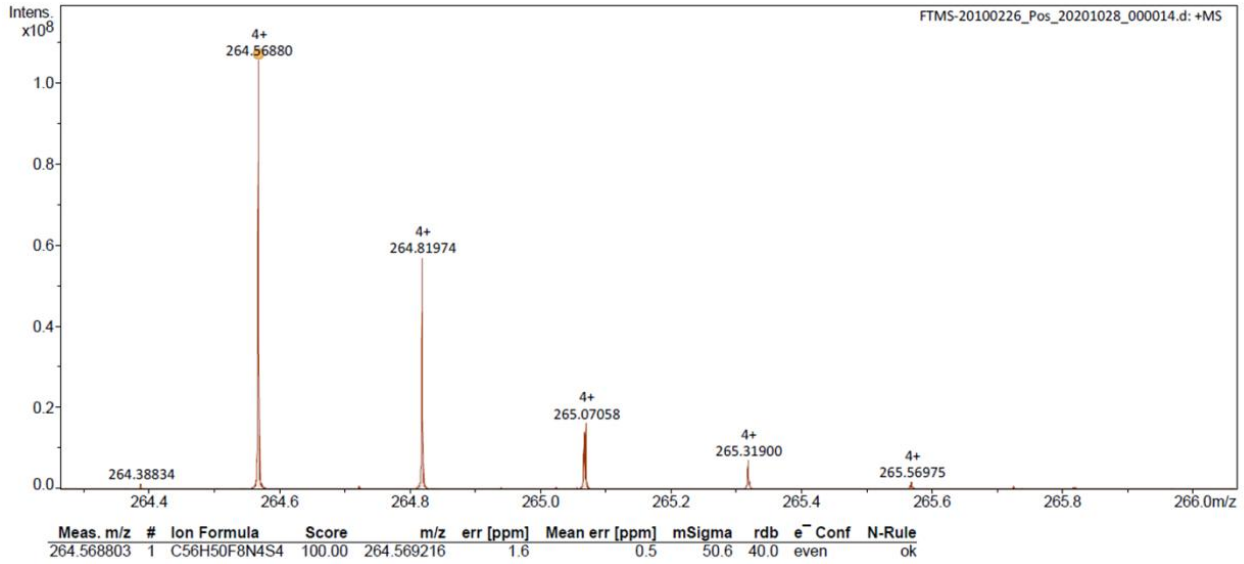

Meas. m/z	#	Ion Formula	Score	m/z	err [ppm]	Mean err [ppm]	mSigma	rdb	e⁻ Conf	N-Rule
264.568803	1	C56H50F8N4S4	100.00	264.569216	1.6	0.5	50.6	40.0	even	ok

Figure S82. HRMS (ESI$^+$-FTICR) spectrum of $\mathbf{P_{11}}$.

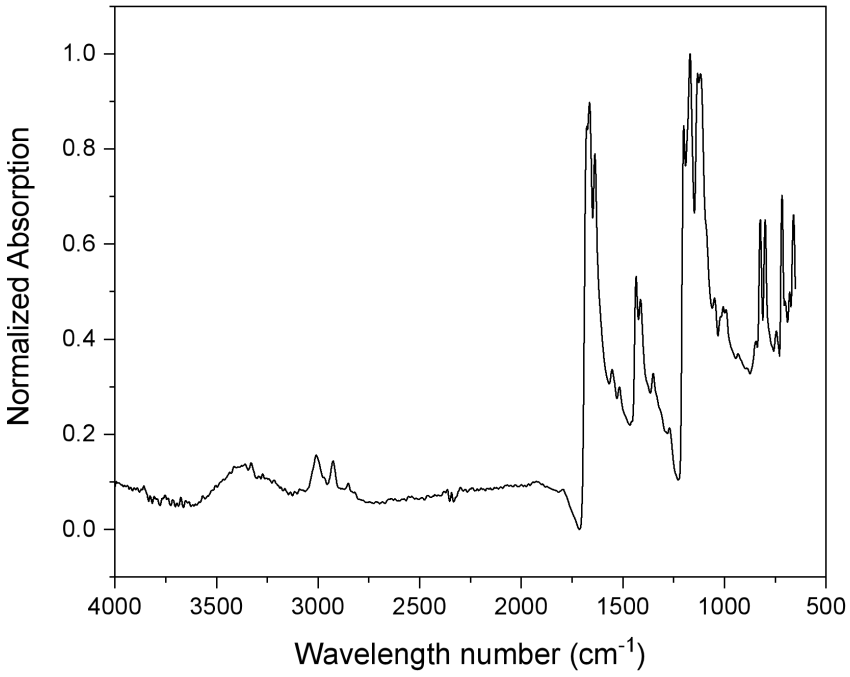

Figure S83. Normalized FT-IR spectrum of $\mathbf{P_{11}}$.

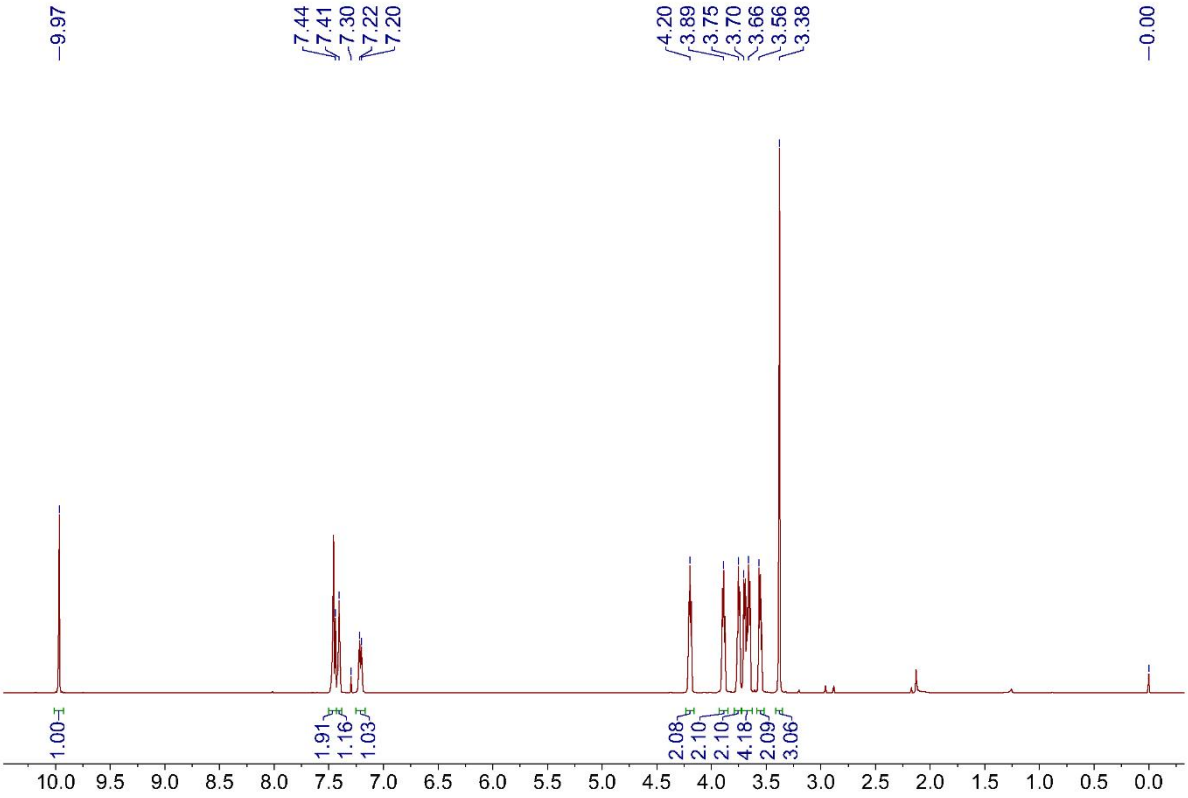

Figure S84. ^{1}H NMR spectrum (400 MHz, Chloroform-*d*) of 3-(2-[2-(2-methoxy-ethoxy)-ethoxy]-ethoxy)-benzaldehyde.

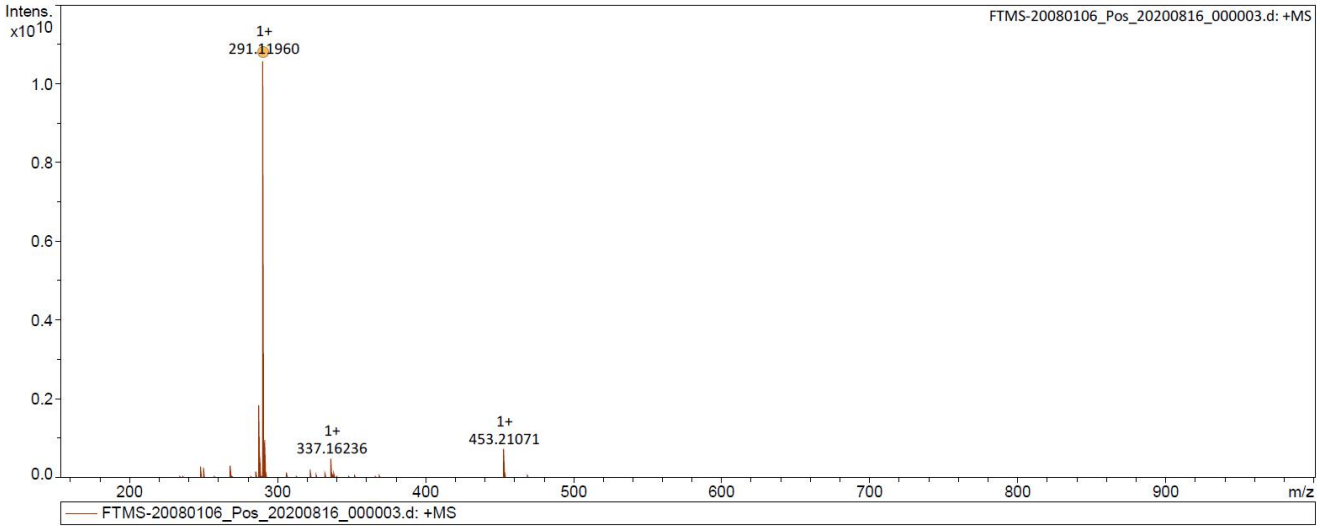

Meas. m/z	#	Ion Formula	Score	m/z	err [ppm]	Mean err [ppm]	mSigma	rdb	e⁻ Conf	N-Rule
291.119595	1	C14H20NaO5	100.00	291.120294	2.4	1.7	31.4	5.0	even	ok

Figure S85. HRMS (ESI$^+$-FTICR) spectrum of 3-(2-[2-(2-methoxy-ethoxy)-ethoxy]-ethoxy)-benzaldehyde.

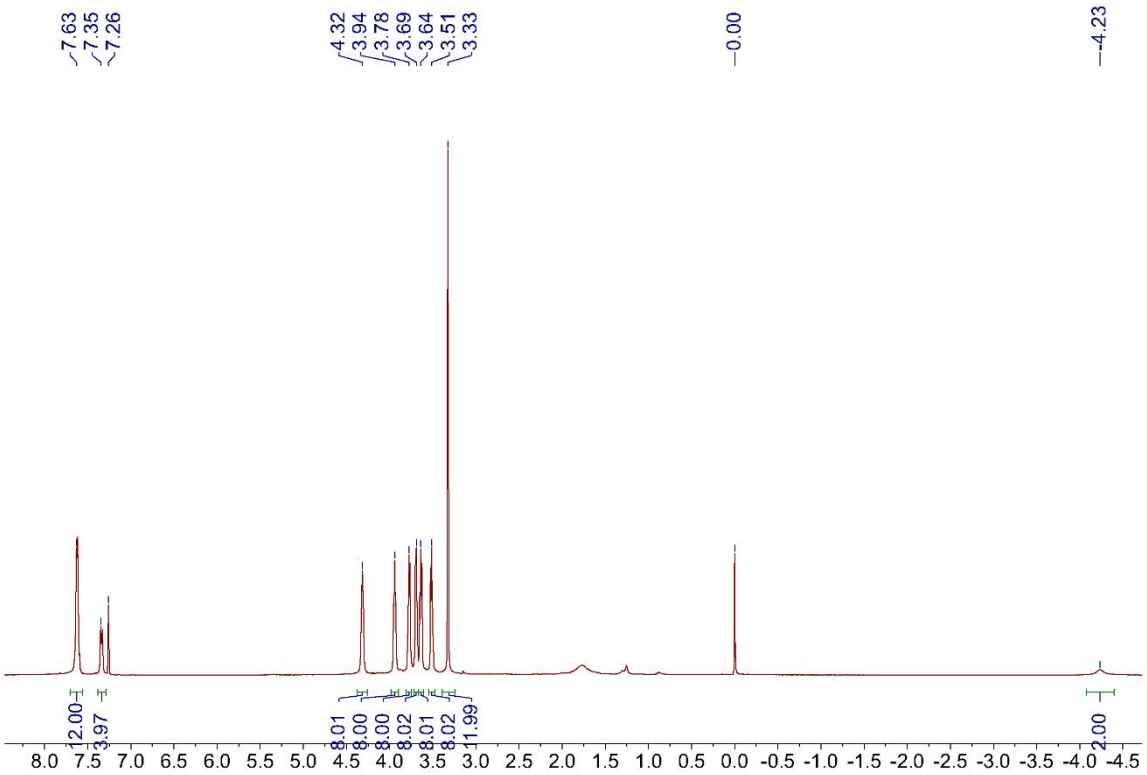

Figure S86. ^{1}H NMR spectrum (400 MHz, Chloroform-*d*) of $\mathbf{P_{12}}$.

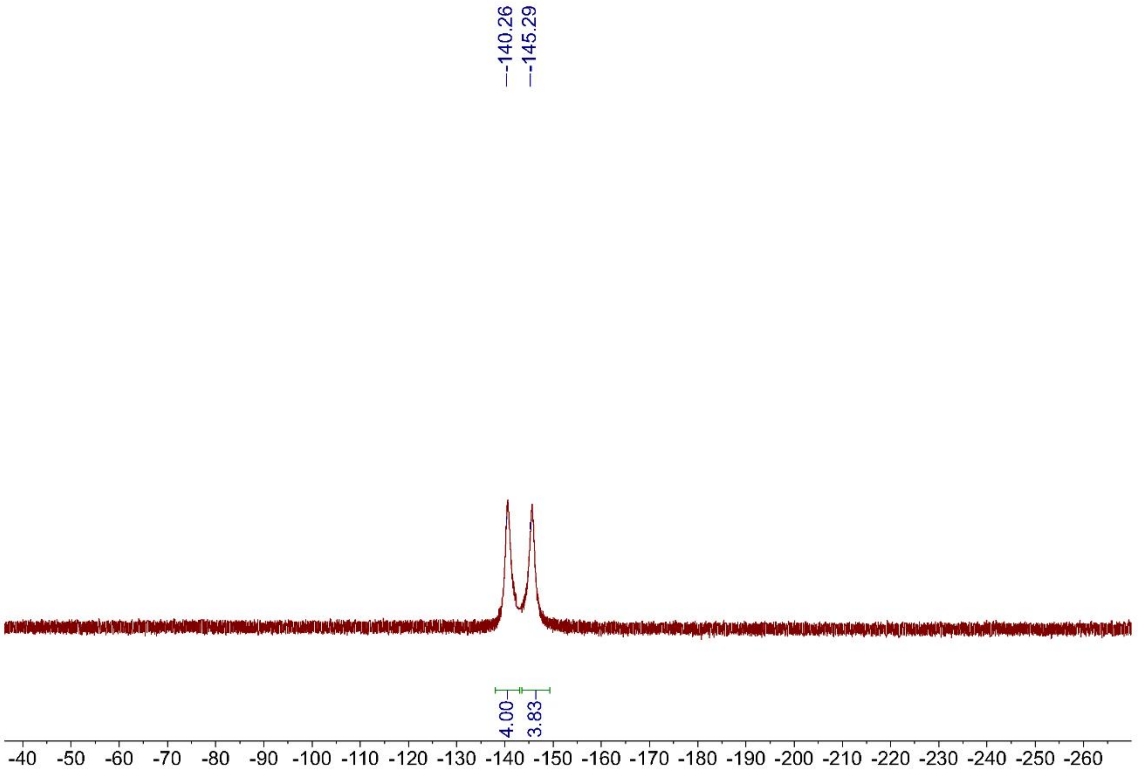

Figure S87. ^{19}F NMR spectrum (471 MHz, Chloroform-*d*) of $\mathbf{P_{12}}$.

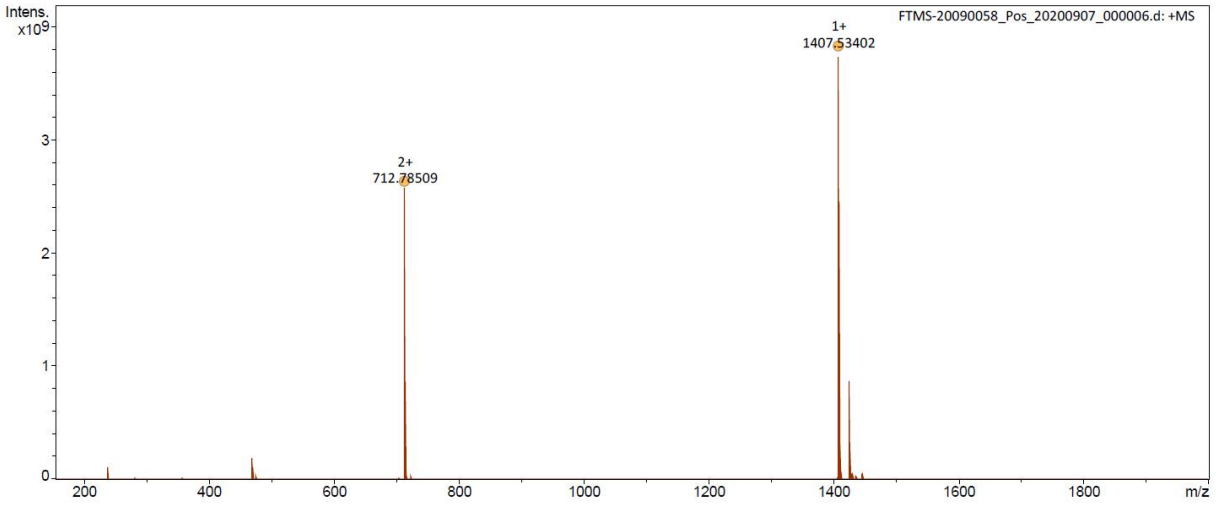

Meas. m/z	#	Ion Formula	Score	m/z	err [ppm]	Mean err [ppm]	mSigma	rdb	e⁻ Conf	N-Rule
712.785086	1	C72H83F8N5O16	100.00	712.784805	-0.4	0.6	12.5	31.0	even	ok
1407.534018	1	C72H79F8N4O16	100.00	1407.535784	1.3	0.4	n.a.	32.0	even	ok

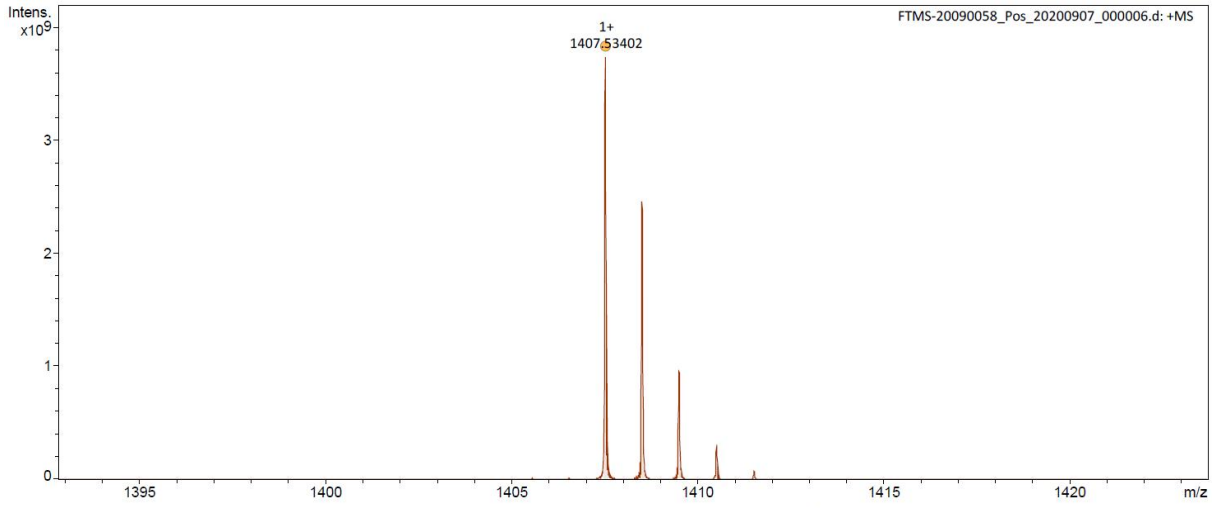

Meas. m/z	#	Ion Formula	Score	m/z	err [ppm]	Mean err [ppm]	mSigma	rdb	e⁻ Conf	N-Rule
712.785086	1	C72H83F8N5O16	100.00	712.784805	-0.4	0.6	12.5	31.0	even	ok
1407.534018	1	C72H79F8N4O16	100.00	1407.535784	1.3	0.4	n.a.	32.0	even	ok

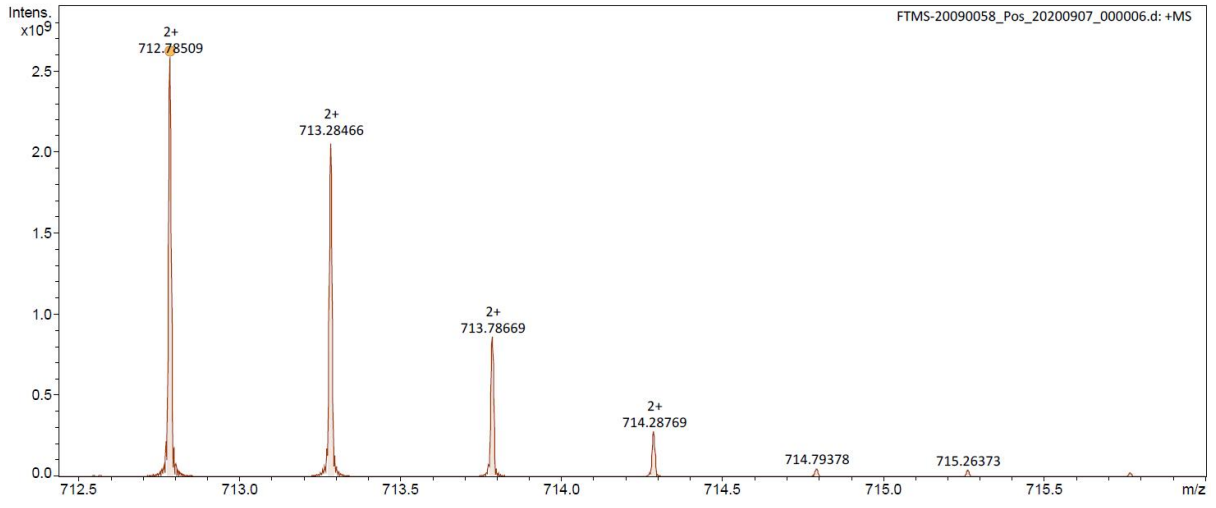

Meas. m/z	#	Ion Formula	Score	m/z	err [ppm]	Mean err [ppm]	mSigma	rdb	e⁻ Conf	N-Rule
712.785086	1	C72H83F8N5O16	100.00	712.784805	-0.4	0.6	12.5	31.0	even	ok
1407.534018	1	C72H79F8N4O16	100.00	1407.535784	1.3	0.4	n.a.	32.0	even	ok

Figure S88. HRMS (ESI$^+$-FTICR) spectrum of **P_{12}**.

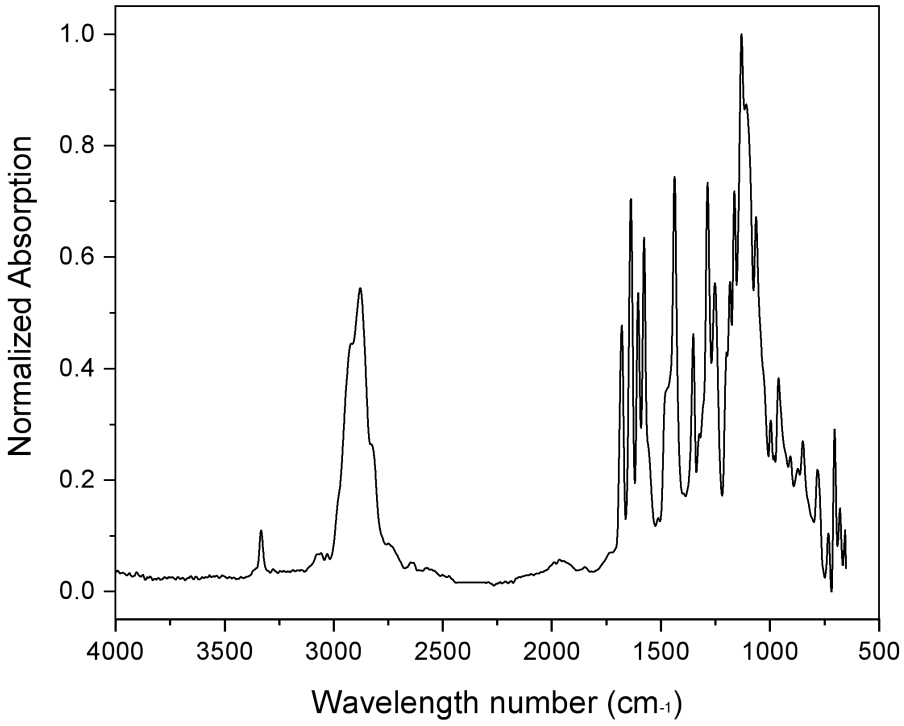

Figure S89. Normalized FT-IR spectrum of $\mathbf{P_{12}}$.

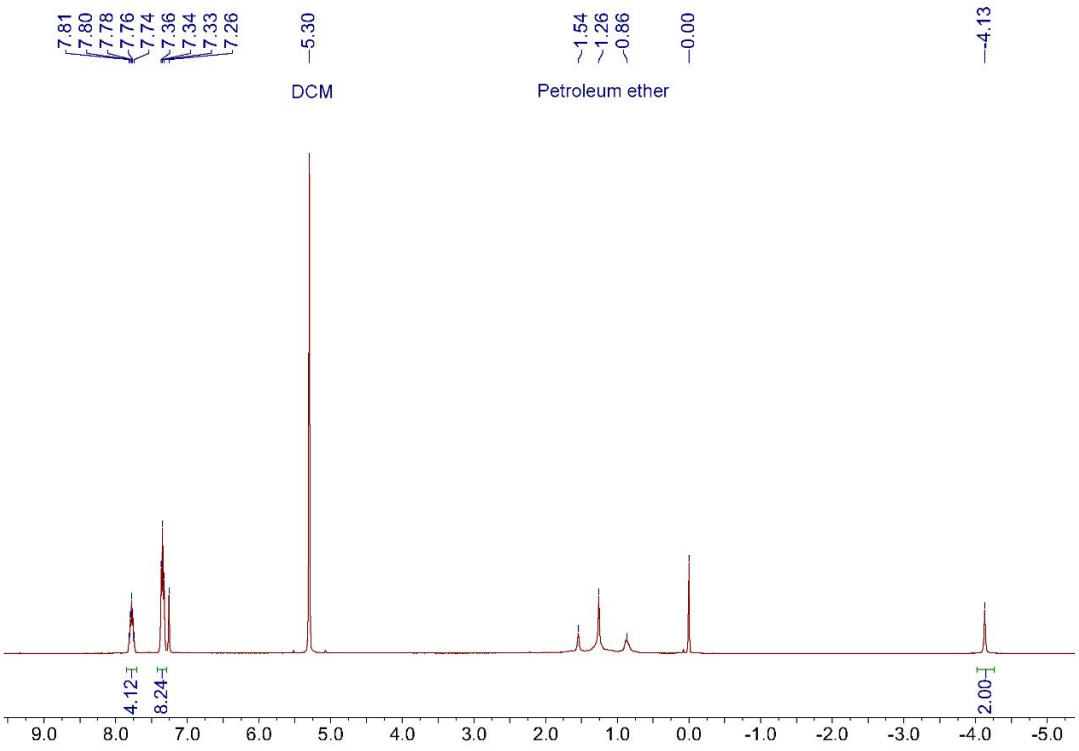

Figure S90. ^{1}H NMR spectrum (400 MHz, Chloroform-*d*) of 2,3,7,8,12,13,17,18-Octafluoro-5,10,15,20-tetrakis(2,6-difluorophenyl)porphyrin.

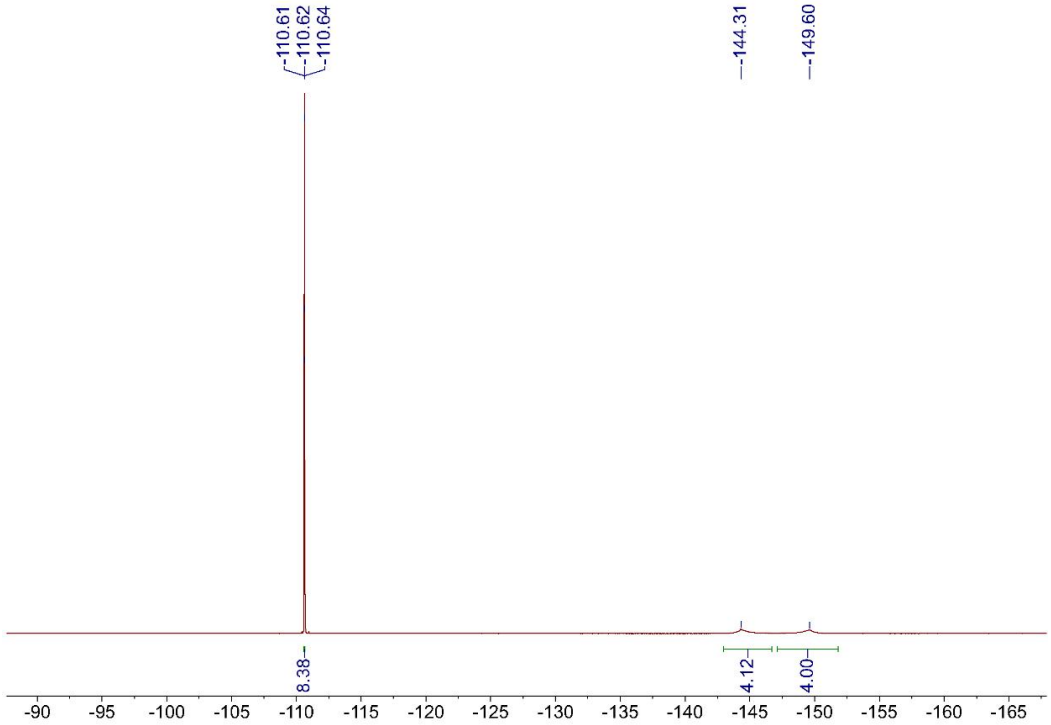

Figure S91. ^{19}F NMR spectrum (400 MHz, Methanol-d_4) of 2,3,7,8,12,13,17,18-Octafluoro-5,10,15,20-tetrakis(2,6-difluorophenyl)porphyrin.

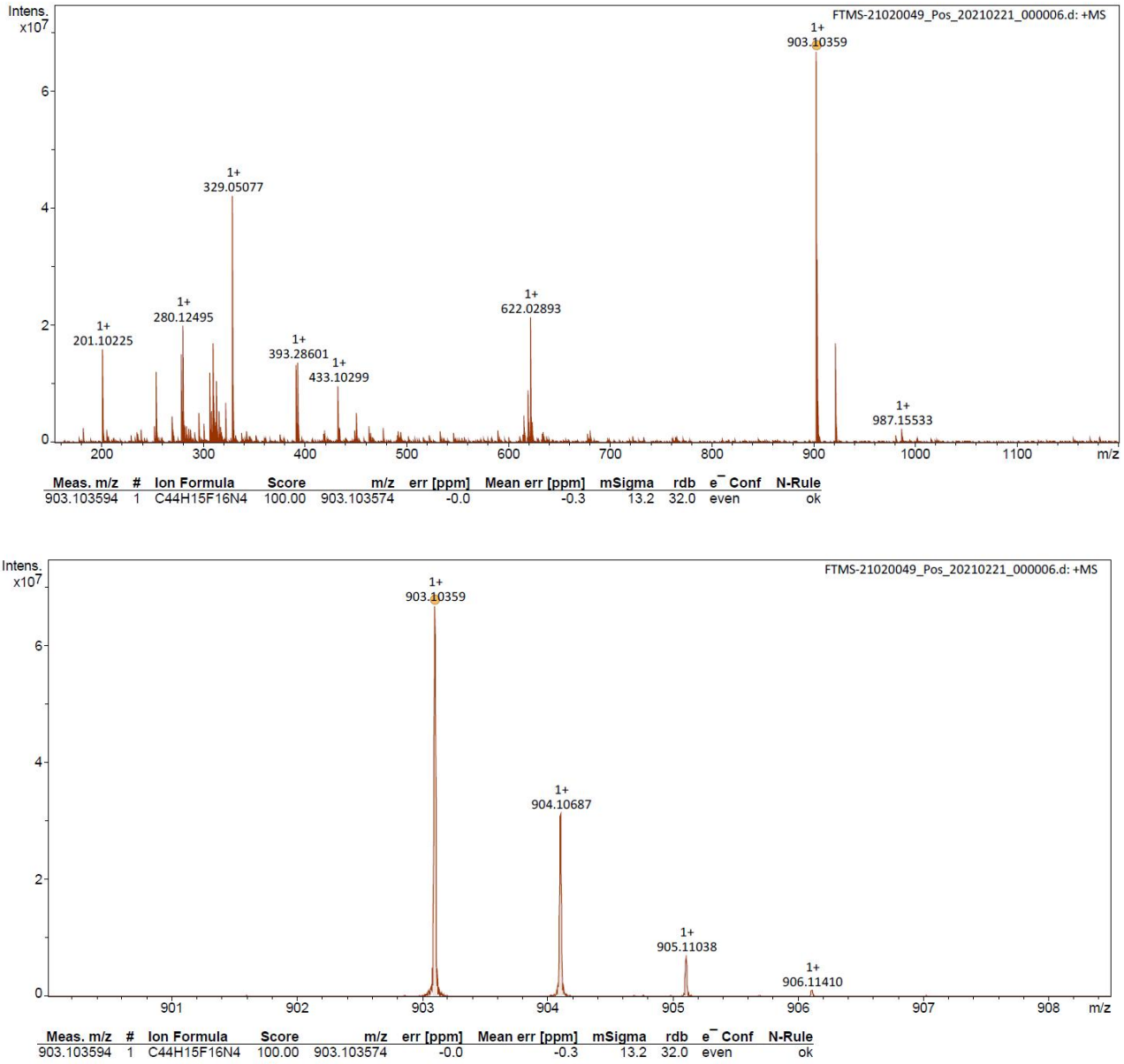

Figure S92. HRMS spectrum (ESI$^+$-FTICR) spectrum of 2,3,7,8,12,13,17,18-Octafluoro-5,10,15,20-tetrakis(2,6-difluorophenyl)porphyrin.

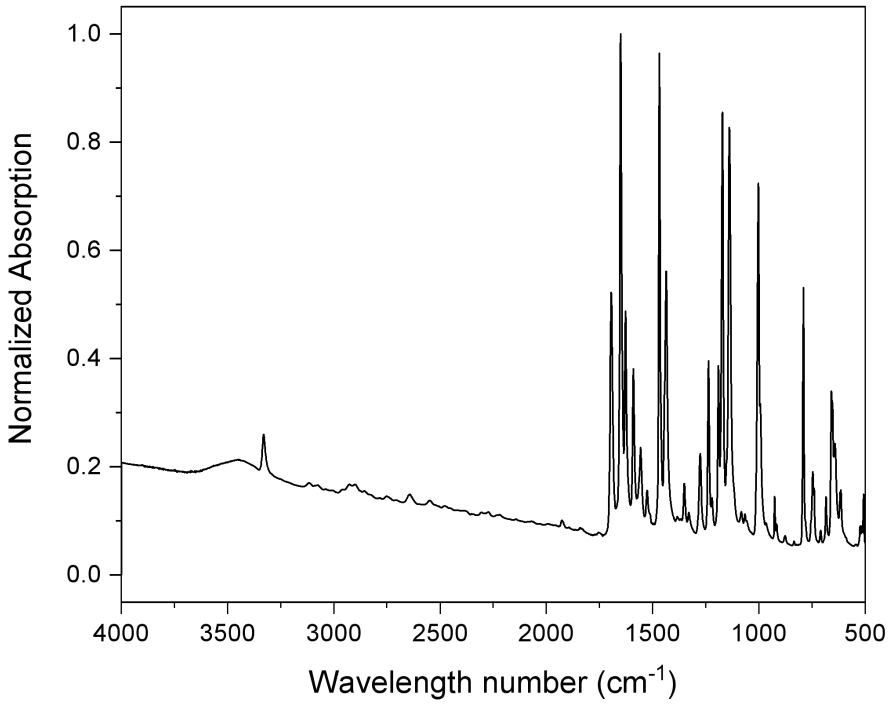

Figure S93. Normalized FT-IR spectrum of 2,3,7,8,12,13,17,18-Octafluoro-5,10,15,20-tetrakis(2,6-difluorophenyl)porphyrin.

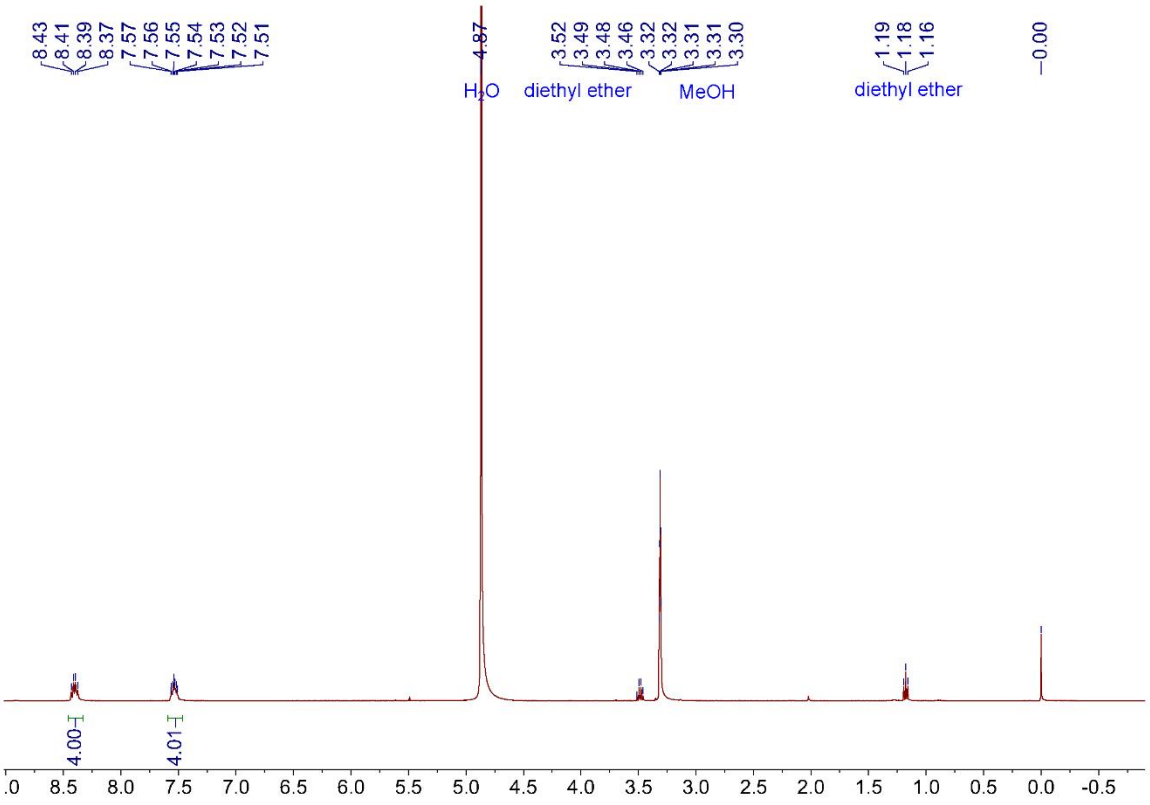

Figure S94.[1]H NMR spectrum (400 MHz, Methanol-d_4) of $\mathbf{P_{13}}$.

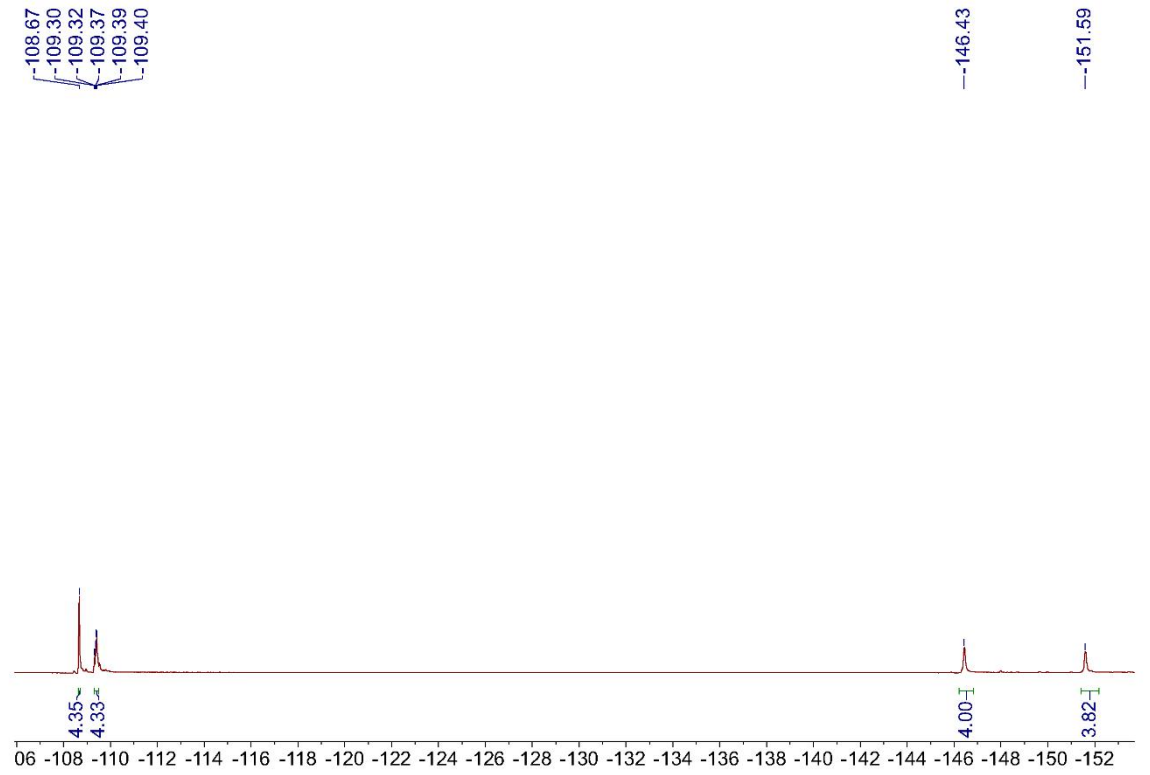

Figure S95. [19]F NMR spectrum (471 MHz, Methanol-d_4) of $\mathbf{P_{13}}$.

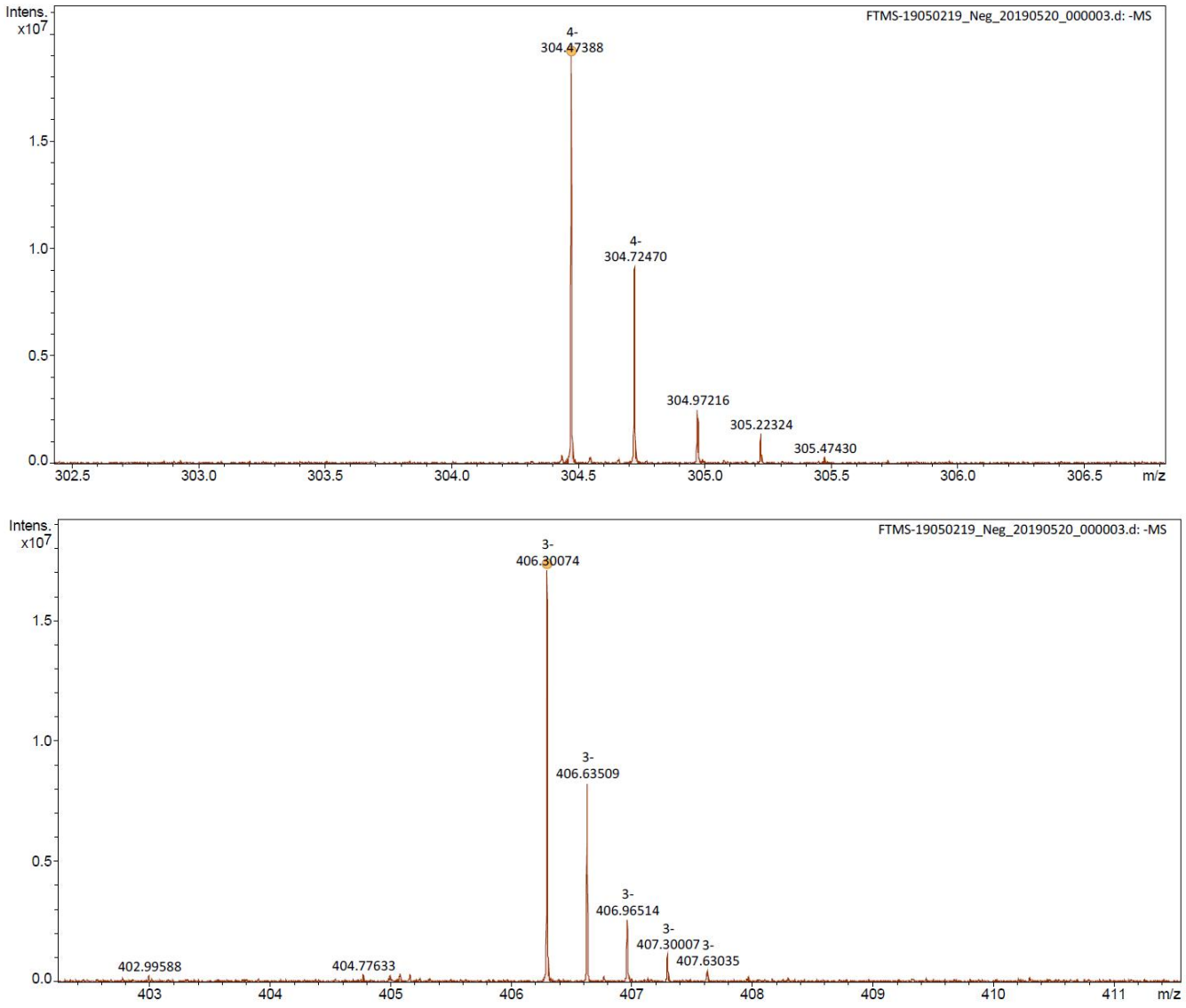

Figure S96. HRMS (ESI$^-$-FTICR) spectrum of $\mathbf{P_{13}}$.

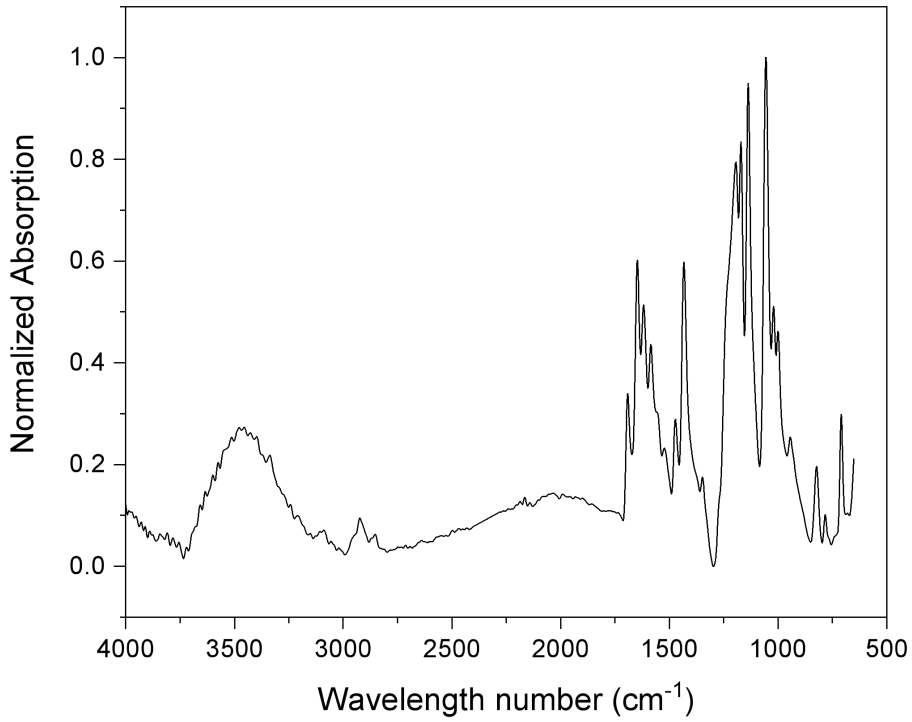

Figure S97. Normalized FT-IR spectrum of $\mathbf{P_{13}}$.

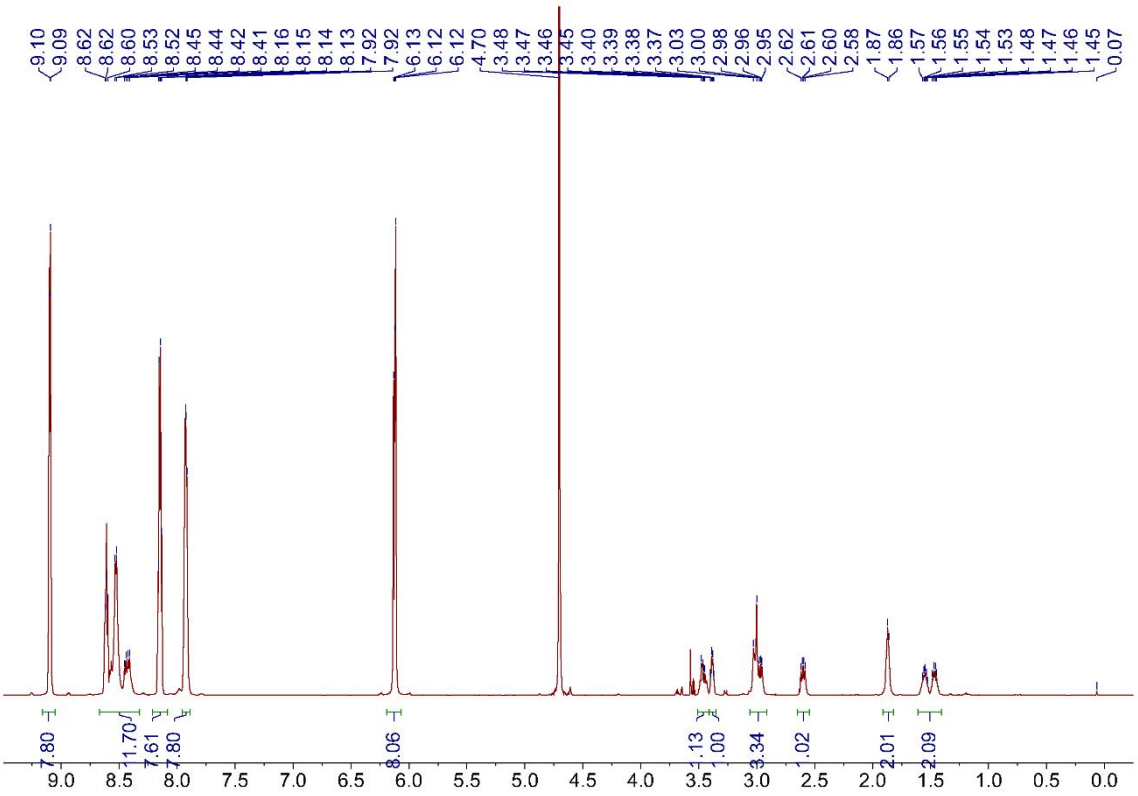

Figure S98. ^{1}H NMR spectrum (600 MHz, Deuterium Oxide) of **P_4-a**.

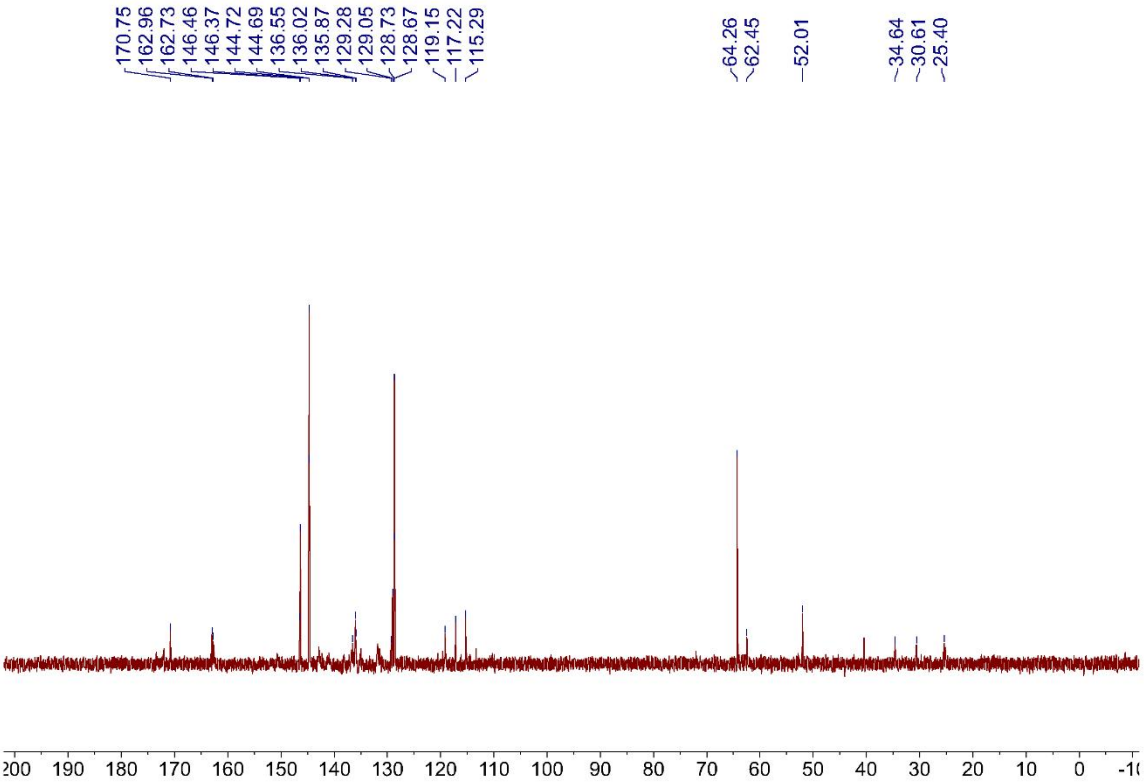

Figure S99. ^{13}C NMR spectrum (151 MHz, Deuterium Oxide) of **P_4-a**.

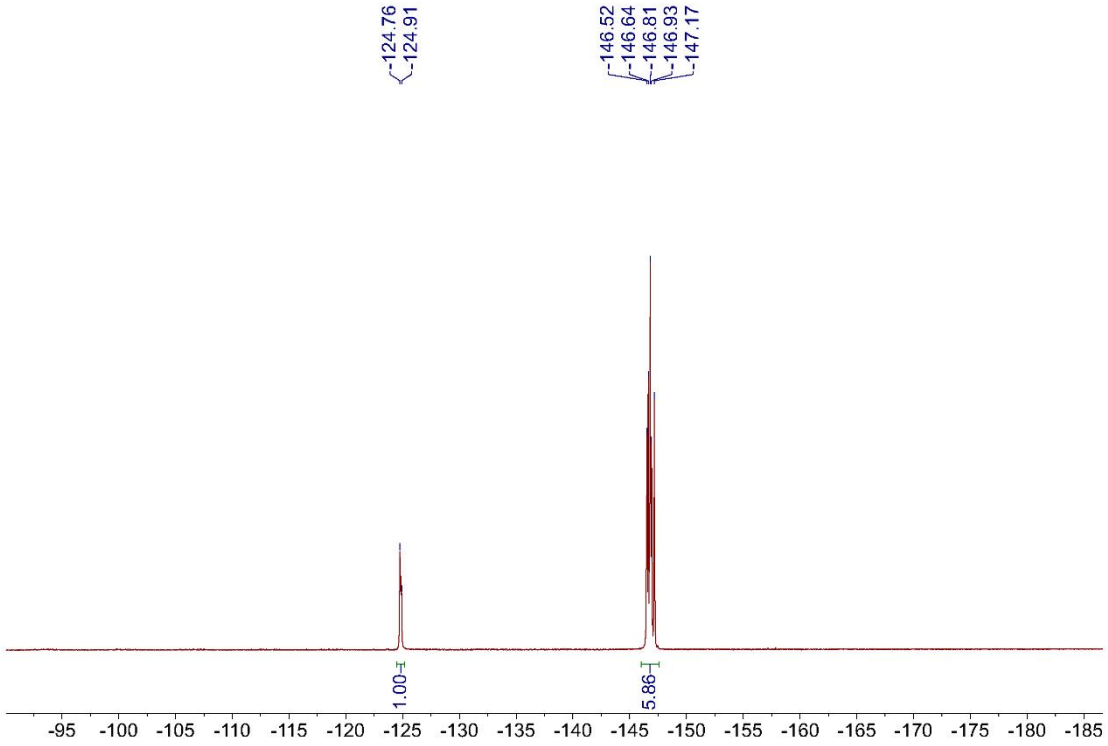

Figure S100. ^{19}F NMR spectrum (565 MHz, Deuterium Oxide) of **P_4-a**.

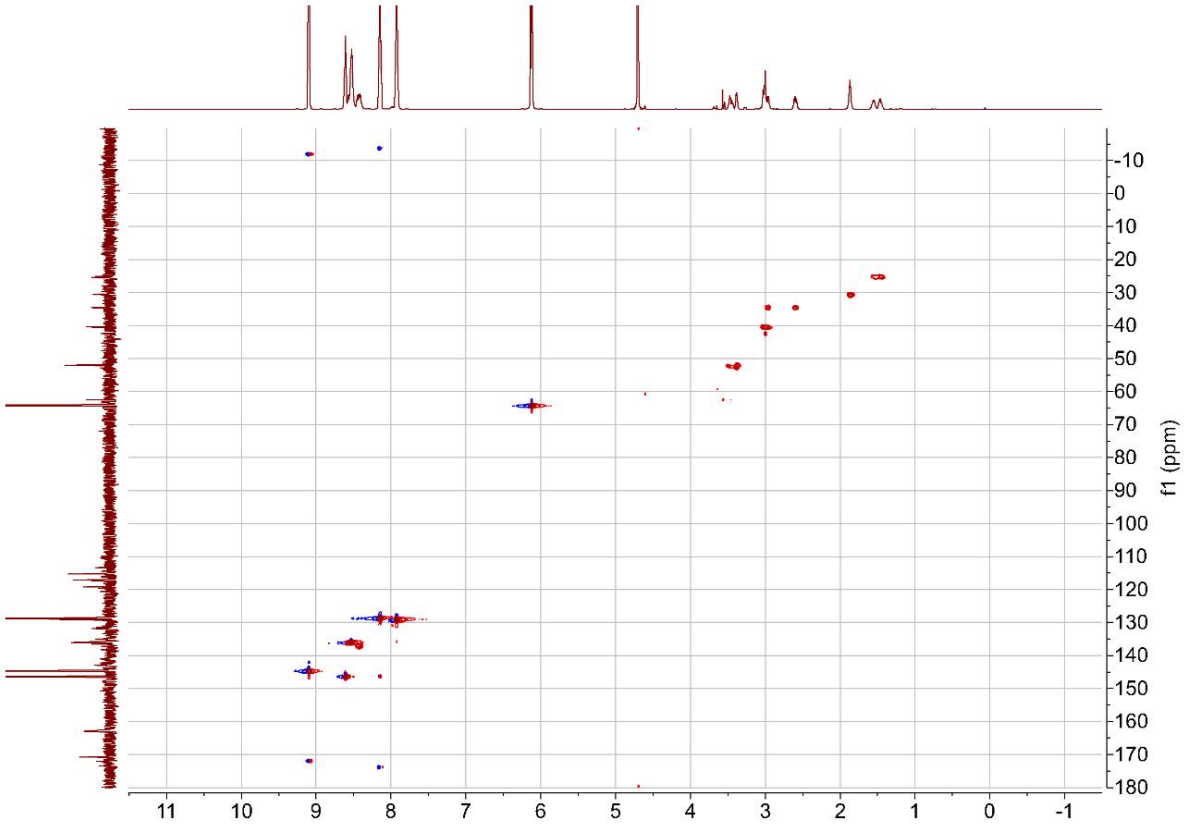

Figure S101. HSQC spectrum (600 MHz, Deuterium Oxide) of **P_4-a**.

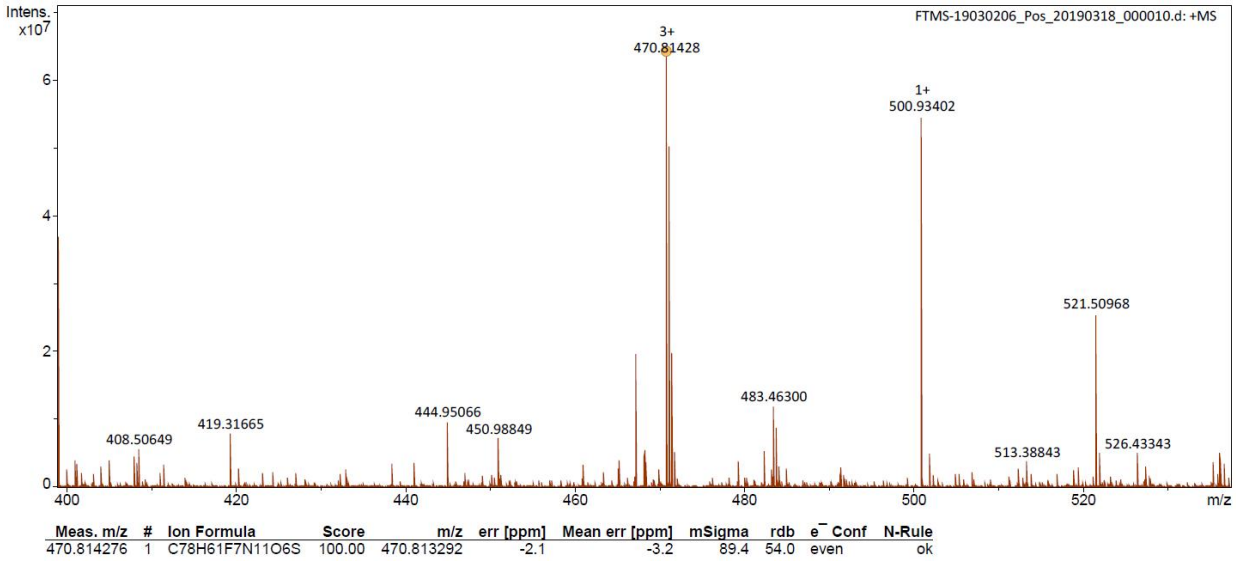

Meas. m/z	#	Ion Formula	Score	m/z	err [ppm]	Mean err [ppm]	mSigma	rdb	e⁻ Conf	N-Rule
470.814276	1	C78H61F7N11O6S	100.00	470.813292	-2.1	-3.2	89.4	54.0	even	ok

Figure S102. HRMS (ESI$^+$-FTICR) spectrum of **P_4-a**.

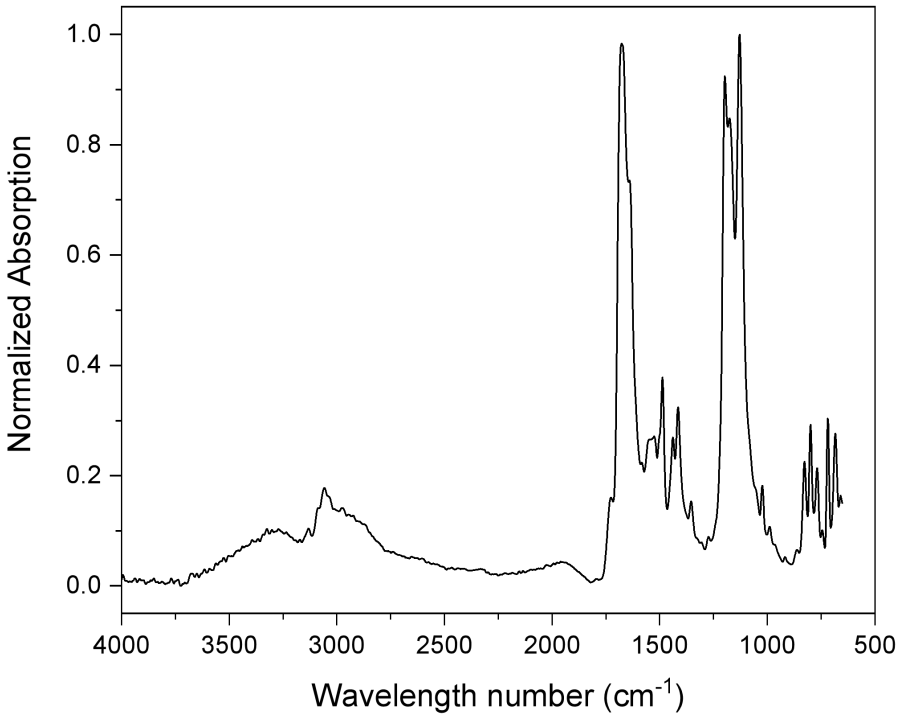

Figure S103. Normalized FT-IR spectrum of **P_4-a**.

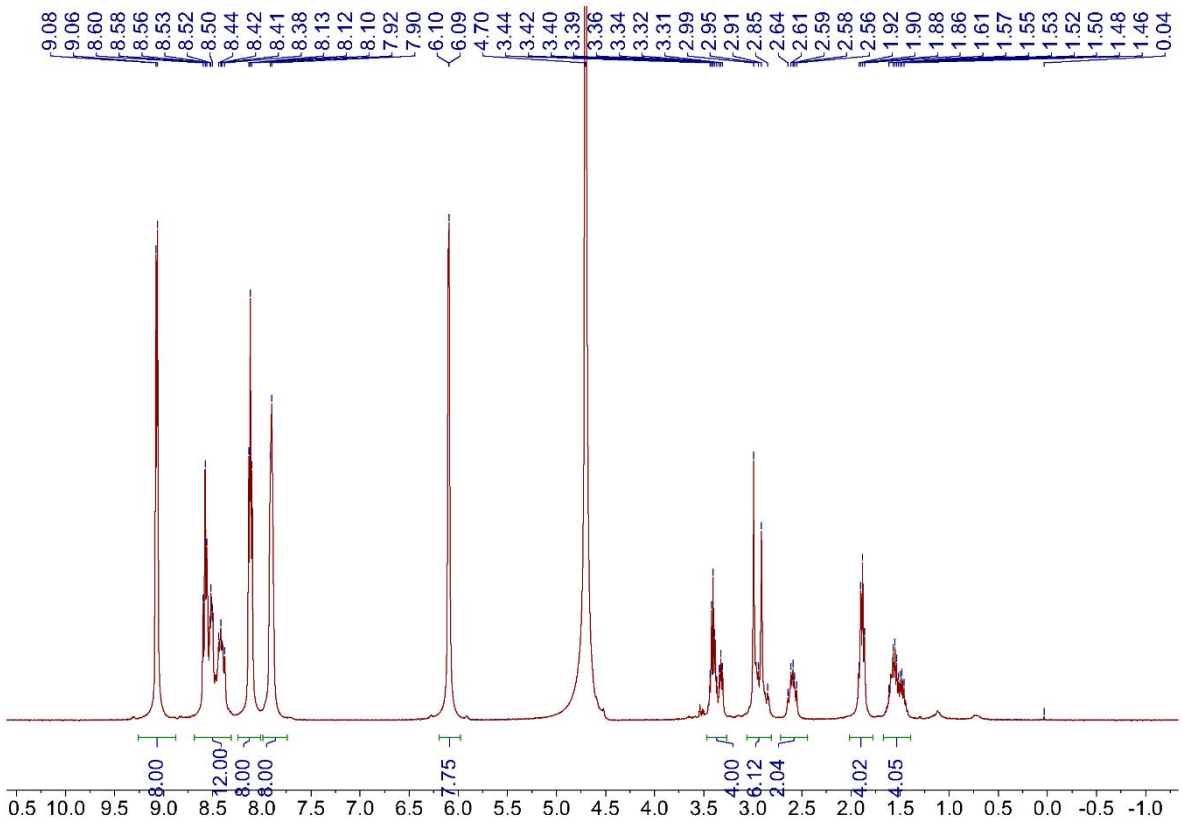

Figure S104. ^{1}H NMR spectrum (400 MHz, Deuterium Oxide) of **P_4-2a**.

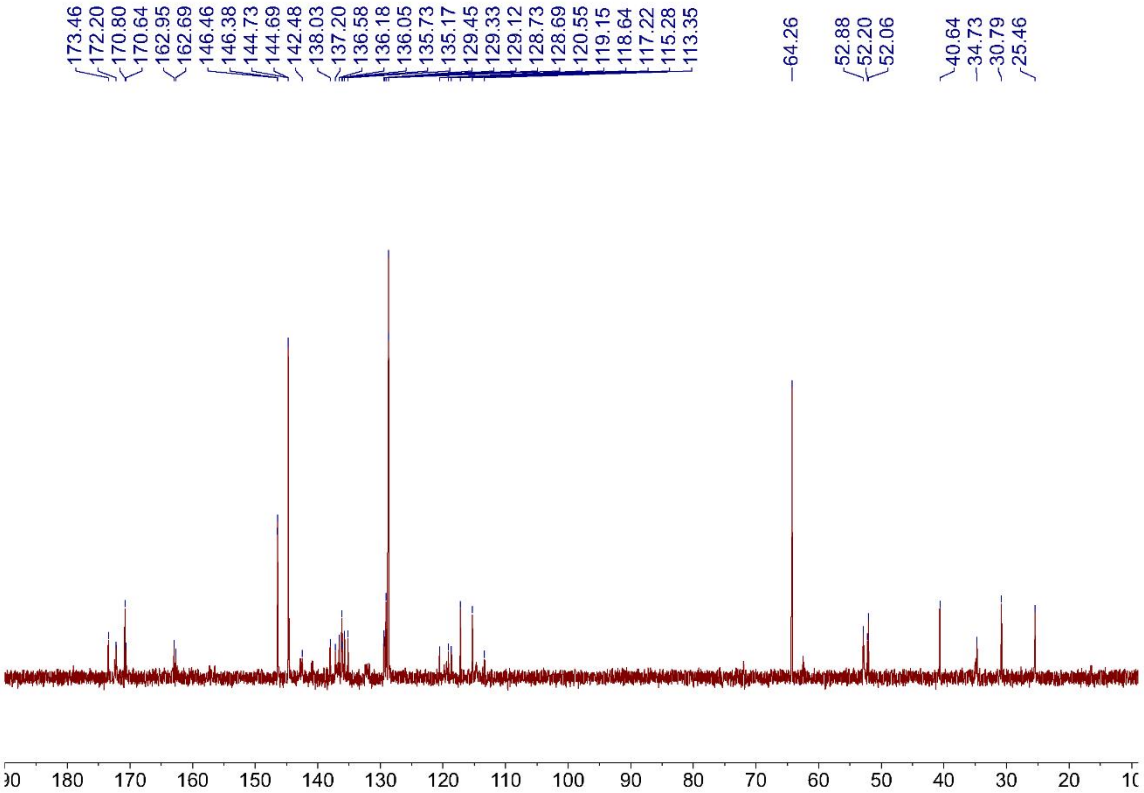

Figure S105. ^{13}C NMR spectrum (151 MHz, Deuterium Oxide) of **P_4-2a**.

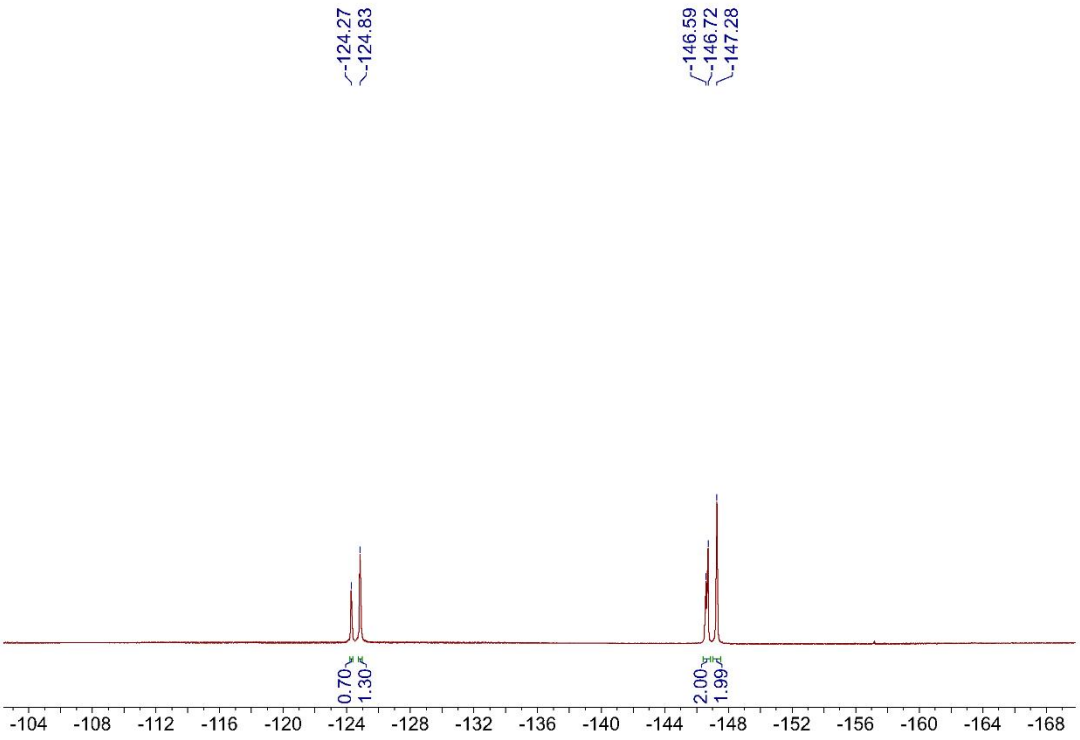

Figure S106. ^{19}F NMR spectrum (565 MHz, Deuterium Oxide) of **P$_4$-2a**.

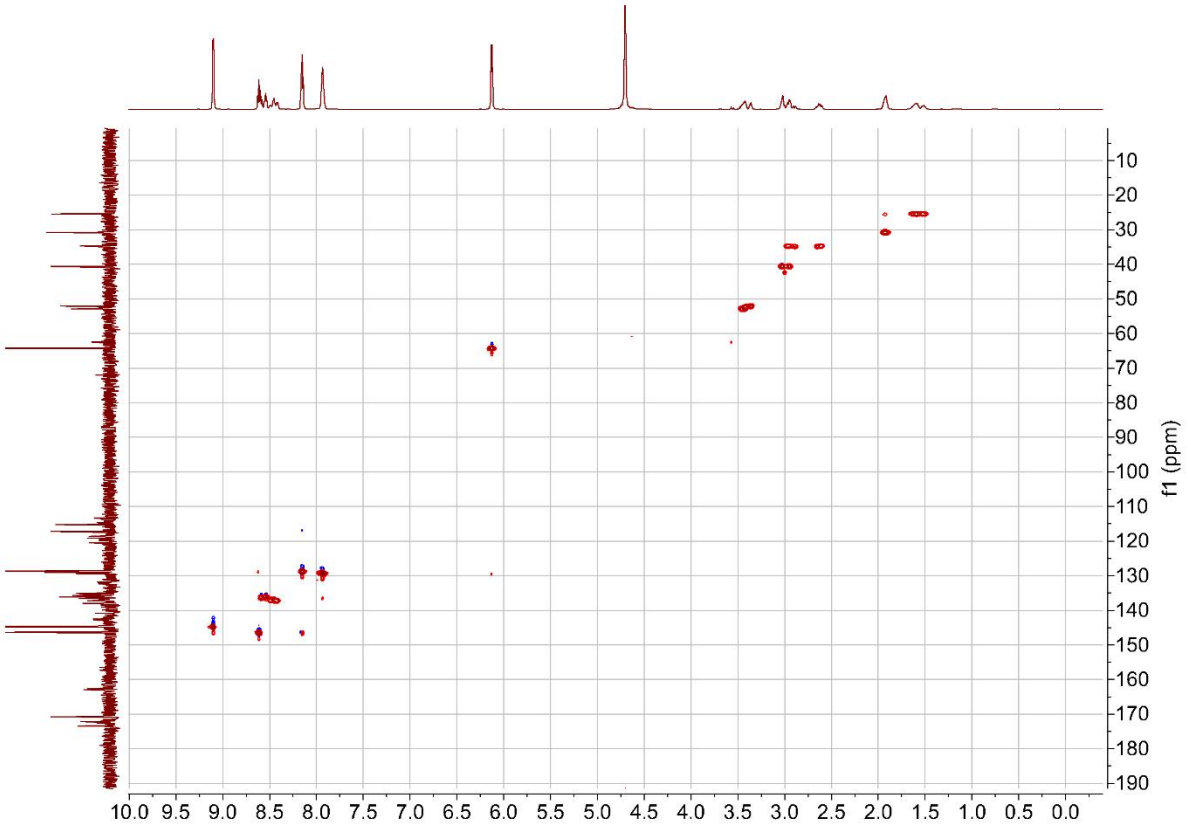

Figure S107. HSQC spectrum (600 MHz, Deuterium Oxide) of **P$_4$-2a**.

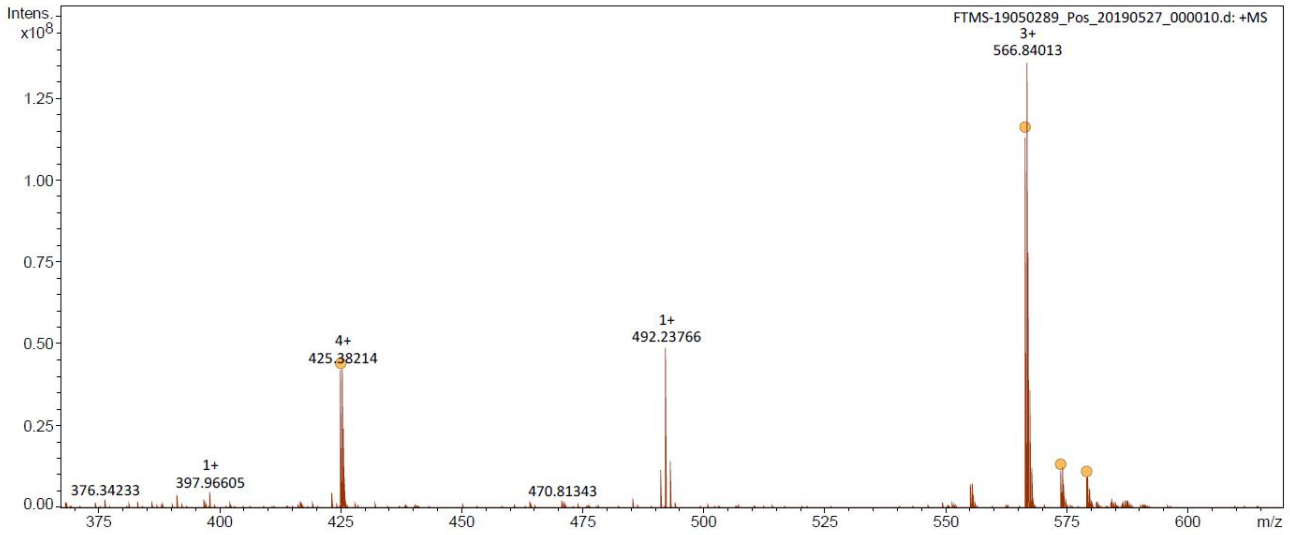

Meas. m/z	#	Ion Formula	Score	m/z	err [ppm]	Mean err [ppm]	mSigma	rdb	e⁻ Conf	N-Rule
425.131468	1	C88H78F6N14O12S2	100.00	425.131183	-0.7	-0.4	40.7	60.0	even	ok
566.506317	1	C88H77F6N14O12S2	100.00	566.505818	-0.9	-0.6	59.4	60.0	even	ok
573.833675	1	C88H76F6N14NaO12S2	100.00	573.833133	-0.9	-2.1	44.1	60.0	even	ok
579.156674	1	C88H76F6KN14O12S2	100.00	579.157779	1.9	1.8	87.1	60.0	even	ok

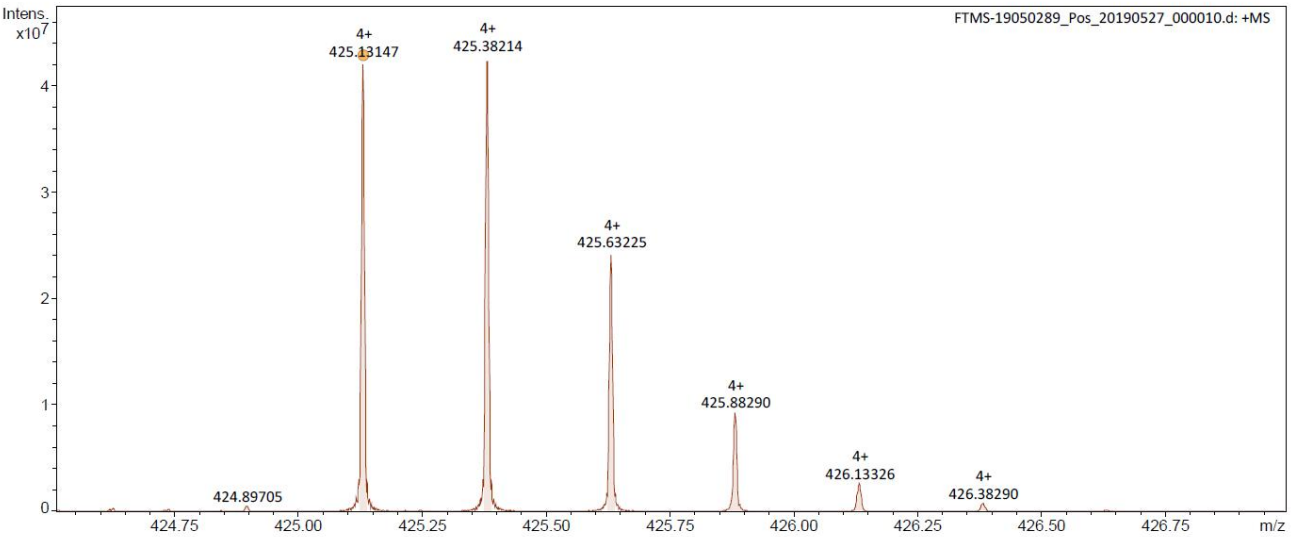

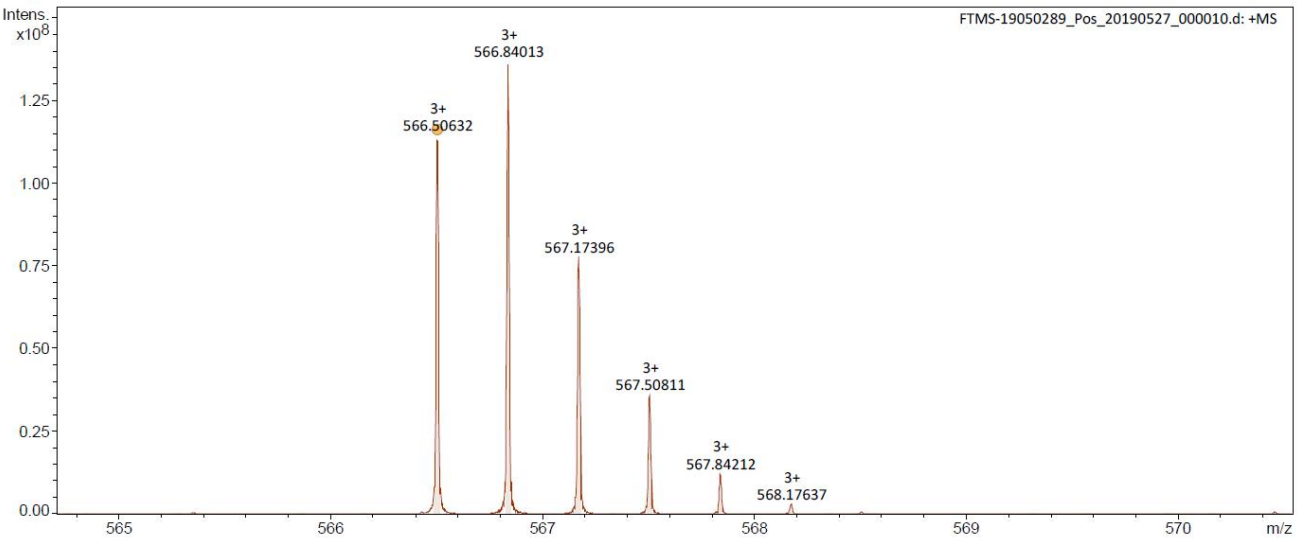

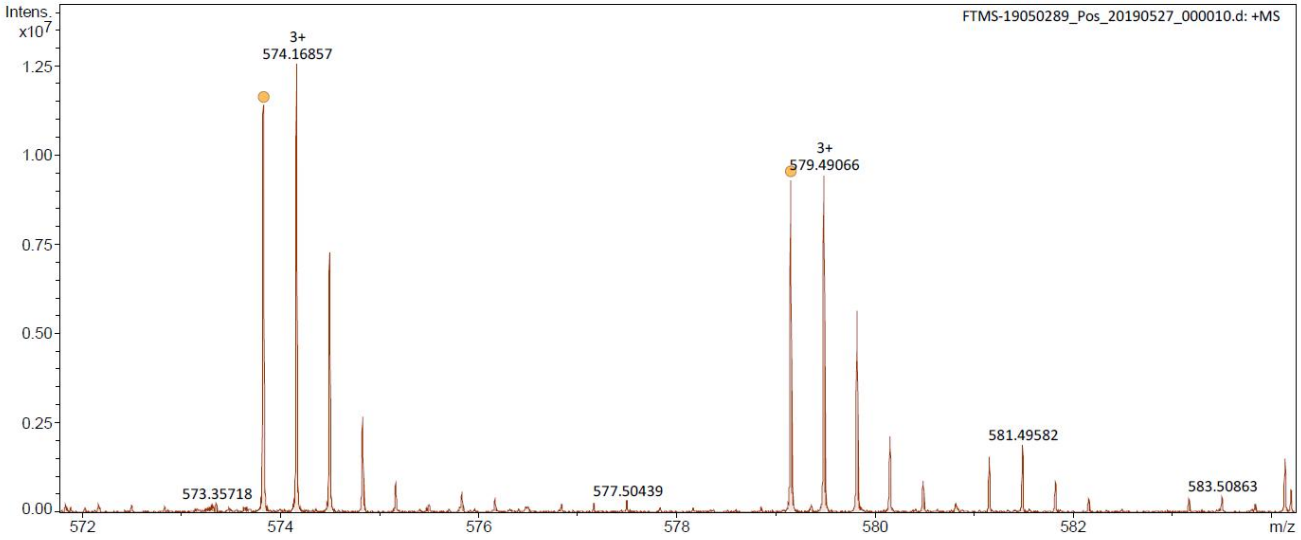

Figure S108. HRMS (ESI$^+$-FTICR) spectrum of **P_4-2a**.

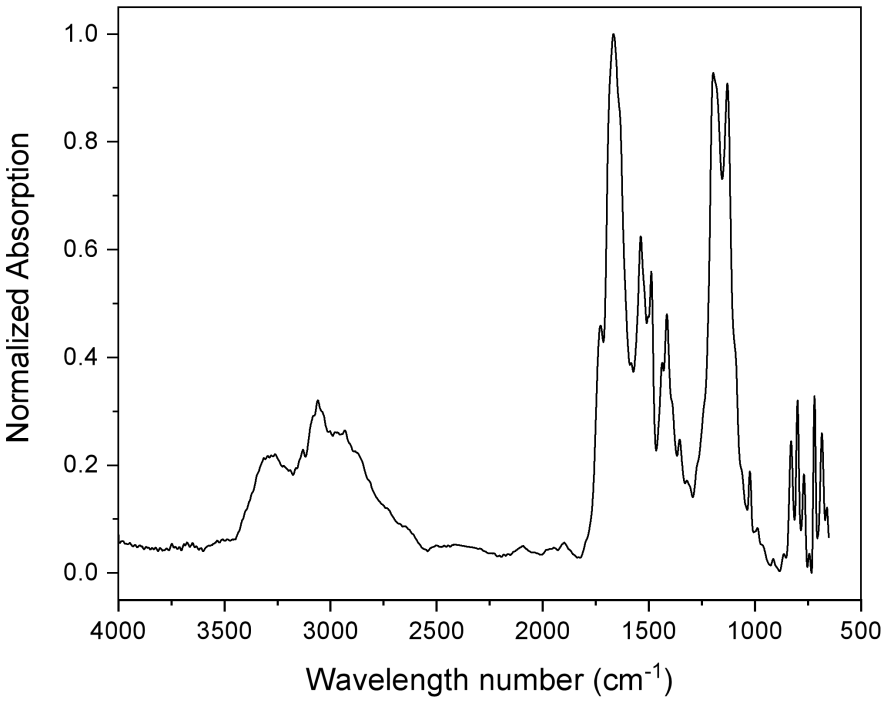

Figure S109. Normalized FT-IR spectrum of **P_4-2a**.

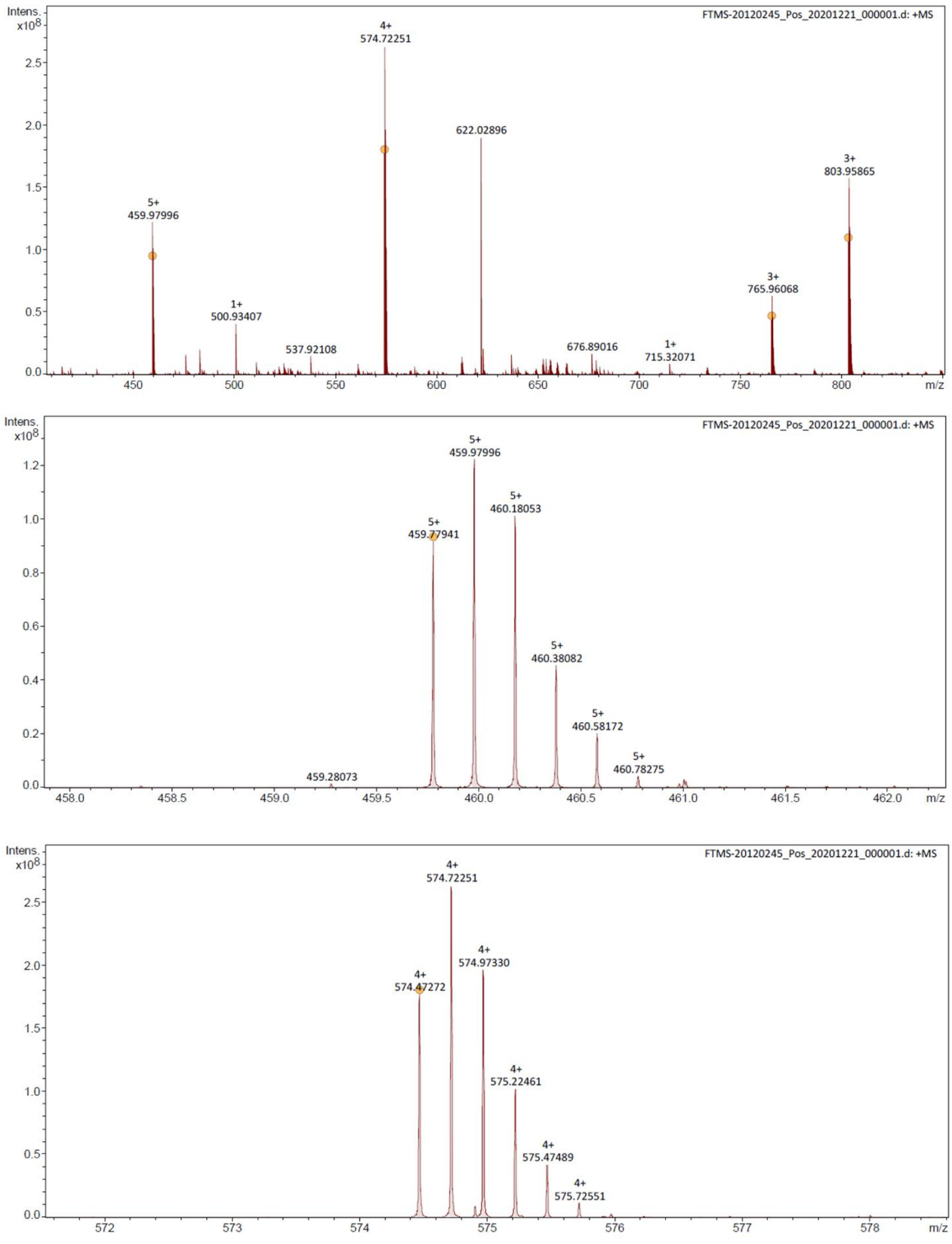
FTMS-20120245_Pos_20201221_000001.d: +MS
Intens.
x10^8
4+
574.72251
622.02896
3+
803.95865
5+
459.97996
3+
765.96068
1+
500.93407
537.92108
676.89016
1+
715.32071
m/z
FTMS-20120245_Pos_20201221_000001.d: +MS
5+
459.97996
5+
460.18053
5+
459.77941
5+
460.38082
5+
460.58172
5+
460.78275
459.28073
m/z
FTMS-20120245_Pos_20201221_000001.d: +MS
4+
574.72251
4+
574.97330
4+
574.47272
4+
575.22461
4+
575.47489
4+
575.72551
m/z

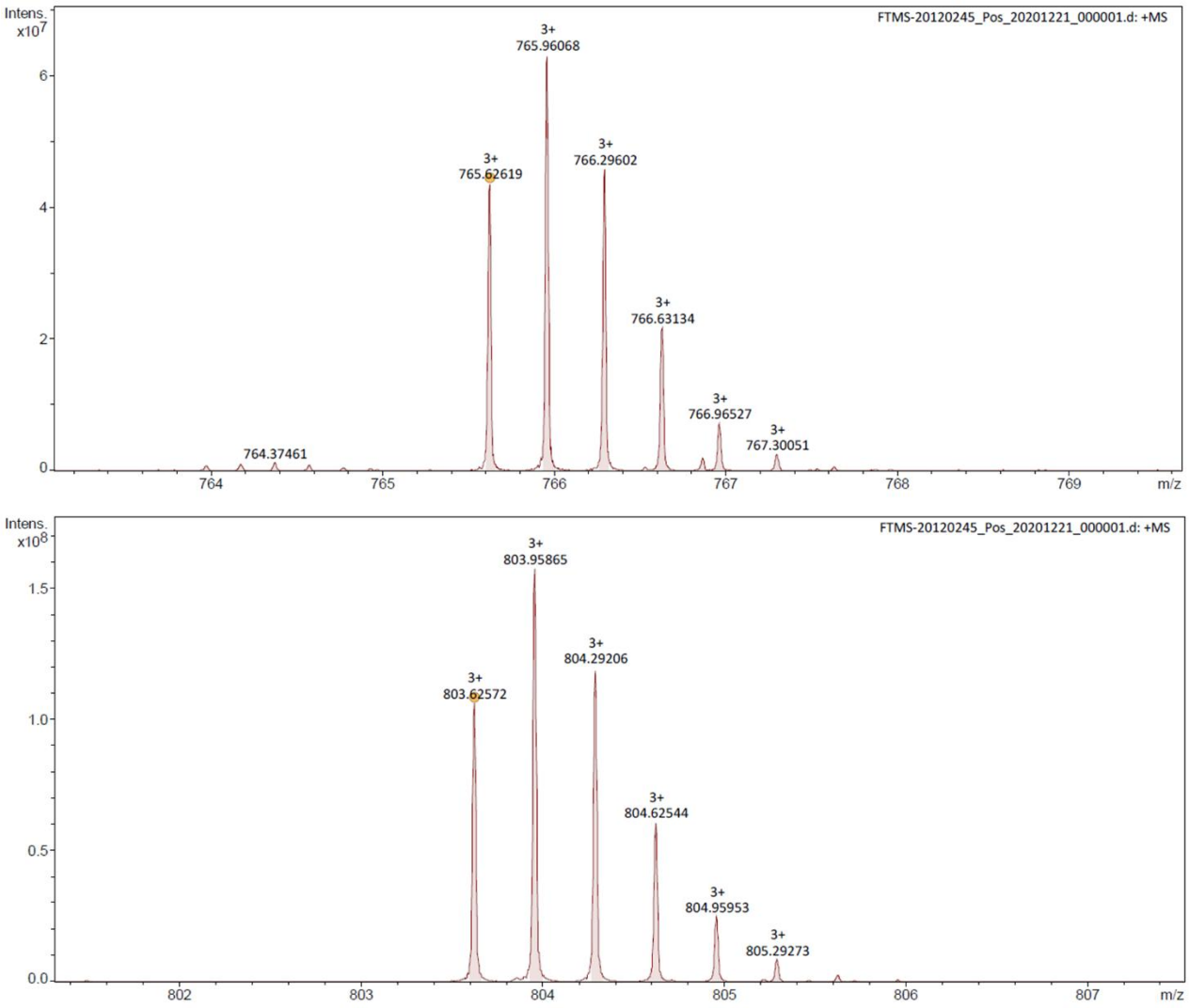

Figure S110. HRMS (ESI$^+$-FTICR) spectrum of **P_4-b**.

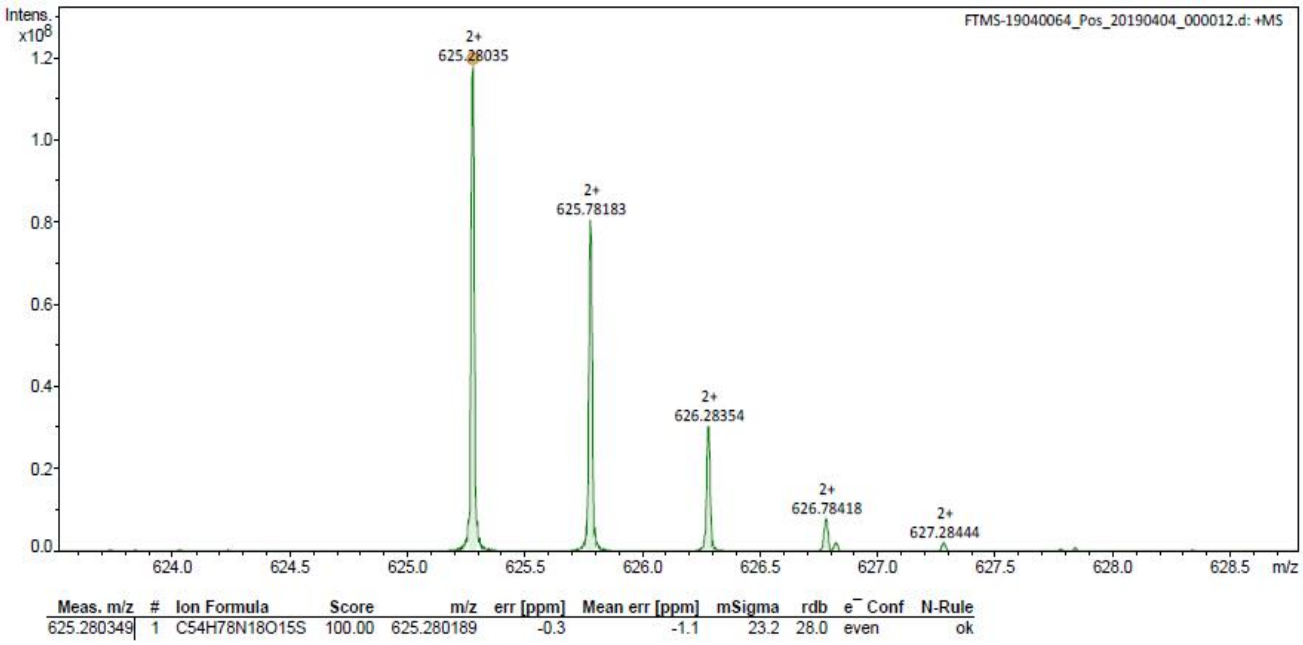

Meas. m/z	#	Ion Formula	Score	m/z	err [ppm]	Mean err [ppm]	mSigma	rdb	e⁻ Conf	N-Rule
625.280349	1	C54H78N18O15S	100.00	625.280189	-0.3	-1.1	23.2	28.0	even	ok

Figure S111. HRMS (ESI$^+$-FTICR) spectrum of **IAA-b**.

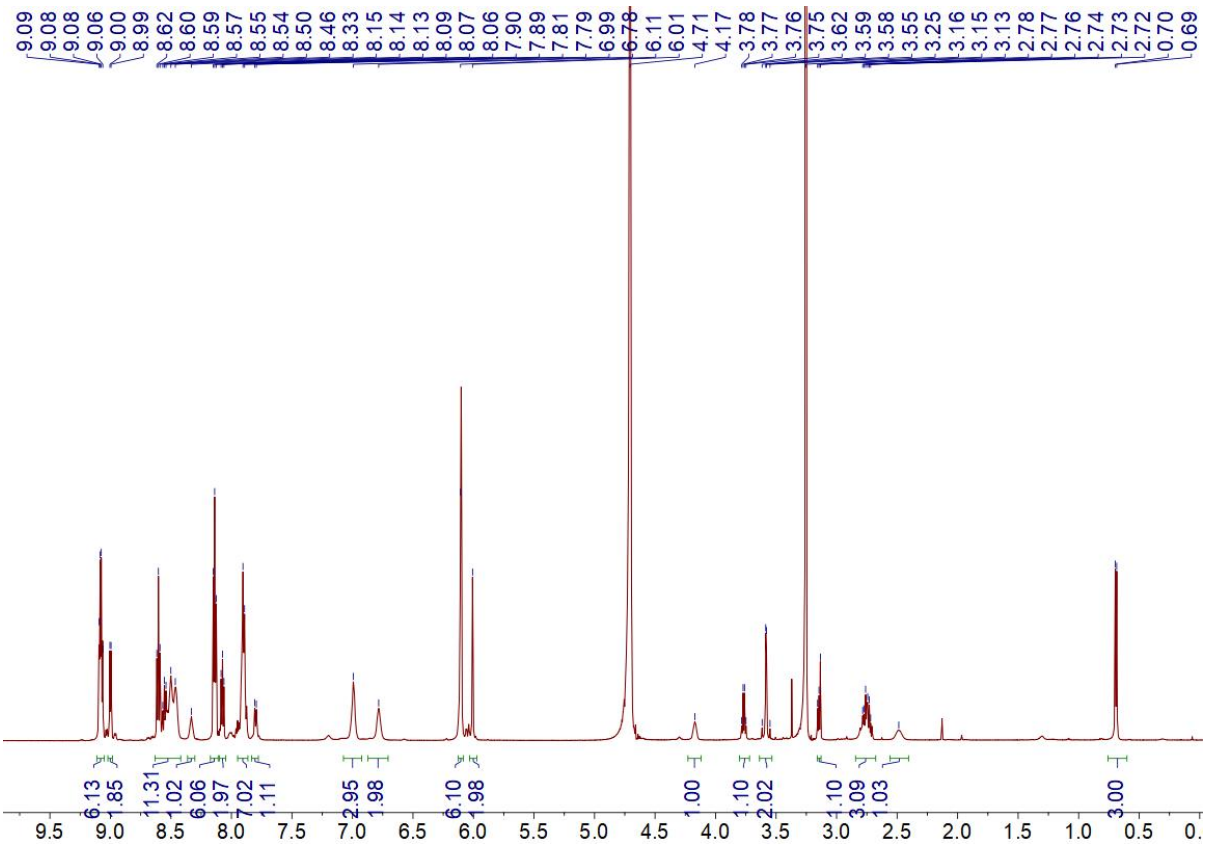

Figure S112. [1]H NMR spectrum (600 MHz, Deuterium Oxide) of **P_4-c**.

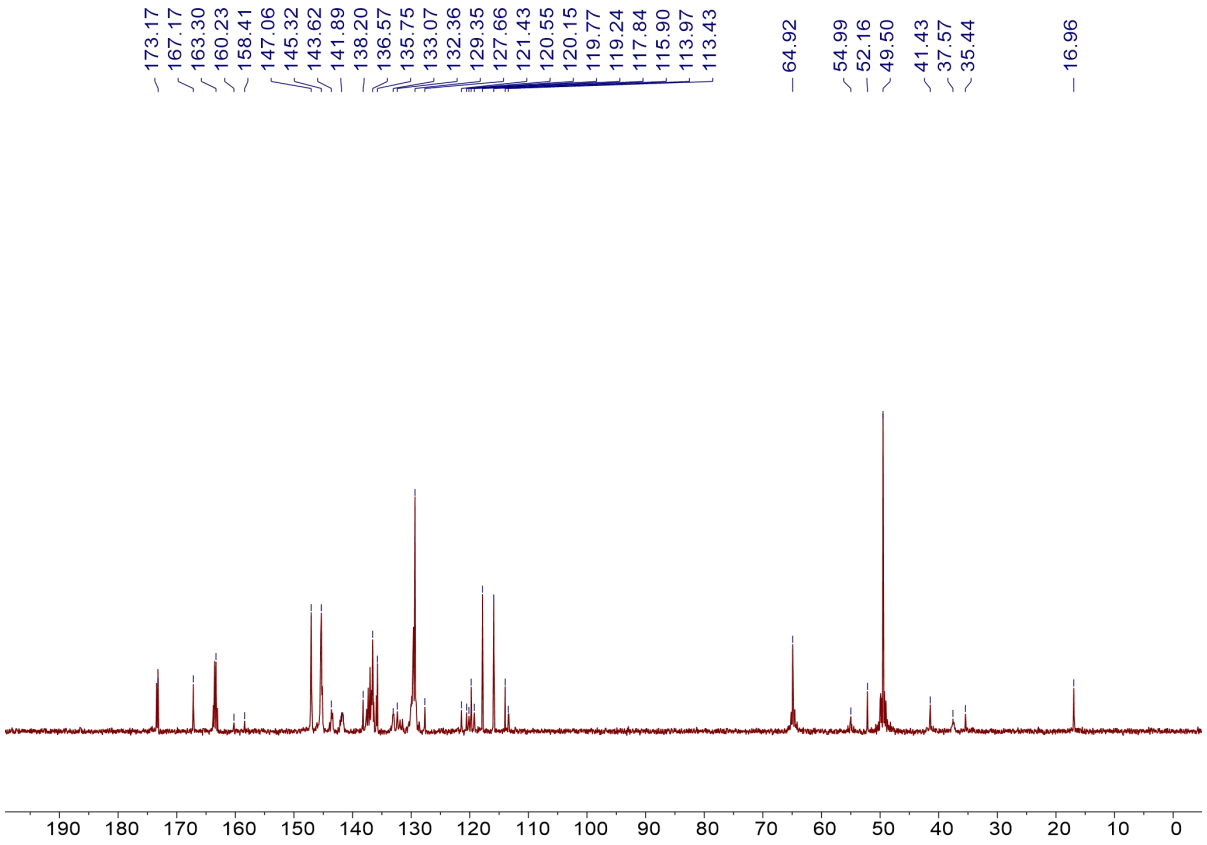

Figure S113. [13]C NMR spectrum (151 MHz, Deuterium Oxide, 1% MeOH) of **P_4-c**.

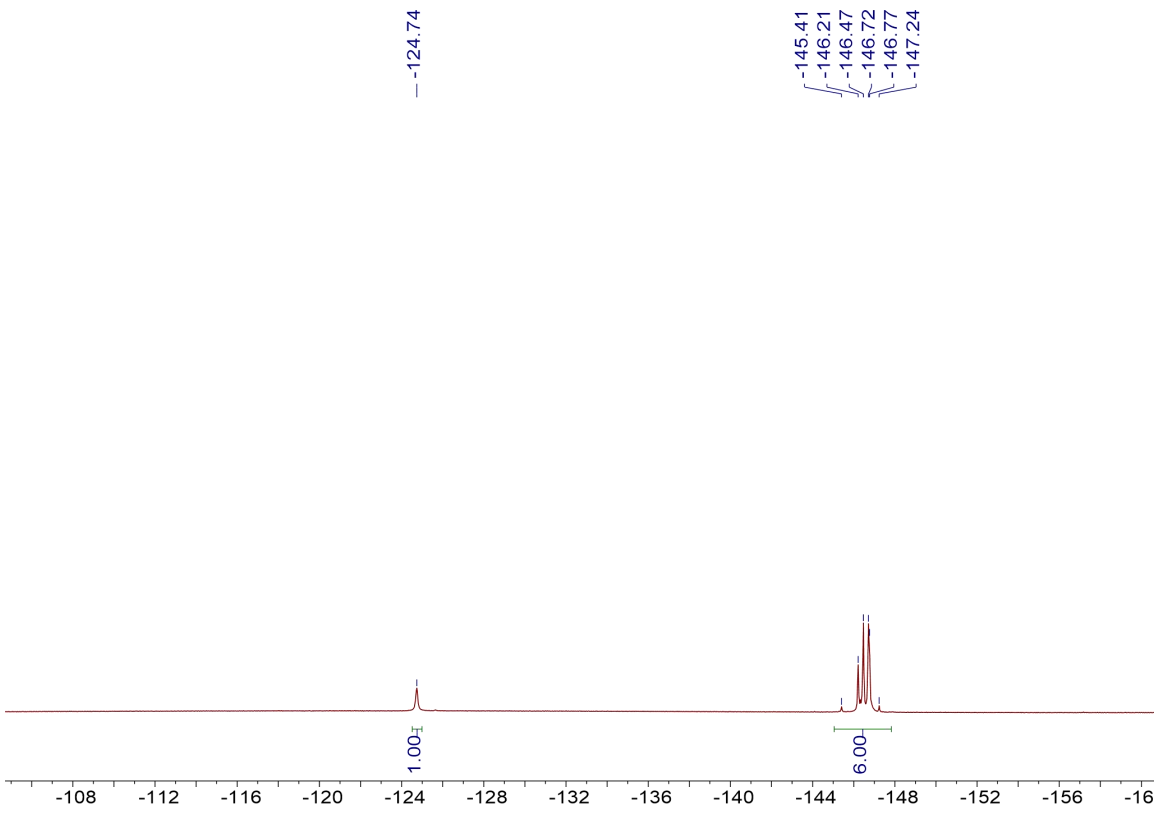

Figure S114. ^{19}F NMR spectrum (565 MHz, Deuterium Oxide, 1% MeOH) of **P$_4$-c**.

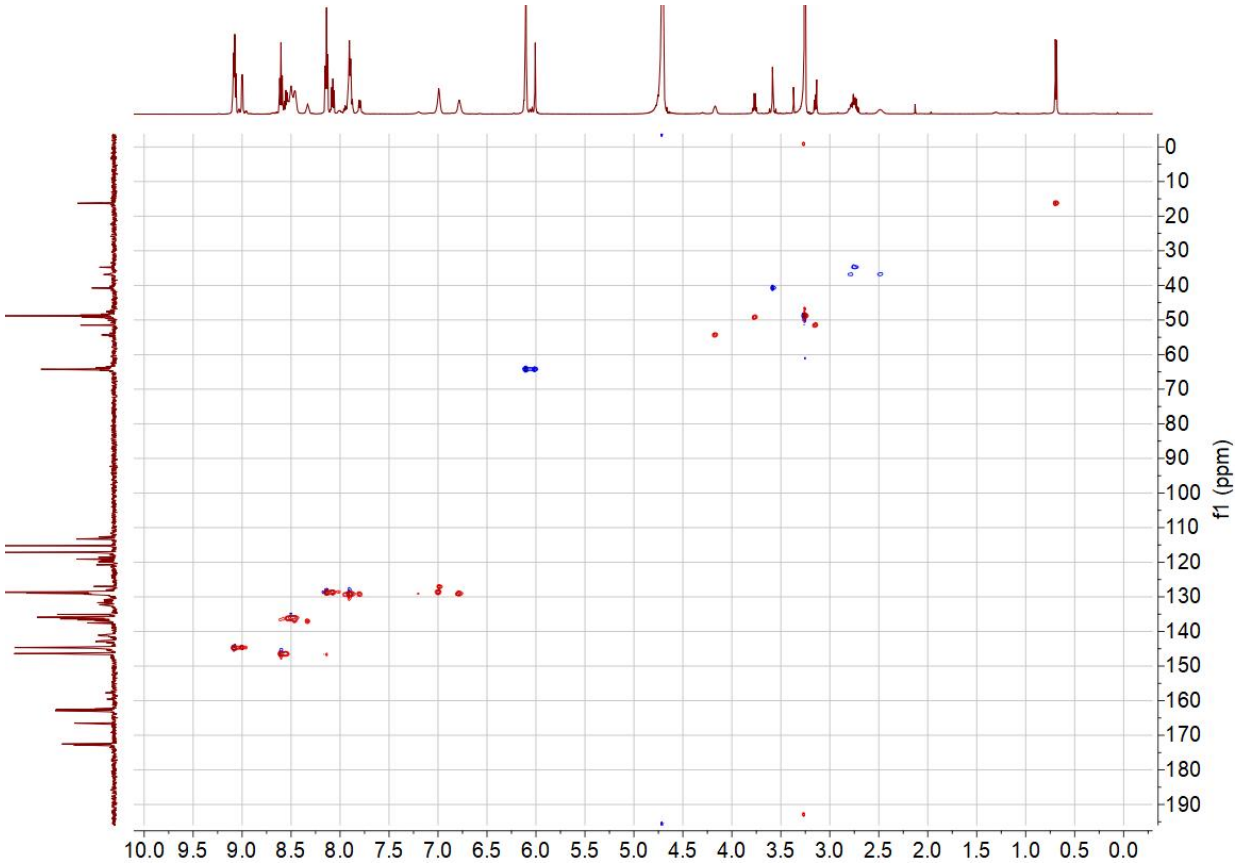

Figure S115. HSQC spectrum (600 MHz, Deuterium Oxide, 1% MeOH) of

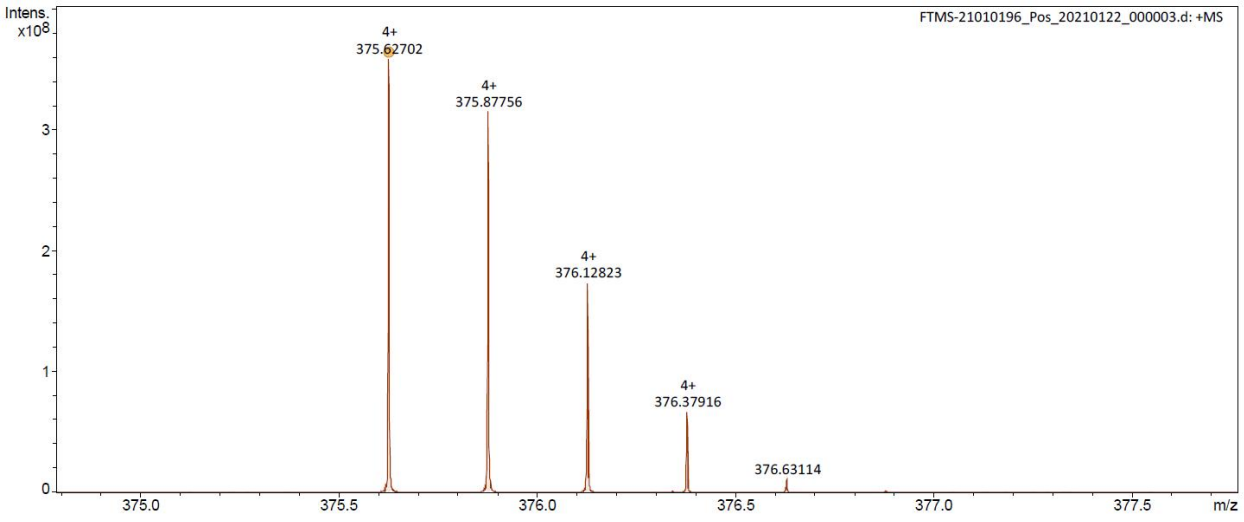

Meas. m/z	#	Ion Formula	Score	m/z	err [ppm]	Mean err [ppm]	mSigma	rdb	e⁻ Conf	N-Rule
375.627016	1	C85H69F7N12O5S	100.00	375.627522	1.3	1.0	47.4	58.0	even	ok
500.501244	1	C85H68F7N12O5S	100.00	500.500937	-0.6	-0.4	45.7	58.0	even	ok
538.499746	1	C87H69F10N12O7S	100.00	538.498558	-2.2	-2.8	66.7	58.0	even	ok

P$_4$-c.

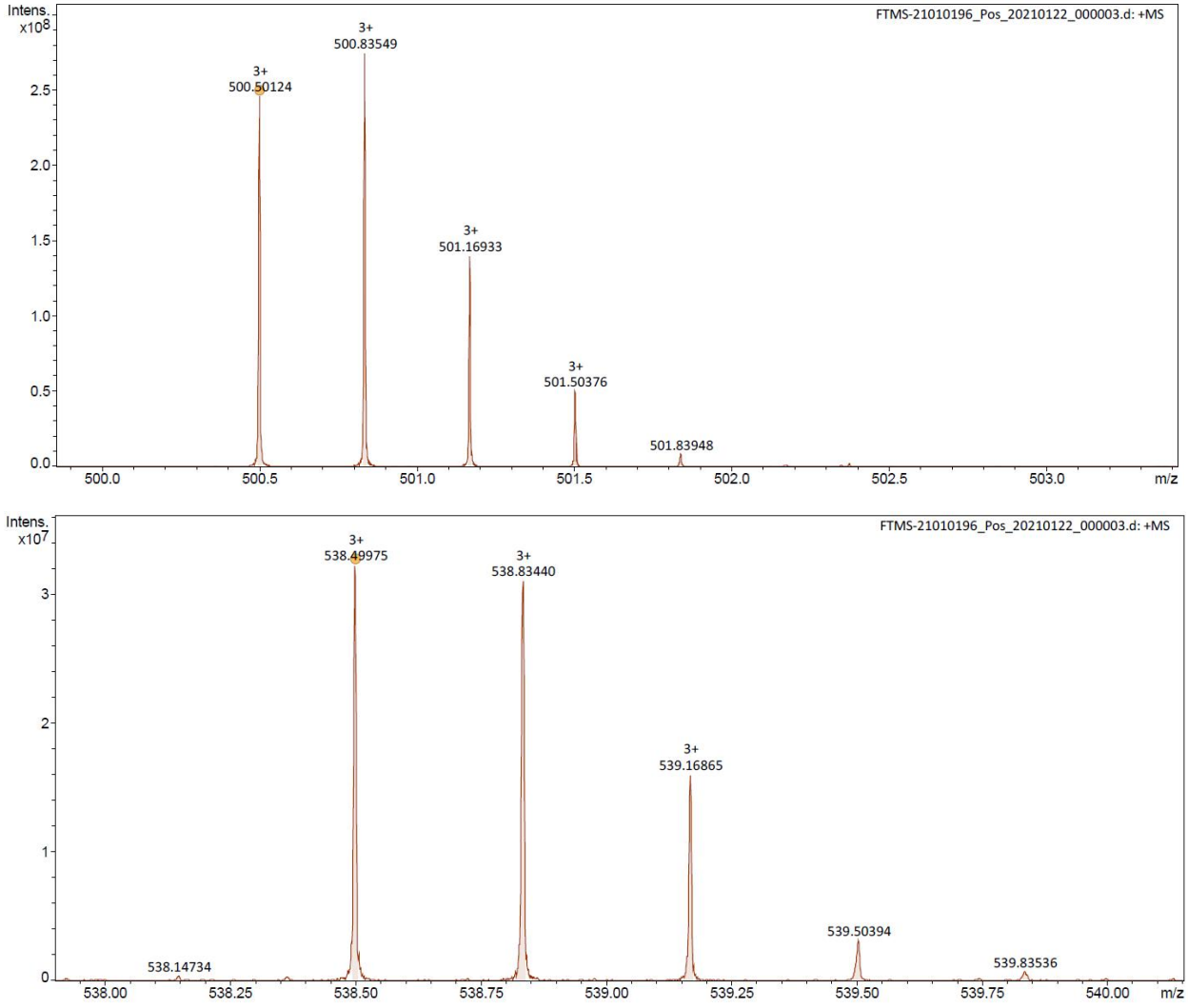

Figure S116. HRMS (ESI$^+$-FTICR) spectrum of **P$_4$-c**.

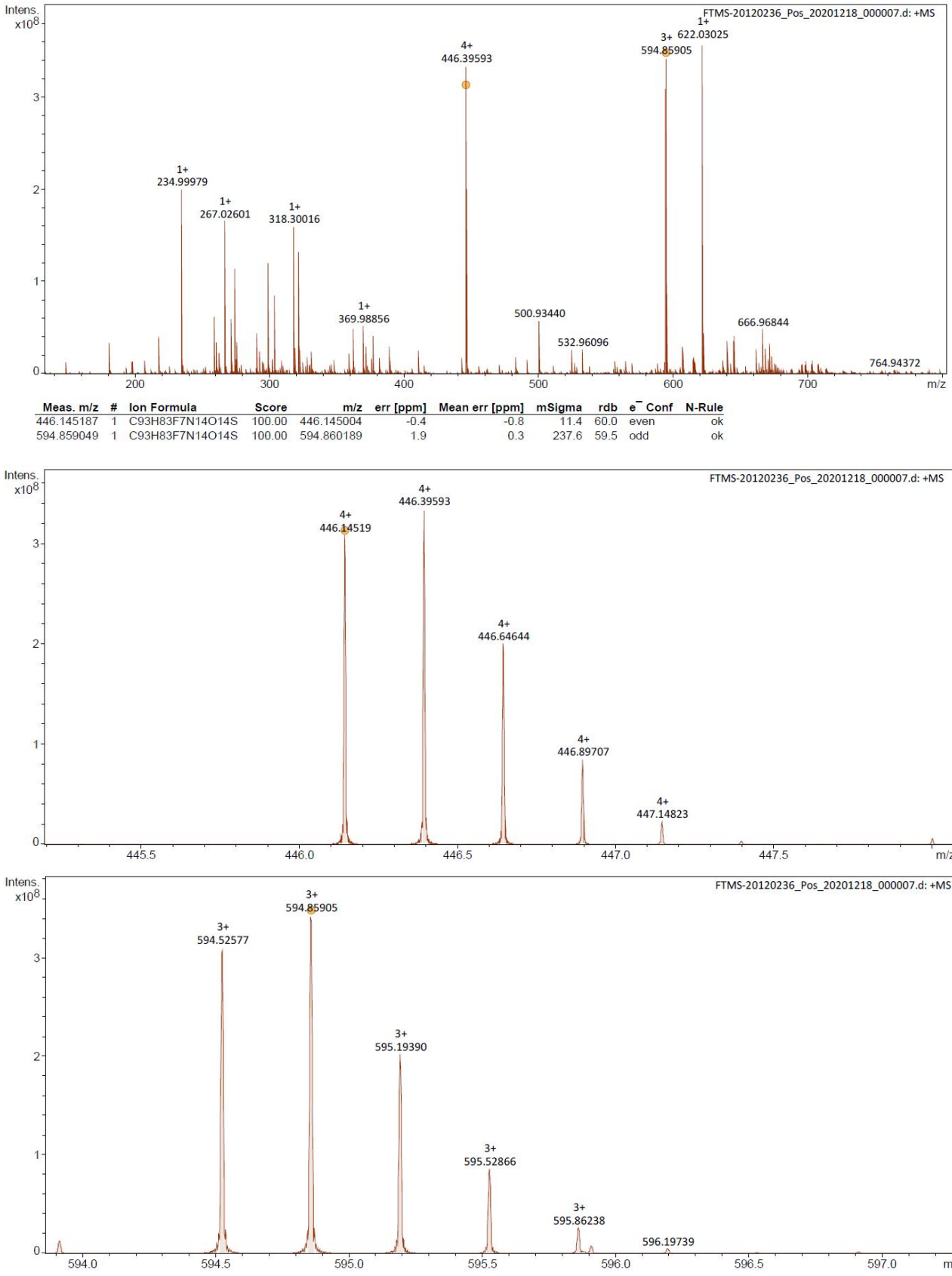

Figure S117. HRMS (ESI$^+$-FTICR) spectrum of **P_4-d**.

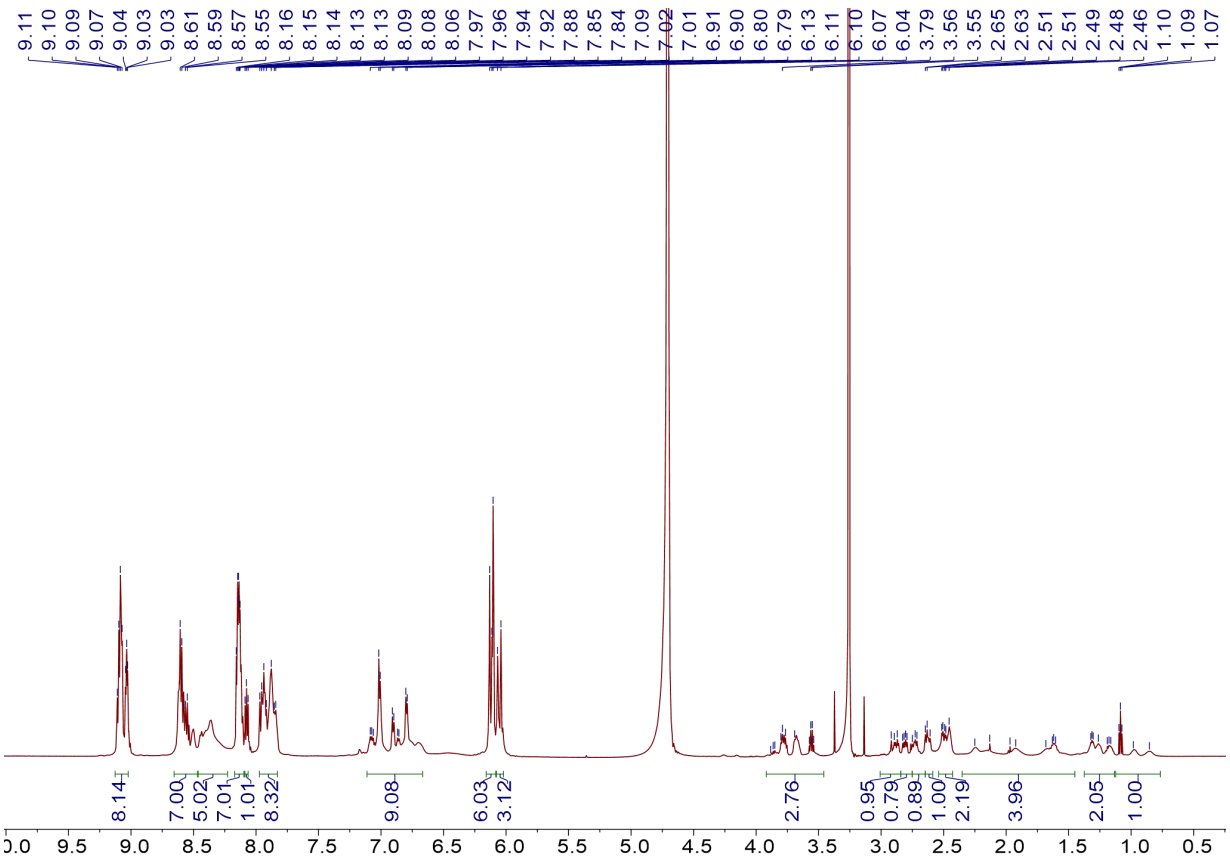

Figure S118. ^{1}H NMR spectrum (600 MHz, Deuterium Oxide, 1% MeOH) of **P_4-e**.

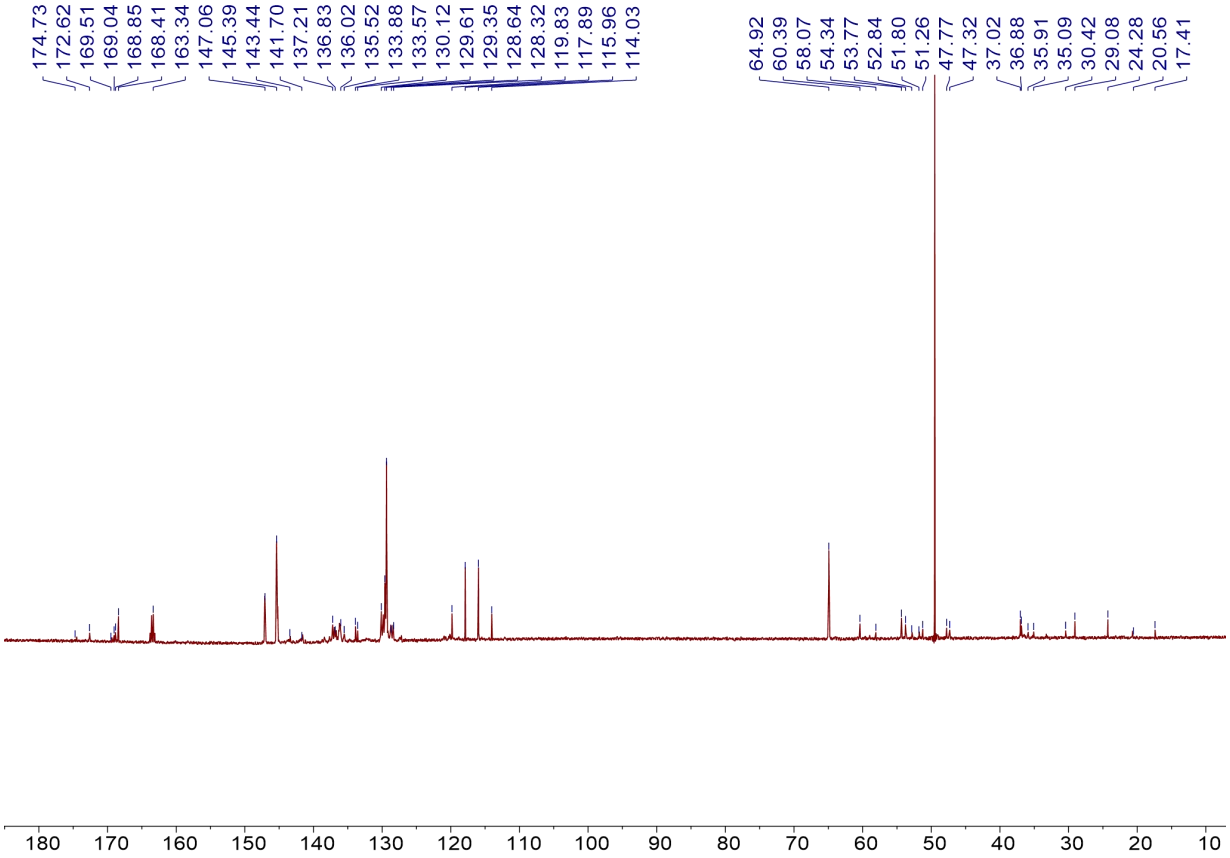

Figure S119. ^{13}C NMR spectrum (151 MHz, Deuterium Oxide, 1% MeOH) of **P_4-e**.

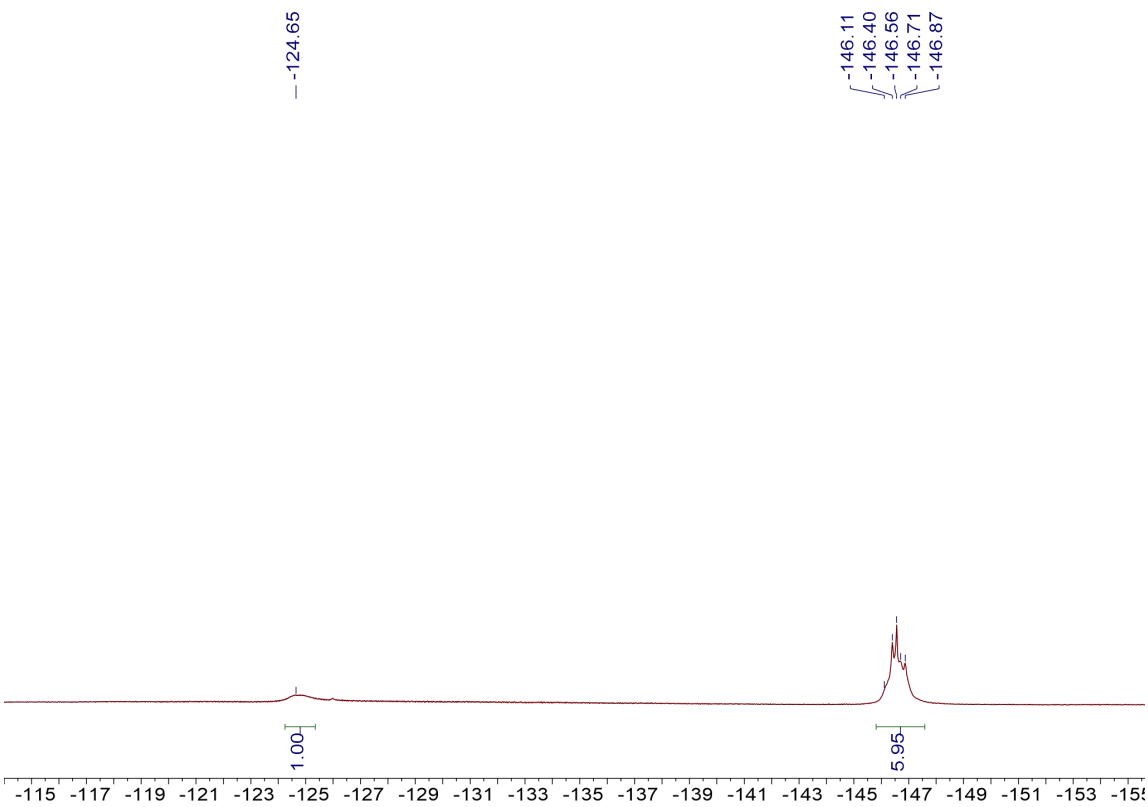

Figure S120. ^{19}F NMR spectrum (565 MHz, Deuterium Oxide, 1% MeOH) of **P$_4$-e**.

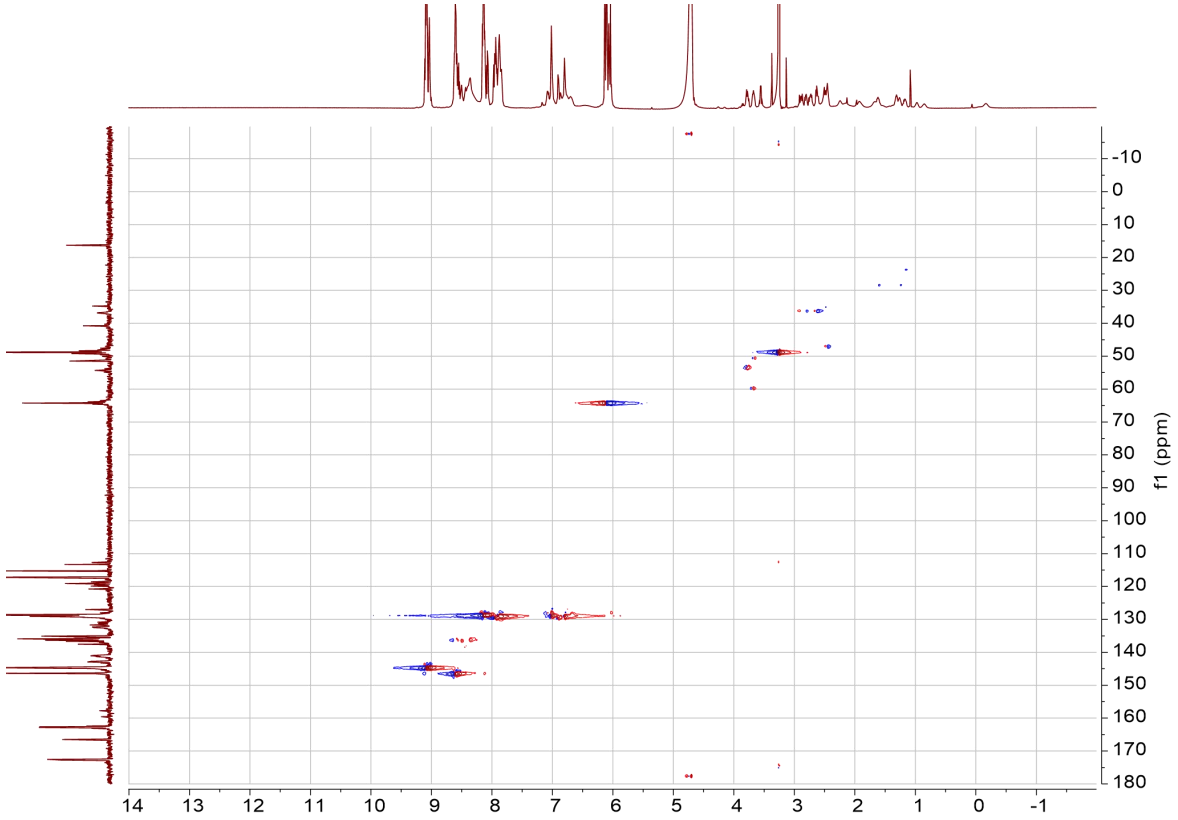

Figure S121. HSQC spectrum (600 MHz, Deuterium Oxide, 1% MeOH) of **P$_4$-e**.

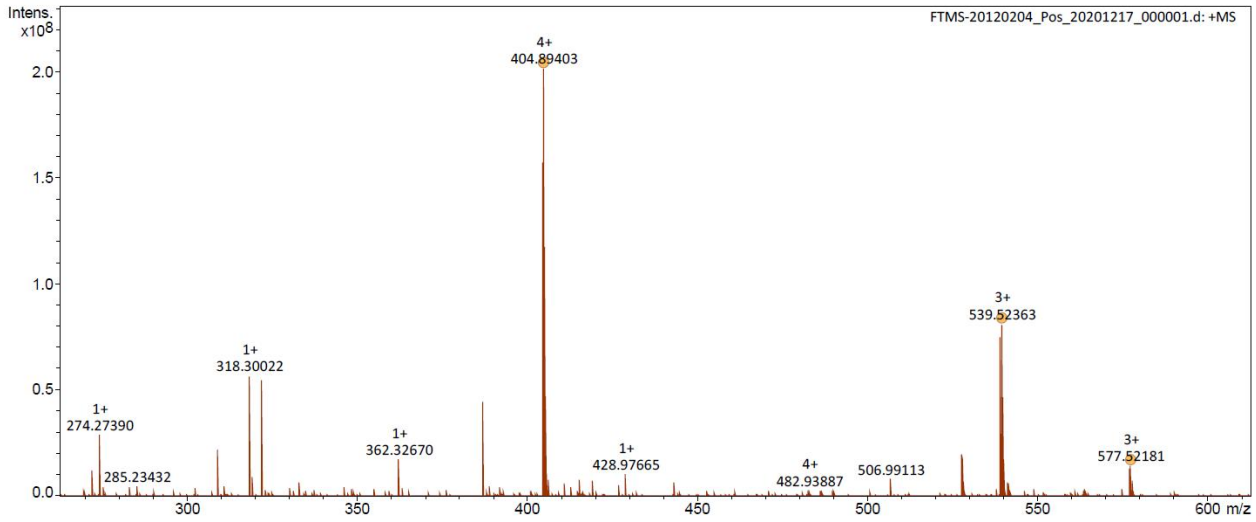

Meas. m/z	#	Ion Formula	Score	m/z	err [ppm]	Mean err [ppm]	mSigma	rdb	e¯ Conf	N-Rule
404.894028	1	C94H77F7N12O5S	100.00	404.643172	-0.2	-0.3	59.9	63.0	even	ok
539.523632	1	C94H76F7N12O5S	100.00	539.188470	-1.5	-2.0	24.1	63.0	even	ok
577.521808	1	C96H77F10N12O7S	100.00	577.186092	-2.3	-2.8	60.0	63.0	even	ok

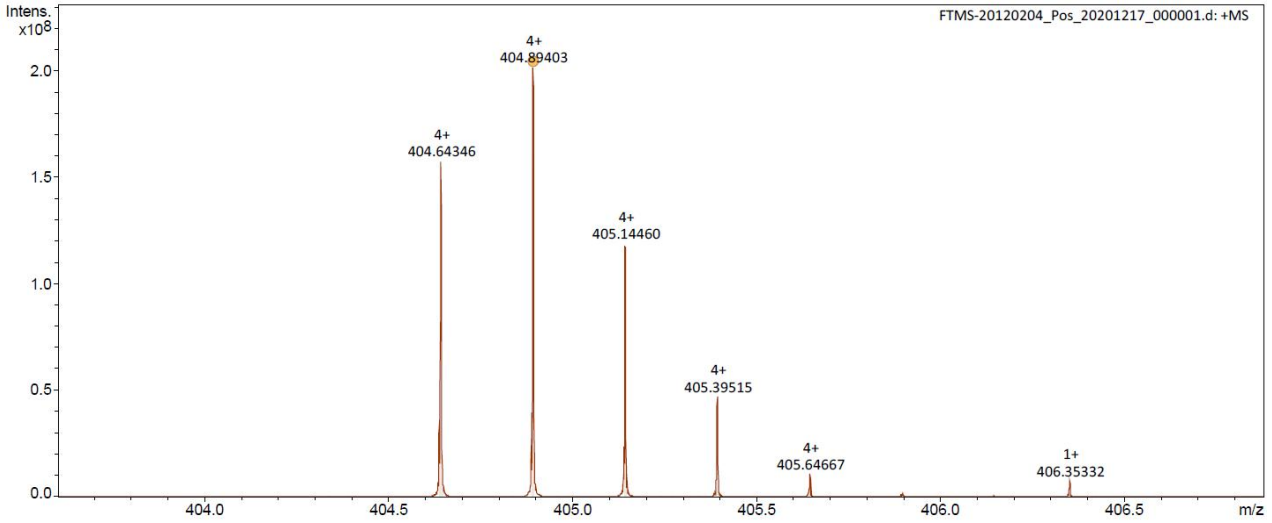

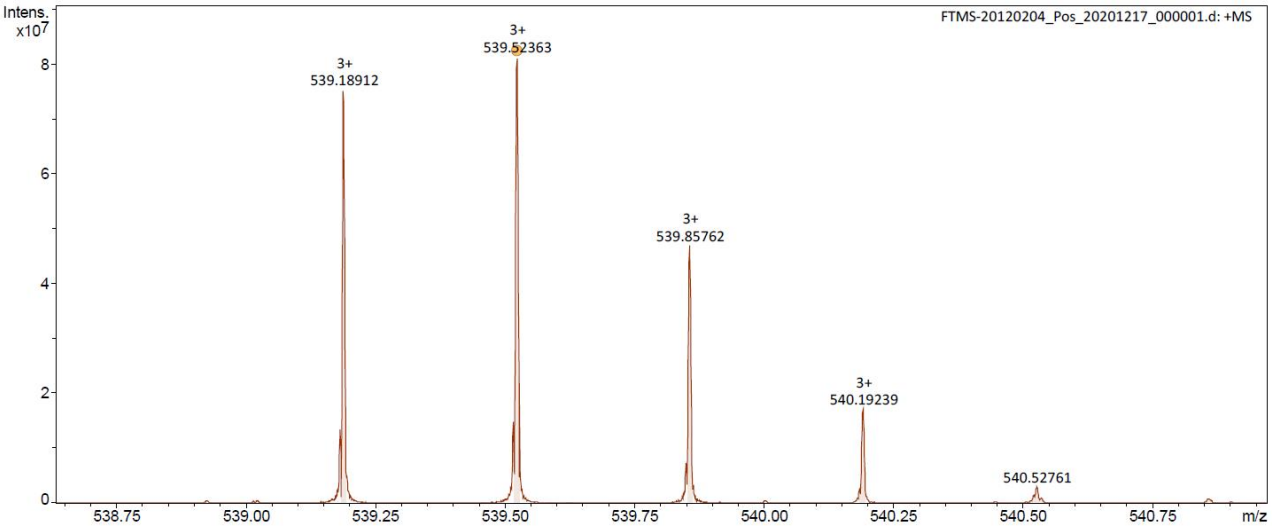

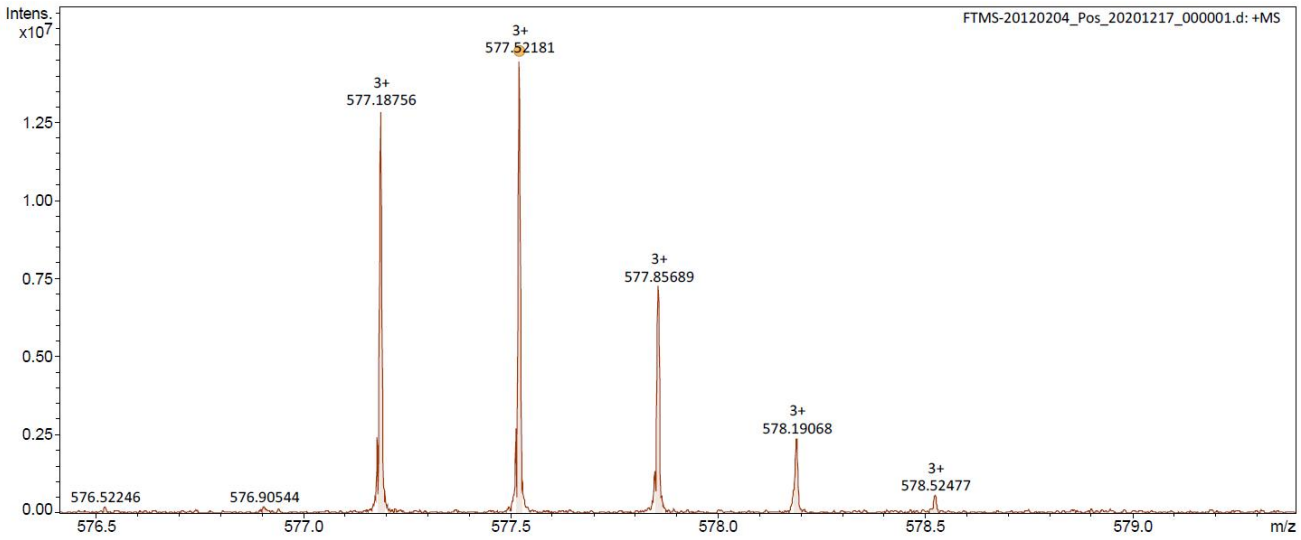

Figure S122. HRMS (ESI$^+$-FTICR) spectrum of **P_4-e**.

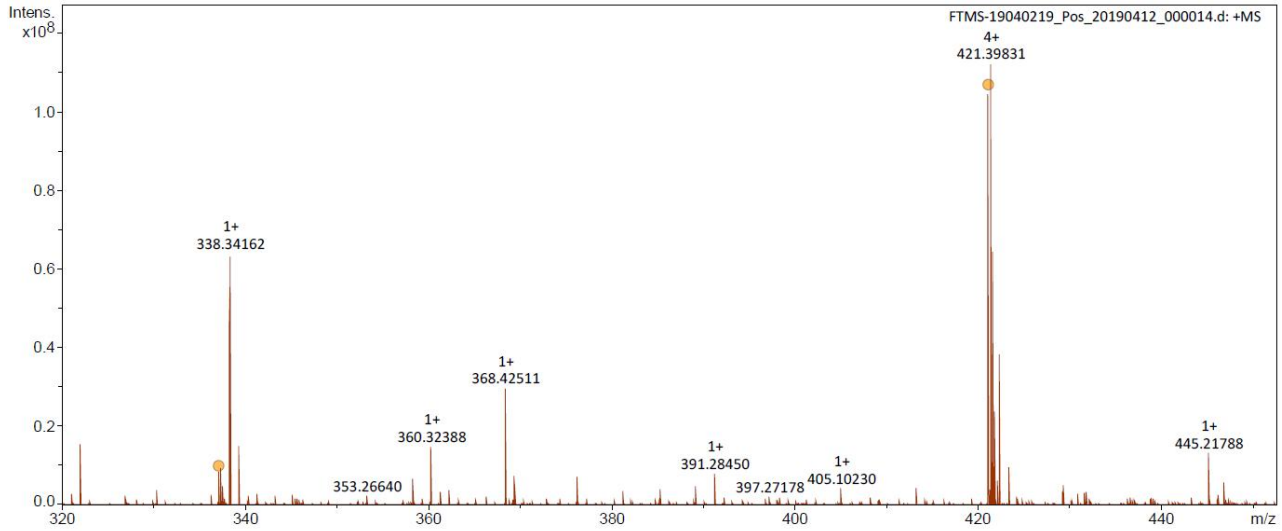

Meas. m/z	#	Ion Formula	Score	m/z	err [ppm]	Mean err [ppm]	mSigma	rdb	e⁻ Conf	N-Rule
337.119630	1	C92H80F7N16O7S	100.00	337.119548	-0.2	-1.3	55.1	62.0	even	ok
421.147583	1	C92H79F7N16O7S	100.00	421.147616	0.1	-0.5	18.8	62.0	even	ok
561.530210	1	C92H79F7N16O7S	100.00	561.530337	0.2	0.3	263.0	61.5	odd	ok

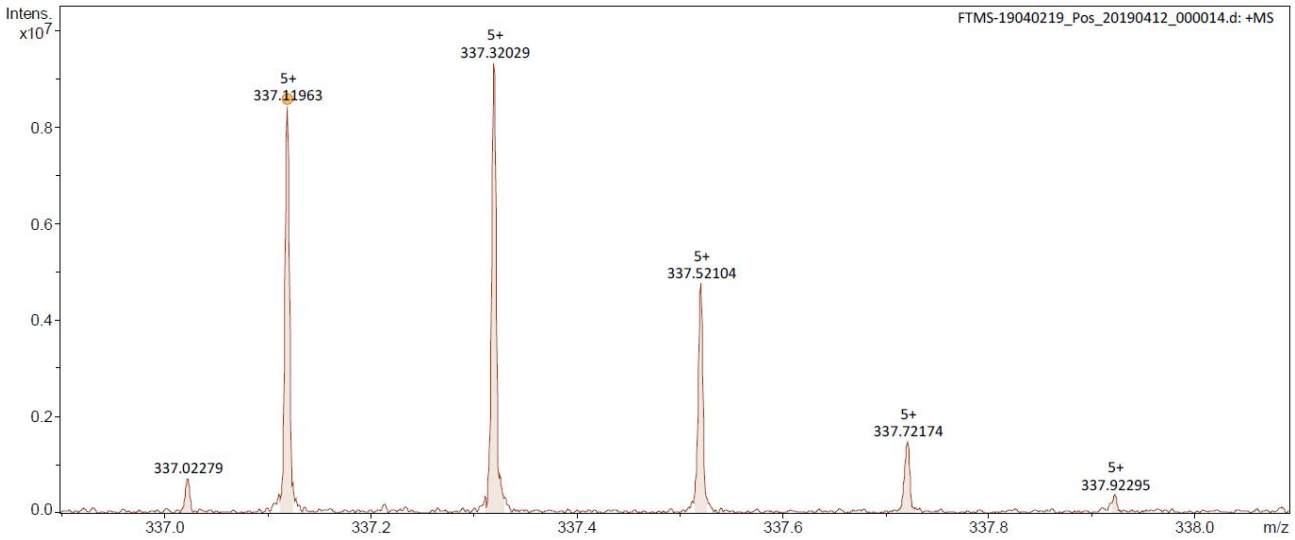

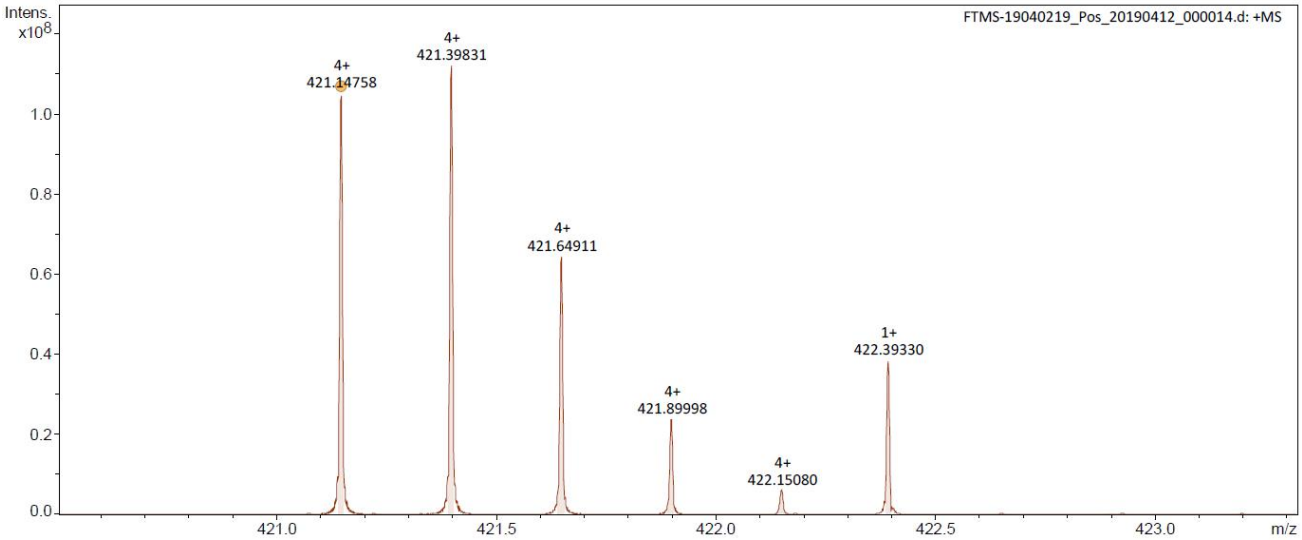

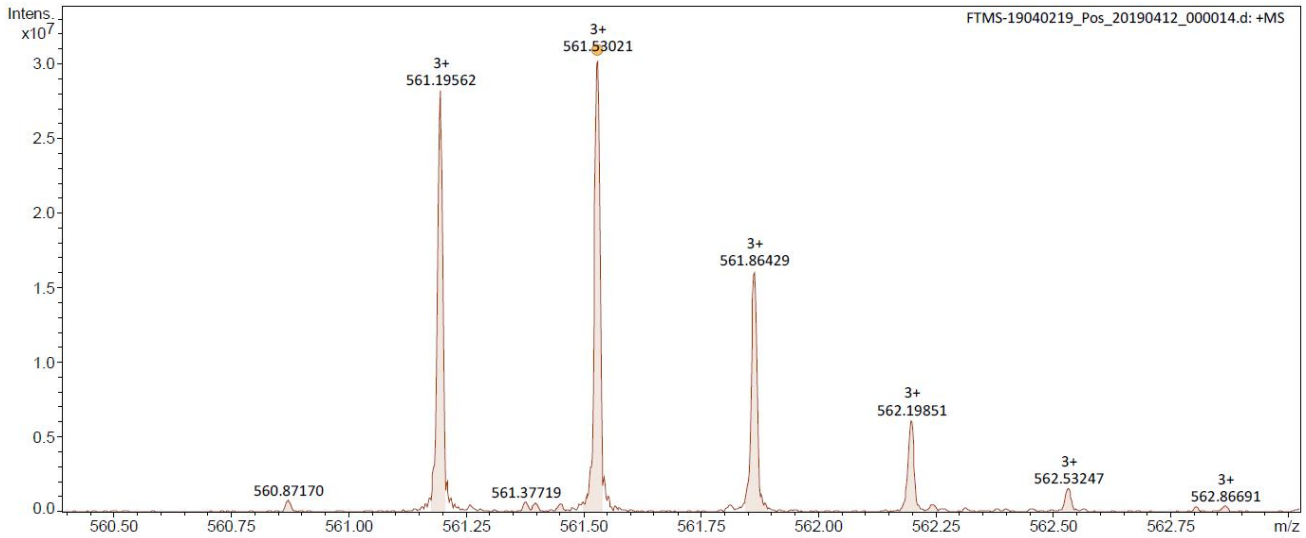

Figure S123. HRMS (ESI$^+$-FTICR) spectrum of **P_4-f**.

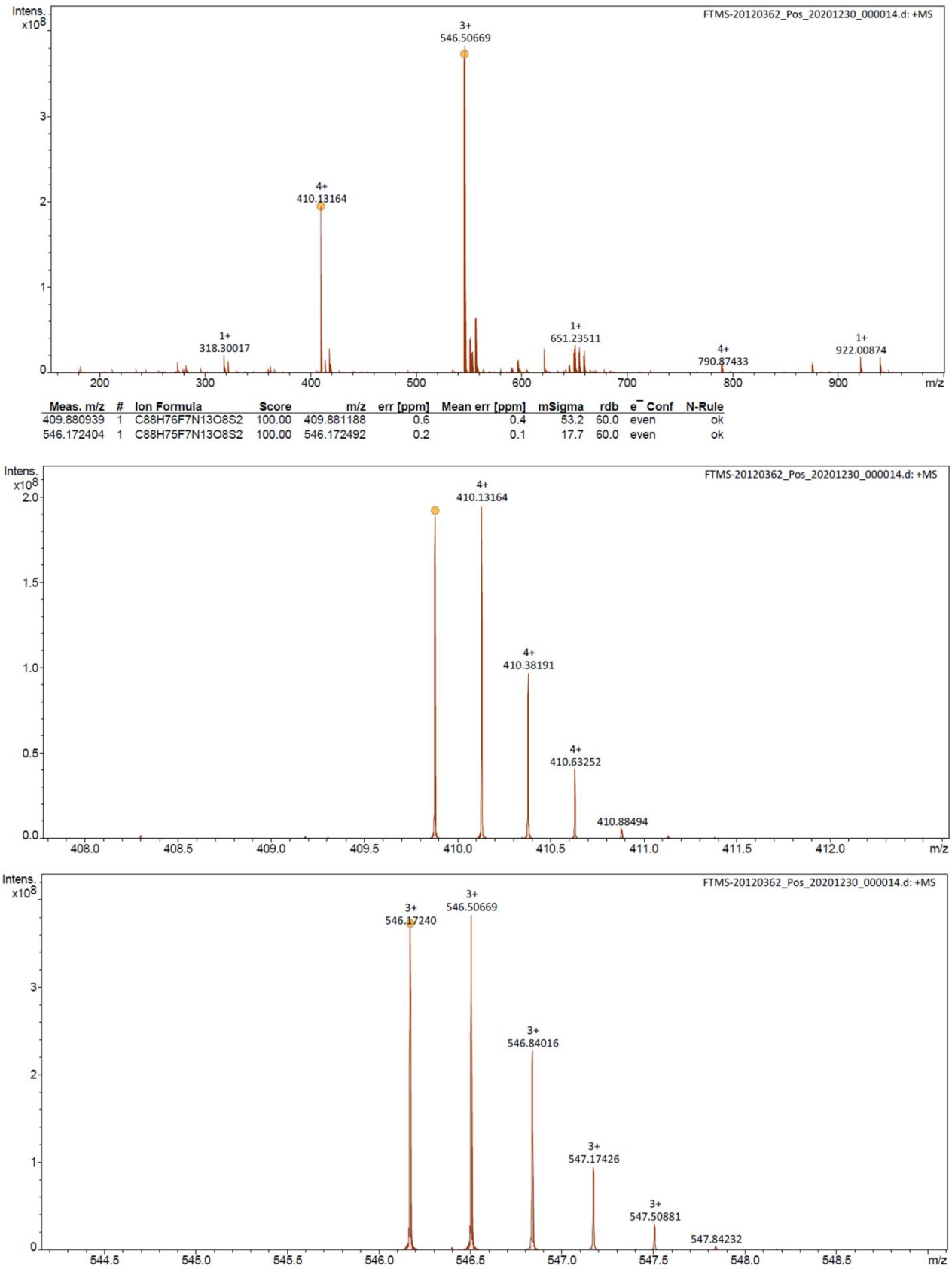

Figure S124. HRMS (ESI$^+$-FTICR) spectrum of **P_4-g**.

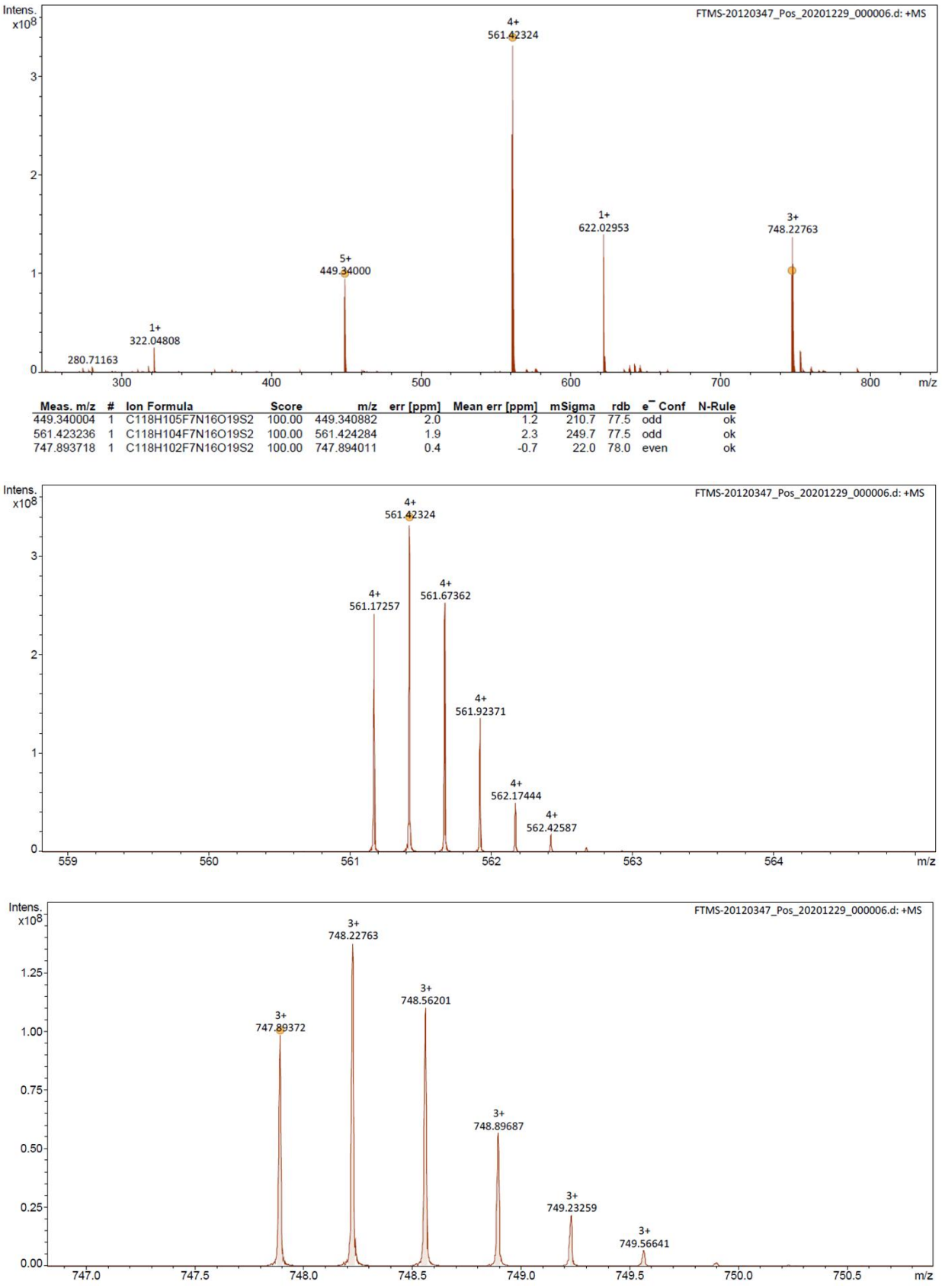

Meas. m/z	#	Ion Formula	Score	m/z	err [ppm]	Mean err [ppm]	mSigma	rdb	e⁻ Conf	N-Rule
449.340004	1	C118H105F7N16O19S2	100.00	449.340882	2.0	1.2	210.7	77.5	odd	ok
561.423236	1	C118H104F7N16O19S2	100.00	561.424284	1.9	2.3	249.7	77.5	odd	ok
747.893718	1	C118H102F7N16O19S2	100.00	747.894011	0.4	-0.7	22.0	78.0	even	ok

Figure S125. HRMS (ESI$^+$-FTICR) spectrum of **P$_4$-k**.

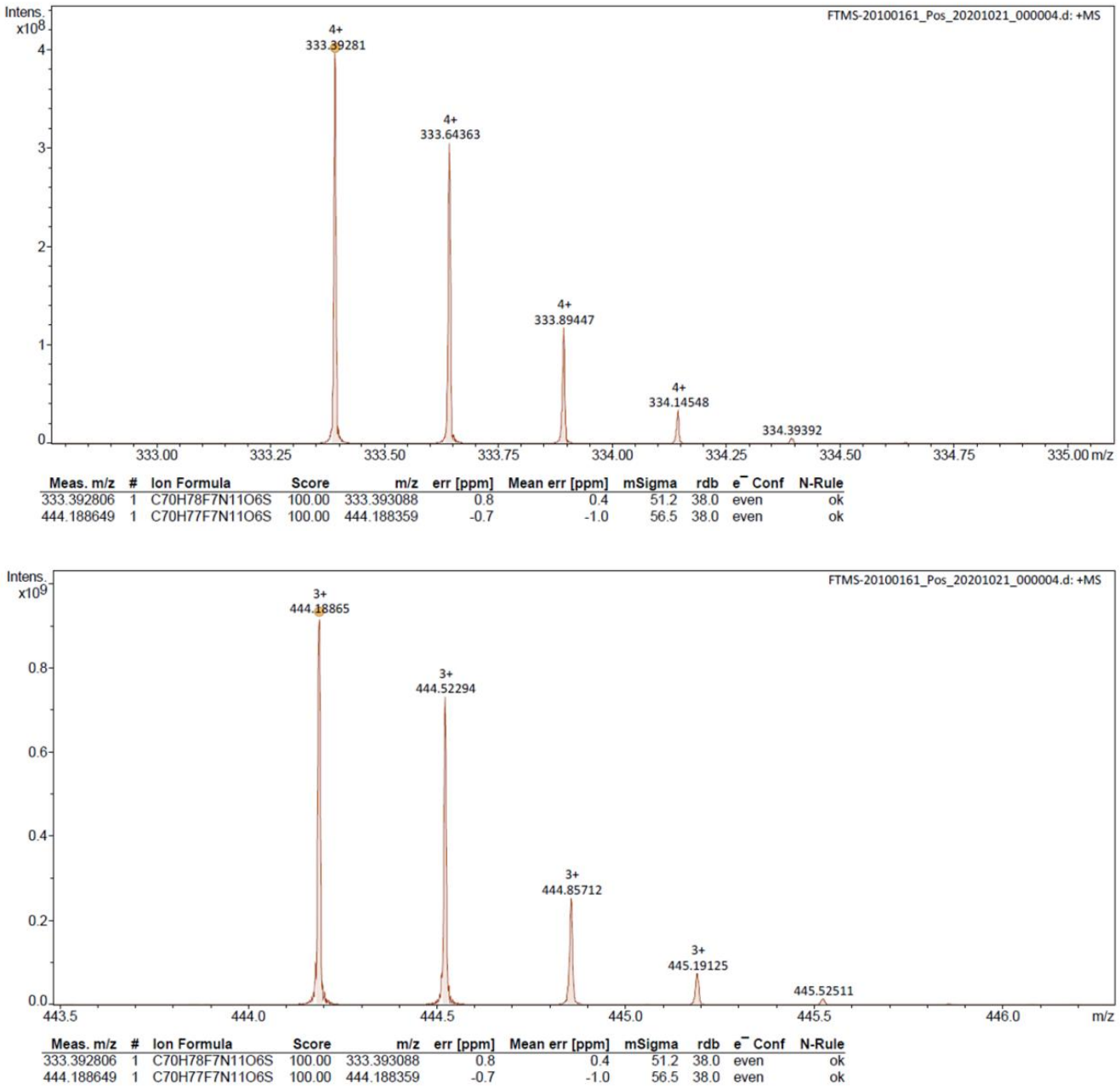

Meas. m/z	#	Ion Formula	Score	m/z	err [ppm]	Mean err [ppm]	mSigma	rdb	e⁻ Conf	N-Rule
333.392806	1	C70H78F7N11O6S	100.00	333.393088	0.8	0.4	51.2	38.0	even	ok
444.188649	1	C70H77F7N11O6S	100.00	444.188359	-0.7	-1.0	56.5	38.0	even	ok

Meas. m/z	#	Ion Formula	Score	m/z	err [ppm]	Mean err [ppm]	mSigma	rdb	e⁻ Conf	N-Rule
333.392806	1	C70H78F7N11O6S	100.00	333.393088	0.8	0.4	51.2	38.0	even	ok
444.188649	1	C70H77F7N11O6S	100.00	444.188359	-0.7	-1.0	56.5	38.0	even	ok

Figure S126. HRMS (ESI$^+$-FTICR) spectrum of **P_5-a**.

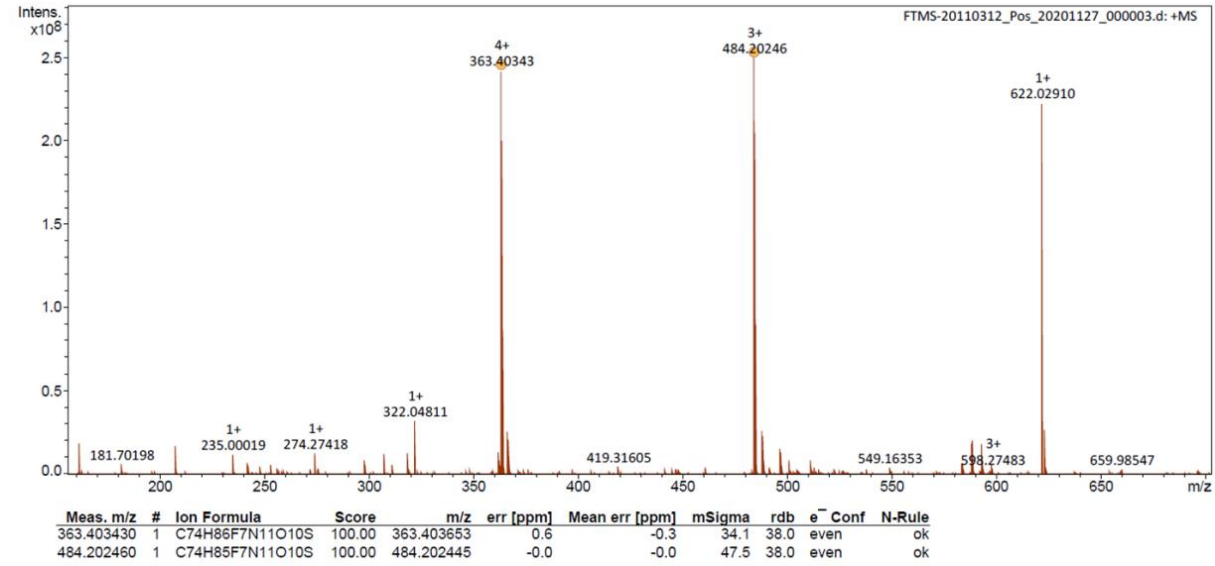

Meas. m/z	#	Ion Formula	Score	m/z	err [ppm]	Mean err [ppm]	mSigma	rdb	e⁻ Conf	N-Rule
363.403430	1	C74H86F7N11O10S	100.00	363.403653	0.6	-0.3	34.1	38.0	even	ok
484.202460	1	C74H85F7N11O10S	100.00	484.202445	-0.0	-0.0	47.5	38.0	even	ok

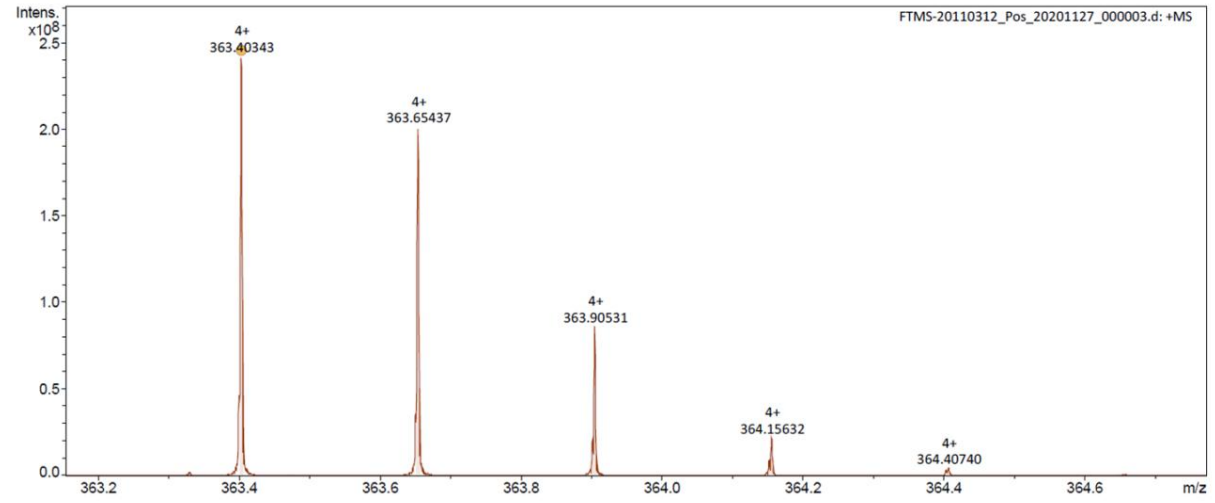

Meas. m/z	#	Ion Formula	Score	m/z	err [ppm]	Mean err [ppm]	mSigma	rdb	e⁻ Conf	N-Rule
363.403430	1	C74H86F7N11O10S	100.00	363.403653	0.6	-0.3	34.1	38.0	even	ok
484.202460	1	C74H85F7N11O10S	100.00	484.202445	-0.0	-0.0	47.5	38.0	even	ok

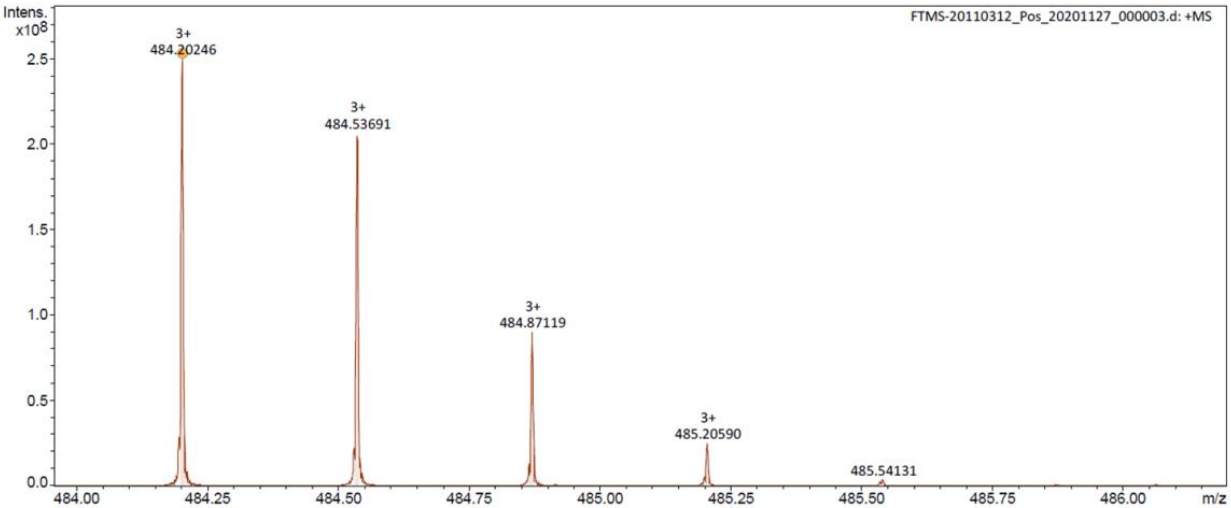

Meas. m/z	#	Ion Formula	Score	m/z	err [ppm]	Mean err [ppm]	mSigma	rdb	e⁻ Conf	N-Rule
363.403430	1	C74H86F7N11O10S	100.00	363.403653	0.6	-0.3	34.1	38.0	even	ok
484.202460	1	C74H85F7N11O10S	100.00	484.202445	-0.0	-0.0	47.5	38.0	even	ok

Figure S127. HRMS (ESI$^+$-FTICR) spectrum of **P_6-a**.

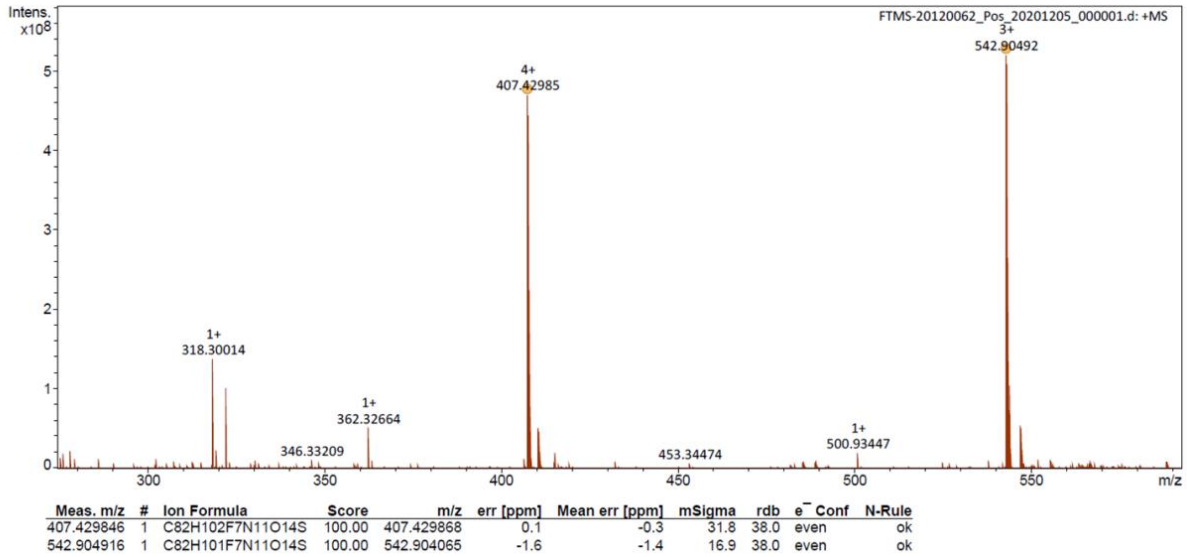

Meas. m/z	#	Ion Formula	Score	m/z	err [ppm]	Mean err [ppm]	mSigma	rdb	e⁻ Conf	N-Rule
407.429846	1	C82H102F7N11O14S	100.00	407.429868	0.1	-0.3	31.8	38.0	even	ok
542.904916	1	C82H101F7N11O14S	100.00	542.904065	-1.6	-1.4	16.9	38.0	even	ok

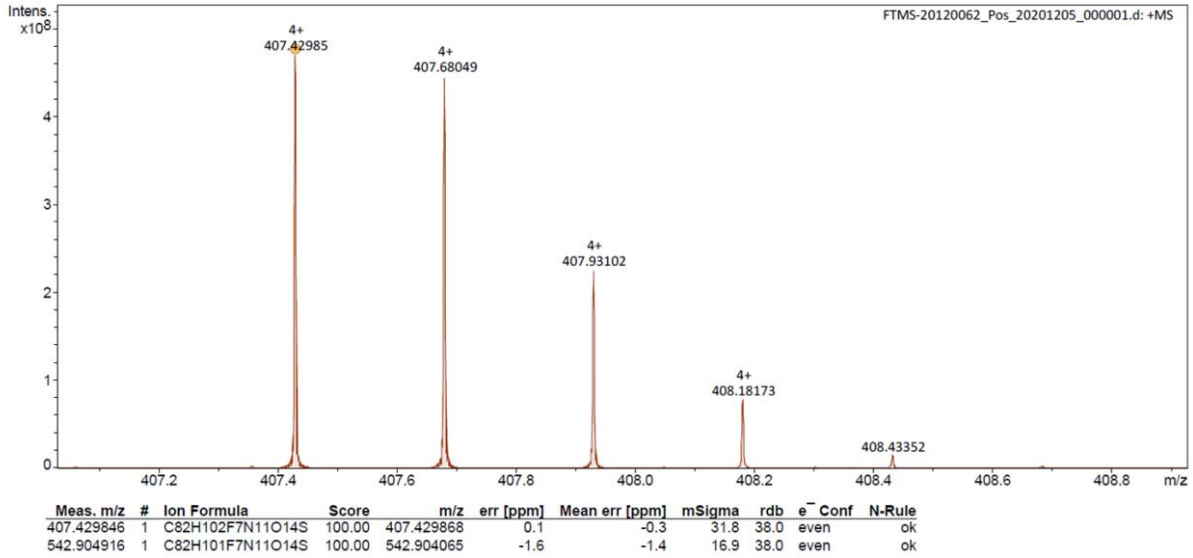

Meas. m/z	#	Ion Formula	Score	m/z	err [ppm]	Mean err [ppm]	mSigma	rdb	e⁻ Conf	N-Rule
407.429846	1	C82H102F7N11O14S	100.00	407.429868	0.1	-0.3	31.8	38.0	even	ok
542.904916	1	C82H101F7N11O14S	100.00	542.904065	-1.6	-1.4	16.9	38.0	even	ok

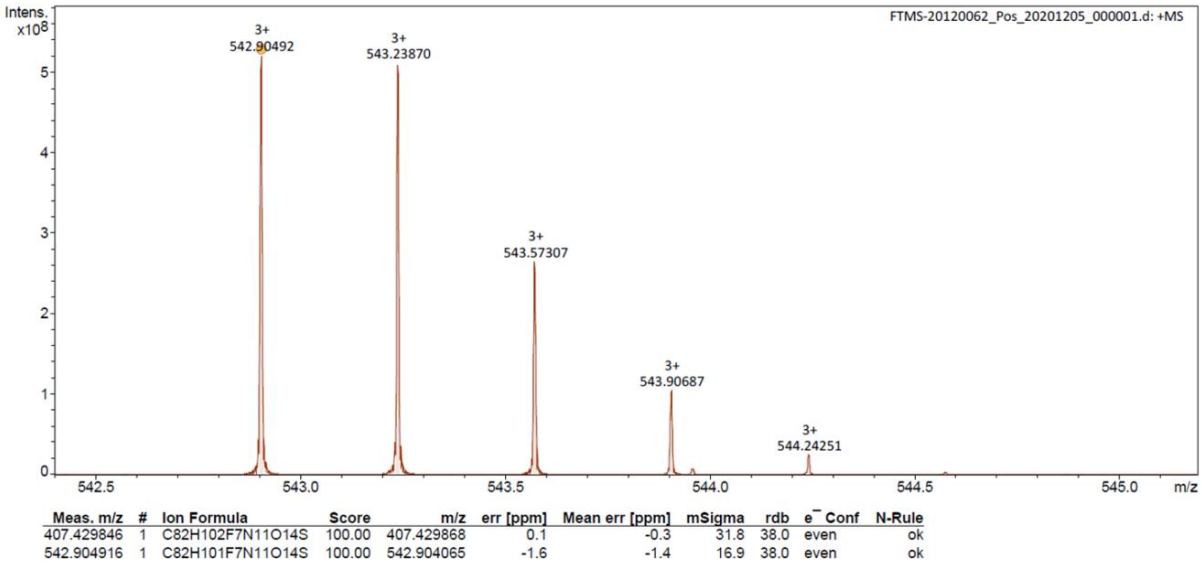

Meas. m/z	#	Ion Formula	Score	m/z	err [ppm]	Mean err [ppm]	mSigma	rdb	e⁻ Conf	N-Rule
407.429846	1	C82H102F7N11O14S	100.00	407.429868	0.1	-0.3	31.8	38.0	even	ok
542.904916	1	C82H101F7N11O14S	100.00	542.904065	-1.6	-1.4	16.9	38.0	even	ok

Figure S128. HRMS (ESI$^+$-FTICR) spectrum of **P$_7$-a**.

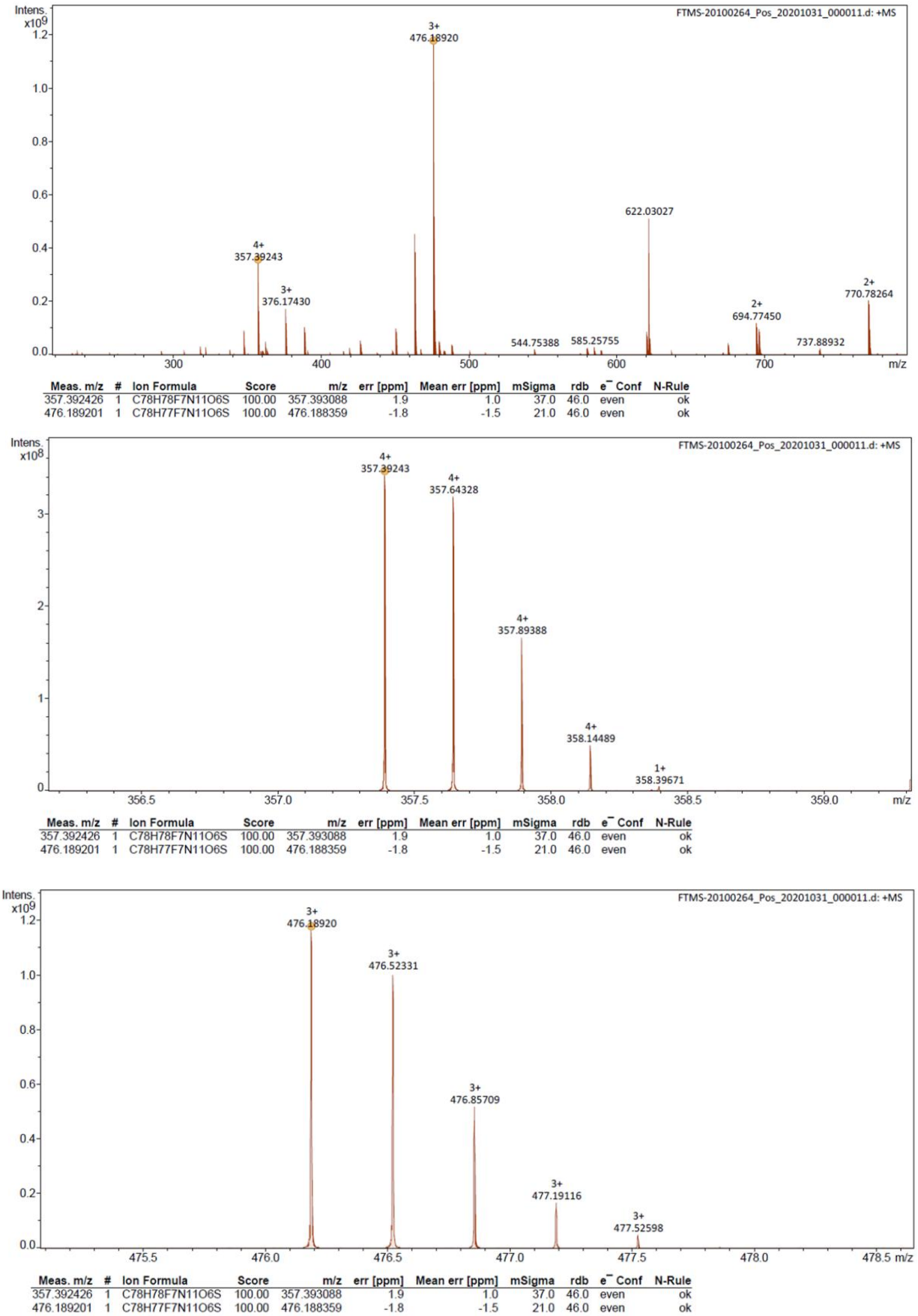

Figure S129. HRMS (ESI$^+$-FTICR) spectrum of **P_8-a**.

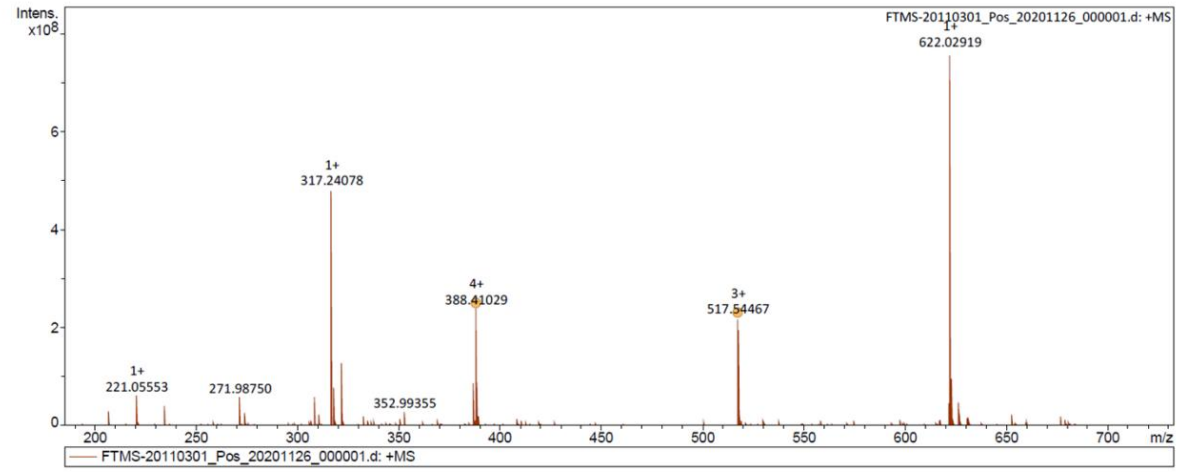

Meas. m/z	#	Ion Formula	Score	m/z	err [ppm]	Mean err [ppm]	mSigma	rdb	e⁻ Conf	N-Rule
388.410290	1	C74H82F7N23O6S	100.00	388.410135	-0.4	-1.4	41.4	46.0	even	ok
517.544675	1	C74H81F7N23O6S	100.00	517.544422	-0.5	-1.4	41.1	46.0	even	ok

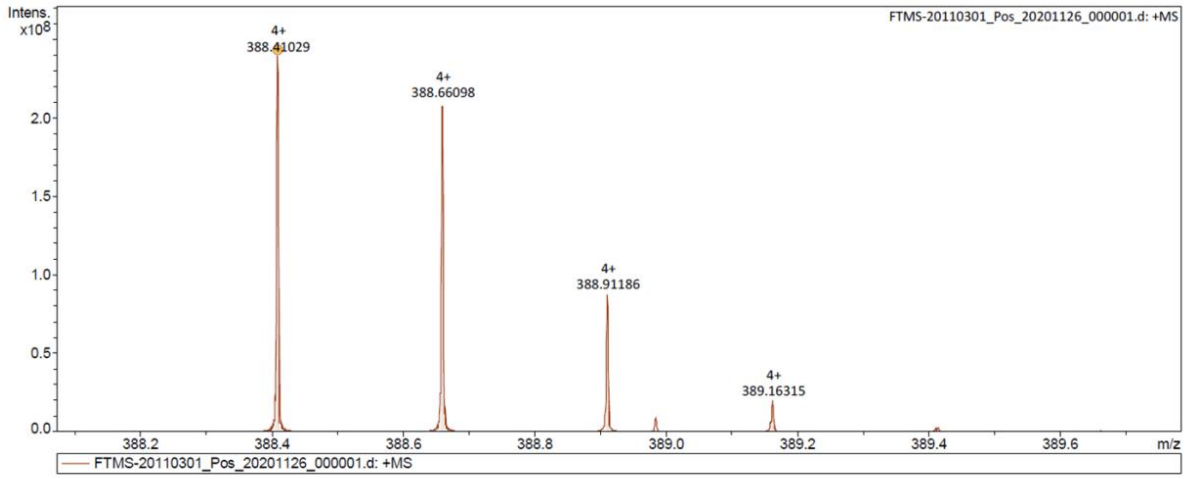

Meas. m/z	#	Ion Formula	Score	m/z	err [ppm]	Mean err [ppm]	mSigma	rdb	e⁻ Conf	N-Rule
388.410290	1	C74H82F7N23O6S	100.00	388.410135	-0.4	-1.4	41.4	46.0	even	ok
517.544675	1	C74H81F7N23O6S	100.00	517.544422	-0.5	-1.4	41.1	46.0	even	ok

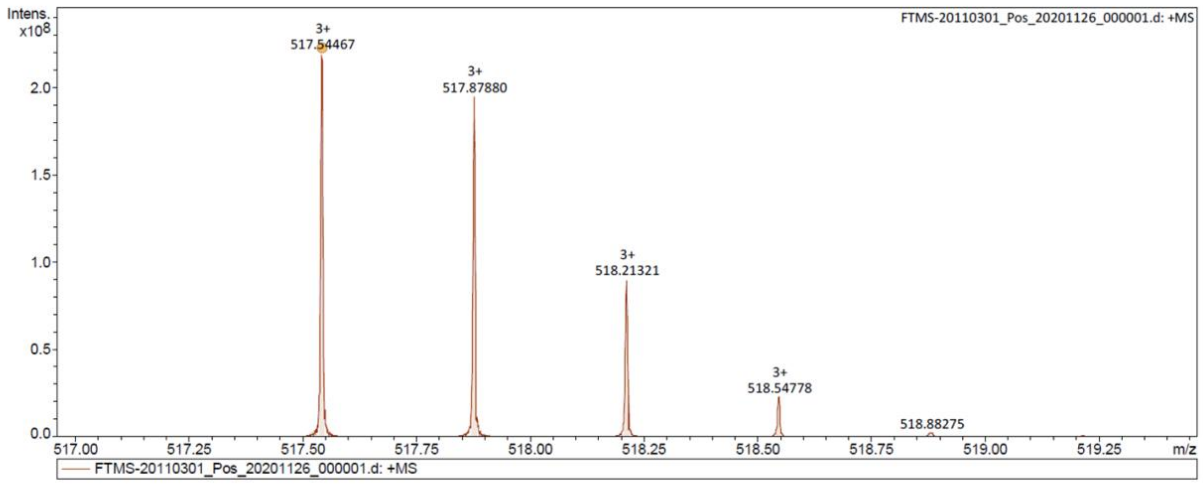

Meas. m/z	#	Ion Formula	Score	m/z	err [ppm]	Mean err [ppm]	mSigma	rdb	e⁻ Conf	N-Rule
388.410290	1	C74H82F7N23O6S	100.00	388.410135	-0.4	-1.4	41.4	46.0	even	ok
517.544675	1	C74H81F7N23O6S	100.00	517.544422	-0.5	-1.4	41.1	46.0	even	ok

Figure S130. HRMS (ESI$^+$-FTICR) spectrum of **P$_9$-a**.

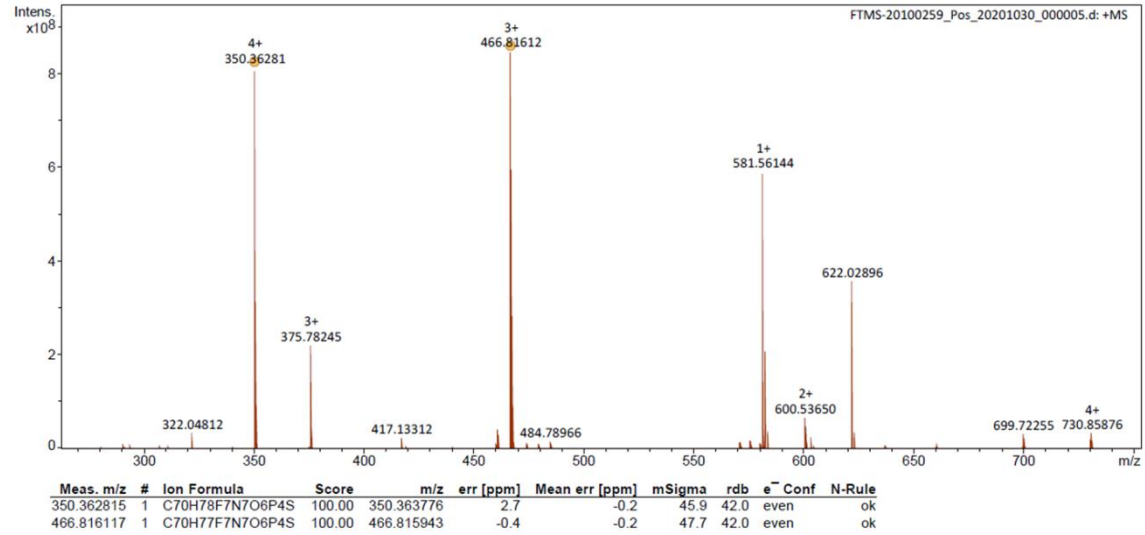

Meas. m/z	#	Ion Formula	Score	m/z	err [ppm]	Mean err [ppm]	mSigma	rdb	e⁻ Conf	N-Rule
350.362815	1	C70H78F7N7O6P4S	100.00	350.363776	2.7	-0.2	45.9	42.0	even	ok
466.816117	1	C70H77F7N7O6P4S	100.00	466.815943	-0.4	-0.2	47.7	42.0	even	ok

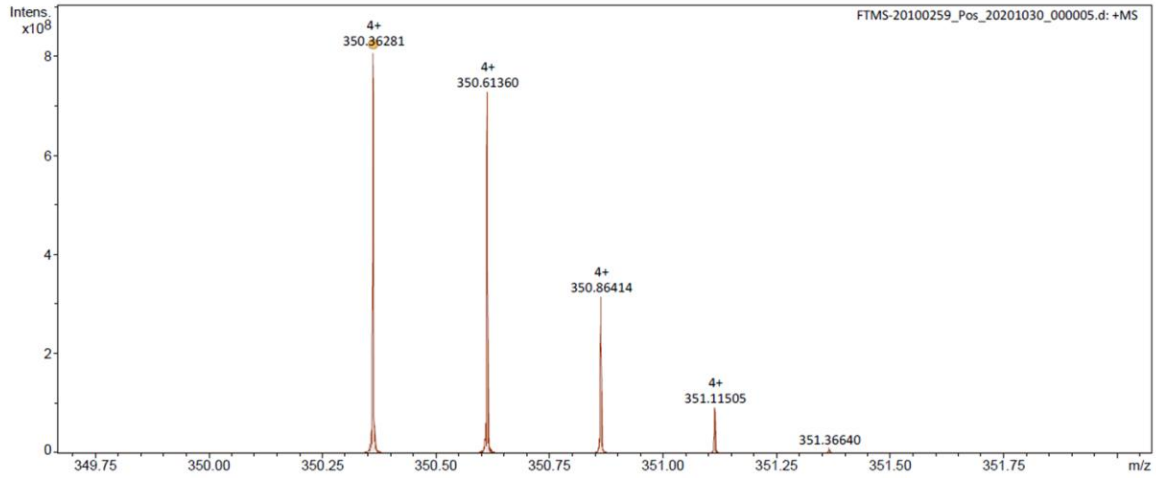

Meas. m/z	#	Ion Formula	Score	m/z	err [ppm]	Mean err [ppm]	mSigma	rdb	e⁻ Conf	N-Rule
350.362815	1	C70H78F7N7O6P4S	100.00	350.363776	2.7	-0.2	45.9	42.0	even	ok
466.816117	1	C70H77F7N7O6P4S	100.00	466.815943	-0.4	-0.2	47.7	42.0	even	ok

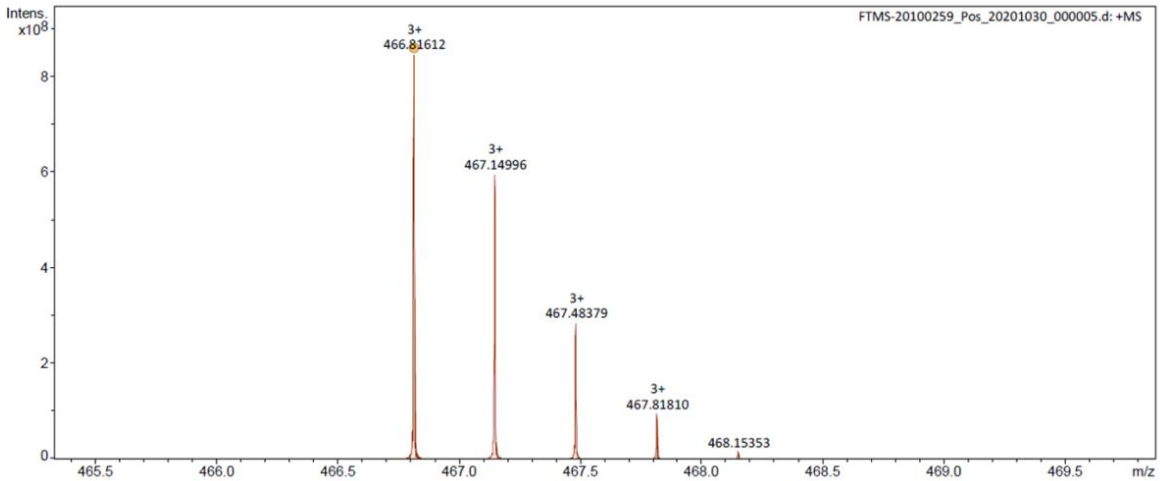

Meas. m/z	#	Ion Formula	Score	m/z	err [ppm]	Mean err [ppm]	mSigma	rdb	e⁻ Conf	N-Rule
350.362815	1	C70H78F7N7O6P4S	100.00	350.363776	2.7	-0.2	45.9	42.0	even	ok
466.816117	1	C70H77F7N7O6P4S	100.00	466.815943	-0.4	-0.2	47.7	42.0	even	ok

Figure S131. HRMS (ESI$^+$-FTICR) spectrum of **P_{10}-a**.

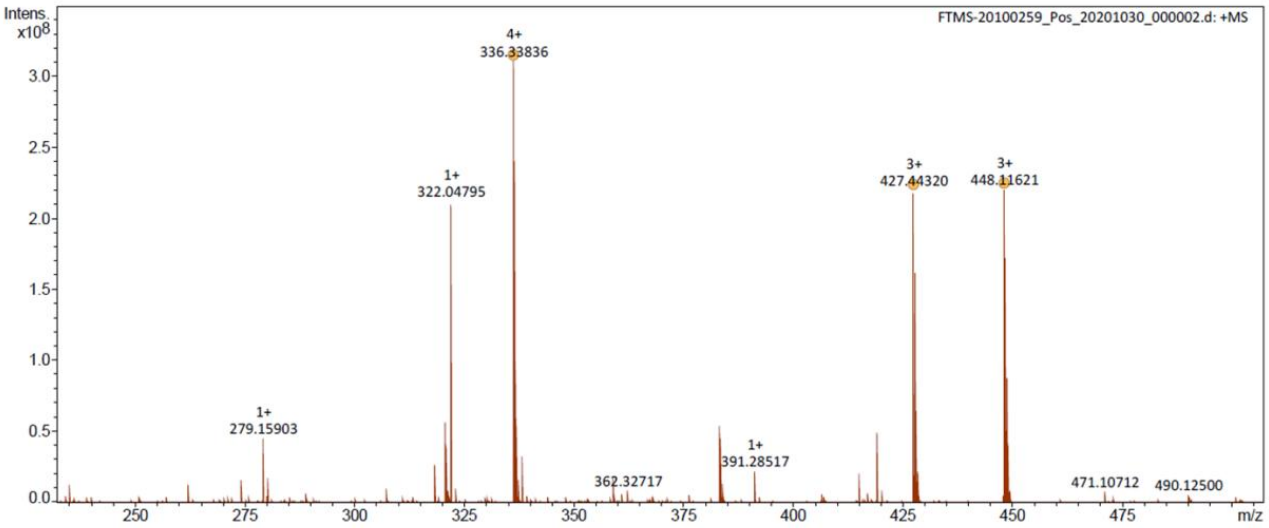

Meas. m/z	#	Ion Formula	Score	m/z	err [ppm]	Mean err [ppm]	mSigma	rdb	e⁻ Conf	N-Rule
336.338364	1	C66H66F7N7O6S5	100.00	336.338610	0.7	-0.3	70.6	46.0	even	ok
427.443196	1	C64H59F7N7O6S4	100.00	427.442715	-1.1	-1.9	84.0	45.0	even	ok
448.116206	1	C66H65F7N7O6S5	100.00	448.115722	-1.1	-1.6	65.6	46.0	even	ok

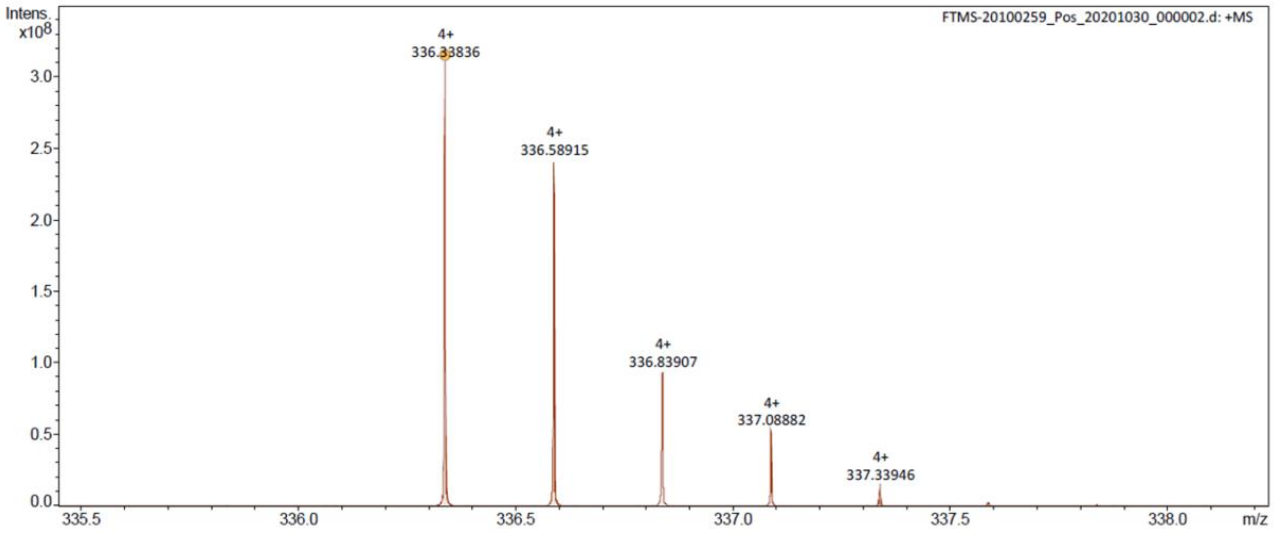

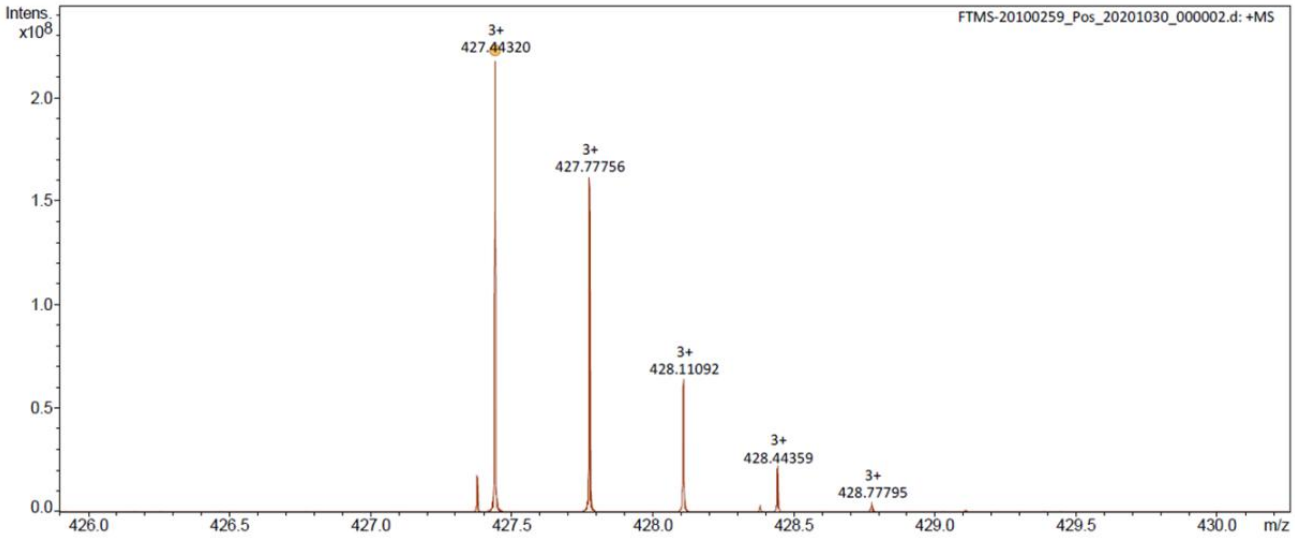

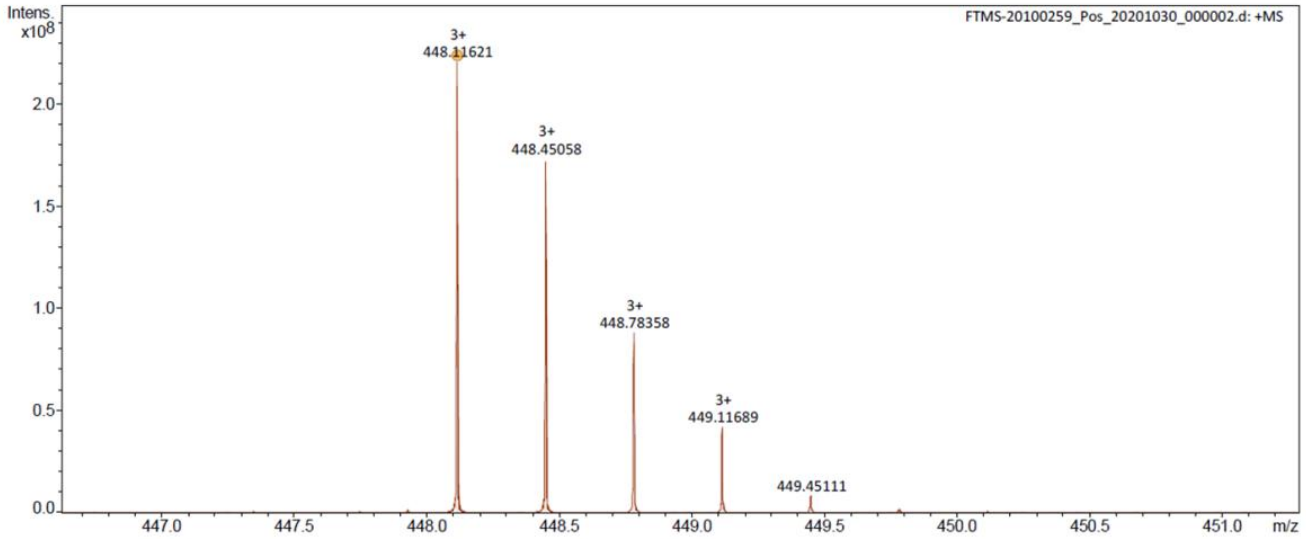

Figure S132. HRMS (ESI$^+$-FTICR) spectrum of **P_{11}-a**.

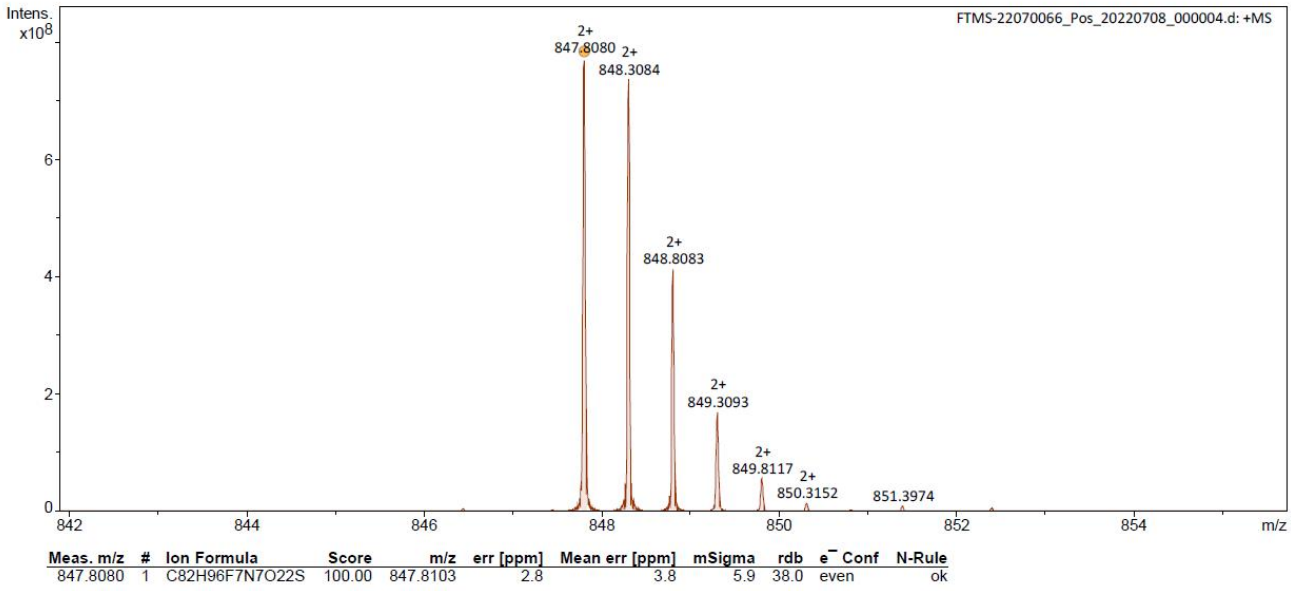

Meas. m/z	#	Ion Formula	Score	m/z	err [ppm]	Mean err [ppm]	mSigma	rdb	e⁻ Conf	N-Rule
847.8080	1	C82H96F7N7O22S	100.00	847.8103	2.8	3.8	5.9	38.0	even	ok

Figure S133. HRMS (ESI$^+$-FTICR) spectrum of **P_{12}-a**.

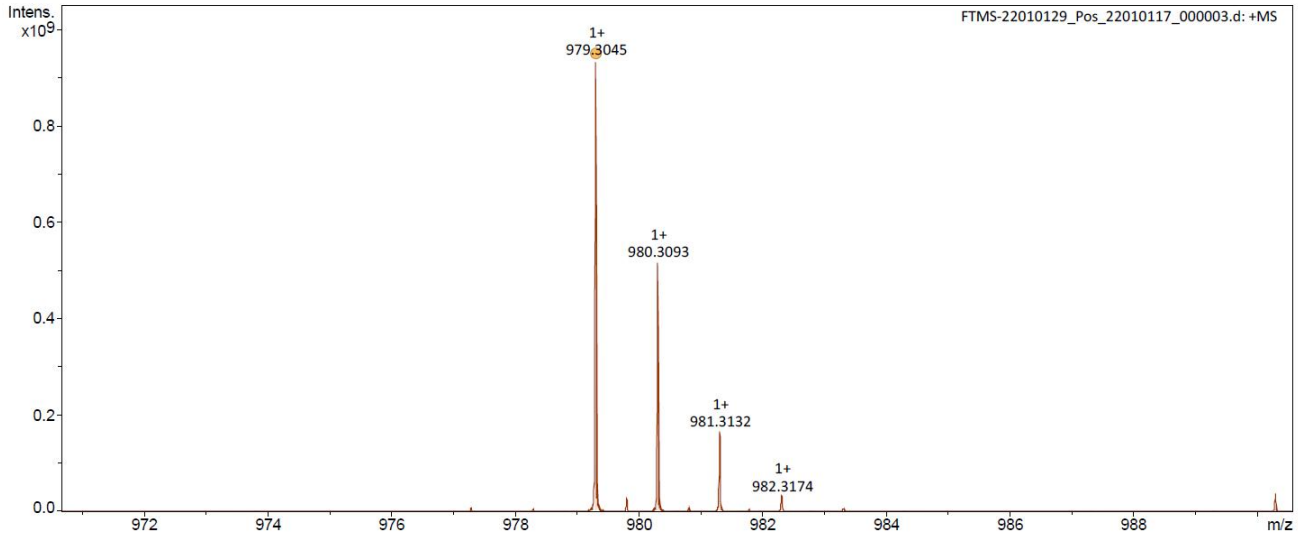

Figure S134. HRMS (ESI$^+$-FTICR) spectrum of **FITC-DEVD**.

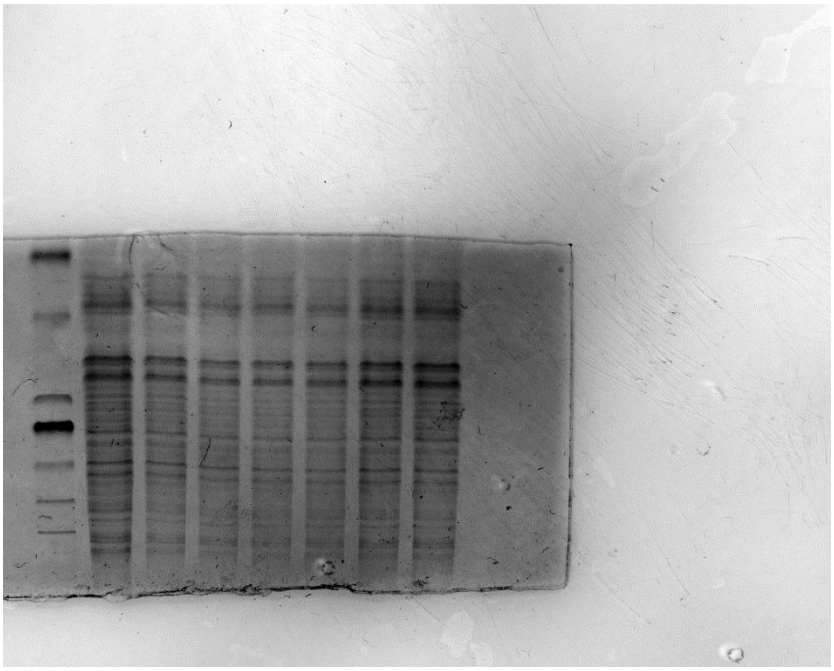

Figure S135. Raw image for **Figure S15**-CBB.

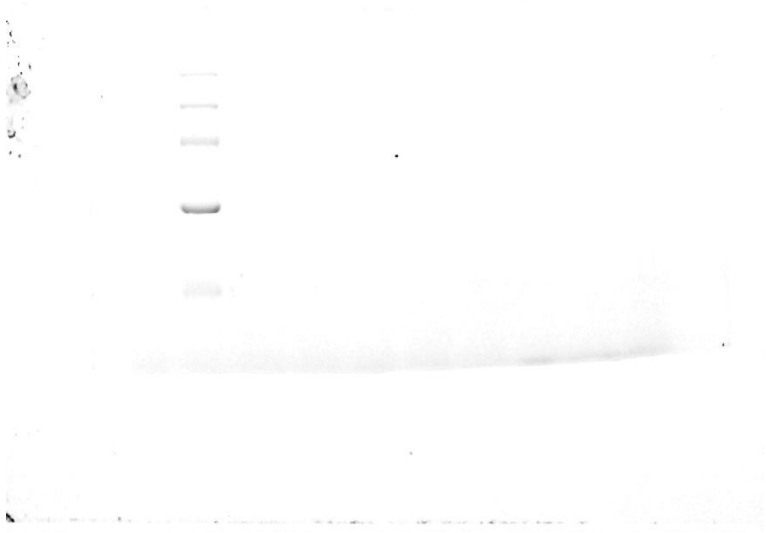

Figure S136. Raw image for **Figure S15**-in gel.

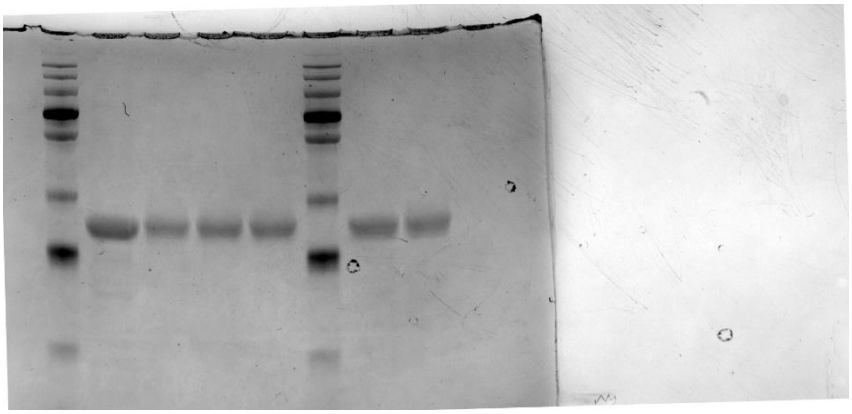

Figure S137. Raw image for **Figure 4c**-CBB.

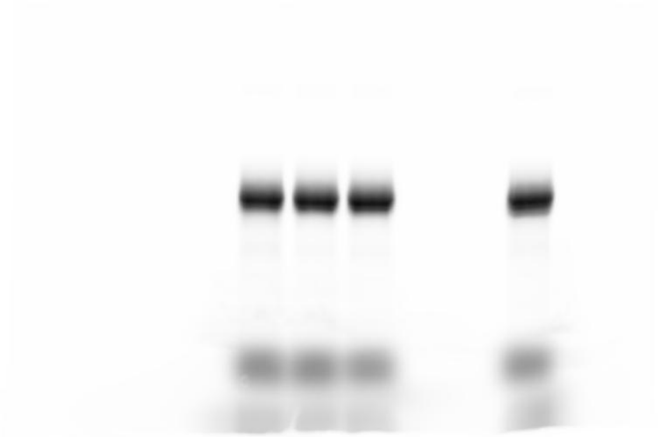

Figure S138. Raw image for **Figure 4c**-in gel.

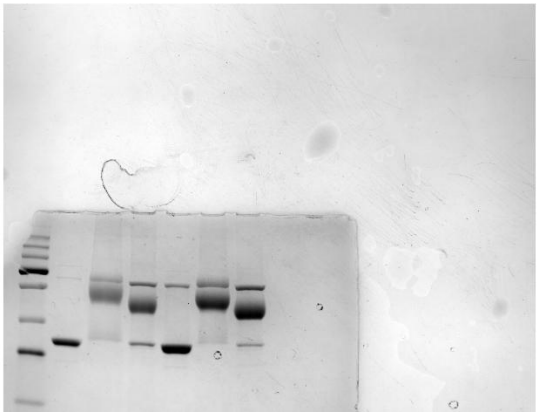

Figure S139. Raw image for **Figure 5b**.

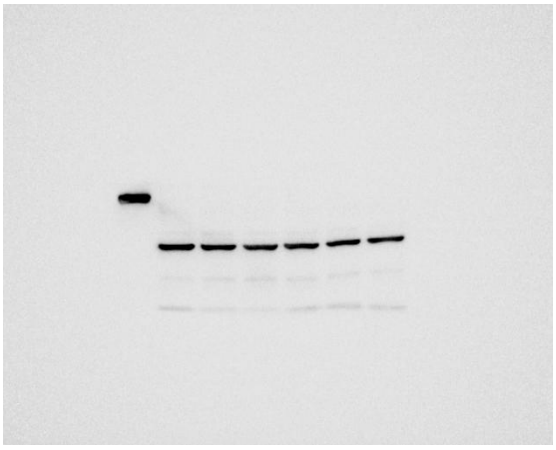

Figure S140. Raw image for **Figure 7g**-β-actin.

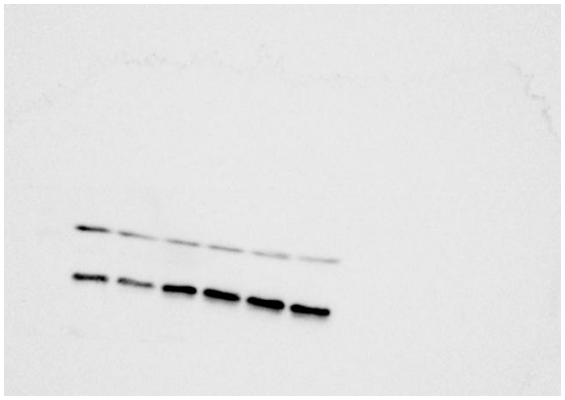

Figure S141. Raw image for **Figure 7g**-caspase 3.

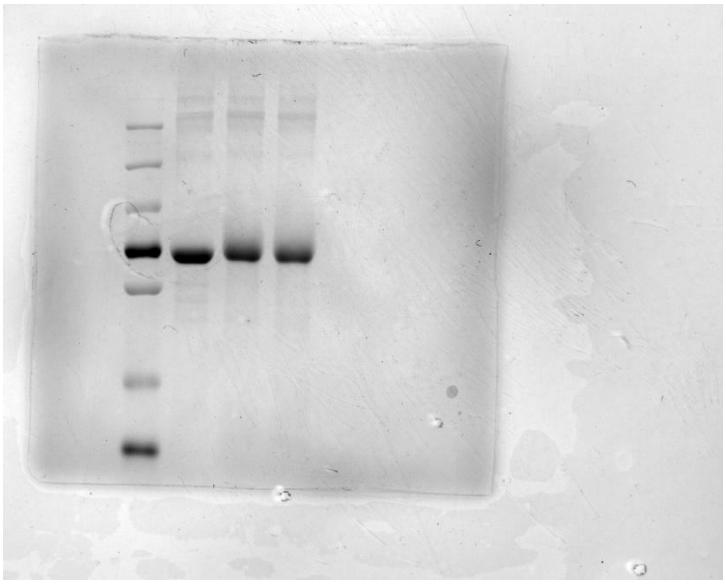

Figure S142. Raw image for **Figure S40**-CBB.

Figure S143. Raw image for **Figure S40**-in gel.

III. Reference

1 Hu, J.-Y. *et al.* Highly near-IR emissive ytterbium(III) complexes with unprecedented quantum yields. *Chem. Sci.* **8**, 2702-2709 (2017).

2 Hou, Y., Yuan, J., Zhou, Y., Yu, J. & Lu, H. A Concise Approach to Site-Specific Topological Protein–Poly(amino acid) Conjugates Enabled by in Situ-Generated Functionalities. *J. Am. Chem. Soc.* **138**, 10995-11000 (2016).

3 Lu, J., Wang, H., Tian, Z., Hou, Y. & Lu, H. Cryopolymerization of 1,2-Dithiolanes for the Facile and Reversible Grafting-from Synthesis of Protein–Polydisulfide Conjugates. *J. Am. Chem. Soc.* **142**, 1217-1221 (2020).

4 M. J. Frisch *et al. Gaussian 09 (Revision E.01)*. (Gaussian Inc., 2009).

5 Francl, M. M. *et al.* Self‐consistent molecular orbital methods. XXIII. A polarization‐type basis set for second‐row elements. *J. Chem. Phys.* **77**, 3654-3665 (1982).

6 Hariharan, P. C. & Pople, J. A. The influence of polarization functions on molecular orbital hydrogenation energies. *Theor. Chem. Acc.* **28**, 213-222 (1973).

7 Marenich, A. V., Cramer, C. J. & Truhlar, D. G. Universal solvation model based on solute electron density and a continuum model of the solvent defined by the bulk dielectric constant and atomic surface tensions. *J. Phys. Chem. B* **113**, 6378-6396 (2009).

8 Chiodo, S. G. & Leopoldini, M. MolSOC: A spin–orbit coupling code. *Computer Physics Communications* **185**, 676-683 (2014).

9 Gao, X. *et al.* Evaluation of spin-orbit couplings with linear-response time-dependent density functional methods. *J. Chem. Theory Comput.* **13**, 515–524 (2017).

10 Niu, Y. L., Peng, Q. A., Deng, C. M., Gao, X. & Shuai, Z. G. Theory of excited state decays and optical spectra: application to polyatomic molecules. *Journal of Physical Chemistry A* **114**, 7817-7831 (2010).

11 Peng, Q., Niu, Y., Shi, Q., Gao, X. & Shuai, Z. Correlation function formalism for triplet excited state decay: combined spin-orbit and nonadiabatic couplings. *J. Chem. Theory. Comput.* **9**, 1132-1143 (2013).

12 Shuai, Z. G., Peng, Q., Niu, Y. L. & Geng, H. *MOMAP, a molecular materials property prediction package, revision 0.2.004*. (Tsinghua University: Beijing, China, 2014).

13 Peng, Q. *et al.* Theoretical study of conversion and decay processes of excited triplet and singlet states in a thermally activated delayed fluorescence molecule. *J. Phys. Chem. C* **121**, 13448-13456 (2017).

14 Niu, Y., Li, W., Qian, P., Hua, G. & Shuai, Z. Molecular materials property prediction package (MOMAP) 1.0: a software package for predicting the luminescent properties and mobility of organic functional materials. *Molecular Physics* **116**, 1-13 (2018).